Less Common Triple-Negative Breast Cancers

12

Poonam Vohra, Yunn-Yi Chen, and Gregor Krings

Adenoid Cystic Carcinoma

Overview and Clinical Presentation

Adenoid cystic carcinoma (AdCC) of the breast is a rare and histologically distinct triple-negative and basal-like cancer, which accounts for <0.1% of all breast carcinomas. Previously termed cylindroma, AdCC of the breast was first described by Geschickter [1]. Classic AdCC follow an indolent clinical course and generally has an excellent prognosis [2–4]. The incidence of mammary AdCC has remained stable over the last 30 years without a notable rise following widespread use of mammography since the 1980s. It occurs more frequently in the sixth or early seventh decade and is extremely unusual in younger and premenopausal women [2]. The incidence ratio for black women is 39% lower than for white women. Although far more common in women, AdCC has also been described in men [5, 6]. The tumor typically presents as a palpable mass that is occasionally tender to palpation. A few reported cases have been detected incidentally on routine screening mammograms of asymptomatic patients. AdCC is often located in the central or subareolar region [7]. Despite this central location, nipple discharge is rarely present. AdCC is only rarely fixed to the overlying skin, nipple, or pectoral muscles [7]. The right and left breasts are equally affected, and there is no predilection for AdCC to develop bilaterally [8].

Gross and Radiologic Features

On gross examination, AdCC is usually circumscribed and nodular, ranging from 0.5 to 12 cm in size, with an average of 3 cm. Microcysts (pink, tan, or gray) may occasionally be noted grossly [9].

On mammography, AdCC can appear either as a well-defined lobulated or ill-defined mass or occasionally as an asymmetric density with microcalcifications [7, 10]. Rare tumors may present as a spiculated lesion. In one case, MRI revealed an unusual pattern of early enhancement (but no washout) extending from the periphery to the center gradually [10]. These tumors exhibit minimal vascularity on color Doppler imaging and on positron emission tomography (PET) scan [11, 12]. AdCC usually does not show the typical appearance of invasive ductal carcinoma (IDC) on either mammogram or ultrasonography due to its well-defined nature with less surrounding architectural disruption and fibrosis. Accordingly, a "negative" finding or a benign-looking breast lesion on imaging cannot completely exclude the possibility of AdCC. On the other hand, the presence of a painful breast lesion without obvious inflammatory signs can lead to diagnostic suspicion [12].

Microscopic Features

AdCC demonstrates distinct histologic features analogous to its counterpart in the salivary glands, lung, and skin. Based on architectural and cytologic features, three subtypes have been recognized by the most recent World Health Organization (WHO) classification of breast tumors: classic AdCC, solid basaloid AdCC (SB-AdCC) and AdCC with high-grade transformation [13]. Classic AdCC constitutes the vast majority of breast AdCC. These tumors are composed of a dual population of luminal epithelial cells and abluminal myoepithelial/basaloid cells, arranged in varied architectural patterns including cribriform, tubular, reticular, solid, and mixed (Figs. 12.1, 12.2, 12.3, 12.4, 12.5, and 12.6). The most frequent cribriform variant is characterized by a sieve-like growth pattern, in which sheets of epithelial cells are punctuated by round or oval gland-like spaces

P. Vohra · Y.-Y. Chen · G. Krings (✉)
Department of Pathology, University of California San Francisco (UCSF), San Francisco, CA, USA
e-mail: Poonam.vohra@ucsf.edu; yunn-yi.chen@ucsf.edu; gregor.krings@ucsf.edu
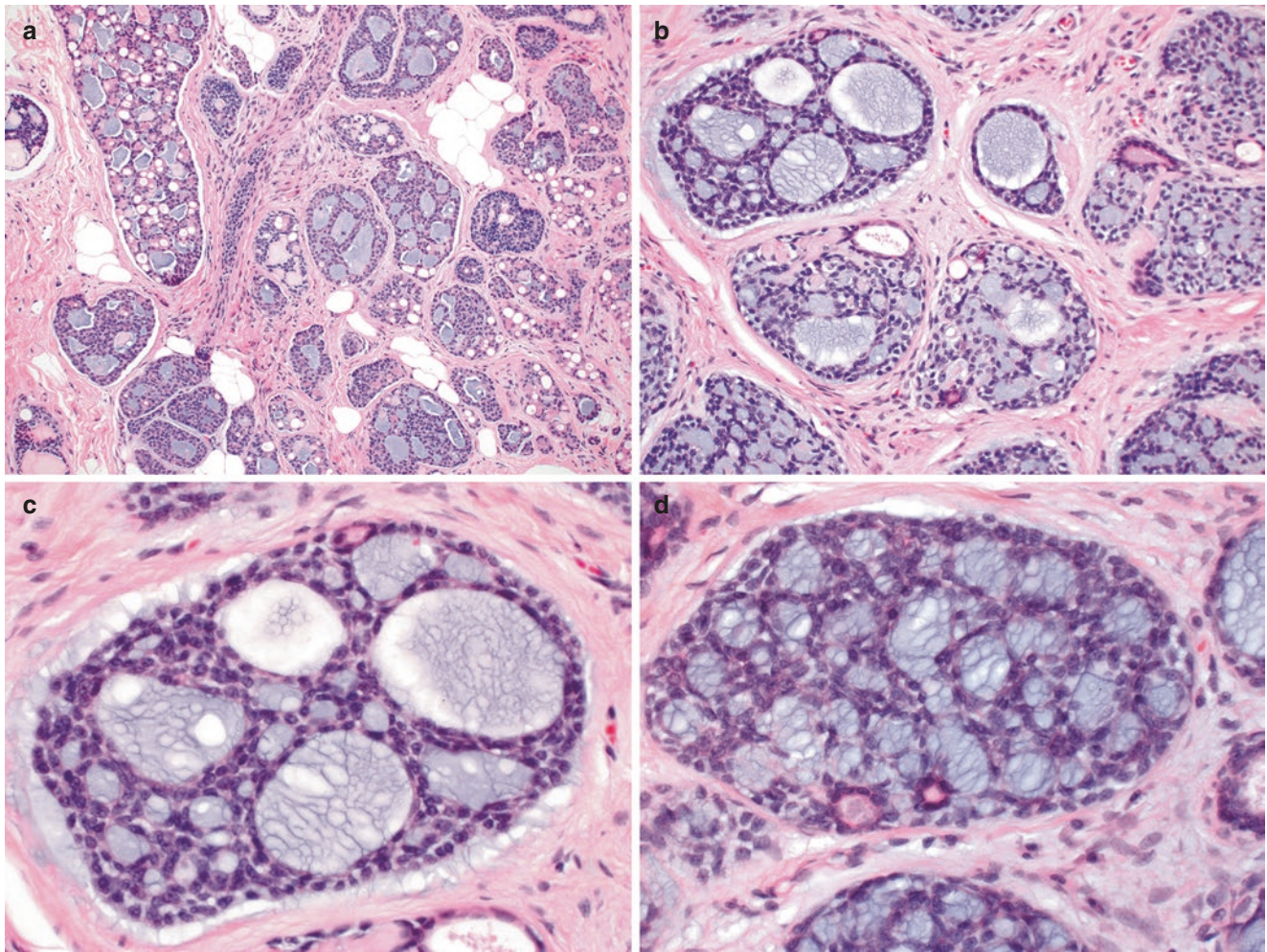
Fig. 12.1 Core needle biopsy of adenoid cystic carcinoma, cribriform growth pattern. (**a–d**) CNB reveals nests of tumor cells with a characteristic sieve-like (cribriform) growth pattern, in which clusters of neo-plastic epithelial and myoepithelial cells are punctuated by round to oval spaces containing myxoid basement membrane material

(Fig. 12.1a–d). The dominant myoepithelial/basaloid cells have scant eosinophilic to clear cytoplasm and angulated to oval, hyperchromatic monomorphic nuclei, whereas the luminal epithelial cells are slightly larger, with modest amounts of eosinophilic cytoplasm and rounded nuclei (Fig. 12.2a–c). Mitotic activity is generally low. Two types of lumens are identified: "pseudolumens," comprising the characteristic cribriform spaces lined by myoepithelial cells, and true glandular lumens, lined by luminal epithelial cells (Fig. 12.4a–e). The pseudolumens contain basement membrane material, which may appear as Alcian blue-positive loose myxoid substance or PASD-positive eosinophilic hyalinized spherules. Immunostains for type IV collagen and laminin highlight the basement membrane components within the pseudolumens [14] (Fig. 12.4f, g). The true glandular lumens may show PAS-positive eosinophilic secretions.

AdCC may also assume a reticular architecture, in which the neoplastic cells are arranged in interconnected thin strands associated with myxoid or hyaline basement membrane material (Fig. 12.5a–d). Interspersed ductules may be appreciated on careful inspection. AdCC with tubular growth pattern comprises ductules or tubules lined by luminal epithelial cells and surrounding abluminal myoepithelial cells. The tubular pattern is often admixed with areas of cribriform growth (Fig. 12.6a–f).

First described by Shin and Rosen in 2002 [15], the rare SB-AdCC subtype is characterized by infiltrating irregular solid nests or islands of basaloid tumor cells within a hyalinized, myxoid, or desmoplastic stroma (Fig. 12.7a–d). Compared to classic AdCC, the tumor cells in the solid-basaloid subtype are larger, with hyperchromatic nuclei, moderate to marked atypia, and increased mitotic activity [15] (Fig. 12.8a, b). Foci of necrosis may be present, and
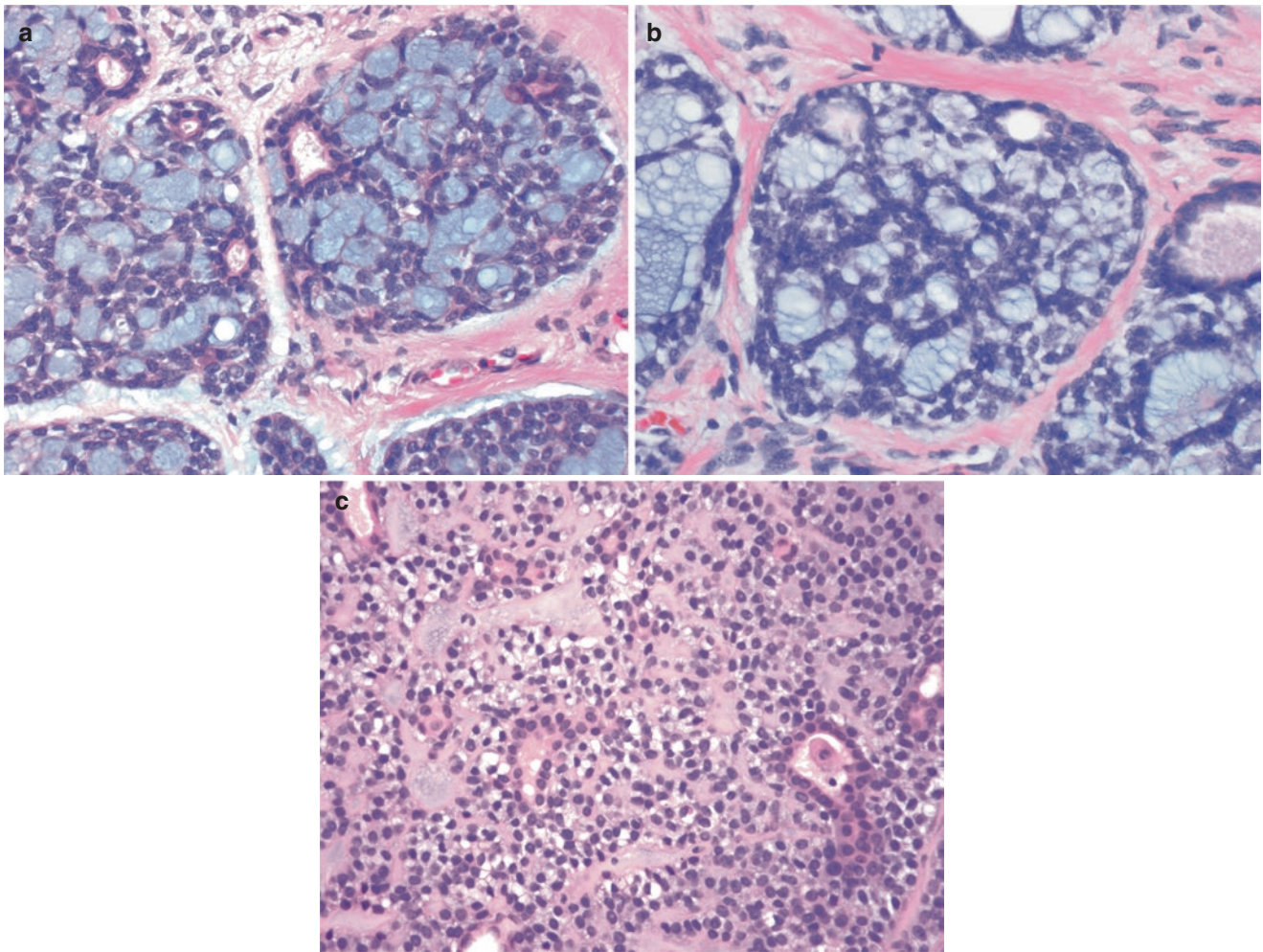
Fig. 12.2 Adenoid cystic carcinoma with dual population of tumor cells. (**a**, **b**) The myoepithelial/basaloid cells in these examples demonstrate scant cytoplasm and enlarged nuclei with irregular borders and open chromatin, whereas the luminal epithelial cells display more distinct eosinophilic cytoplasm and slightly smaller nuclei. (**c**) The myo-epithelial cells of this case show scant pale to clear vacuolated cytoplasm and oval hyperchromatic nuclei. The luminal epithelial cells are larger, with more eosinophilic cytoplasm and rounded nuclei. Note the lumen formation by both populations of tumor cells in these examples

perineural invasion and lymphovascular invasion are frequent findings. Whereas a dual population of ductal and myoepithelial cells is considered to be the cardinal feature for diagnosis of AdCC, this phenotype is not conspicuous in the solid basaloid subtype, with the tumor showing basaloid cells, apparent loss of the biphasic cellular components, and decrease or loss of myoepithelial marker expression [15–18]. Immunostaining is often required to highlight any focal, subtle second cell population and true glandular lumens in SB-AdCC (Fig. 12.9a–f). The identification of so-called intercalated ducts, which appear eosinophilic in the background of dark basaloid cells, is helpful in recognizing this variant (Fig. 12.9). It has been suggested that the basaloid tumor cells probably represent poorly differentiated or undif-ferentiated primitive precursor cells capable of differentiating into myoepithelial-like or luminal-type cells [15, 16].

AdCC with high-grade transformation has been well documented in the salivary gland but is vanishingly rare in the breast. This subtype is characterized by either classic or SB-AdCC associated and merged with a high-grade carcinoma, which has been reported to include high-grade triple-negative breast cancer (TNBC) of no special type [19, 20] and small cell neuroendocrine carcinoma [21]. A rare metaplastic carcinoma with an associated AdCC component has been described [22].

In rare cases, the epithelial cells of AdCC can demonstrate squamous or sebaceous differentiation [2]. AdCC has been observed in association with microglandular adenosis,
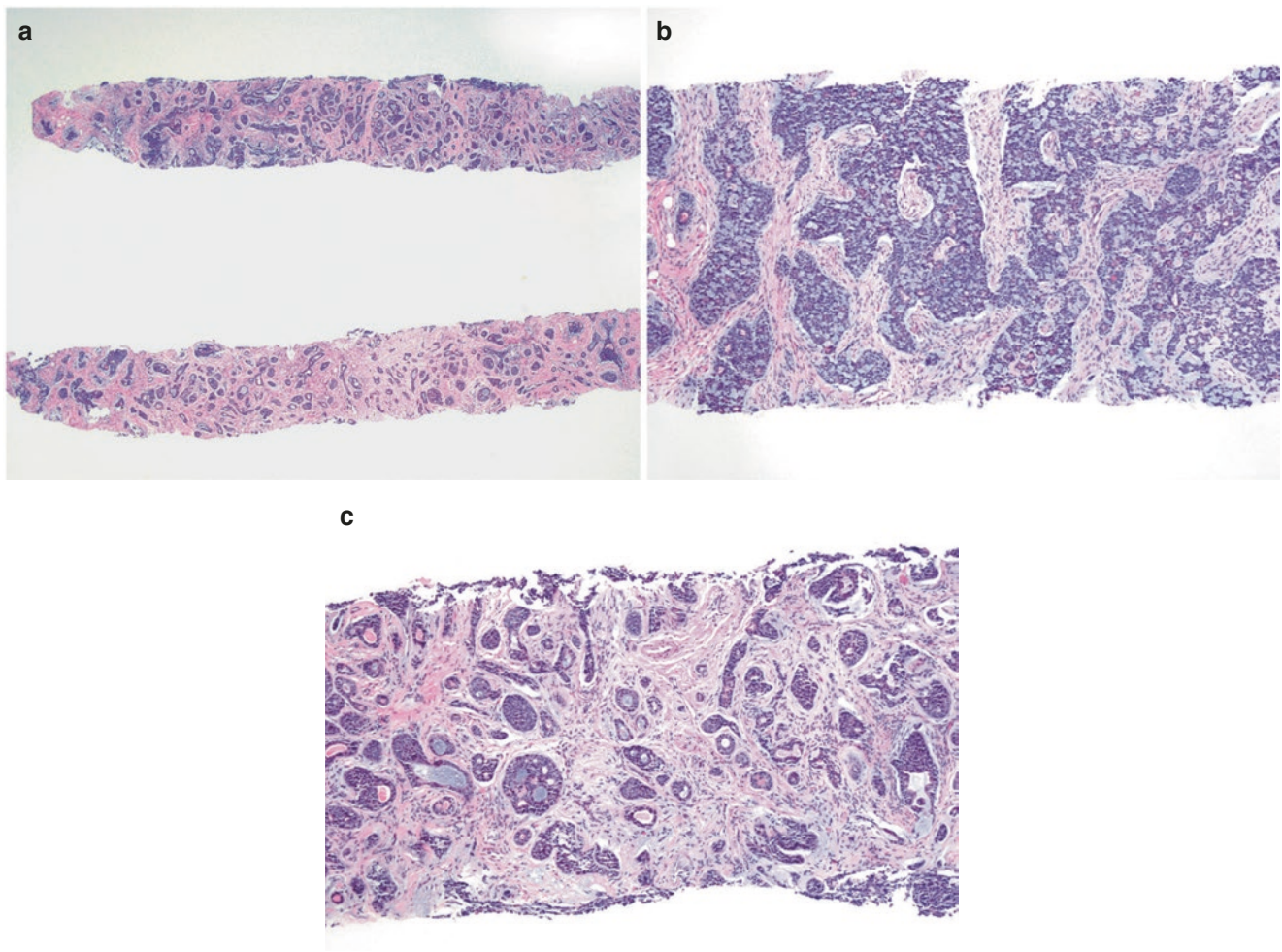
Fig. 12.3 Core needle biopsy of adenoid cystic carcinoma, mixed growth patterns. (**a**) This AdCC demonstrates varied growth patterns, (**b**) including some areas with irregular infiltrating trabeculae, (**c**) and other areas showing nested and glandular growth with focal cribriforming

tubular adenosis, papilloma, adenomyoepithelioma, and low-grade adenosquamous carcinoma [3, 23–25], suggesting a close relationship between breast lesions displaying biphasic epithelial–myoepithelial differentiation (Fig. 12.10). An in situ lesion with adenoid cystic features has been described [15, 23]. However, the distinction between in situ and invasive AdCC may be challenging.

Similar to its counterpart in the salivary gland but to a much lower frequency, AdCC of the breast can demonstrate perineural invasion [26, 27], which may be associated with the clinical finding of a painful breast mass (Fig. 12.11). Lymphatic tumor emboli are extremely uncommon in classic AdCC. As mentioned above, perineural invasion and lymphovascular invasion are more frequently observed in SB-AdCC. Despite being well circumscribed on imaging and gross evaluation, the tumor borders are usually at least focally infiltrative microscopically. In fact, scant tubular or cribriform glands may be noted at some distance (>1 cm

away) from the grossly identified mass, sometimes in the form of perineural invasion. This feature may partly contribute to the local recurrence observed in some patients with AdCC after breast-conserving surgery.

Ro et al. suggested that AdCC can be stratified into three grades based on the proportion of solid growth within the tumor: grade I—no solid component; grade II—<30% solid component; and grade III—>30% solid component. Grade II and III tumors tended to be larger and were more likely to recur and rarely metastasize [3, 28]. However, the prognostic significance of this histologic grading scheme has not been confirmed by other studies [16, 29]. The current (eighth edition) American Joint Commission on Cancer staging manual recommends that the modified Scarf-Bloom-Richardson (SBR) grading system be applied for all breast cancer subtypes, including AdCC. Using the SBR grading system, most classic AdCC are grade 2, whereas SB-AdCC can be either grade 2 or 3 [18, 30]. Given the unclear significance of histo-

logic grading and the overall excellent prognosis of AdCC, except for the solid basaloid subtype, we generally do not grade these tumors on core needle biopsies (CNB).

Immunohistochemistry

The two different cell types of classic AdCC can be readily distinguished by immunohistochemistry. The myoepithelial cells are typically positive for high-molecular-weight cyto-keratins (HMWCK; CK5/6, CK14, CK17) and a subset of myoepithelial cell markers (p63, smooth muscle actin [SMA], S100 protein), but are usually negative for other myoepithelial markers, which can include calponin, smooth muscle myosin (SMM), and CD10 (Figs. 12.12b–f, 12.13b, and 12.14c, d). This suggests an incomplete or aberrant myo-epithelial phenotype. Which myoepithelial cell markers are positive or negative in a given tumor is not predictable. The luminal epithelial cells show positivity for CK7, CK8/18, CD117 (c-kit), epithelial membrane antigen (EMA), and car-
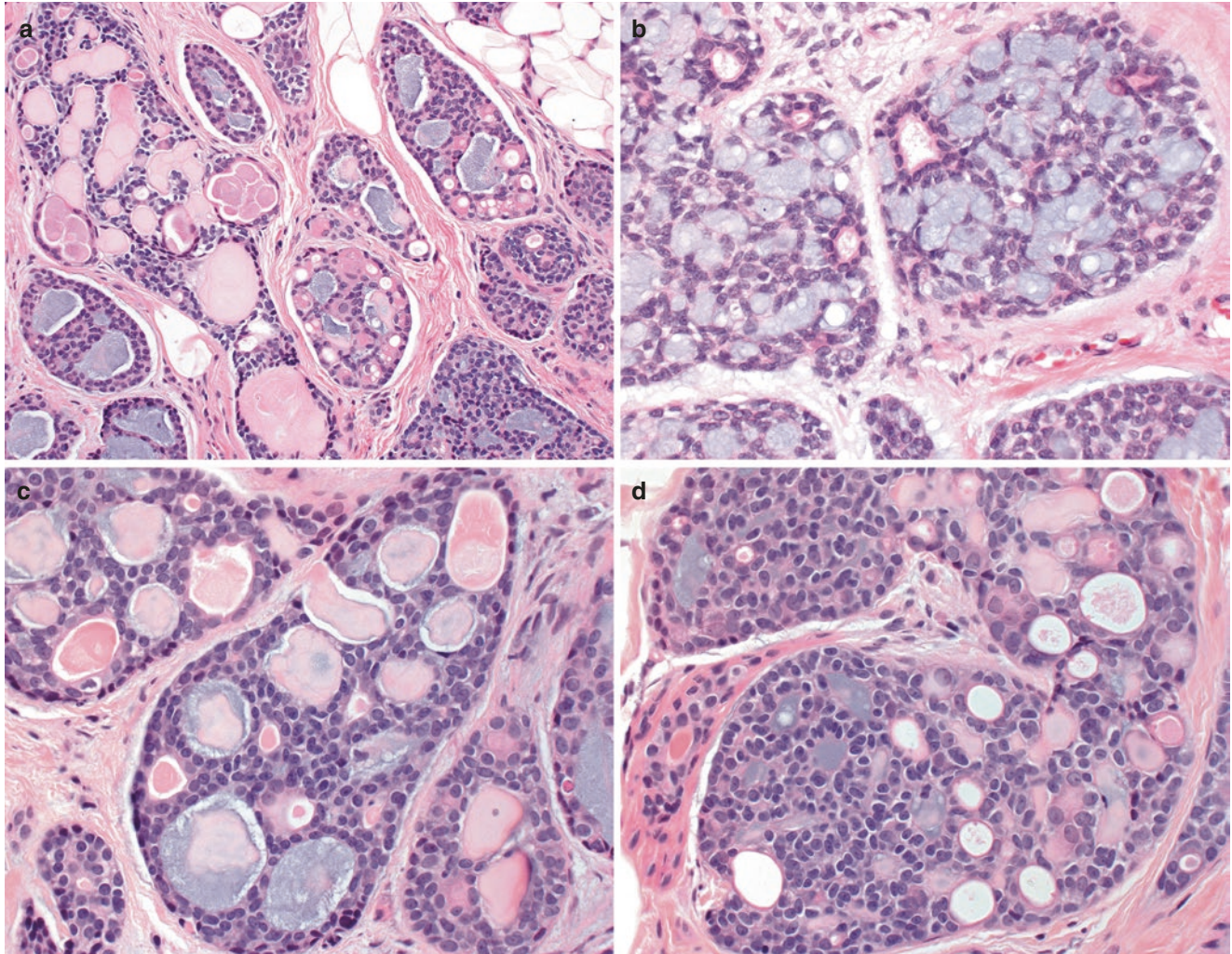
Fig. 12.4 True lumens and pseudolumens of adenoid cystic carci-noma. (**a–e**) Pseudolumens are lined by myoepithelial cells and often contain basement membrane material, which may appear as either loose myxoid substance or eosinophilic hyalinized spherules. In contrast, true glandular lumens are lined by luminal epithelial cells and may be empty or show intraluminal eosinophilic secretions. Immunostains for laminin (**f**) and (**g**) collagen type IV highlight the basement membrane material within pseudolumens
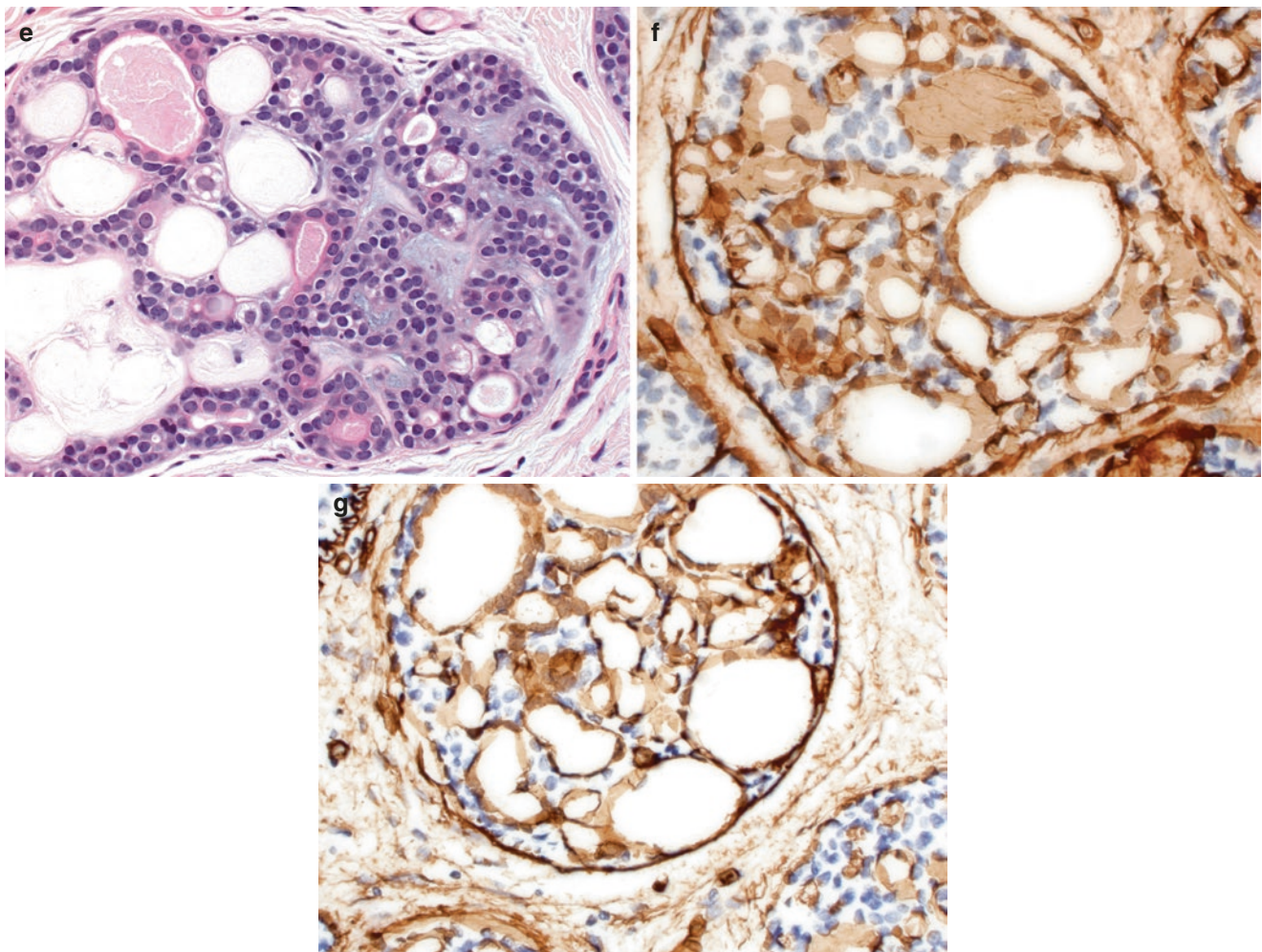
Fig. 12.4 (continued)

cinoembryonic antigen (CEA) [31] (Figs. 12.9c, 12.12f, 12.13c, and 12.14e). The basaloid cells in the SB-AdCC are often diffusely CK7 positive, and p63 may be negative or only focally positive, sometimes at the periphery of the tumor nests [15, 18, 30] (Figs. 12.9f and 12.15c). Therefore, negative or minimal staining for myoepithelial markers in a tumor with basaloid features does not exclude the diagnosis of SB-AdCC [15]. The MYB transcription factor is expressed predominantly in the myoepithelial cells of classic AdCC and is often positive in the basaloid cells of SB-AdCC [18, 32] (Figs. 12.14f and 12.15e). MYB expression is typically diffuse and strong in SB-AdCC on CNB, whereas only peripheral tumoral staining may be seen in some excised tumors, which may be due to short protein half-life and incomplete formalin fixation [18, 33]. SOX10 is expressed by both epithelial and myoepithelial cells [34] (Fig. 12.15d).

Expression of CD117, a tyrosine kinase receptor, is identified in virtually all AdCC. CD117 reactivity is usually limited to the ductular epithelial cells but may exhibit a more diffuse pattern in some cases, especially in SB-AdCC [18, 22] (Figs. 12.8c, 12.13c, and 12.14e). Although CD117 expression is helpful in the diagnosis of AdCC, this marker is not specific for this tumor type. Despite a high level of protein expression, recurrent *KIT* gene aberrations have not been identified [31].

AdCC are usually negative for estrogen receptor (ER) and progesterone receptor (PR) and consistently lack HER2 protein overexpression and gene amplification [35]. However, a small subset of AdCC may be ER/PR positive [15, 29, 35]. A novel 36 kDa isoform of ER (ER-α36) has been detected in AdCC [36]. Androgen receptor (AR) is usually negative [37, 38].
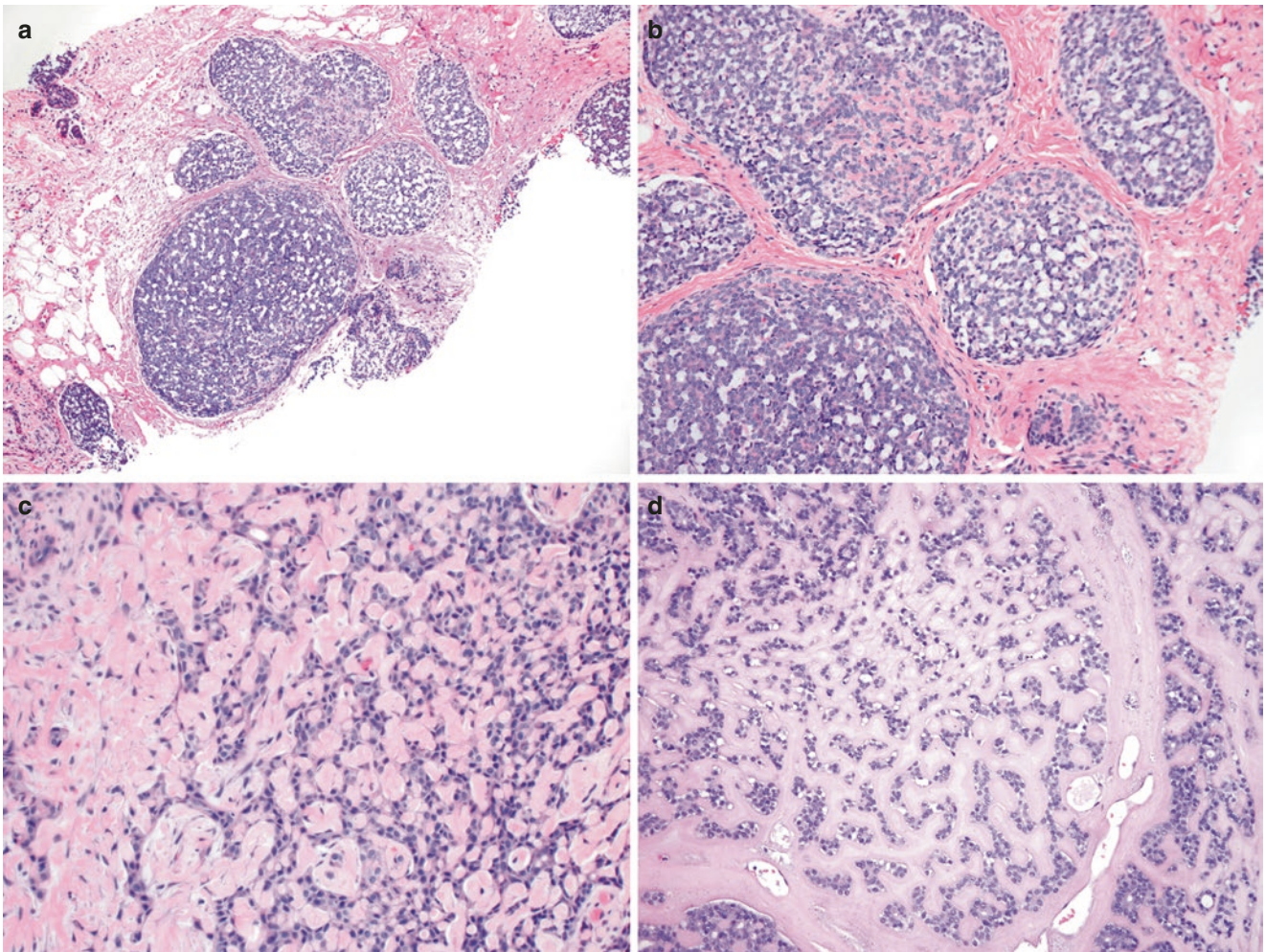
Fig. 12.5 Core needle biopsy of adenoid cystic carcinoma, reticular growth pattern. (**a–d**) The reticular growth pattern is characterized by neoplastic cells arranged as interconnected thin strands with associated myxoid or hyaline matrix. The matrix material may compress the glands

Although other TNBC generally have high proliferative activity, several studies have reported a low Ki-67 proliferation rate in classic AdCC (average ~5 to 10%) [18, 39, 40]. The SB-AdCC subtype, in agreement with increased mitotic count compared to classic AdCC, has a significantly higher Ki-67 proliferation index (average ~30%) [17, 18] (Fig. 12.15f).

Differential Diagnosis

The differential diagnosis of AdCC depends largely on the growth pattern. Cribriform pattern AdCC can mimic and be confused with invasive cribriform carcinoma, cribriform ductal carcinoma in situ (DCIS), and collagenous spherulosis, especially in small tissue samples obtained by CNB

(Fig. 12.16a–f). The cribriform glands of invasive cribriform carcinoma are usually angulated, lined by a single population of luminal-type epithelial cells, and present within desmoplastic stroma. Luminal contents may contain calcifications and mucin. In contrast, cribriform AdCC demonstrates a dual cell population, with pseudolumens filled with basement membrane material. Immunophenotypically, invasive cribriform carcinoma is negative for myoepithelial markers and positive for ER and PR, whereas AdCC expresses at least some myoepithelial markers and is usually hormone receptor (HR) negative. Cribriform DCIS reveals a lobulocentric arrangement, with a single population of luminal-type epithelial cells comprising the proliferative component. Although myoepithelial cells are present in cribriform DCIS, they are limited to the periphery of the ducts and are not admixed with the epithelial cells as in AdCC. In
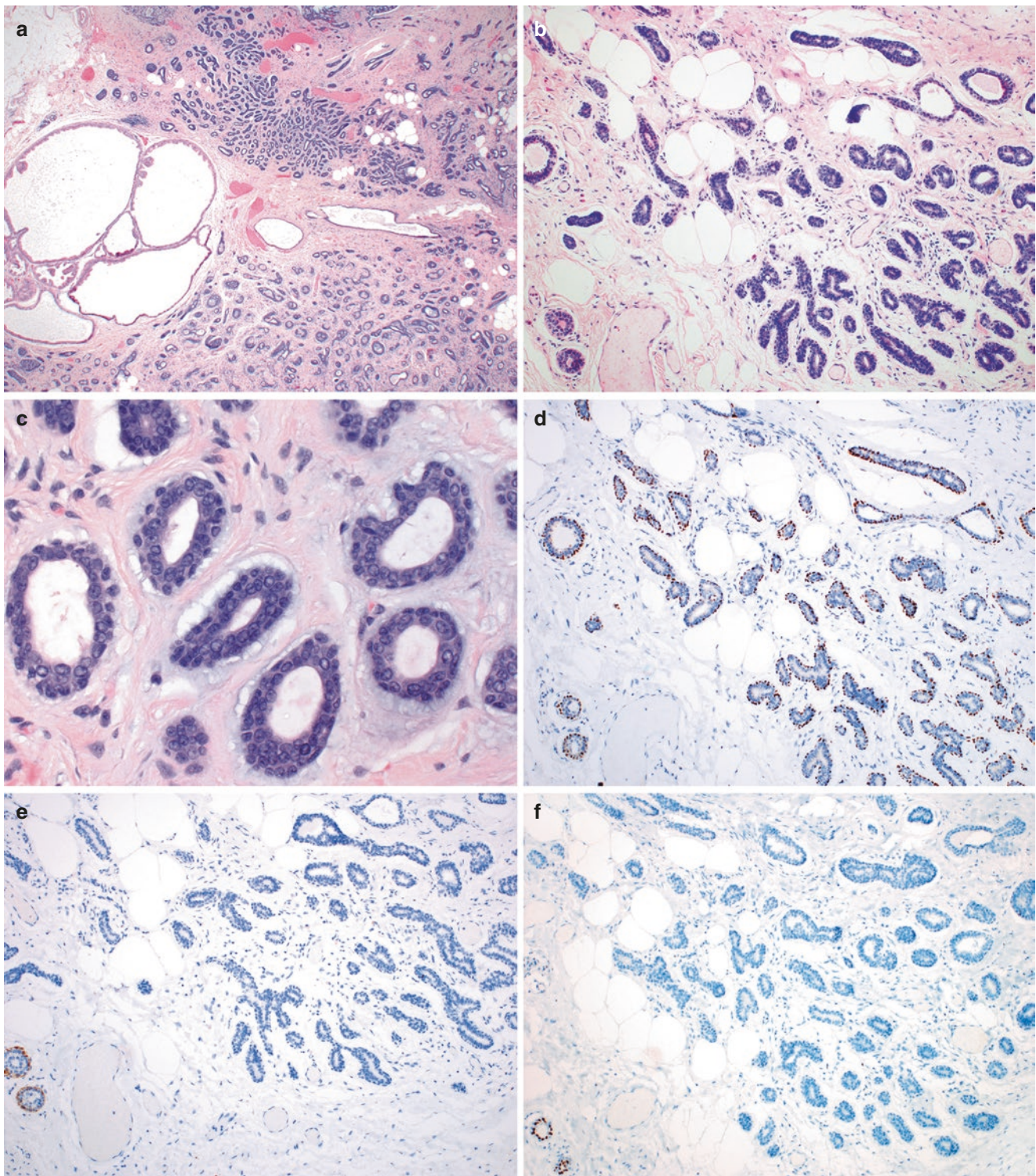
Fig. 12.6 Adenoid cystic carcinoma, tubular growth pattern. (**a**) The tubular growth pattern of AdCC demonstrates distinctly infiltrative ductules, (**b**, **c**) which on higher power are noted to be composed of luminal epithelial and abluminal myoepithelial cells. (**d**) The tubular glands show positive immunohistochemical staining for p63, which can be mistaken for a benign glandular proliferation such as a sclerosing lesion. Note the presence of two benign ducts in the lower left corner. Immunostains for other myoepithelial markers such as calponin (**e**) and SMM, and ER (**f**) are helpful in such cases, as calponin and SMM are usually negative in the neoplastic myoepithelial cells of AdCC but positive in myoepithelial cells associated with benign glandular lesions, while ER is negative in AdCC but patchy positive in benign glands
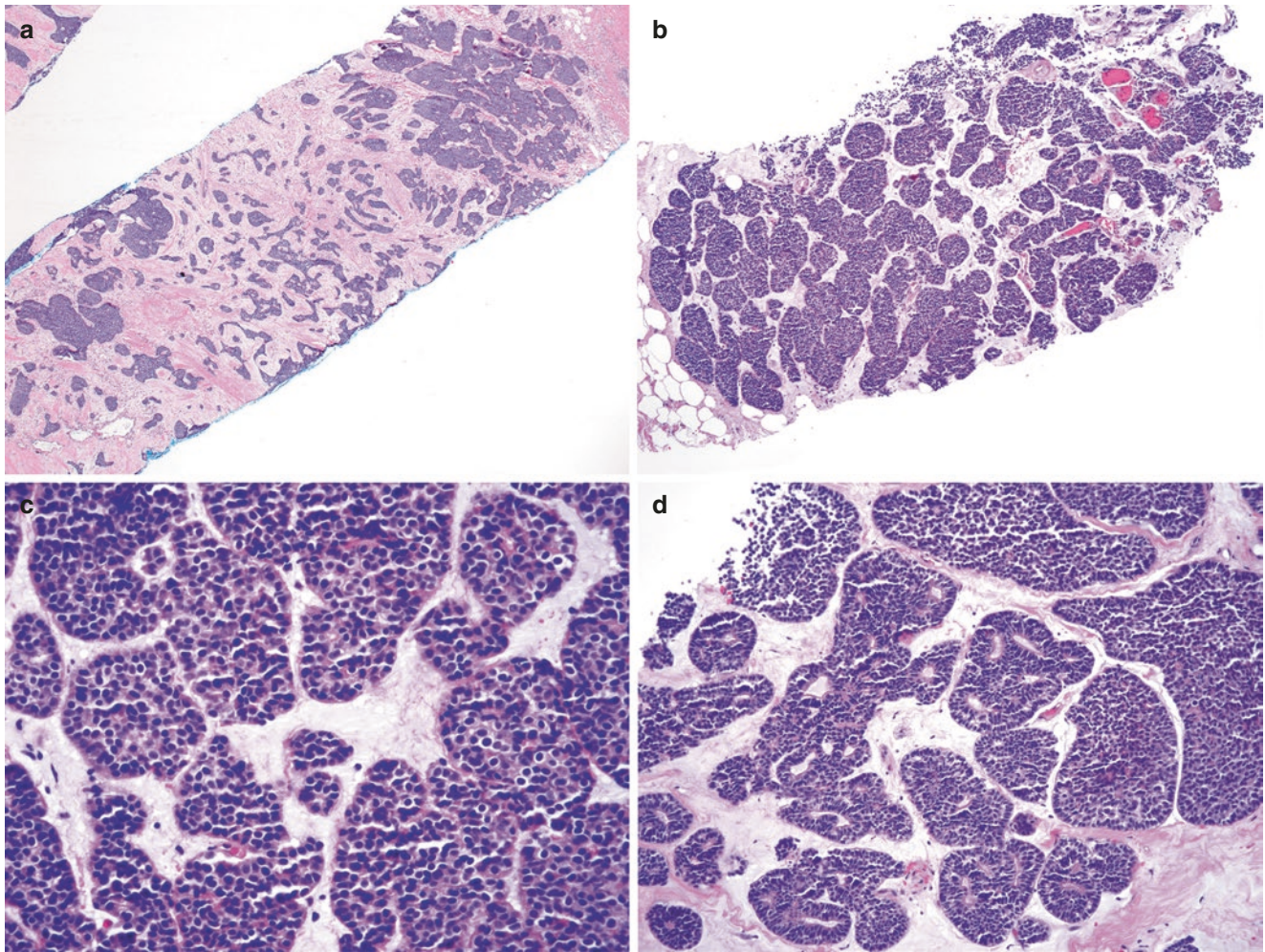
Fig. 12.7 Core needle biopsy of adenoid cystic carcinoma, solid-basaloid subtype. (**a**, **b**) Lower power view shows infiltrating irregular trabeculae and "geographic" solid nests in a hyalinized stroma. (**b**, **c**) Medium- and high-power views demonstrate solid nests of tumor cells with basaloid features. (**d**) Note the admixture of solid nests and focal cribriform growth in some areas

addition, cribriform DCIS is typically ER positive. CD117 immunoreactivity can be a helpful diagnostic adjunct in differentiating AdCC from invasive cribriform carcinoma and cribriform DCIS. The latter two cribriform lesions generally do not express CD117, as opposed to positive CD117 staining in most AdCC. However, it is important to note that lack of CD117 staining in a CNB does not necessarily exclude the cribriform pattern of AdCC, because CD117-positive ductular cells may be sparsely present. The distinction of AdCC from collagenous spherulosis may be challenging due to the biphasic nature of the epithelial–myoepithelial proliferation, the presence of true glandular and pseudolumens, and the accumulation of myxoid material and eosinophilic spherules shared by both lesions. However, collagenous spherulosis is a benign entity confined to preexisting ducts, lobules, or proliferative lesions and is not infiltrative. Furthermore, although

both lesions demonstrate p63- and SMA-positive myoepithelial cells surrounding pseudolumens, the myoepithelial cells of AdCC often lack expression of SMM and calponin, whereas these markers are positive in the true myoepithelial cells of collagenous spherulosis (Fig. 12.16a–f). Figure 12.17 depicts a flow chart that is helpful in evaluating cribriform proliferations of the breast, and the characteristic immuno-profiles of these lesions are summarized in Table 12.1.

The tubular component of AdCC should be distinguished from tubular carcinoma, microglandular adenosis (MGA) and radial sclerosing lesion. Attention to the cellular components (single cell type versus biphasic epithelial-myoepithelial populations) and luminal contents (presence of basement membrane material) in conjunction with a selective panel of immunohistochemical markers are helpful to make the distinction, which are summarized in Table 12.2.
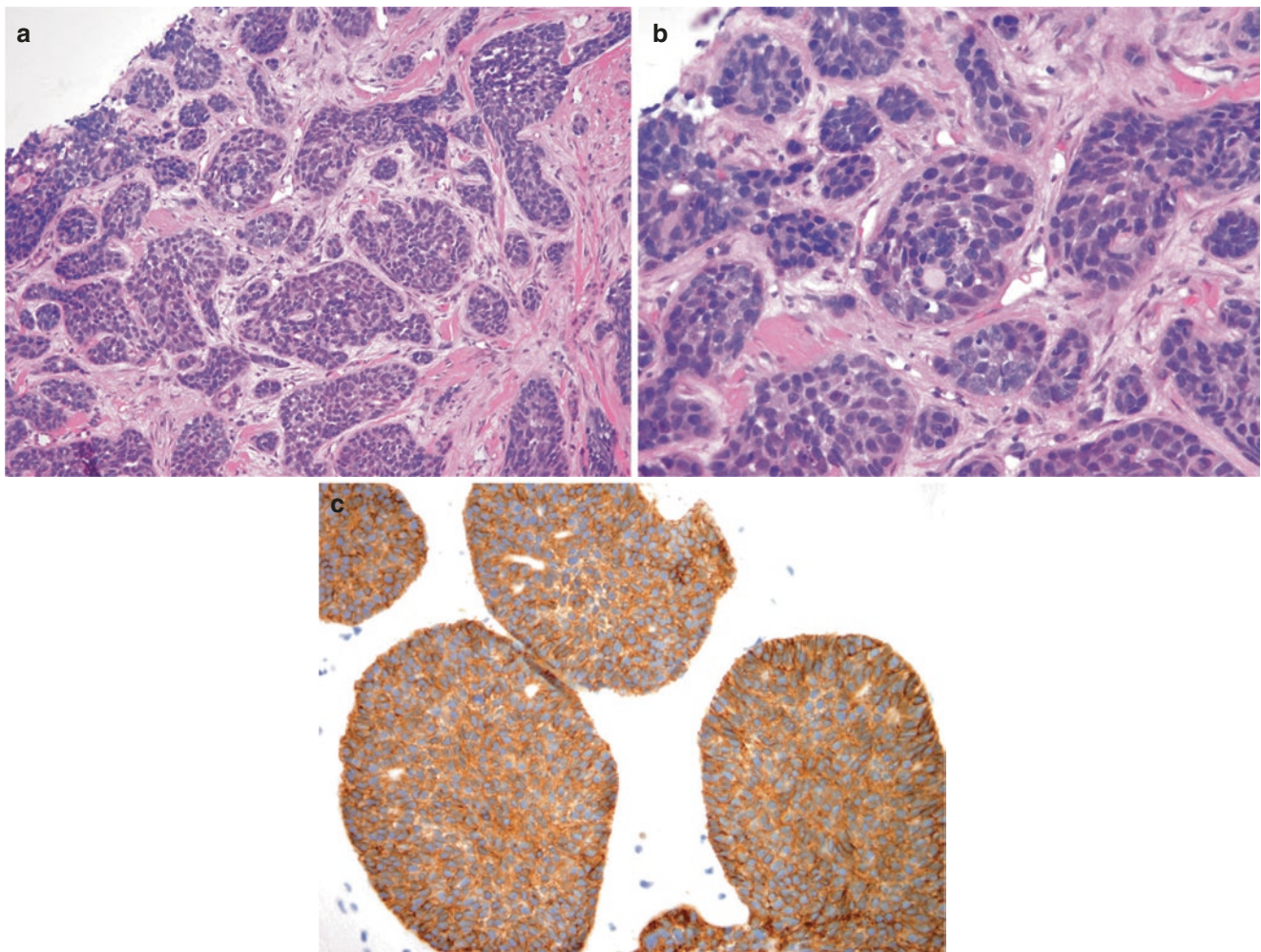
Fig. 12.8 Core needle biopsy of adenoid cystic carcinoma, solid-basaloid subtype. (**a**) High magnification reveals medium to large basaloid cells with scant cytoplasm, round to oval hyperchromatic nuclei, and inconspicuous nucleoli. The stroma is slightly desmoplastic in this case. (**b**) Note nuclear atypia is severe. (**c**) Diffuse positive immunostaining of the tumor cells for CD117

The main differential diagnosis for SB-AdCC includes high-grade IDC (especially tumors with basal-like features), small cell carcinoma (primary and metastatic), solid papillary carcinoma, Merkel cell carcinoma, lymphoma, and cylindroma of the breast. High-grade IDC with basal-like features often demonstrate large necrotic or fibrotic foci, pushing borders, and/or a prominent lymphoplasmacytic infiltrate. Small cell carcinoma is distinguished from SB-AdCC by prominent nuclear molding, necrosis with frequent apoptotic bodies, and significantly higher mitotic activity and Ki-67 proliferative index. In contrast to SB-AdCC, neuroendocrine markers may be positive in small cell carcinoma and Merkel cell carcinoma, the latter of which typically also expresses CK20 and neurofilament. Identification of intercalated ducts in SB-AdCC may be useful. In most cases, immunostains will be required to help establish the correct diagnosis. Table 12.3 summarizes the immunohistochemical markers useful in the workup of lesions with solid and "basaloid" features.

Cylindroma of the breast (dermal analog tumor) is a rare benign tumor with eccrine phenotype that can be confused with SB-AdCC, especially in CNB, as both tumors have nodular and trabecular patterns, basaloid cells with admixed duct structures, and hyaline globules of basement membrane material. However, infiltrative growth, cytologic atypia, mitotic activity, and lack of continuous, thickened basement membrane around tumor cell nests in SB-AdCC can help to differentiate the two. In addition, AdCC may be associated with mucin production, a feature not observed in cylindroma [41, 42].

Pathogenesis and Risk Factors

Although the origin of AdCC of the breast has been debated, it is generally accepted that this tumor is likely derived from undifferentiated cells that have the capacity to differentiate toward ductal and myoepithelial lineages [15, 16, 43].
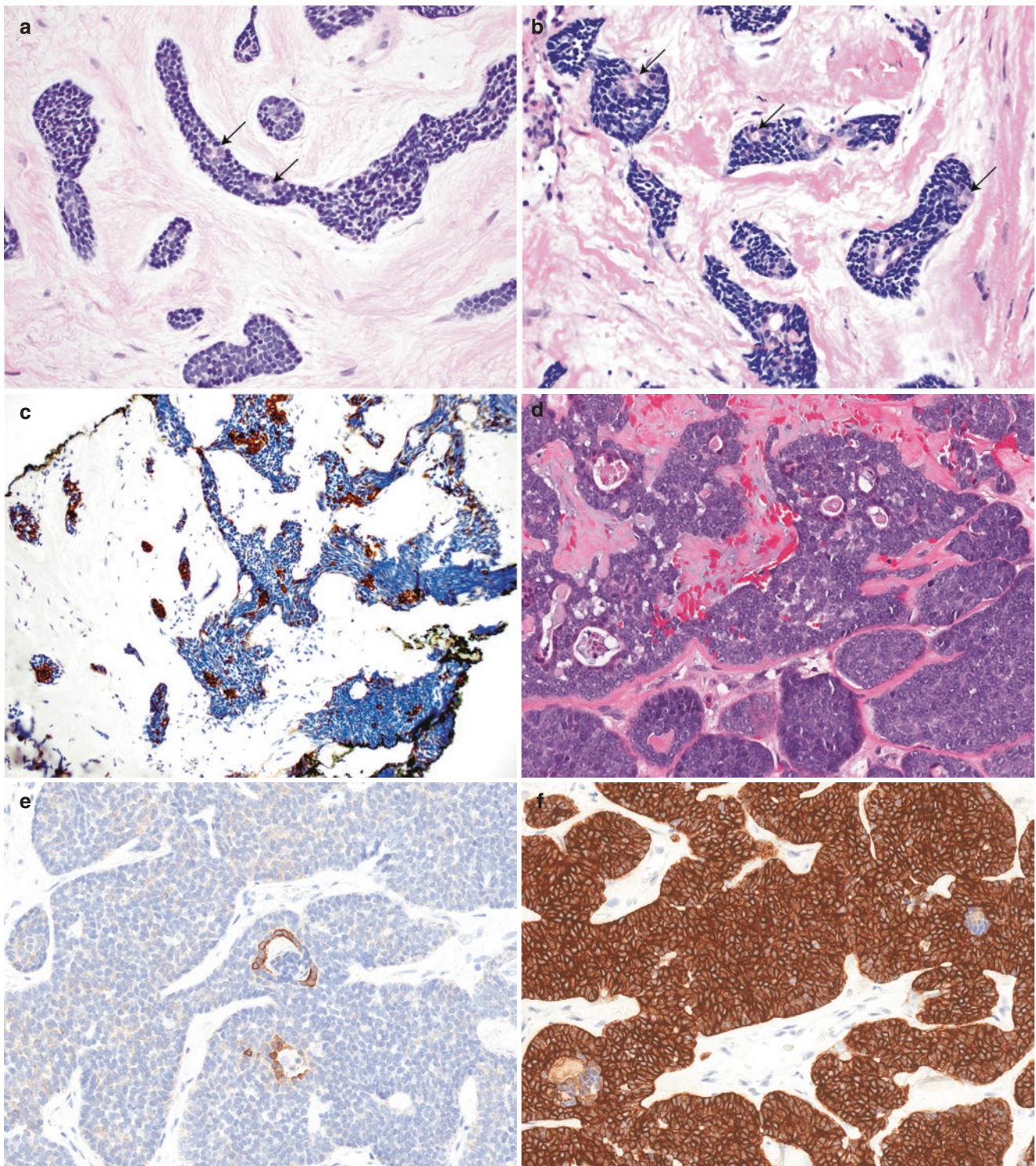
Fig. 12.9 Solid-basaloid subtype of adenoid cystic carcinoma, intercalated ducts. (**a**, **b**) Note slightly eosinophilic intercalated ducts subtly embedded within nests of dark basaloid cells. (**c**) CK7 highlights the glandular component and is negative in the basaloid cells. (**d–f**) Another example of SB-AdCC showing dispersed intercalated ducts within solid nests (**d**). The glandular component in this SB-AdCC is positive for CK5/6 (**e**) but negative for CK7 (**f**), while the basaloid cells are diffusely positive for CK7. These two examples illustrate that cytokeratin expression pattern is variable between different cases of SB-AdCC, likely reflecting the poorly differentiated state of the neoplastic cells
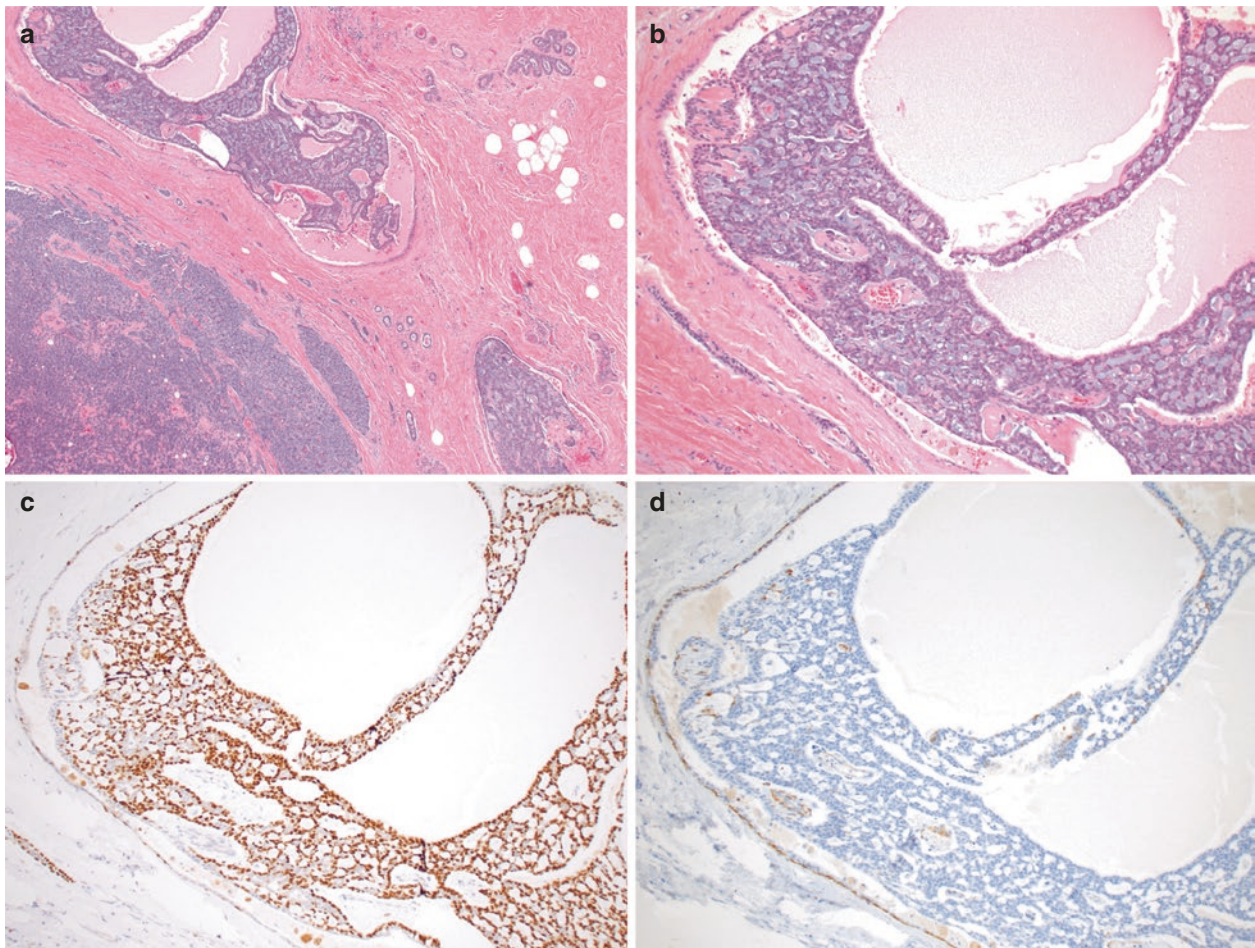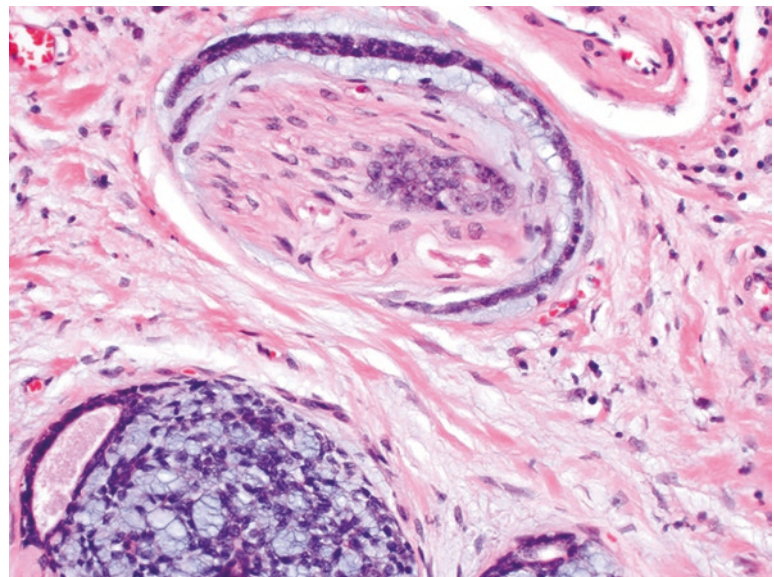
Fig. 12.10 Adenoid cystic carcinoma arising in association with intraductal papilloma. (**a**) This invasive AdCC (*lower left*) is arising in association with intraductal papillomas (*upper right*). (**b**) Higher power magnification demonstrates the typical biphasic epithelial and myoepithelial tumor cells of adenoid cystic carcinoma involving an underlying papilloma. Note the presence of residual papillary fibrovascular cores. (**c**) An immunohistochemical stain for p63 shows positive staining of the tumor cells and benign myoepithelial cells lining the periphery of the involved duct. (**d**) In contrast, an immunohistochemical stain for SMM is characteristically negative in the tumor cells but also highlights the benign myoepithelial cells of the involved duct

Fig. 12.11 Adenoid cystic carcinoma with perineural invasion. Similar to its counterpart in the salivary gland, albeit less frequently, AdCC of the breast can demonstrate perineural invasion and may be associated with clinical findings of a painful breast mass
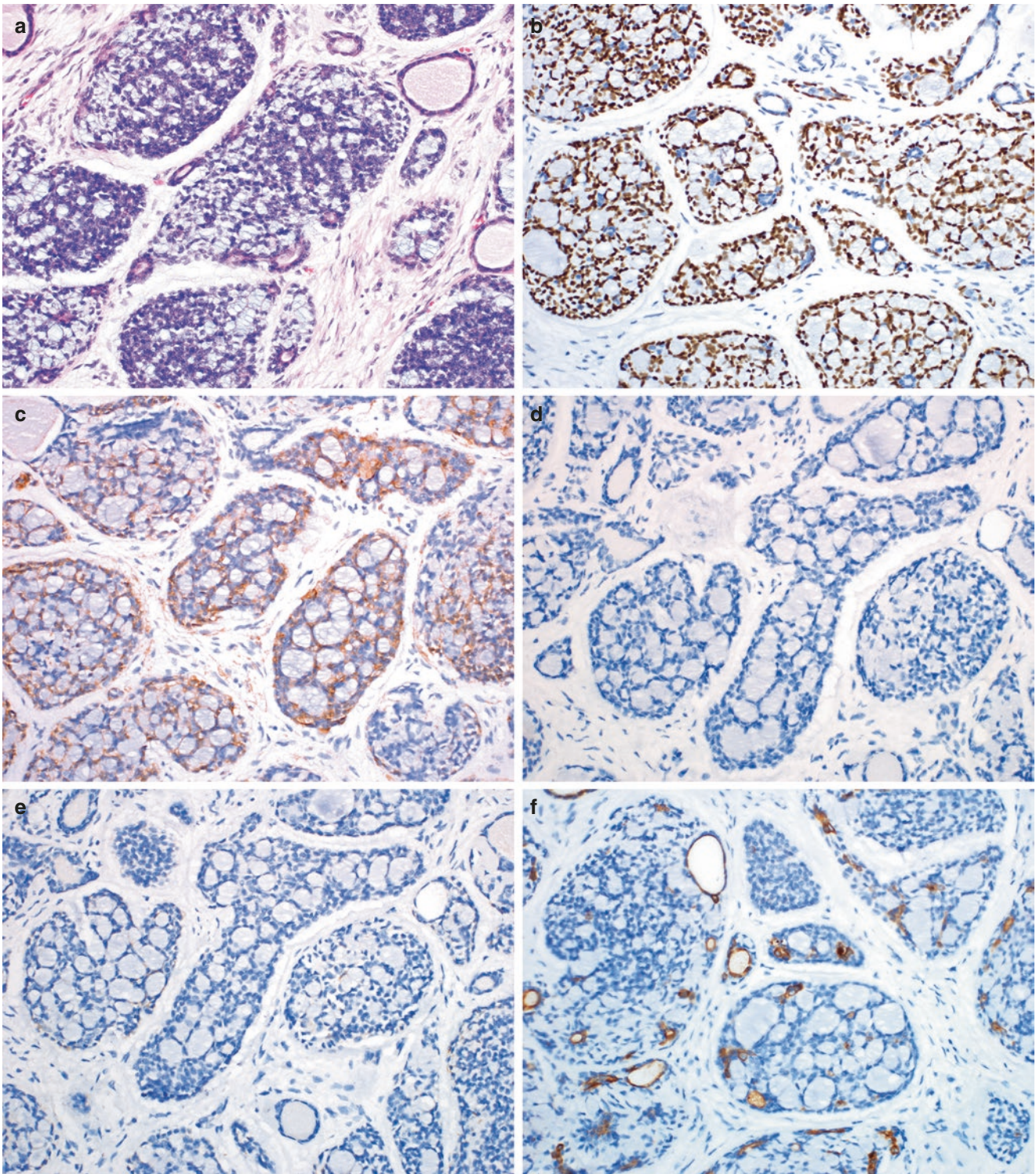
Fig. 12.12 Immunohistochemistry highlights the dual neoplastic cell populations in adenoid cystic carcinoma. (**a**) The neoplastic myoepithelial cells are immunopositive for (**b**) p63 and (**c**) SMA but are negative for (**d**) SMM and (**e**) calponin. In contrast, the neoplastic epithelial cells are decorated by (**f**) CK7
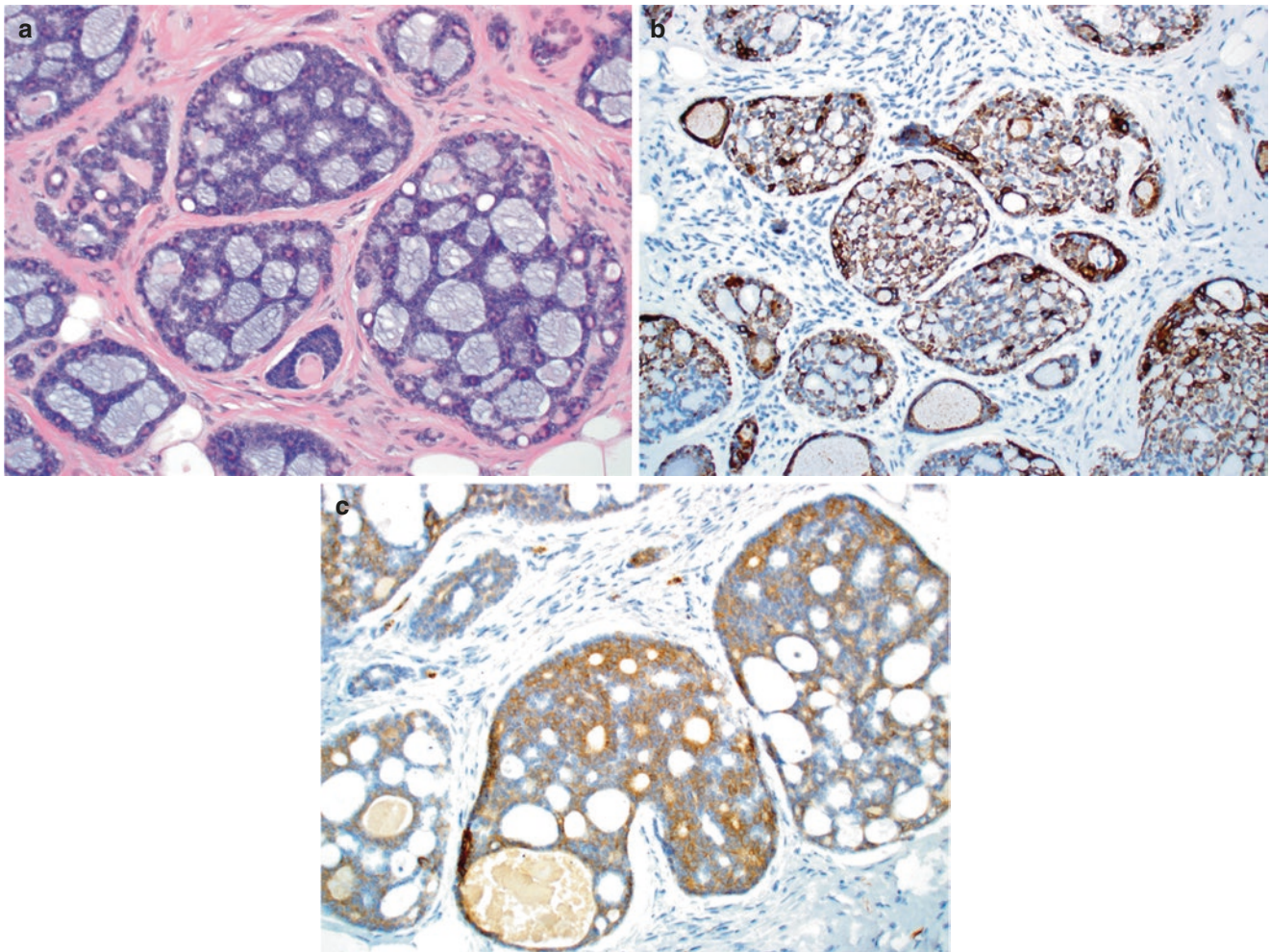
Fig. 12.13 Immunohistochemistry reveals a basal-like phenotype in AdCC. (**a**) This cribriform AdCC shows easily identified dual tumor cell populations. (**b**) The basaloid cells are typically immunoreactive for high-molecular-weight cytokeratins, such as CK5/6. (**c**) The basal marker CD117 is positive in most AdCC, often preferentially staining the luminal epithelial cells, as seen in this example

Similar to its counterpart at other anatomic sites, most classic AdCC of the breast harbor a t(6:9)(q22–23:p23–24) chromosomal translocation, which results in an expressed *MYB-NFIB* fusion gene [30, 44–46]. The fusion is thought to upregulate *MYB* RNA and MYB protein by removing microRNA binding sites in the *MYB* 3′ untranslated region or by super enhancer translocation [44]. The prevalence of *MYB-NFIB* is reported to be 33–100% in AdCC of the breast [39, 44, 47]. Alternate genetic drivers in AdCC lacking the *MYB-NFIB* fusion gene include *MYB* amplification, deletion of downstream sequences harboring presumed *MYB* regulatory element(s), and rearrangements involving *MYBL1*, which encodes A-MYB, a protein sharing extensive homology with c-MYB (encoded by *MYB*) [48]. In contrast to TNBC of no special type, classic AdCC have simple genomes, a low exonic mutation burden, and absence of

PIK3CA and *TP53* mutations. Similar to salivary gland AdCC, classic breast AdCC harbor mutations in chromatin remodeling, cell adhesion, and canonical signaling pathway genes [45]. *MYB-NFIB* fusions are much less common (~13–19%) in SB-AdCC than classic AdCC [18, 30]. In contrast to classic AdCC and TNBC of no special type, SB-AdCC frequently harbor inactivating mutations in *CREBBP* and activating mutations in *NOTCH1* or *NOTCH2* [18]. SB-AdCC were also found to have less genomic instability and less frequent *TP53* mutations than TNBC of no special type [18]. The majority of AdCC (classic and SB-AdCC) express high levels of MYB protein, suggestive of a convergent phenotype in which activation of *MYB* and *MYBL1* and downstream targets can be driven by various mechanisms. Genetic analysis of AdCC with high-grade transformation is limited, but two tumors with transformation to high-grade TNBC were found
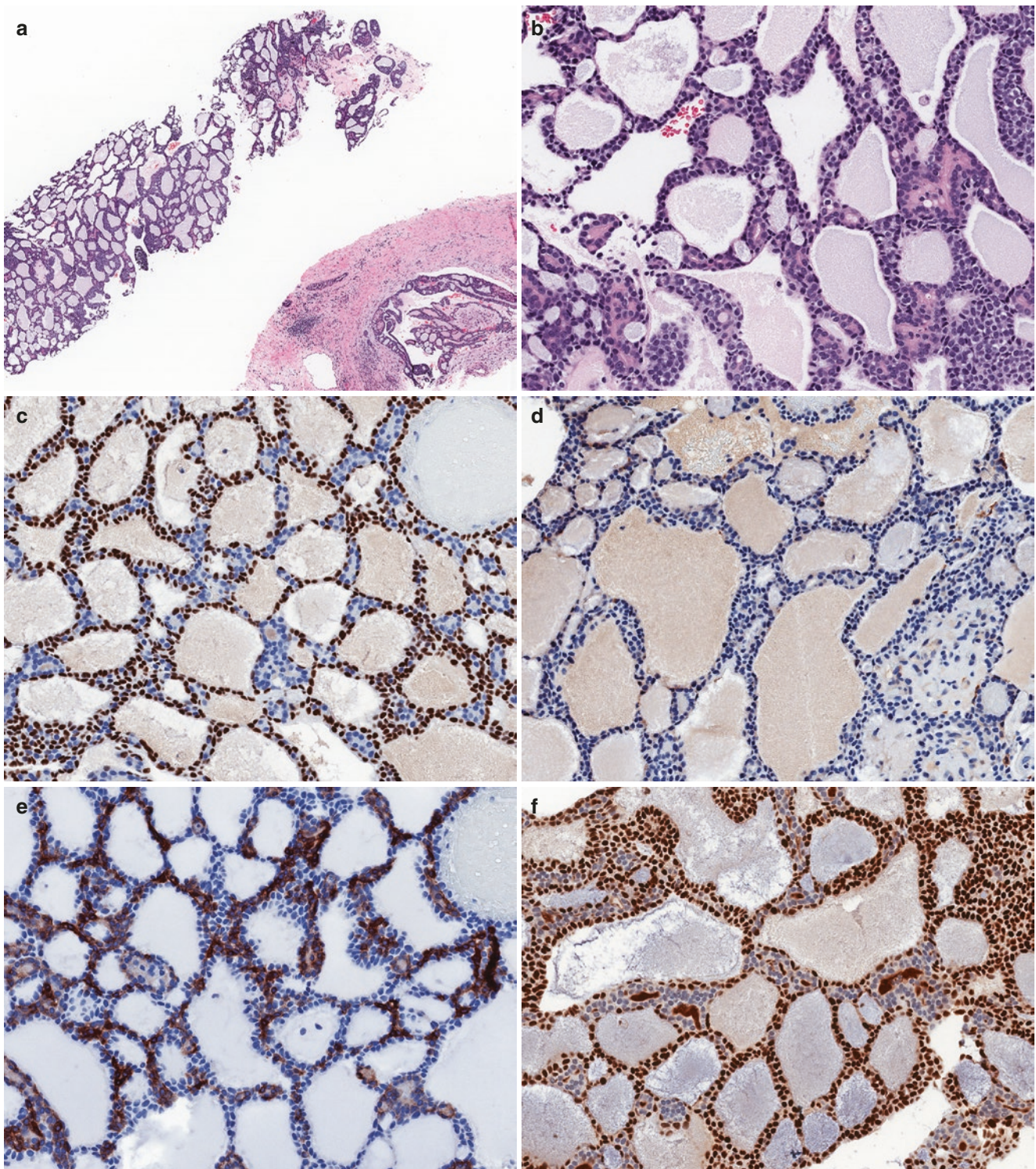
Fig. 12.14 Core needle biopsy of adenoid cystic carcinoma. (**a**) Low-power magnification shows an epithelial neoplasm arranged in cribriform growth pattern. (**b**) High magnification demonstrates dual neoplastic populations comprising basaloid cells surrounding larger lumens and slightly eosinophilic epithelial cells forming smaller lumens. Note the presence of lightly basophilic myxoid substance in the larger lumens. The basaloid cells are positive for p63 (**c**) and negative for calponin (**d**), while CD117 stain decorates the epithelial cells (**e**). The neoplastic cells show strong nuclear expression of MYB (**f**), predominantly in the basaloid cells. The morphologic features and immunophenotype support the diagnosis of AdCC, classic subtype
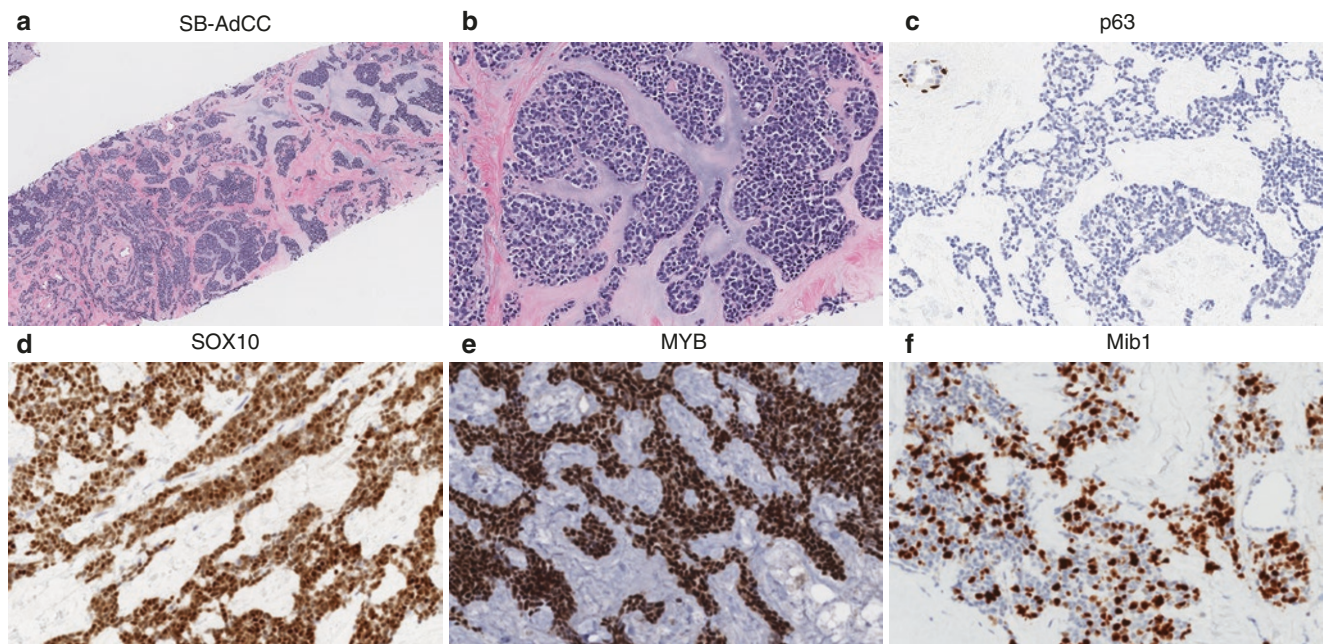
Fig. 12.15 Core needle biopsy of adenoid cystic carcinoma, solid-basaloid subtype. (**a**) Low-power view reveals an epithelial neoplasm infiltrating as irregular solid nests in a hyalinized and focally myxoid stroma. (**b**) High-power view demonstrates basaloid cells with high nuclear-to-cytoplasmic ratio and moderate to marked nuclear atypia. The neoplastic cells lack expression of myoepithelial markers p63 (**c**) and SMM (not shown) and are strongly positive for SOX10 (**d**) and MYB (**e**). The morphologic features and immunophenotype support the diagnosis of SB-AdCC. Note SB-AdCC has a higher Ki-67 proliferation index (**f**) than what is observed in classic AdCC

to harbor *MYB-NFIB* fusions in both the AdCC and high-grade TNBC components, with additional clonal aberrations in high-grade TNBC [20].

Because AdCC characteristically show MYB activation, MYB testing can be useful as a robust ancillary test in the workup of challenging cases where AdCC is included in the differential diagnosis. This includes (1) fluorescence in situ hybridization (FISH) using *MYB* break-apart probe, *MYB-NFIB* fusion probe, or *MYBL1* break-apart probe [30, 48] (Fig. 12.18a); (2) Next-generation sequencing, (3) detection of MYB protein overexpression by immunohistochemistry (Figs. 12.14f, 12.15e, and 12.18b) [18, 32, 48]; and (4) *MYB* RNA in situ hybridization (ISH) [49, 50]. FISH is very specific but least sensitive. Immunohistochemistry (with a positive result defined as strong staining in ≥50% tumor cells) is sensitive and readily available in many laboratories, but less specific. Immunohistochemistry is overall likely to be more useful in CNB than excision specimens due to poor staining in central areas of some excised tumors, which is likely related to fixation [18, 48]. In the salivary gland, *MYB* RNA ISH has been shown to provide superior sensitivity for the diagnosis of AdCC compared with *MYB* FISH and superior specificity compared with MYB immunohistochemistry [49].

AdCC displays a triple-negative and basal-like phenotype and clusters with basal-like breast cancers by gene expression profiling [37, 43, 51]. However, in contrast to other triple-negative tumors such as metaplastic carcinomas, AdCC forms a separate subgroup within the basal-like group by hierarchical clustering [37]. These findings further support the distinction of AdCC as a specific subtype of basal-like cancer. Some AdCC may belong to the claudin-low molecular subgroup, which is characterized by stem cell-like features and low expression of claudins, E-cadherin, and proliferation genes [31]. A characteristic CD44+/CD24—stem cell marker immunophenotype, which has been associated in some studies with tumor initiation, progression and survival and resistance to therapy, has been observed in AdCC [31, 52].

Prognosis and Clinical Management

Recognition of AdCC as a distinct subtype of TNBC is of clinical relevance due to the indolent behavior and excellent prognosis of classic AdCC [3, 4, 28]. Classic AdCC presents mostly as a localized disease (pathologic stage T1 or T2) with a low incidence of lymph node (0–5%) or dis-
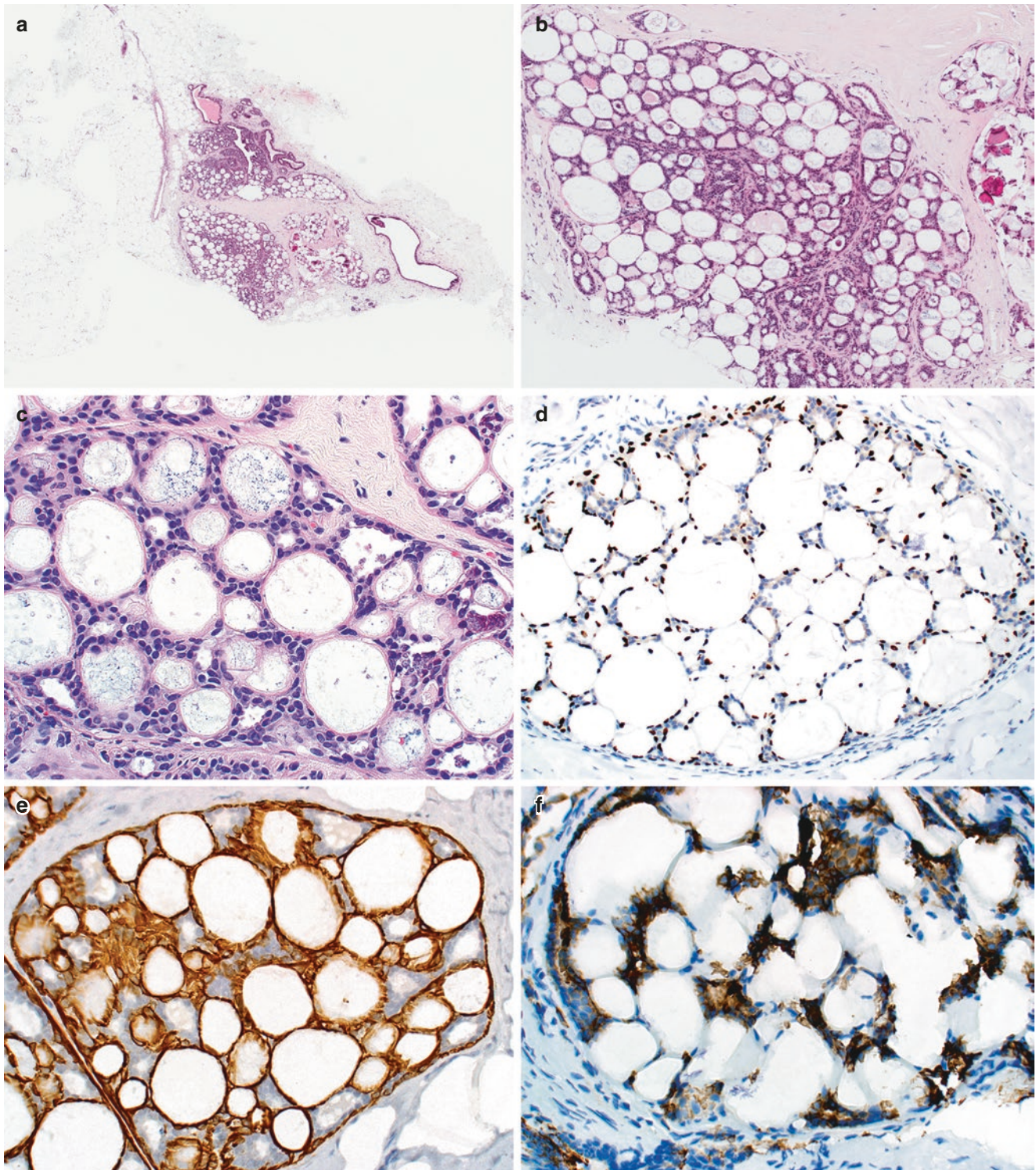
Fig. 12.16 Collagenous spherulosis (CS). (**a**, **b**) Core needle biopsy of CS, showing cribriform glands with associated calcifications. (**c**) The cribriform pattern with dual epithelial and myoepithelial cell populations and the presence of basement membrane material within pseudolumens can mimic the cribriform pattern of AdCC. Note the eosinophilic cuticles lining pseudolumens of CS, which are not a feature of AdCC. Immunohistochemical stains for (**d**) p63 and (**e**) SMM highlight the myoepithelial cells of CS, whereas neoplastic myoepithelial cells of AdCC are often negative for SMM. (**f**) The luminal epithelial cells of CS are immunoreactive for CAM5.2

tant (<3%) metastasis at the time of diagnosis [2, 51]. The most common sites of distant metastases are the lung and bone [2, 27, 53], in contrast to other TNBC, which frequently affect the brain and lung. At variance with TNBC

Fig. 12.17 Flow chart for cribriform proliferations of the breast

of no special type, which usually recurs within the first 3 years after diagnosis, AdCC can recur both locally and with metastatic disease many years after the initial presentation. However, even with local recurrence or distant metastases, these patients have a prolonged and indolent clinical course, with a 10-year survival of 90–100% [38, 53, 54]. Death from AdCC of the breast is extremely unusual [55]. The development of a second malignancy following the diagnosis of AdCC has been documented, and all patients should continue to be followed for this risk [2, 53, 56].

Limited data in the literature provide either no evidence or conflicting results on the prognostic value of histologic or nuclear grading and proliferative activity [16, 28, 29]. However, SB-AdCC appears to be associated with a more aggressive clinical course, with increased risk of axillary lymph node involvement and distant metastasis [17, 18, 30, 31]. Even with metastasis, patients with SB-AdCC may survive for an extended period, suggesting that this subtype is not as aggressive as high-grade TNBC of no special type.
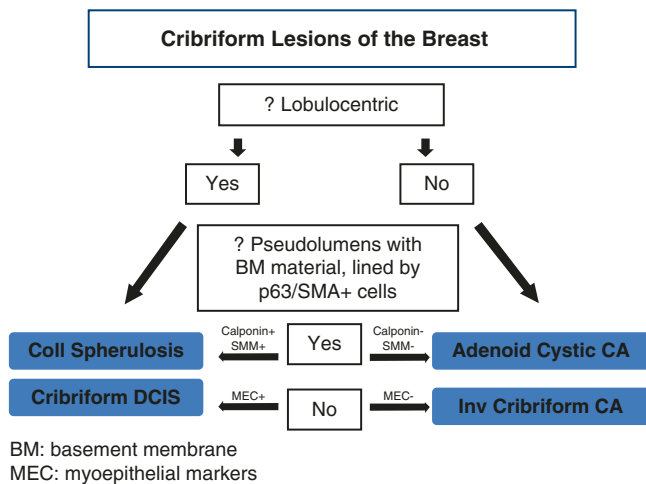
Table 12.1 Immunophenotype of cribriform breast lesions

Immunostain	AdCC	Invasive cribriform carcinoma	Cribriform DCIS	Collagenous spherulosis
p63 and SMA	Myoepithelial cells +	–	Periphery of duct +	Myoepithelial cells within and at periphery of duct +
Calponin and SMM	Usually –	–	Periphery of duct +	Myoepithelial cells within and at periphery of duct +
Low-molecular-weight keratins (CK7, CAM5.2)	Epithelial cells +	Diffusely +	Diffusely +	Epithelial cells +
CD117	+, Usually in epithelial cells	–	–	– To patchy + in epithelial cells
Estrogen receptor (ER)	Usually –	Diffusely +	Diffusely +	Epithelial cells patchy +

Table 12.2 Morphologic features and immunohistochemical markers helpful in the distinction of tubular variant adenoid cystic carcinoma from histologic mimics

Histopathologic features	AdCC (tubular variant)	Tubular carcinoma	Microglandular adenosis	Radial sclerosing lesion
Cell types	Epithelial and myoepithelial	Epithelial	Epithelial	Epithelial and myoepithelial
Luminal contents	True lumens: Mucin or eosinophilic secretions Pseudo lumens: Myxoid or hyalinized basement membrane material	+/− Calcifications	PASD-positive colloid-like eosinophilic secretions	+/− Calcifications
Immunohistochemistry for myoepithelial markers (p63, SMM, calponin, SMA)	Positive for p63 and SMA; often negative (or variable staining) for calponin and SMM	Negative for all myoepithelial markers	Negative for all myoepithelial markers	Positive for all myoepithelial markers (attenuation in some cases)
Estrogen receptor	Negative	Diffusely and strongly positive	Negative	Positive, patchy staining with variable intensity
Other immunohistochemical markers	Diffusely and strongly positive for MYB (predominantly in myoepithelial cells)		Strongly positive for S100 protein; negative for MYB	

Table 12.3 Immunohistochemical markers useful in the distinction of solid basaloid AdCC from histologic mimics

	Pankeratin	CK 7	CK 20	p63	TTF-1	NSE	SYN	CHROMO	LCA
SB-AdCC	+	+[a]	−	−/+[b]	−	−	−	−	−
Small cell carcinoma (primary)	+[c]	+	−	−	−/+	+	+/−	+/−	−
Small cell carcinoma (secondary from lung)	+[c]	−	−	−	+	+	+/−	+/−	−
Merkel cell carcinoma of the skin	+[c]	−	+	−	−	+	+/−	+/−	−
Lymphoma	−	−	−	−	−	−	−	−	+

[a] Positive in basaloid cells
[b] Often negative or only focally positive
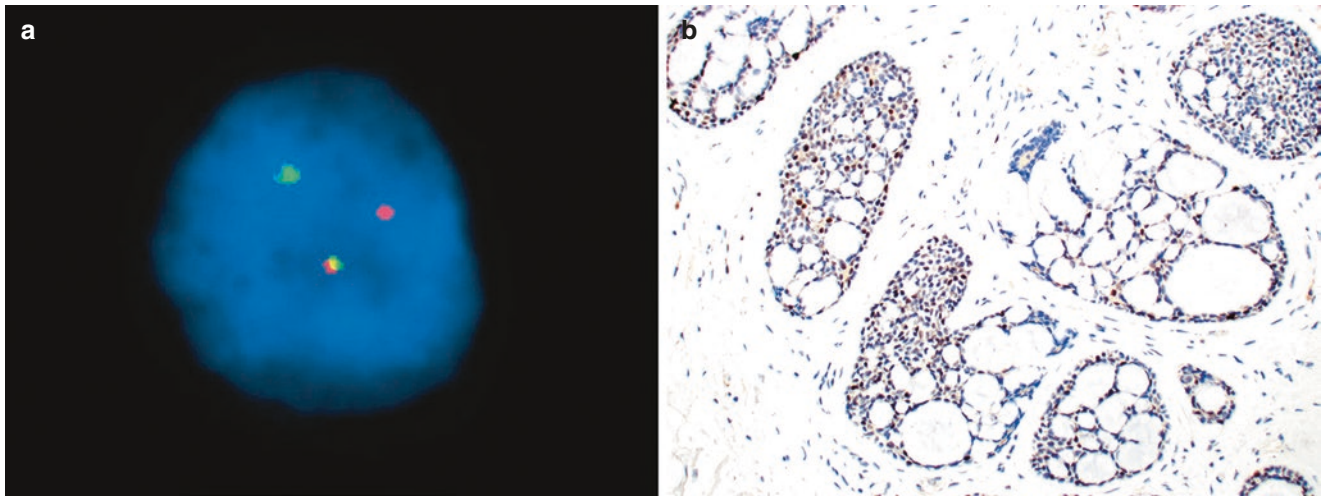[c] May be patchy and weak, with perinuclear dot-like pattern

Fig. 12.18 *MYB-NFIB* translocation and MYB protein overexpression in adenoid cystic carcinoma. (**a**) Fluorescence in situ hybridization demonstrates evidence of *MYB* rearrangement (*MYB* break-apart probe). (**b**) The *MYB-NFIB* fusion results in MYB overexpression, which is highlighted by MYB immunostaining in this example of AdCC

Due to the rarity of AdCC in the breast, there is no consensus on the optimal management of patients with these tumors [33]. Current treatment generally includes complete surgical resection with or without axillary sentinel lymph node sampling or adjuvant radiotherapy [29]. In one study, a high rate (42%) of positive surgical margins was observed after breast-conserving surgery [57]. Reported recurrence rates ranged from 6 to 37% after local excision only [26, 29, 53, 56]. A large study from the California Cancer Registry reported a significant benefit for adjuvant radiotherapy on overall survival and disease-specific survival in patients with AdCC [58], and some suggest that postoperative radiation should be considered for all patients after lumpectomy irrespective of margin status, given the high rate of positive margins after breast-conserving surgery [55, 59]. Most patients are not eligible for hormonal therapy due to negative hormonal receptor status. For most patients with classic AdCC, chemotherapy is likely not indicated [60]. More frequent axillary and distant metastases in SB-AdCC may suggest a role for chemotherapy in patients with this rare subtype, and most reported SB-AdCC cases in the literature have received chemotherapy. Given their frequency in SB-AdCC, activating *NOTCH* mutations could be a potential future therapeutic target [61].

Tall Cell Carcinoma with Reversed Polarity

Overview and Clinical Presentation

Tall cell carcinoma with reversed polarity (TCCRP) is a rare triple-negative invasive breast carcinoma with characteristic histologic and molecular features, an indolent clinical course, and favorable prognosis [62–66]. TCCRP was first described by Eusebi et al. [62] in 2003 as "breast tumor resembling tall cell variant of papillary thyroid carcinoma" because of its morphological resemblance to papillary thyroid carcinoma (PTC), with less than 100 cases reported in the literature since [62, 64–78]. This tumor has also been referred to as "solid papillary carcinoma with reverse polarity" [63] and "solid papillary carcinoma resembling the tall cell variant of papillary thyroid carcinoma" [62–64, 66,

79]. The fifth edition of the WHO classification of breast tumors has included TCCRP as a distinct type of invasive breast carcinoma [80].

TCCRP primarily affect patients in the sixth decade (range of 39–89 years, median age 64), with all reported cases having been in women [63–78, 81, 82]. TCCRP usually presents as a palpable and well-defined nodule that is occasionally tender to palpation [71], or less frequently as a screen-detected non-palpable lesion with associated microcalcifications [64, 68, 70–73, 75, 77, 78].

Gross and Radiologic Features

On gross evaluation, TCCRP usually appears as a well-circumscribed, firm, white to gray mass ranging in size from 0.6 to 8.5 cm, with an average of 2.6 cm [62, 66–69, 72, 75, 77, 78]. The cut surface is generally solid and grayish-white to tan in color [77]. A brownish, translucent, multinodular cut surface resembling hyperplastic thyroid tissue may occasionally be observed [67].

TCCRP is often interpreted as benign on mammography or ultrasound examination due to its circumscribed margins. On mammography, these tumors present either as a mass or pleomorphic calcifications [68, 77]. On ultrasound, they can appear either as a round, mildly hypoechoic mass with microlobulated margins without acoustic shadowing [68, 70] or a well-circumscribed, hypoechoic mass with mixed posterior shadowing and enhancement and increased vascularity [77].

Microscopic Features

TCCRP has distinct morphology with cytoarchitectural features analogous to the tall cell variant of PTC. At low power, most tumors have overall pushing margins (Fig. 12.19a); however, focal infiltrative growth into fat and entrapment of benign glands can usually be appreciated on closer evaluation, which may help suggest an invasive process, especially in a CNB specimen [63, 64, 78] (Figs. 12.19b and 12.20). The tumor is composed of multiple circumscribed nests and nodules of epithelial cells haphazardly distributed in stroma. In some cases, the cellular nests are arranged in a jigsaw pattern (Fig. 12.20). Many of the nodules are solid and contain thin papillae with delicate fibrovascular cores, creating a solid papillary pattern, whereas others are partly cystic with more conspicuous papillae, imparting a papillary appearance [62, 63, 65, 66] (Fig. 12.21a, c). Aggregates of foamy histiocytes are frequently present within the fibrovascular cores (Fig. 12.21b). Foci of cystically dilated glands or follicle-like structures containing eosinophilic amorphous colloid-like material with a scalloped periphery, reminiscent of a thyroid follicular pattern, can be seen in some tumors [64, 66] (Fig. 12.21d). The tumoral stroma is usually collagenous with little to no desmoplasia. Networks of small capillary-like vessels are present in a delicate garland-like fashion encircling the tumor nests [64, 83].

Cytologically, the tumor cells in TCCRP are cuboidal to tall columnar, usually with abundant granular eosinophilic cytoplasm (Fig. 12.22). Occasionally, the cytoplasm can be less granular but strongly eosinophilic [64]. The characteris-
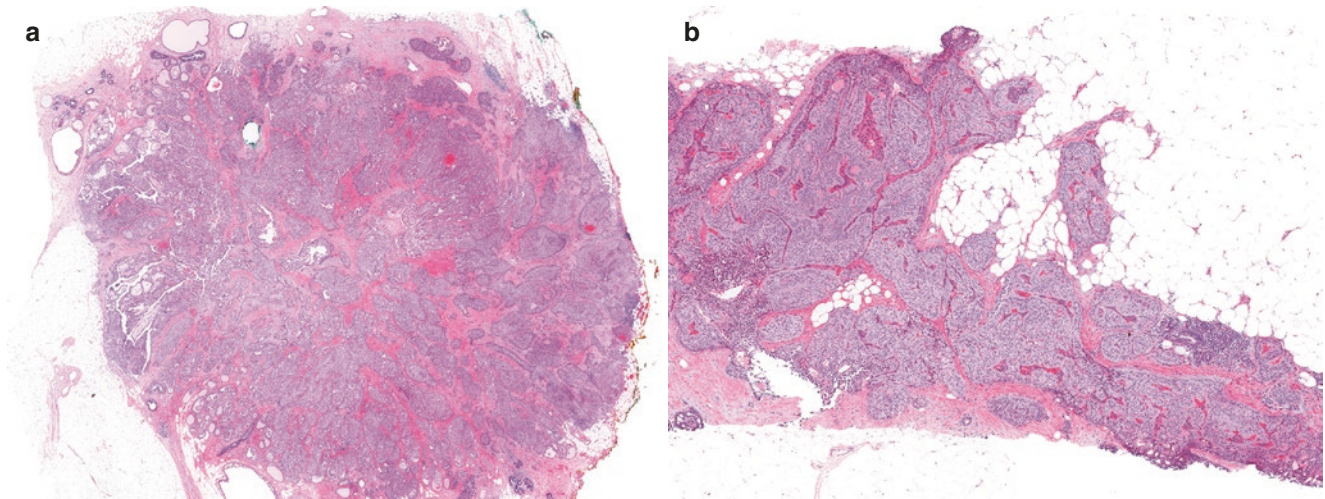
Fig. 12.19 Tall cell carcinoma with reversed polarity, tumor border. (**a**) Whole mount view of an excision for TCCRP demonstrates an overall circumscribed tumor with pushing margins that is often observed in this neoplasm. Note that the tumor is composed of multiple nodules and nests in the background of fibrotic stroma. (**b**) A CNB of TCCRP shows relatively circumscribed tumor-stroma interface, but with infiltration of tumor nests into fat
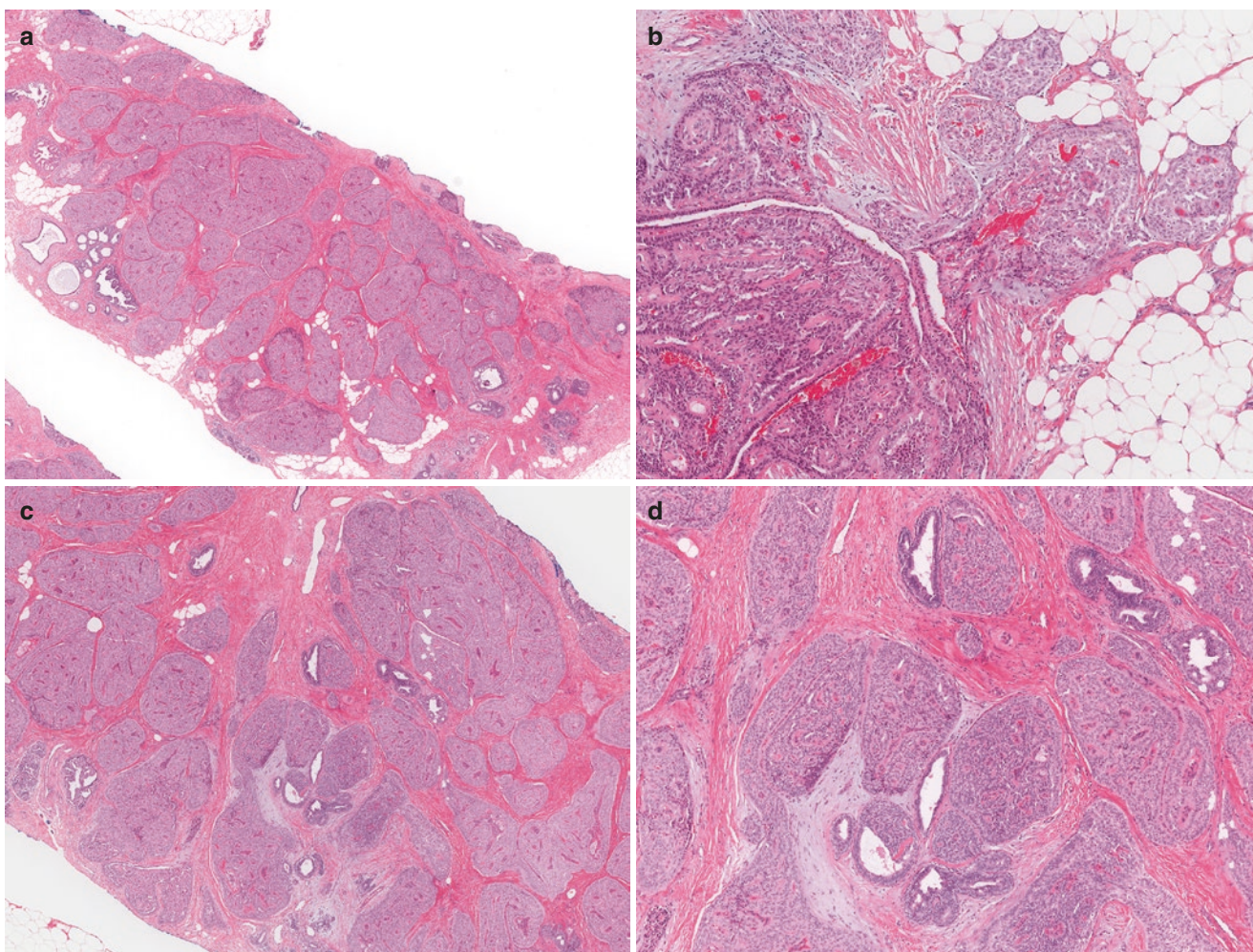
Fig. 12.20 Core needle biopsy of tall cell carcinoma with reversed polarity. (**a**) This example of TCCRP shows multiple solid circumscribed nodules haphazardly distributed throughout the breast stroma imparting a jigsaw pattern. (**b**) The presence of focal tumor nests in the fat raises the possibility of an invasive process in a CNB. (**c**) Low mag- nification demonstrates circumscribed solid papillary nodules growing around and between normal ducts, suggesting an invasive lesion. (**d**) Higher magnification further highlights normal ducts between tumor nodules. The stroma of TCCRP is typically collagenous and fibrotic, but may rarely show focal desmoplasia (lower central field)

tic cytoplasm has been shown to reflect the presence of abundant mitochondria using an anti-mitochondrial antibody [62, 66]. The neoplastic cells have round to oval, low- to intermediate-grade nuclei that often exhibit optical clearing, nuclear grooves, stratification, and cytoplasmic pseudoinclusions [62–65, 72, 78], similar to the nuclei of PTC (Fig. 12.22c). The most distinguishing cytologic feature is reverse polarization, with the nuclei localized to the apical or adluminal, rather than at the basal, pole of the columnar tumor cells [62–65, 72, 77] (Fig. 12.22d–f). Psammoma bodies [77] or granular calcifications may be identified within the colloid-like material or associated with the proliferative epithelium [62, 64, 66, 68, 77]. Mitotic activity is generally low, and there is no necrosis, or vascular or perineural invasion. Areas of mucinous differentiation or apocrine metaplasia may rarely be present [77]. Using the Nottingham grading system, most tumors are histological grade 1, receiving 2 points for nuclear grade, 1 point for mitotic activity, and 2 points for glandular differentiation.

An in situ component has been described in some cases of TCCRP [66]. The distinction between in situ and invasive cancer can be challenging in tumors that are composed of well-circumscribed round nodules, but myoepithelial markers such as p63 and SMM are helpful [63, 64]. Foci of flat epithelial atypia (FEA) have been observed at the periphery of the tumor in a few cases [64].

Immunohistochemistry

TCCRP typically shows strong and diffuse cytoplasmic expression for low-molecular-weight keratins (LMWCK,
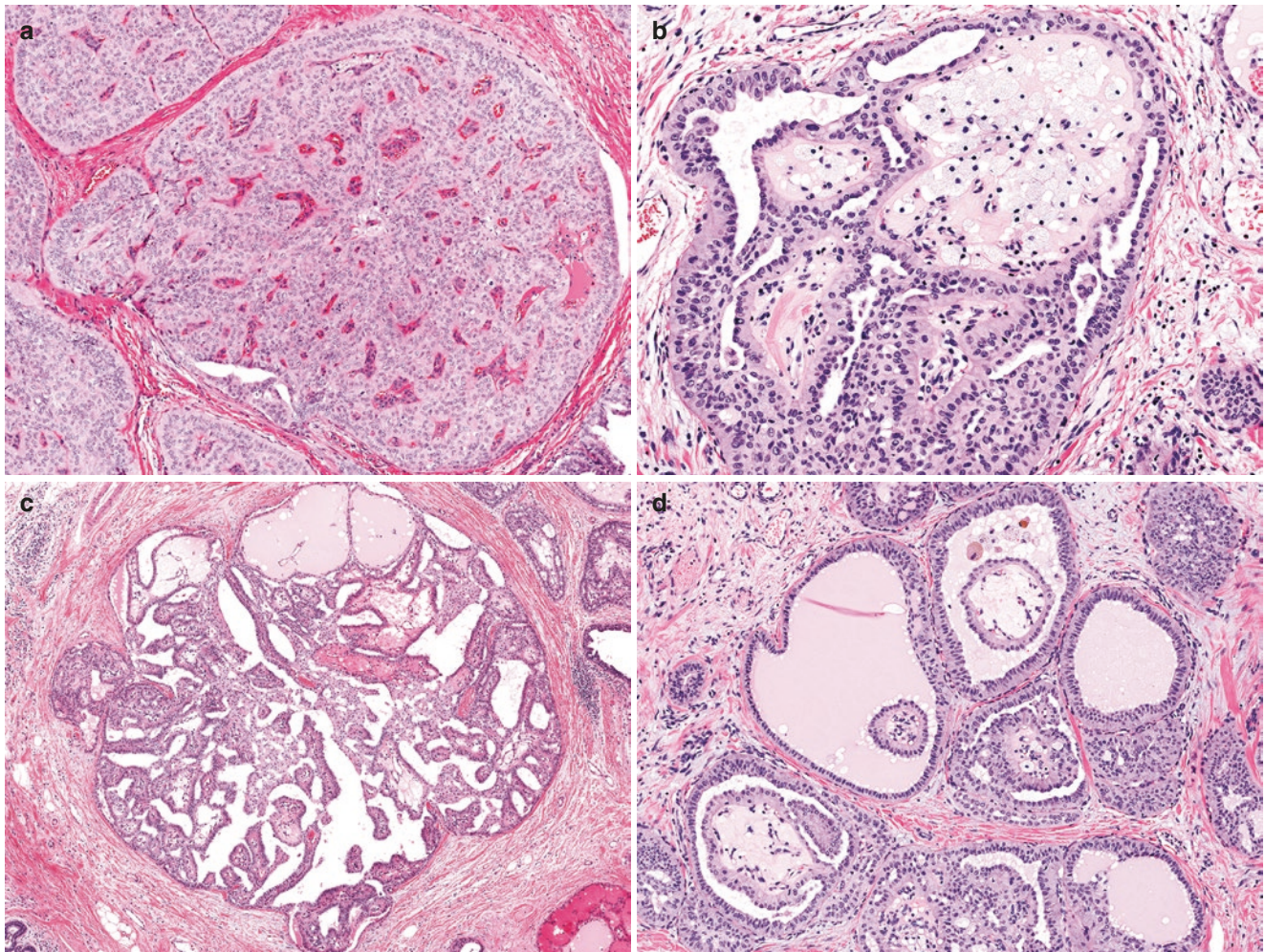
Fig. 12.21 Tall cell carcinoma with reversed polarity, architectural patterns. Tumor cells in TCCRP can be arranged in various growth patterns. (**a**) A major pattern is characterized by solid nodules containing thin papillae with delicate fibrovascular cores, imparting a solid papillary appearance. (**b**) The fibrovascular cores of tumor nodules often contain aggregates of foamy histiocytes. (**c**) Some tumor nodules are partly cystic with more conspicuous papillae, creating a frankly papillary appearance. (**d**) A follicular pattern features cystically dilated glands containing eosinophilic colloid-like material with a scalloped periphery, resembling thyroid follicles

e.g., CK7, CK19) and HMWCK (e.g., CK5/6, CK14 and CK34bE12) [62, 64, 66, 76] (Fig. 12.23). The tumor cells are also immunoreactive for calretinin (diffuse or focal), S100 protein, mitochondrial antigen (accentuated at the basal pole), CEA, and BCL-2 [64, 65, 69, 71]. Despite the morphologic resemblance to PTC, TTF-1, thyroglobulin, and HBME 1 are negative [70, 76, 77]. Breast origin is confirmed by variable staining for GATA3, mammaglobin, and GCDFP-15 (Fig. 12.23f, g), which are positive in ~60% of cases [64, 71, 75, 76].

E-cadherin stain shows strong lateral membrane expression with absent apical or basal expression, whereas MUC1 and EMA highlight localization of the nucleus to the apical aspect of the tumor cells (Fig. 12.23h), supporting the morphologic impression of reverse polarity [63]. No myoepithelial cells are identified along the fibrovascular cores or at the periphery of the papillary, solid, or follicular structures with immunohistochemical stains for p63, calponin, SMM, and CD10 [64, 65, 69, 71, 78] (Fig. 12.23b, c). The lack of a peripheral myoepithelial layer, together with the haphazard distribution of the tumor nodules and infiltrative growth, supports TCCRP as an invasive process.

TCRRPs are usually negative for ER and PR and consistently lack HER2 protein overexpression and gene amplification (Fig. 12.23i). However, a small subset of TCCRP may show weak and focal ER and PR expression in 1–10% of tumor cells [63, 66, 69, 77]. Most cases have either absent or low AR expression, arguing against apocrine differentiation [64, 82]. The Ki-67 proliferation index is low (Fig. 12.23j), ranging from 1 to 5% in most tumors [64, 65, 69, 71]. The rich capillary network around tumor nests can be highlighted by vascular markers, such as CD31, ERG, or CD34.

Antibodies against IDH2 R172 mutant proteins have been shown to be highly sensitive (>90%) and specific (100%) for
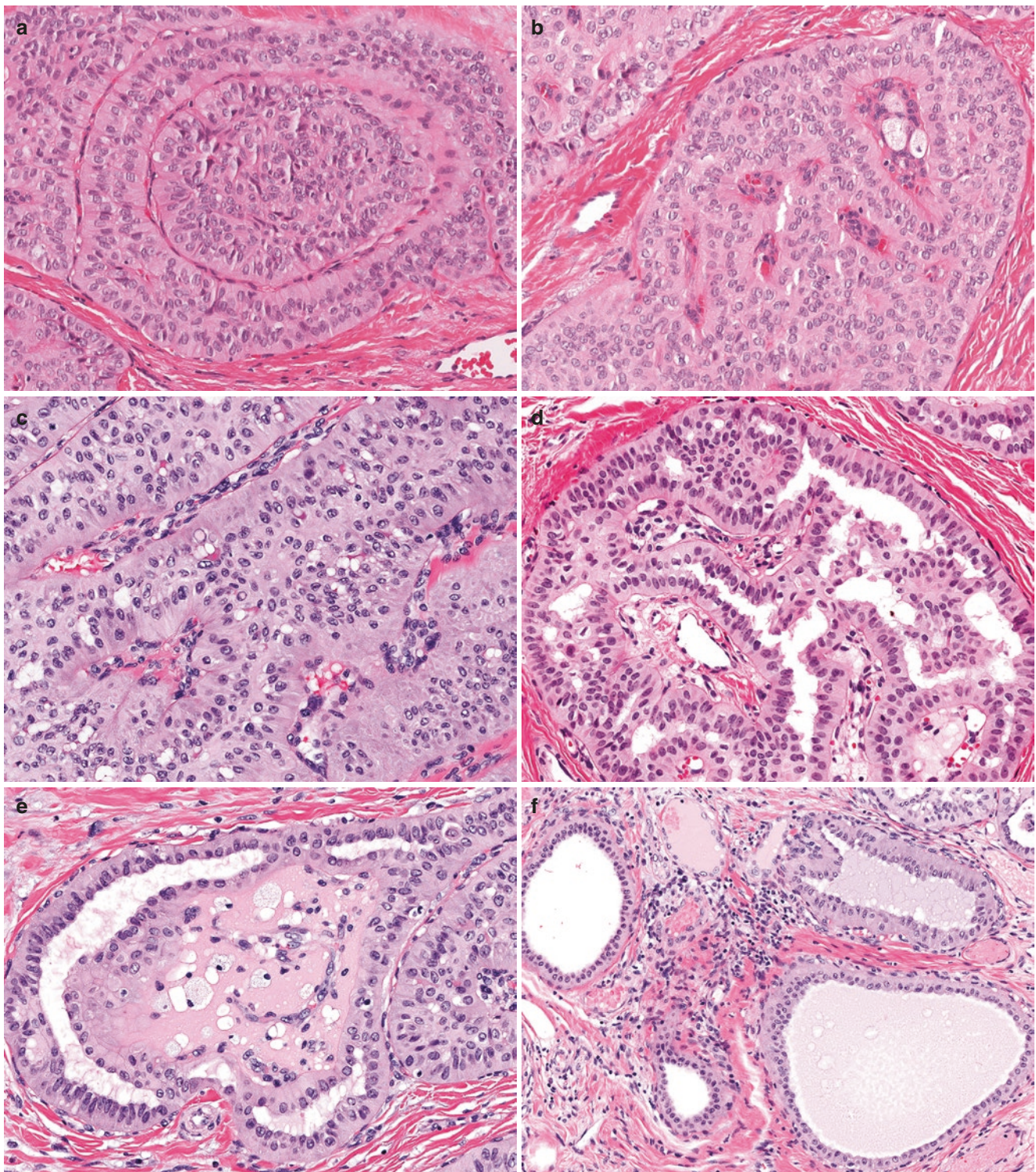
Fig. 12.22 Tall cell carcinoma with reversed polarity, cytologic features. (**a**, **b**) The tumor cells are tall columnar with abundant eosinophilic cytoplasm and low- to intermediate-grade nuclei. (**c**) The nuclei are crowded and overlapping and exhibit nuclear grooves with scattered cytoplasmic pseudoinclusions, features mimicking thyroid papillary carcinoma. (**d**–**f**) These images highlight the characteristic reverse polarization of TCCRP in which the nuclei are localized in the apical rather than at the basal poles of the neoplastic columnar cells

the detection of the *IDH2* R172 hotspot mutations in TCCRP, including in CNB [75, 82]. Using an antibody directed at IDH2 R172S, all tumors with either *R172S* or *R172T* muta-tions were found to be immunoreactive, showing diffuse and strong staining with a cytoplasmic granular pattern (Fig. 12.24). The single tumor in this study with *IDH2* R172I
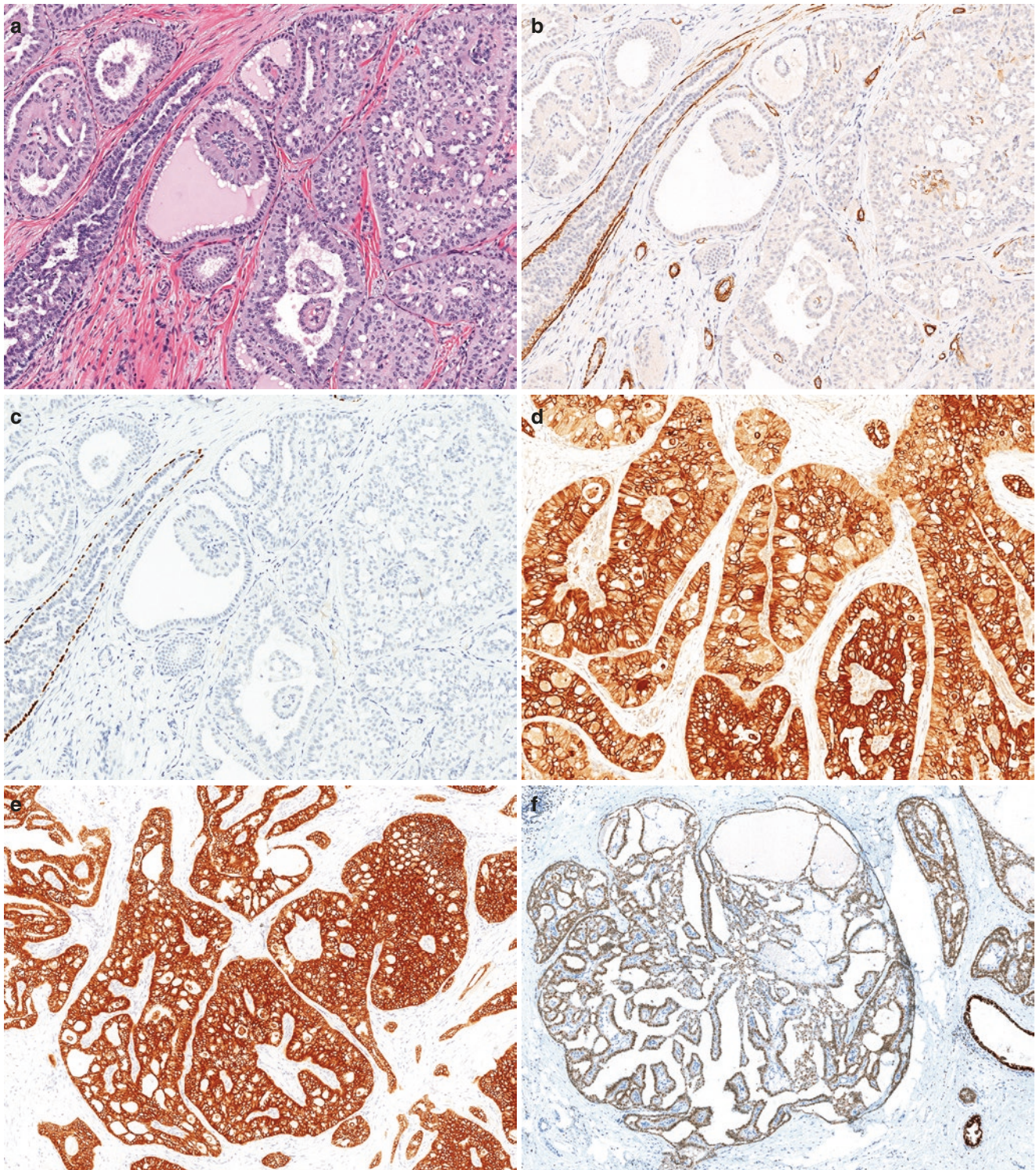
Fig. 12.23 Tall cell carcinoma with reversed polarity, immunophenotype. (**a–c**) Although the tumor nests are circumscribed with a rounded contour on H&E section (**a**), they lack an investing myoepithelial layer as shown by the SMM (**b**) and p63 (**c**) immunostains, supporting the invasive nature of TCCRP. Note the absence of myoepithelial cells both at the periphery of the tumor nodules and along all the fibrovascular cores, while the entrapped benign ducts are positive for SMM and p63. The neoplastic cells demonstrate diffuse and strong expression of both HMWCK CK5/6 (**d**) and LMWCK CAM5.2 (**e**). Breast markers GATA3 (**f**) and mammaglobin (**g**) are variably positive in the tumor cells. (**h**) An EMA immunostain decorates the apical side of the columnar cells where the nuclei are situated, confirming the reversed polarity of TCCRP. (**i**) The majority of these tumors are negative for ER (note positive staining in the entrapped normal ducts), PR (not shown), and HER2 (not shown). (**j**) The Ki-67 proliferation index is low
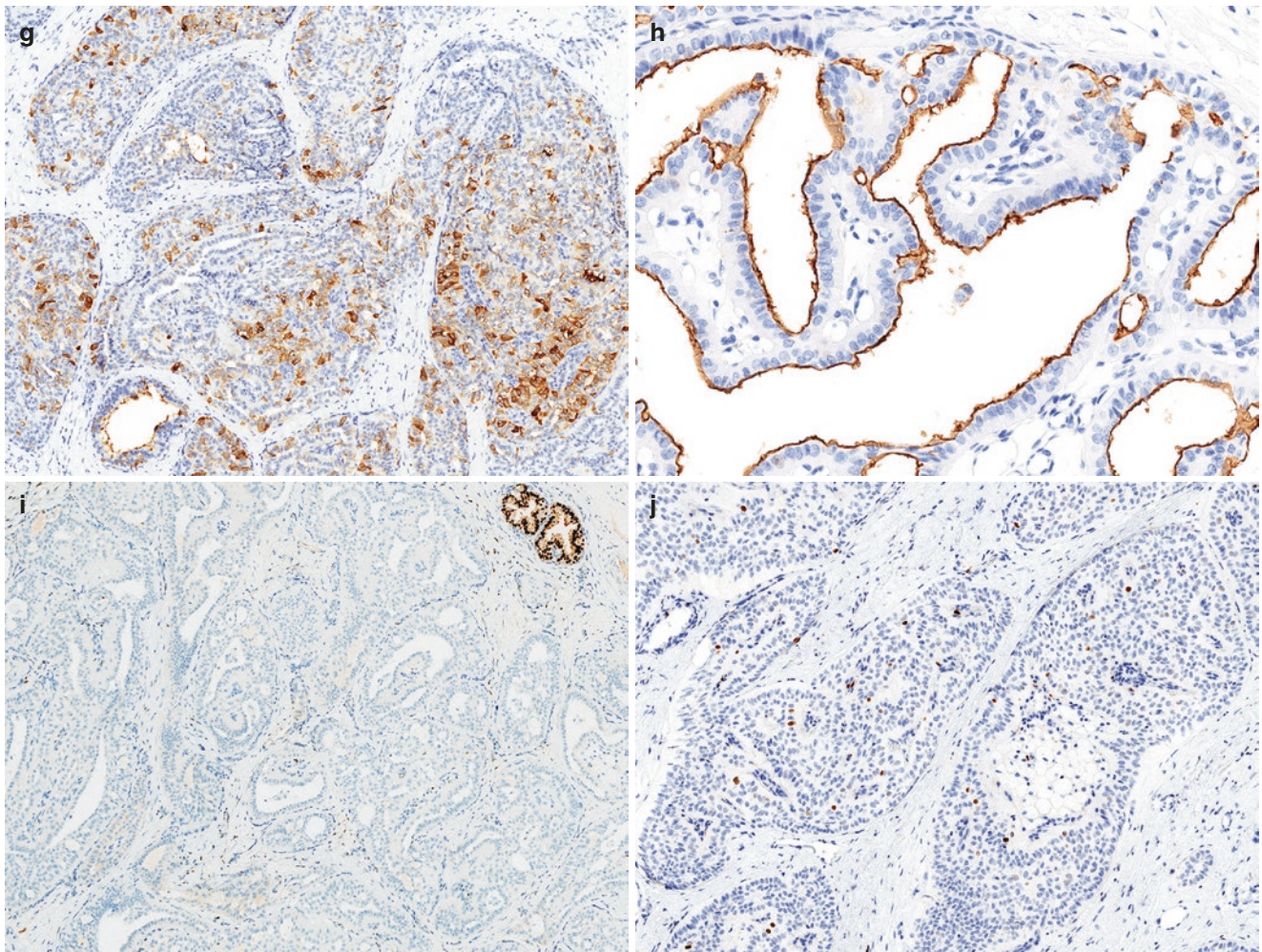
Fig. 12.23 (continued)

mutation was negative [82]. In another study, an antibody recognizing IDH2 epitopes R172A/C/D/E/G/L/Q/S/Y (MsMab-1) showed strong and diffuse immunopositivity in 6 of 7 TCCRP with *IDH2* mutations (R172G and R172S), with another tumor harboring an R172T mutation showing weak staining [75]. Other papillary neoplasms and all conventional TNBC tested in these studies were negative, with the exception of weak staining (H-score ≤ 40) in 3 non-TCCRP papillary lesions with MsMab-1 [75, 82]. Immunohistochemistry with IDH2 R172 mutation-specific antibodies can therefore be useful as a surrogate for genetic analysis or to triage tumors for sequencing of the *IDH2* R172 hotspot locus [75, 82], with the caveat that TCCRP with some less common *IDH2* R172 mutations may be negative with one or the other antibody, and tumors lacking *IDH2* mutations will be missed [63]. Accordingly, the diagnosis of TCCRP should not be excluded in cases displaying the unique histopathologic features of this entity if IDH2 R172 immunohistochemistry is negative.

Differential Diagnosis

Other papillary lesions of the breast: Due to its rarity, papillary architecture and unusual immunoprofile, TCCRP may be confused with other more common benign or malignant papillary neoplasms of the breast, especially in limited CNB material. These lesions include intraductal papilloma with usual ductal hyperplasia, solid papillary carcinoma (SPC), papillary pattern DCIS, and encapsulated papillary carcinoma (EPC) (Table 12.4). The cytologic features, including nuclear grooves and pseudoinclusions, and strong CK5/6 expression in TCCRP could mimic intraductal papilloma with usual ductal hyperplasia. However, TCCRP lacks myoepithelial cells along the fibrovascular papillae or around the papillary nodules and is typically ER negative, whereas papilloma has intact myoepithelial cell layers and is ER positive in a heterogeneous pattern. Like TCCRP, SPC is composed of circumscribed nodules with solid papillary architecture and an absence of myoepithelial cells along the fibrovascular cores.
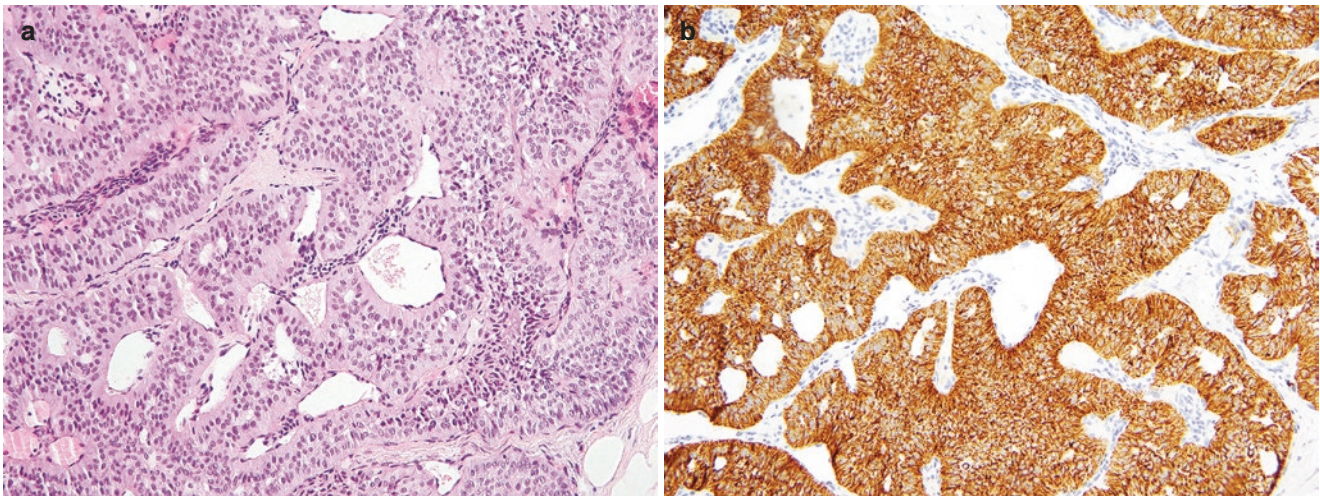
Fig. 12.24 Tall cell carcinoma with reversed polarity, detection of mutant IDH2 by mutant-specific antibody. TCCRP harbors recurrent *IDH2* mutations at R172. (**a**, **b**) Immunohistochemistry using an antibody to IDH2 R172 mutant protein demonstrates diffuse and strong staining with cytoplasmic granular pattern in the tumor cells, helpful in confirming the diagnosis of TCCRP (*Courtesy of Dr. Fresia Pareja*, Department of Pathology, Memorial Sloan Kettering Cancer Center with permission)

Table 12.4 Immunohistochemical markers helpful in the differential diagnosis of TCCRP and papillary mimics

	Tall cell carcinoma with reverse polarity	Papilloma with usual ductal hyperplasia	Solid papillary carcinoma (in situ and invasive)	Papillary pattern DCIS and encapsulated papillary carcinoma
CK5/6	Positive, diffuse	Positive, mosaic pattern	Negative	Negative
ER	Negative or focal weak	Positive, heterogeneous	Positive, diffuse	Positive, diffuse
Myoepithelial cell markers (p63, SMM, calponin)	Negative along papillae and around nodules	Positive along papillae and around ducts	Negative along papillae; Positive or negative around nodules	Negative along papillae; Positive around DCIS, negative around EPC
IDH2 R172	Positive	Negative	Negative	Negative

The helpful distinguishing morphologic features include tall columnar cells with apically located nuclei in TCCRP versus polygonal cells with evenly spaced round to oval nuclei, often accompanied by areas of spindled or plasmacytoid cytology, in SPC. Immunophenotypically, TCCRP is diffusely CK5/6 positive and ER negative, while SPC has the opposite staining pattern. Furthermore, SPC often expresses the neuroendocrine markers synaptophysin and chromogranin, which are consistently negative in TCCRP. The finding of circumscribed papillary ducts lacking myoepithelial cells in TCCRP could also raise the consideration of papillary pattern DCIS or EPC. Immunohistochemical analysis with CK5/6 and ER is again helpful in the distinction, as in the distinction from SPC. Furthermore, most TCCRP display strong and diffuse immunolabeling with an IDH2 R172-specific antibody, in contrast to the other papillary neoplasms in the differential. Careful evaluation of cytoarchitectural features supplemented by judicious use of immunohistochemical markers can therefore help establish the correct diagnosis, even in a CNB specimen (Table 12.4).

Metastatic papillary thyroid carcinoma: Because of the striking morphologic similarities between PTC and TCCRP and because ~5% of metastases to the breast are of thyroid origin [84], metastatic thyroid carcinoma is often considered in the differential diagnosis for TCCRP. Immunohistochemistry with tissue-specific markers is helpful in this context. TCCRP lacks expression of thyroid-specific markers, including TTF-1, thyroglobulin, and PAX8 [62, 66, 67, 75, 77], and instead shows positive, albeit patchy, staining for breast markers GATA3, mammaglobin, and GCDFP-15.

Infiltrating epitheliosis (IE): Another lesion that shares morphologic features and immunophenotype with TCCRP is infiltrating epitheliosis (IE), an exceedingly rare complex sclerosing lesion with overt CK5/6-positive epithelial proliferation [85], weak/patchy to absent ER expression, and attenuated to absent myoepithelial cell layers around the proliferating cells, similar to TCCRP. Moreover, *PIK3CA* or *PIK3R1* mutations have been reported in IE, and are also seen in TCCRP [86]. It has been suggested that there is a continuum between IE and TCCRP and that these papillary lesions represent a spectrum, with IE at the sclerosis-rich/ epithelium-poor end and TCCRP at the epithelium-rich/ stroma-poor end of the spectrum [65].

Pathogenesis and Risk Factors

TCCRP characteristically harbors recurrent *IDH2* hotspot mutations (often R172S or R172T), which have been reported in >80% of cases [63, 65, 71–73, 75, 78]. *IDH2* mutations appear to be pathognomonic for TCCRP in the context of breast neoplasms [63] but have also been identified in gliomas [87], myeloid leukemias [88], sinonasal undifferentiated carcinomas [89], chondrosarcomas [90], and cholangiocarcinomas [91]. *IDH2* encodes the mitochondrial enzyme isocitrate dehydrogenase 2. The precise mechanisms by which *IDH2* mutations function in cancer remain unknown. However, *IDH2* mutations lead to gain-of-function enzymatic activity that allows for NADPH-dependent reduction of α-ketoglutarate (αKG) to 2-hydroxyglutarate, which in turn inhibits αKG-dependent dioxygenases, including TET2, and alters genome-wide histone and DNA methylation, cell differentiation and survival, and extracellular matrix maturation [65, 75, 92–94]. In TCCRP, *IDH2* mutations often co-exist with genetic alterations in phosphatidylinositol-3 kinase (PI-3 K) signaling pathway genes, including activating *PIK3CA* and *PIK3R1* mutations [63, 65, 72, 75, 78]. Whereas PI-3 K pathway gene mutations are common in breast cancer, *IDH2* hotspot mutations are extremely rare or non-existent in other breast tumors, and their identification can be used as a confirmatory molecular finding for TCCRP [72, 95–97]. Functional studies have shown that forced expression of *IDH2* R172S and *PIK3CA* H1047R together result in a reverse polarization phenotype resembling that of TCCRP [63]. Truncating *TET2* mutations have been identified in a subset of TCCRP lacking the *IDH2* mutations [63, 65, 72, 75, 78]. Given that mutant IDH2 is thought to function through inhibition of TET2, TCCRP may be an example of a convergent phenotype stemming from *IDH2* or *TET2* mutations functioning in the same pathway [63, 87]. TCCRP has thus joined a growing list of breast tumors with unique genotypic-phenotypic correlation (Table 12.5) [72].

Table 12.5 Breast tumors with genotype-phenotype correlation

Tumor	Genetic Alterations
Lobular carcinoma in situ and invasive lobular carcinoma	*CDH1* mutation
Adenoid cystic carcinoma	*MYB-NFIB* fusion *MYBL1-NFIB* fusion *MYB* amplification
Secretory carcinoma	*ETV6-NTRK3* fusion
Mucoepidermoid carcinoma	*CRTC1-MAML2* fusion
Pleomorphic adenoma	*PLAG1* arrangement *HMGA2-WIF1* fusion
Fibroepithelial tumor (fibroadenoma and phyllodes tumor)	*MED12* exon 2 mutation
Tall cell carcinoma with reversed polarity	*IDH2* R172 mutation

BRAF mutations and *RET/PTC* rearrangements, which are frequently found in PTC and are thought to be responsible for the specific nuclear features in PTC, are consistently absent in TCCRP [77].

RNA sequencing of 9 TCCRP revealed expression profiles of either luminal A or basal intrinsic molecular subtypes [75].

Prognosis and Clinical Management

Limited available follow-up data on a small number of cases suggests that the majority of TCCRP follow an indolent clinical course with excellent prognosis despite the triple-negative or weakly ER-positive biomarker profile [62–71, 73, 75, 77]. TCCRP presents mostly as localized disease with a low incidence of lymph node metastasis at the time of diagnosis (reported in only 4 patients, including one intramammary node) [64, 66, 69, 76]. The single patient with intramammary lymph node metastases was alive and free of local or distant recurrence 10 years after diagnosis. Only one case with distant metastasis (to bone) has been reported [69]. However, it is not clear if this tumor was truly TCCRP, as it was ER positive and associated with DCIS with comedonecrosis, and with lymphovascular invasion.

Due to the rarity of TCCRP, there are no guidelines or consensus on the management of patients with these tumors. Current treatment generally includes surgical excision with lumpectomy or mastectomy [63–65]. Local recurrence has been reported, and complete excision with adequate margin is considered optimal. The role of radiation or systemic therapy is unclear. *IDH2* mutations may serve as a future target for therapeutic intervention in metastatic lesions.

Mucoepidermoid Carcinoma

Overview and Clinical Presentation

Mucoepidermoid carcinoma (MEC) of the breast is a triple-negative salivary gland-like tumor that shares distinctive histopathologic features, immunophenotype, and genetic alterations with its counterpart arising in other anatomic sites [98–100]. Whereas MEC is the most common salivary gland malignancy, it is an exceedingly rare diagnosis and less frequent than other salivary gland-like neoplasms in the breast, such as AdCC, secretory carcinoma, and adenomyoepithelioma. The estimated incidence has been cited as 0.2–0.3% of all breast cancers [101, 102], although it appears to be even less common in practice. Since the first description by Patchefsky et al. [103] in 1979, less than 50 cases of breast MEC have been reported in the English literature, mostly as single case reports [100, 102, 104].

All reported MEC cases are in adult women, ranging in age from 27 to 86 years (mean age 56 years) [104]. Patients usually present with a palpable lump that is often well-circumscribed but occasionally ill-defined on physical examination and may be tender to palpation [99, 103, 104]. Nipple discharge may be present when the tumor arises in the retroareolar region [99]. Some cases have been detected by screening mammography [100, 105, 106].

Gross and Radiologic Features

Most MEC are well circumscribed, gray to white, and firm with a solid or solid cystic cut surface. Cysts are often filled with mucoid material. Tumor size ranges from 0.5 to 11 cm (median 2.5 cm).

Radiographically, some MEC are considered to be benign. On mammography, MEC often presents as a round nodule and less frequently as an ill-defined mass. Ultrasonography demonstrates a hypoechoic or mixed hyperechoic and hypoechoic mass with smooth or irregular contours that may show posterior shadowing [100, 104, 105, 107, 108]. Some cases appear as a complex cystic and solid nodule [104, 109, 110]. An enhancing mass is observed on MRI [107, 108].

Microscopic Features

At scanning magnification, most MEC appear as a solid or partly cystic nodular lesion with pushing margins (Fig. 12.25). Some tumors are surrounded by a fibrous pseudocapsule [99, 108]. Stellate or irregular margins may be seen, usually in high-grade tumors. A dense lymphoplasmacytic infiltrate is frequently observed at the tumor periphery, which in the salivary gland has been termed tumor-associated lymphoid proliferation (TALP) (Fig. 12.25). MEC comprises a mixed population of mucinous (mucin-secreting) cells, epidermoid/squamous cells, and intermediate cells in varying proportions and arranged in overall circumscribed macrocystic, microcystic/glandular, and solid patterns (Figs. 12.26, 12.27, and 12.28). Prominent extracellular basophilic and/or eosinophilic secretions often fill the cystic and glandular spaces.

Mucinous cells are usually located at the luminal/central aspects of the cysts, glands, and nests (Figs. 12.27a and 12.28c, g). These cells may be tall columnar or goblet shaped with obvious cytoplasmic mucin, or more subtle, requiring special stains, such as PASD, mucicarmine, or Alcian blue to highlight the mucin (Fig. 12.27b). Intermediate cells, which are most concentrated at the periphery of cysts and nodules, are small with relatively high nuclear-to-cytoplasmic ratio and oval hyperchromatic nuclei (Figs. 12.27a and 12.28g). Epidermoid cells are polygonal with well-defined cell borders and abundant eosinophilic cytoplasm (Figs. 12.27a and 12.28c, g). Focal intercellular bridges may be observed in rare cases, but true keratinization, such as squamous pearls or individual cell keratinization, should be absent. In addition to the most common three cell types as described above, salivary gland MEC may also have cells with prominent cytoplasmic clearing (clear cell changes), oncocytic cells, spindle cells, and rarely ciliated cells and cells with sebaceous differentiation. Clear cell changes are also observed in breast MEC and can be quite prominent in some tumors (Fig. 12.27c). An in situ component may be present and displays similar features, including the three characteristic cell types, mucinous/eosinophilic secretions, and periductal lymphoplasmacytic infiltrates [99, 108, 111] (Fig. 12.29).
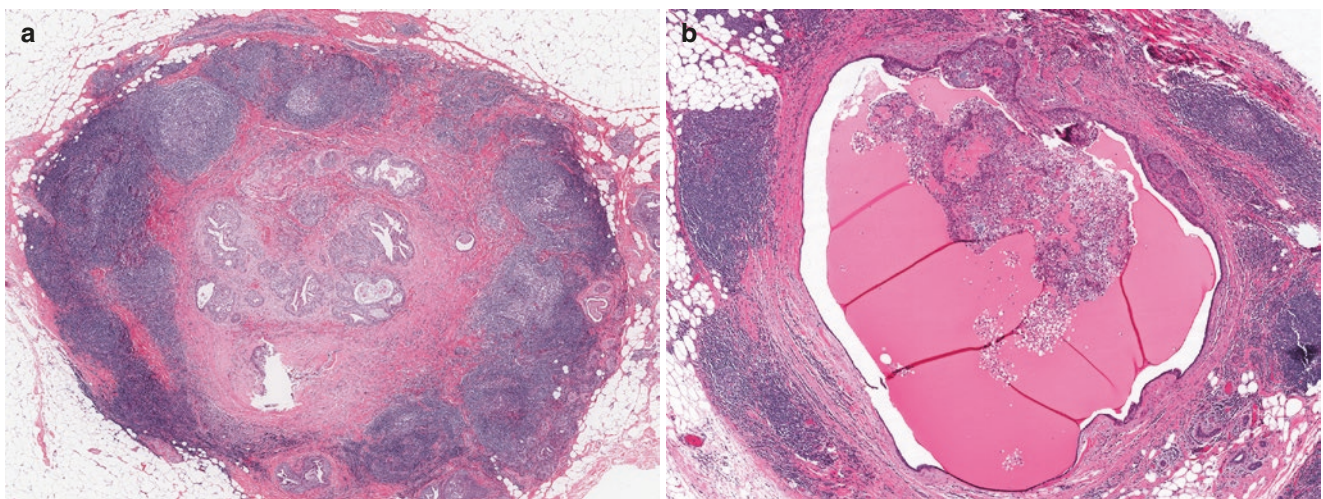

Fig. 12.25 Mucoepidermoid carcinoma, tumor border. (**a**, **b**) At scanning magnification, these two examples of MEC appear circumscribed with pushing margins. Note the prominent lymphoplasmacytic infiltrate at the periphery of the tumor, including lymphoid aggregates with germinal center formation. The tumor can be solid (**a**), cystic (**b**), or solid and cystic
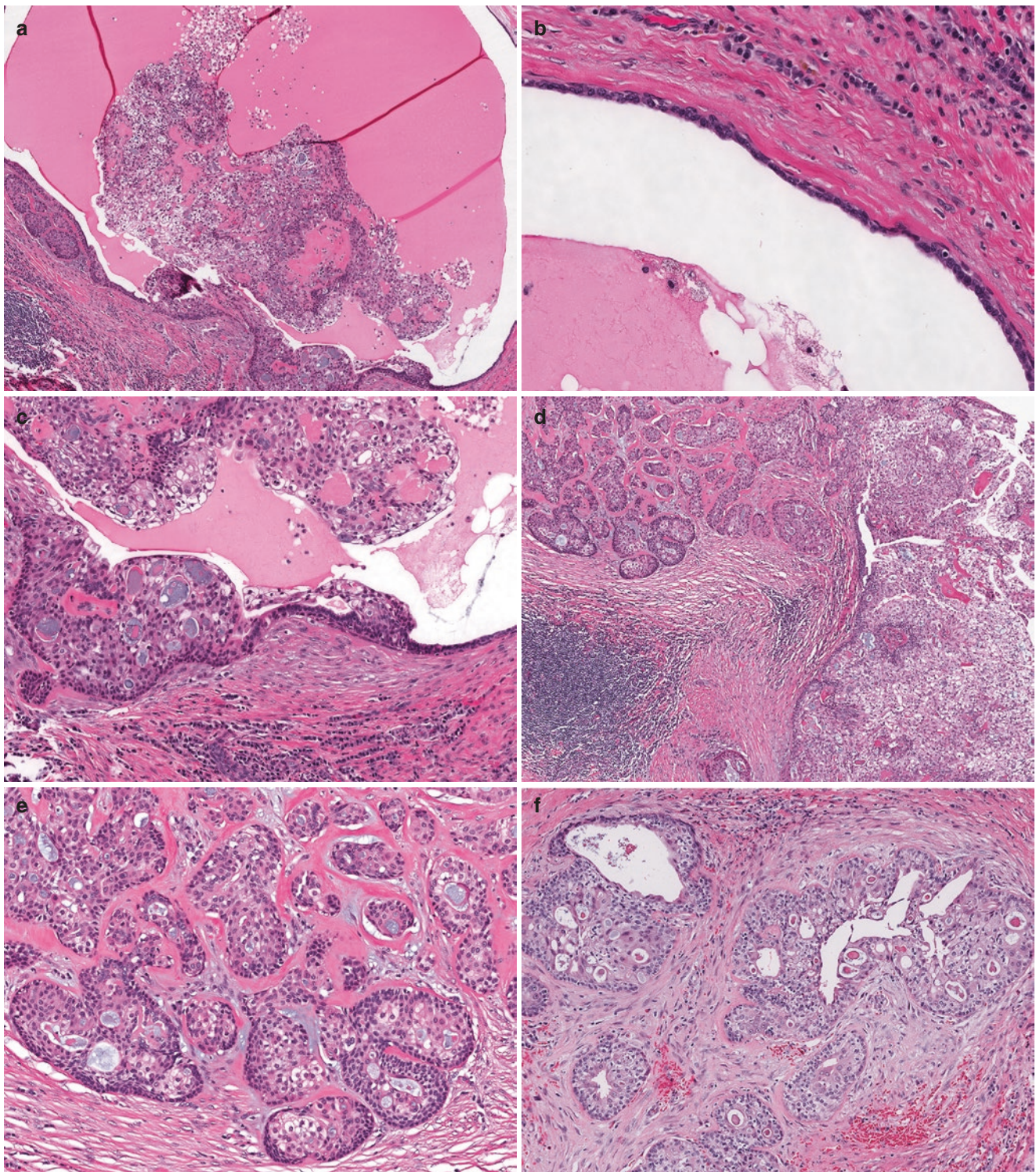
Fig. 12.26 Mucoepidermoid carcinoma, architectural pattern. The tumor cells in MEC can be arranged in macrocystic structures (**a–c**), solid nests (**d**, **e**) or microcystic/fenestrated glandular pattern (**e**, **f**), usually with varying proportion in a given lesion. In the macrocystic pattern, the tumor cells can grow as a mural papillary nodule (**a**); while the majority of the cyst wall can be lined by one to a few layers of neoplas-

tic epithelial cells (**b**, **c**). In the solid growth pattern, the nests can be large (**d**, right) or small (**d**, left, and **e**). The small solid nests may be admixed with microcystic elements (**e**). Note the presence of prominent secretions within the macrocytic spaces and glandular lumens, which can be eosinophilic or basophilic. The stroma associated with the tumor nests/glands can be hyalinized/fibrotic (**e**) or desmoplastic (**f**)
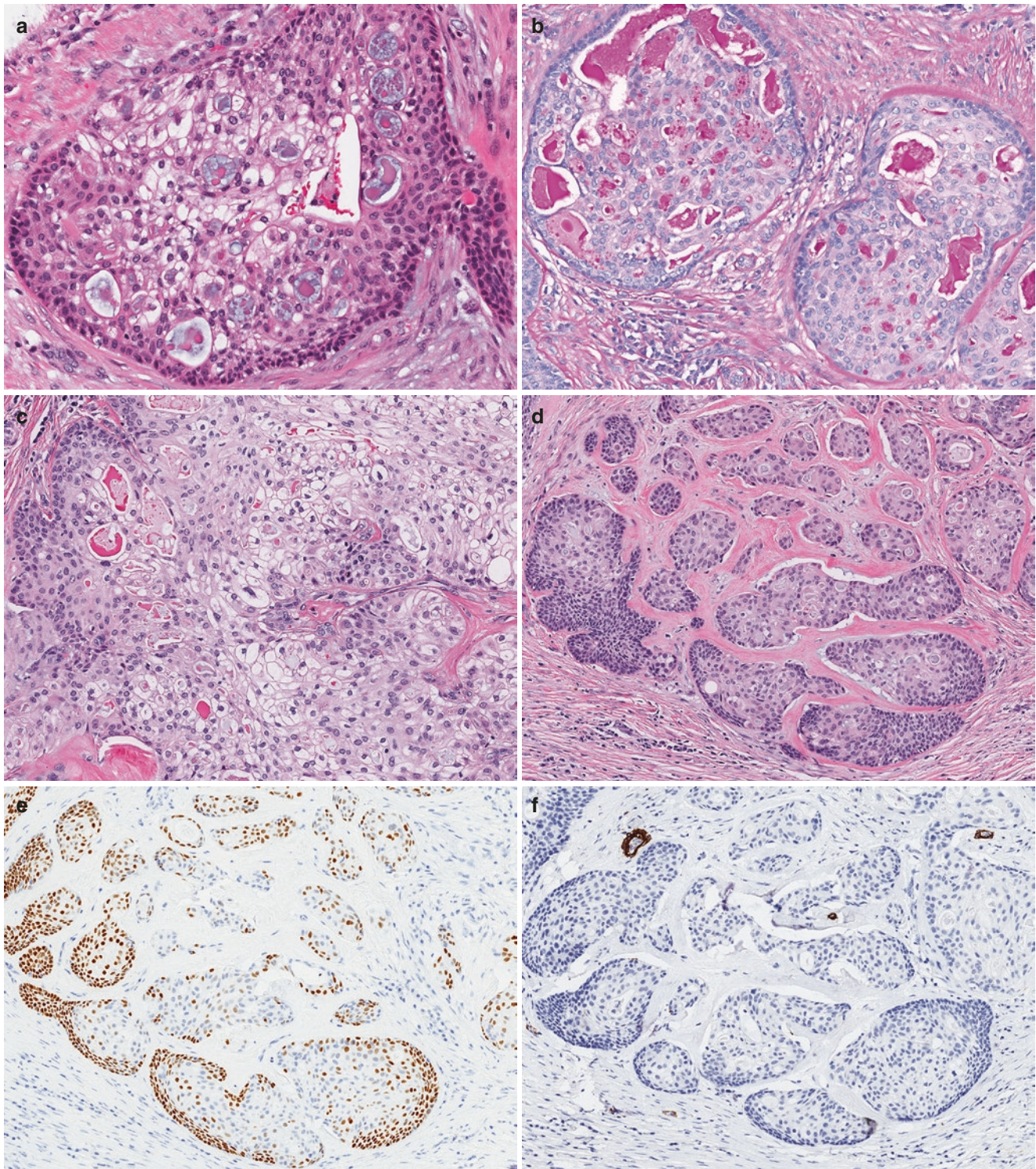
Fig. 12.27 Mucoepidermoid carcinoma, cytologic features. (**a**) MEC is composed of a mixed population of intermediate cells (which are most concentrated at the periphery of the tumor cysts/glands/nests), epidermoid/squamoid cells (which have distinct cell borders and abundant eosinophilic cytoplasm), and mucin-secreting cells (which are preferentially localized at the luminal/central aspects of tumor cysts/glands/nests). (**b**) A PASD stain highlights the intracytoplasmic mucin in the mucin-secreting cells as well as the mucinous secretion within the glandular lumens. (**c**) Clear cell changes may be observed in the neoplastic cells and are prominent in this example. (**d**) The various tumor cell types and their spatial arrangement create a distinct appearance to the tumor nests with darker cells at the periphery and paler cells toward the center. The intermediate cells (and to various extent, the epidermoid cells) are positive for p63 immunostain (**e**), which may be mistaken as being myoepithelial cells. However, the tumor nests and glands are negative for other myoepithelial markers, including SMM (**f**), calponin and SMA (not shown)
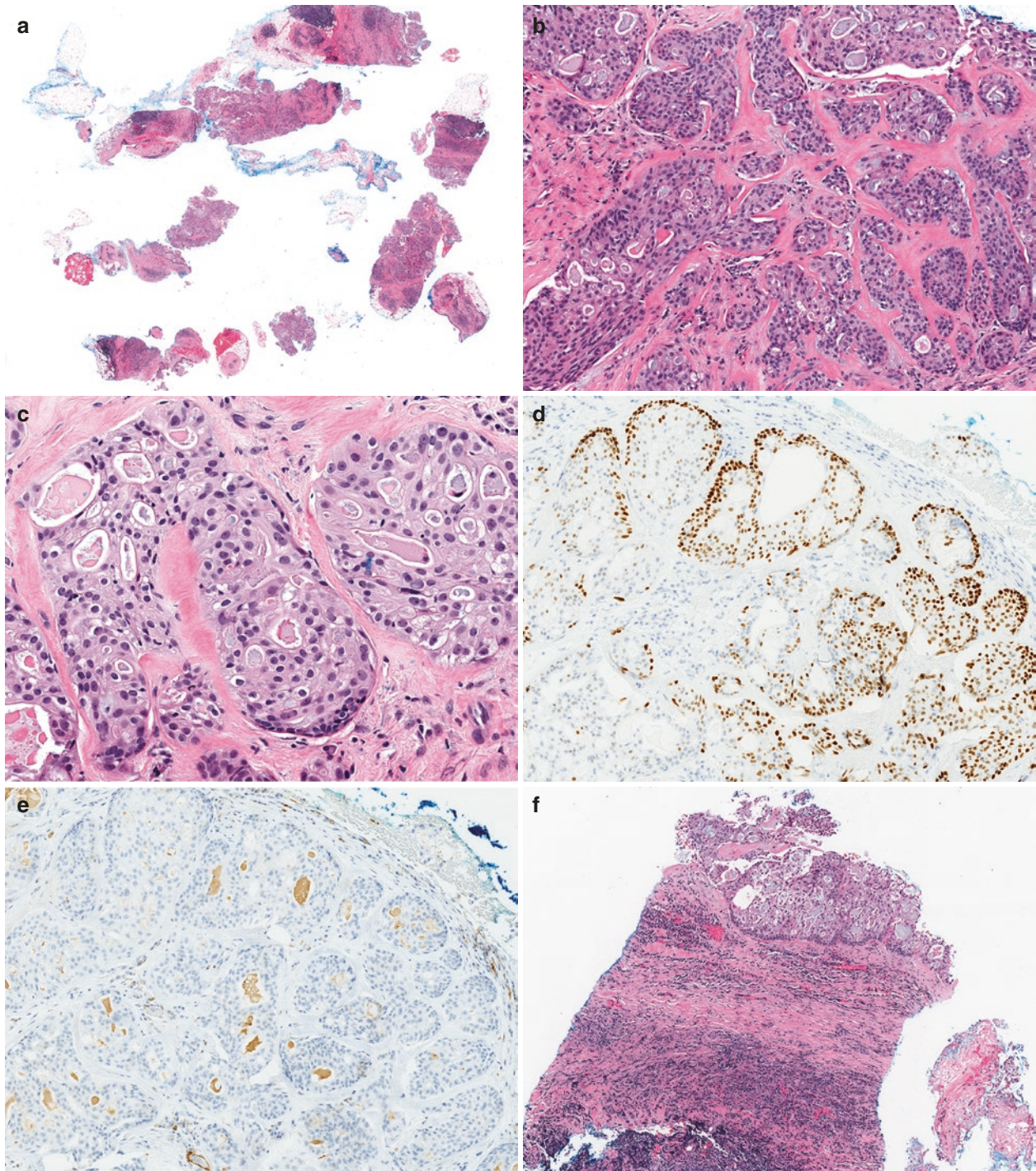
Fig. 12.28 Mucoepidermoid carcinoma, features in core needle biopsy specimen. The characteristic architectural and cytologic features of MEC can be appreciated in this CNB specimen targeted for a breast mass (**a**). (**b**) Some core fragments contain microcystic glands and small solid nests in a fibrotic/hyalinized stroma. (**c**) High magnification reveals a mixed cell population and eosinophilic/basophilic secretions within glandular lumens (**c**). The microcystic glands and solid nests have peripheral p63-positive cells (**d**) and are negative for SMM immunostain (**e**). (**f–i**) One core fragment appears to sample part of a cyst wall that is lined by multiple layers of epithelial cells. Note the prominent lympho-plasmacytic infiltrate in the cyst wall (**f**), and the mixed intermediate cells (dark cells with high nuclear-to-cytoplasmic ratio at the periphery of the cyst), epidermoid cells, and mucin-secreting cells (**g**). Also noted

is the basophilic to eosinophilic secretory material within the glandular spaces. Similar to the microcystic elements and solid nests, the macro-cystic structure is positive for p63 immunostain with a predominant peripheral staining pattern (**h**) and negative for SMM (**i**). (**j–l**) Another core fragment samples a part of a cyst that is lined by only one to two flat layers of bland epithelial cells, which could easily be misinterpreted as a benign simple cyst. Again, note the presence of a dense lymphoplasma-cytic infiltrate in the cyst wall. Also note the presence of subtle mucin secretion in the thin cyst lining (upper part of the cyst in **j**), which would not be expected in simple cyst. The cyst is lined by p63-positive cells (**k**), but is completely negative for SMM (**l**), which along with other features (dense lymphoplasmacytic infiltrate and mucin secretion) should alert the pathologist to question the impression of a benign simple cyst
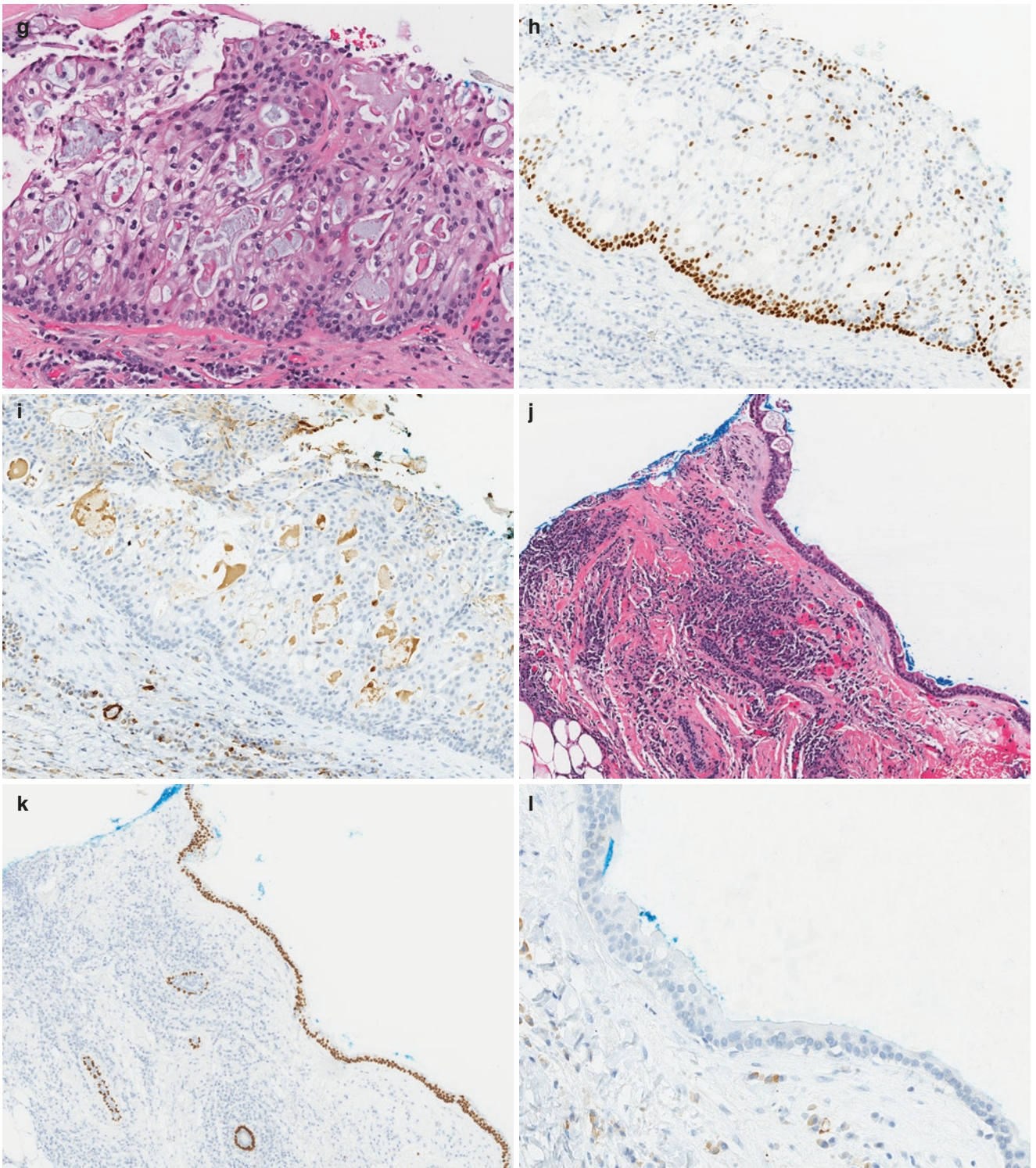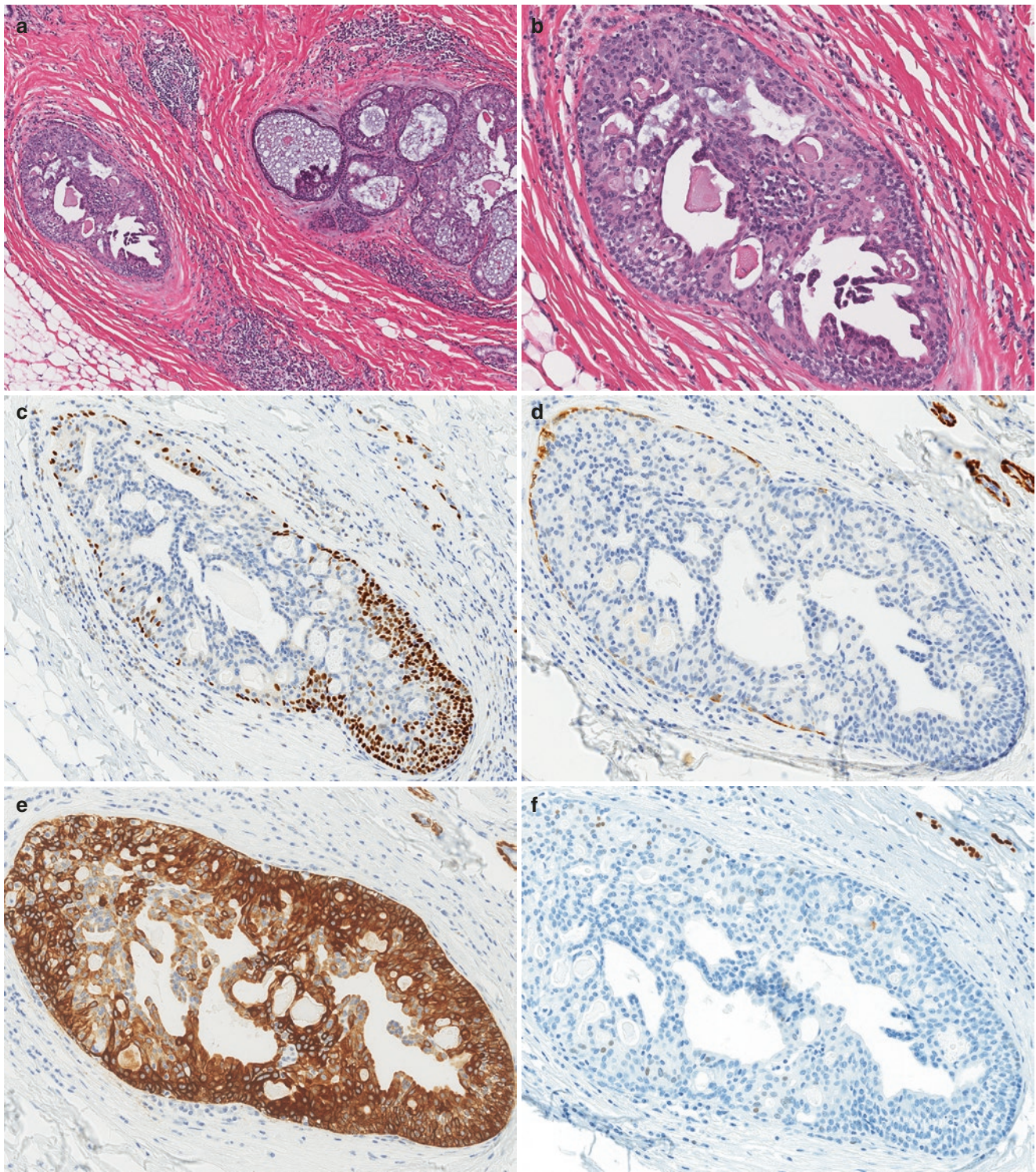
Fig. 12.28 (continued)

Fig. 12.29 Mucoepidermoid carcinoma, in situ component. (**a–f**) An in situ component of MEC may be present in some cases and exhibit similar features as those observed in the invasive component, including the associated lymphoplasmacytic infiltrate (**a**) and the mixed population of neoplastic cells and luminal secretions (**b**). The mixed (hence appearing to be heterogeneous) epithelial types with squamoid features and irregular fenestrations could mimic usual ductal hyperplasia. Strong expression for CK5/6 (**e**) further complicates the issue. However, the neoplastic cells in the MEC (both in situ and invasive forms) are completely negative to minimally positive for ER (in the range 1–2%) (**f**), which helps to distinguish the lesion from usual ductal hyperplasia. The in situ component of MEC is invested by a myoepithelial layer, highlighted by p63 (**c**) and calponin (**d**) immunostains

Accurate grading of breast MEC is important in providing prognostic information. In the salivary gland, the most commonly used grading systems for MEC are The Brandwein and Armed Forces Institute of Pathology (AFIP) methods, which are three-tiered and point-based systems incorporating various adverse histologic features (Table 12.6). For breast MEC, the AFIP system and the modified Scarff-Bloom-Richardson (SBR) system appear to be largely interchangeable and yield similar prognostic data [99]. With the AFIP grading scheme, ~55% of breast MEC are low grade, <10% are intermediate grade, and ~40% are high grade [100, 104, 112].

Cystic architecture with abundant mucinous cells predominates in low-grade MEC, and the tumor cells have bland round to oval nuclei and infrequent mitoses (0–3/10 HPF). High-grade MEC are usually arranged in solid nests with scant mucinous cells, greater nuclear atypia, and increased mitotic activity. Infiltration of tumor nests into surrounding breast tissue may be present. Necrosis, lymphovascular invasion, and perineural invasion are typically only identified in high-grade tumors. Accurate diagnosis of high-grade MEC can be challenging based on morphologic grounds alone. High-grade MEC of the salivary gland has been well documented in the literature to include a heterogeneous group of different entities upon re-review by expert pathologists. FISH is a useful ancillary test to help identify MEC in the breast (see section "Pathogenesis" and "Differential Diagnosis").

Table 12.6 AFIP and Brandwein semiquantitative methods for assessing histological grade in salivary gland MEC

	AFIP method	Brandwein method
Intracystic component	2 (<20%)	2 (<25%)
Border/invasive front	NA	2 (small nests and islands)
Nuclear anaplasia/pleomorphism	4	2
Mitosis	3 (≥4/10 HPF)	3 (≥5/10 HPF)
Perineural invasion	2	3
Necrosis	3	3
Lymphovascular invasion	NA	3
Bony invasion	NA	3
	Total score	Total score
Low grade	0–4	0
Intermediate grade	5–6	2–3
High grade	7–14	4+

Adapted from Cipriani et al. [113]

Immunohistochemistry

MEC is overall positive for LMWCK (CK7, CAM5.2), HMWCK (CK5/6, CK14), and p63 [99, 100] (Figs. 12.27e, 12.28d, h, k, 12.30, and 12.31b). Expression of these markers is correlated with cell type, and immunohistochemistry is helpful in highlighting the various cell populations and their distribution in the tumor nests and cysts. Intermediate cells are typically positive for p63 and HMWCK and negative for LMWCK; epidermoid cells usually react with both LMWCK and HMWCK, with variable staining for p63; and mucinous cells preferentially express LMWCK. This differential staining pattern with LMWCK-positive cells concentrated in the central/luminal part of the tumor nests and HMWCK-positive cells predominantly located in the outer layers of the nests creates a "zoning phenomenon" (Fig. 12.30), that is shared by salivary gland and breast MEC and is helpful in
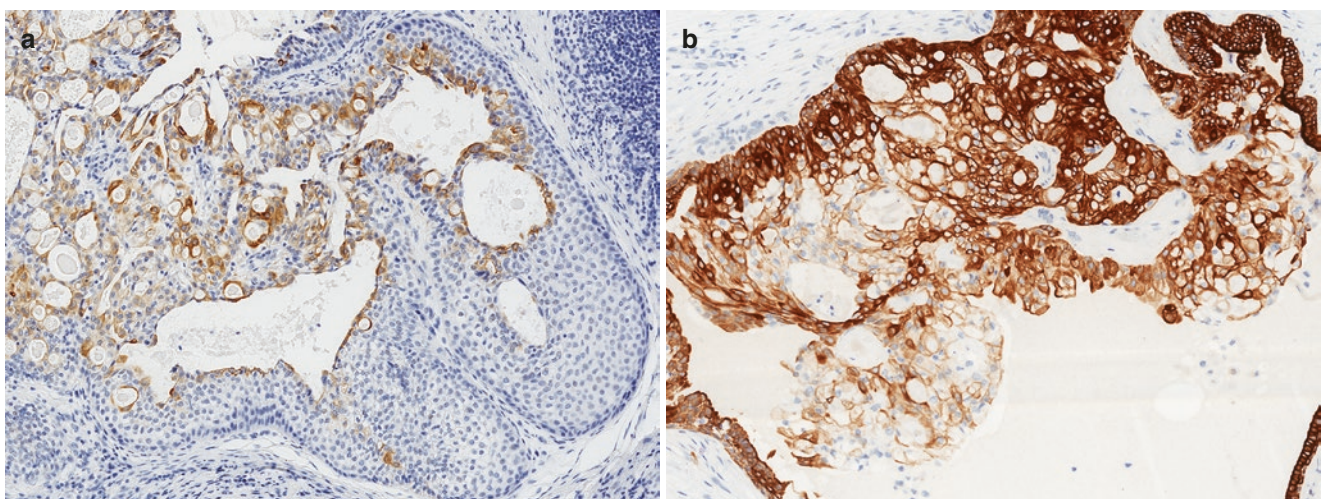
Fig. 12.30 Mucoepidermoid carcinoma, zoning phenomenon with cytokeratin immunostains. (**a**, **b**) The various cell types in MEC tend to exhibit different expression for cytokeratins, in which LMWCK such as CAM5.2 shows preferential staining of the mucin-secreting cells (**a**) whereas HMWCK such as CK14 decorates predominantly the intermediate and epidermoid cells (**b**), creating a distinctive "zoning" phenomenon that is helpful for the diagnosis of MEC

establishing the diagnosis [99]. Expression of p63 by intermediate cells at the periphery of tumor nests and cysts may be misinterpreted as myoepithelial differentiation; however, the tumor cells are negative for other myoepithelial cell markers, including SMM, calponin, and SMA [99] (Figs. 12.27f and 12.28e, i, l). On the other hand, the in situ component has a peripheral myoepithelial layer that can be highlighted with SMM, calponin, SMA stains, in addition to p63 (Fig. 12.29d).

All reported breast MEC have been ER and PR negative or rarely weakly positive and are consistently HER2 negative (Fig. 12.31c). Therefore, MEC falls into the group of basal-like triple-negative breast cancers by immunophenotype.

There is limited information about expression of other markers in MEC. Based on analyses of two breast MEC, these tumors were also patchy or diffusely positive for MUC4, GATA3, and mammaglobin and negative for GCDFP-15 [100] (Fig. 12.31d).

Differential Diagnosis

The characteristic histological features and immunophenotype of MEC are distinctive in the breast. However, pathologists may not necessarily consider this very rare subtype of breast cancer, and MEC can be confused with various benign and malignant lesions when assessing limited CNB material, depending on the architectural pattern and dominant cell type sampled.

Simple cysts: CNB which samples only a portion of a macrocyst lined by one to a few layers of intermediate cells with or without epidermoid cells could easily be misinterpreted as a simple cyst with or without squamous metaplasia (Figs. 12.26b and 12.28j). Features that would be unusual for simple cyst include the presence of mucinous cells (which can be very subtle), a prominent lymphoplasmacytic infiltrate in the cyst wall, and lack of myoepithelial cells at the cyst periphery by SMM and calponin immunohistochemistry
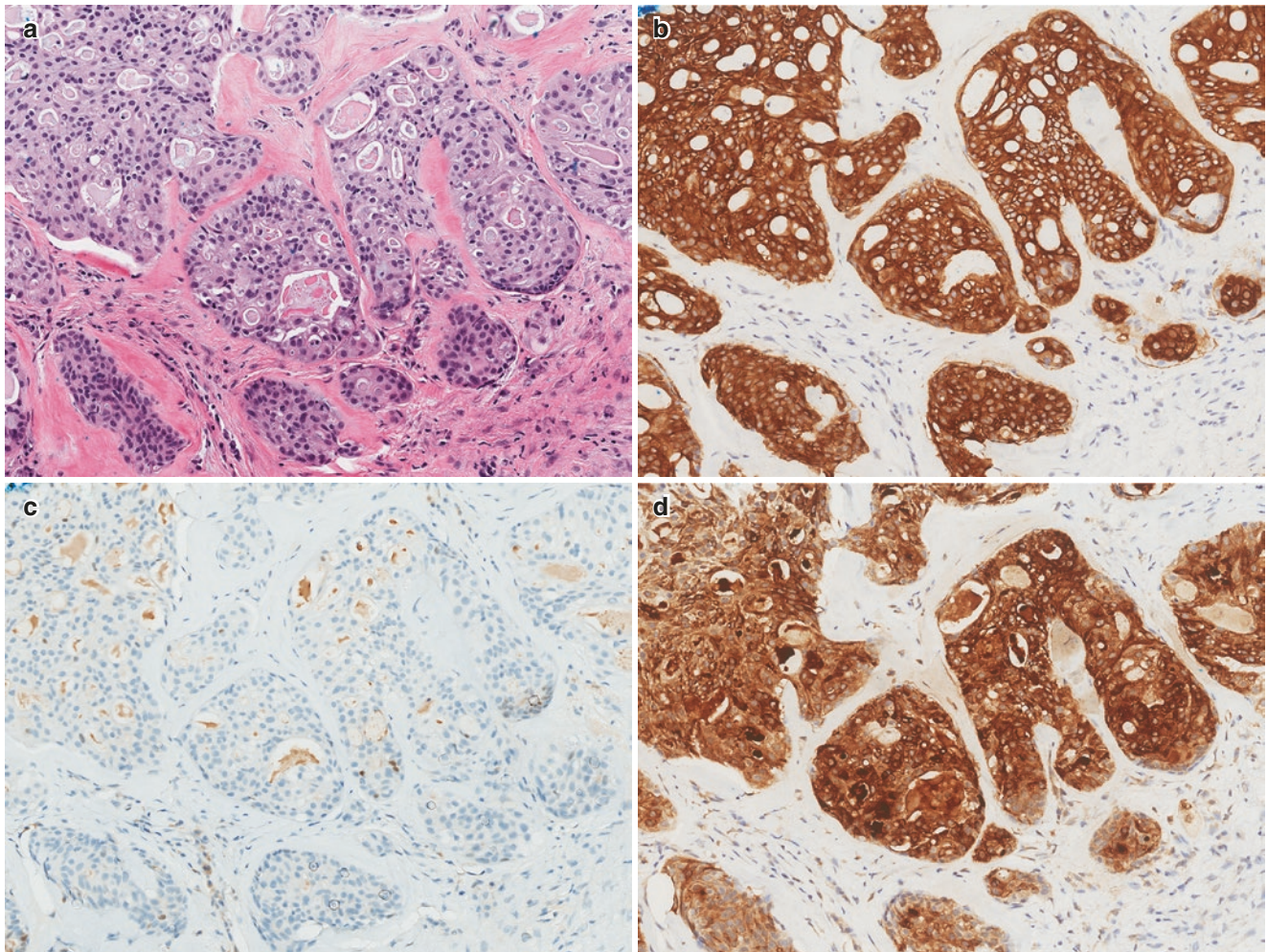

Fig. 12.31 Mucoepidermoid carcinoma, additional immunostaining profile. (**a–d**) The neoplastic cells in MEC are positive for CK5/6 (**b**) and negative for ER (**c**), PR (not shown), and HER2 (now shown), thus exhibiting a basal-like and triple-negative immunophenotype. MEC typically shows strong expression of mammaglobin (**d**)

(Fig. 12.28j–l). In these situations, radiologic-pathologic correlation is important to determine the presence of discordant findings and the need for re-biopsy to pursue a conclusive diagnosis.

Usual ductal hyperplasia: The bland cytology, different cell types (heterogeneous cell population), and often irregular microcystic spaces of MEC, especially in the DCIS component, may mimic usual ductal hyperplasia (Fig. 12.29a, b). Clues to the correct diagnosis include recognizing tumor cells with epidermoid, mucinous, and intermediate features, the presence of mucin, and the associated periductal lymphoplasmacytic infiltrate. CK5/6 and ER immunohistochemistry is helpful in making the distinction, with positive CK5/6 (in zonal pattern) and negative ER expression in MEC, and positive CK5/6 (in mosaic pattern) and heterogeneous ER expression in usual ductal hyperplasia (Fig. 12.29).

Ductal carcinoma in situ: Epidermoid cells with well-defined cell borders and microcystic architecture in MEC can also raise consideration of cribriform pattern DCIS of no special type. Helpful features for the correct diagnosis are the heterogeneous cell population, as well as the CK5/6-positive,

ER-negative, and p63-positive phenotype in MEC, compared to the uniform cell population with negative CK5/6 and p63 and strongly ER-positive expression pattern in DCIS.

Papillary lesions: MEC with macrocystic structures containing mural cellular nodules can resemble either intraductal papilloma with usual ductal hyperplasia and squamous metaplasia or papillary carcinoma, including EPC (Fig. 12.26a). As in the discussion for usual ductal hyperplasia and DCIS above, appreciation of the various cell types and characteristic immunophenotype can help to arrive at the correct diagnosis.

Secretory carcinoma: Low-grade MEC can be mistaken for secretory carcinoma, another rare salivary gland-type carcinoma. Both tumors can have a prominent cystic component, abundant PASD-positive secretory material, and cytologically bland cells that may have eosinophilic, clear, or vacuolated cytoplasm (Fig. 12.32). In addition, both tumors express MUC4, GATA3, and mammaglobin [100, 114]. However, in contrast to the strong S100 protein-positive and p63-negative profile of secretory carcinoma, MEC is consistently positive for p63 and is negative or only focally positive
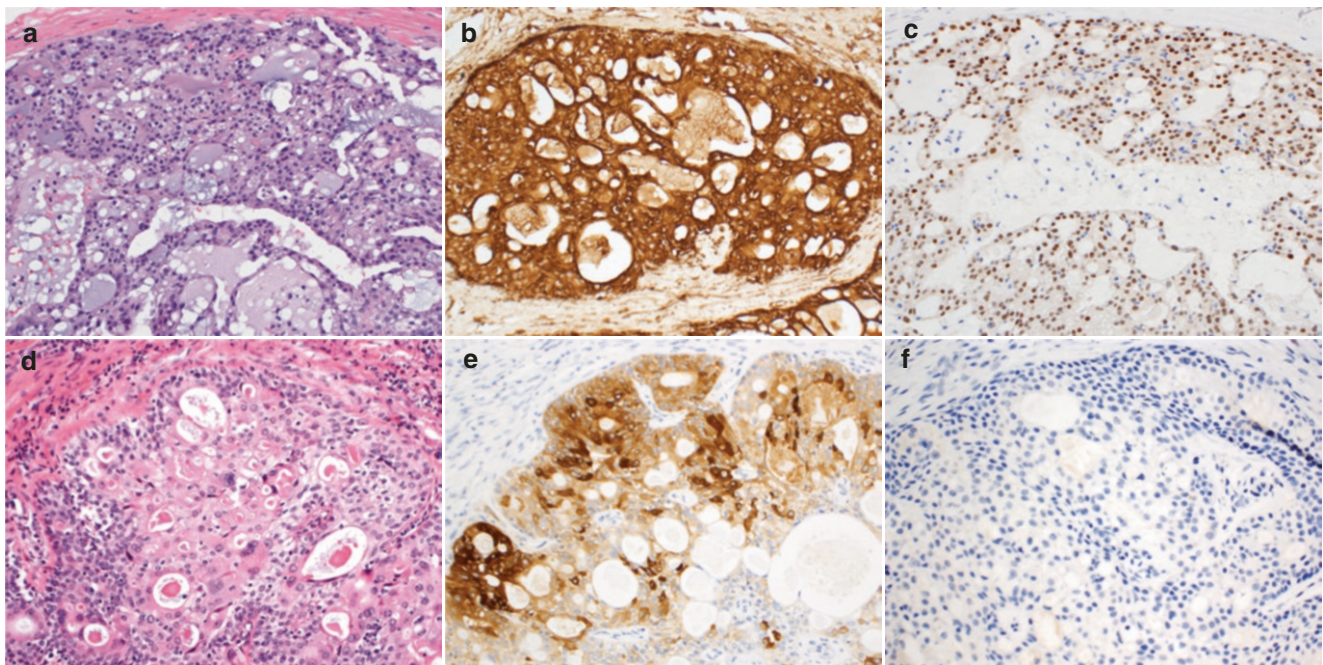

Fig. 12.32 Mucoepidermoid carcinoma versus secretory carcinoma. Secretory carcinoma (**a–c**) and MEC (**d–f**) are both salivary gland-like carcinomas with a triple-negative biomarker profile, share similar morphologic features with a microcystic pattern, bland cytology and prominent secretions (**a**, **d**) and strong mammaglobin expression (**b**, **e**), and may be confused with each other. However, each tumor type is charac-terized by a distinct chromosomal translocation, with *ETV6-NTRK3* fusion gene in secretory carcinoma and *CRTC1-MAML2* fusion gene in MEC. The diagnosis can therefore be supported by immunohistochemistry with a pan-TRK antibody, which shows nuclear staining in secretory carcinoma (**c**) and is negative in MEC (**f**)
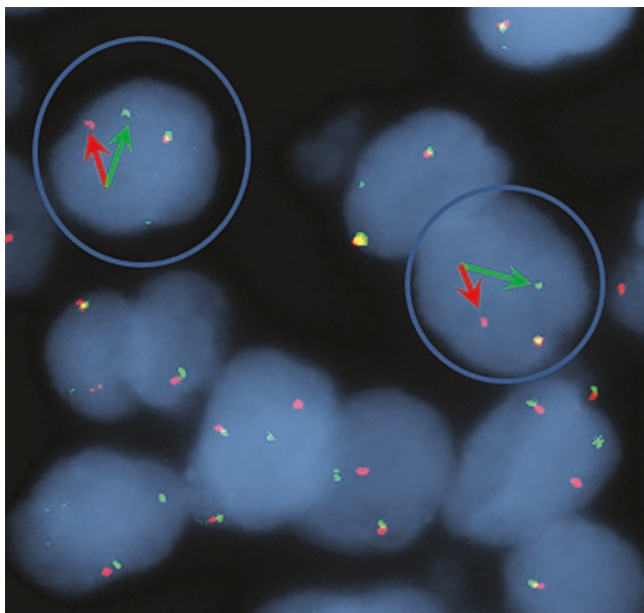
Fig. 12.33 *CRTC1-MAML2* translocation in mucoepidermoid carcinoma. The hallmark chromosomal translocation in MEC, *CRTC1-MAML2*, can be detected using a break-apart fluorescence in situ hybridization (FISH) probe to *MAML2* gene. Note the split-apart green and orange signals of the altered *MAML2* allele and the fused yellow signal from the normal *MAML2* allele. This FISH result is from the case shown in Fig. 12.28. (*Courtesy of Dr. Joaquin Garcia*, Department of Laboratory Medicine and Pathology, Mayo Clinic with permission)

for S100 protein. Furthermore, the tumors each harbor pathognomonic chromosomal translocations and resultant fusion genes (*CRTC1-MAML2* in MEC and *ETV6-NTRK3* in secretory carcinoma), allowing for distinction by FISH using *MAML2* and *ETV6* break-apart probes or sequencing technologies (Fig. 12.33). Immunostaining with a pan-TRK antibody can also be useful, with the majority of secretory carcinomas showing positive nuclear expression, while MEC are negative [115, 116] (Fig. 12.33c, f).

Metaplastic carcinoma: The epidermoid cells and immunophenotype (positive CK5/6 and p63, triple negative) of MEC may raise consideration of metaplastic squamous cell carcinoma. This distinction has significant management implications as diagnosis of metaplastic carcinoma in a CNB may lead to treatment with neoadjuvant chemotherapy. MEC is composed of circumscribed nodules and cysts with mixed cell types including mucinous cells, whereas metaplastic squamous cell carcinoma infiltrates as irregular nests lacking mucinous cells. The presence of true keratinization is not observed in MEC and favors metaplastic squamous cell carcinoma. Low-grade adenosquamous carcinoma may also enter into the differential diagnosis, but this tumor has a different growth pattern consisting of small glands with varying

degree of squamous differentiation and lacks mucinous cells (see section "Metaplastic Carcinoma").

Breast tumors with clear cell cytology: MEC with prominent clear cell features and positive p63 expression may be confused with adenomyoepithelioma exhibiting clear cell change of the neoplastic myoepithelial cells. MEC lacks myoepithelial differentiation and is negative for myoepithelial markers SMM, calponin, and SMA. MEC with clear cell features must also be differentiated from invasive breast carcinomas with glycogen-rich clear cell carcinoma pattern and lipid-rich carcinoma pattern. Both of these latter tumors lack mucinous cells and are usually negative for CK5/6 and p63.

Metastatic renal cell carcinoma: Metastatic renal cell carcinoma is also a potential consideration in the differential diagnosis of MEC with prominent clear cell changes. Correlation with history and radiologic findings together with immunohistochemistry is helpful in establishing the diagnosis. Tissue-specific markers (mammaglobin, GATA3, and PAX8) and cytokeratins (CK7 and CK5/6) are differentially expressed in these tumors, with MEC being positive for mammaglobin, GATA3, CK7, and CK5/6, whereas clear cell renal cell carcinoma expresses PAX8 and is negative for CK7 and CK5/6.

Hidradenoma arising in the breast: Hidradenoma (HA) is a skin adnexal tumor that shares overlapping morphological features and immunophenotype with MEC (see Chap. 25). In addition, the signature *MAML2* rearrangement of MEC has also been identified in HA, predominantly as a *CRTC1-MAML2* translocation and rarely as a *CRTC3-MAML2* translocation [117, 118]. These findings raise the question as to whether HA is a distinct cutaneous adnexal neoplasm that shares histopathologic and genetic characteristics with MEC, or whether it represents a cutaneous counterpart of MEC. HA in the breast usually arises in the nipple and subareolar region, although it may also be located in the deeper parenchyma. Differentiating HA of the breast skin from low-grade MEC is diagnostically challenging, if not impossible, in a CNB [119–121]. An infiltrative growth pattern or irregular borders favor MEC, while the presence of ductal or tubular structures lined by SOX10-positive basophilic cuboidal cells is suggestive of HA [122]. Complete excision to evaluate the entire lesion is required for a definitive diagnosis.

Finally, although metastatic MEC from the salivary gland or other anatomic locations could be considered in the differential diagnosis, this is very unlikely. Salivary gland tumors rarely metastasize to the breast, and low-grade MEC does not carry a risk for distant metastasis. Nevertheless, clinical history is helpful in excluding metastasis. A DCIS component, if present, supports MEC of the breast.

Pathogenesis

MEC arising in salivary gland and other sites are characterized by recurrent chromosomal translocations involving the *MAML2* gene, most commonly t(11;19), which results in *CRTC1-MAML2* fusion, and less frequently t(11;15), which results in *CRTC3-MAML2* fusion [123–125]. *MAML2* gene rearrangements and *CRTC1-MAML2* fusions have also been identified in breast MEC by FISH, reverse transcription polymerase chain reaction (RT-PCR), and RNA sequencing [100, 105, 111, 112]. *MAML2* rearrangements are thus considered the hallmark genetic alteration of MEC regardless of anatomic location. Detection of *MAML2* rearrangement using a commercially available *MAML2* break-apart FISH probe (Fig. 12.33) or detection of *CRTC1-MAML2* fusion by RT-PCR or sequencing technologies can be performed on formalin-fixed paraffin-embedded tissue to confirm the diagnosis of this rare breast cancer subtype, especially in challenging CNB specimens.

CRTC1 (*C*REB *R*egulated *T*ranscriptional *C*oactivator) controls the expression of specific CREB-activated genes, and *MAML2* gene is a member of the mastermind-like family that augments Notch signaling. The *CRTC1-MAML2* fusion gene has been shown to activate Notch signaling and has transforming activity in cell lines, with silencing of the fusion inhibiting tumor growth [126]. Expression of *CRTC1-MAML2* in a transgenic mouse model causes formation of salivary gland tumors that resemble histological and molecular characteristics of human MEC [127]. Together, in vitro and in vivo studies support *CRCT1-MAML2* fusion as the major oncogenic driver in MEC.

In addition to *CRTC1-MAML2* fusions, breast MEC have been found to have simple genomes with no copy number alterations and a very low exonic mutational burden, similar to other fusion gene-driven special breast cancer subtypes (e.g., AdCC and secretory carcinoma) and distinct from high-grade TNBC of no special type [100].

Prognosis and Clinical Management

The prognosis of breast MEC is correlated with histologic grade and clinical stage. High-grade tumors portend aggressive behavior with frequent metastasis to axillary lymph nodes and distant organs. Approximately 30% of high-grade MEC in the literature developed distant metastasis and eventually led to death. In contrast, only rare axillary metastasis and no distant spread have been documented for low- and intermediate-grade MEC, and none of the patients died of disease [104, 105, 122]. Low-grade MEC of the breast can be considered to have indolent biological behavior and favorable clinical outcome, similar to other salivary gland-like carcinomas in the breast, such as AdCC and secretory carcinoma.

Given the rarity of MEC in the breast, there is limited data to guide treatment. Complete excision with clear margins has been proposed as the standard surgical approach. Most patients are not eligible for hormonal therapy due to the triple-negative status of these tumors. Radiation has been offered to some patients in case reports. Chemotherapy is not likely to be recommended for node-negative low-grade tumors [104, 105].

Secretory Carcinoma

Overview

Secretory carcinoma is a rare salivary gland-type breast carcinoma characterized by distinct morphologic and immunophenotypic features and underpinned by a hallmark t(12;15)(p13;q25) chromosomal translocation and resultant *ETV6-NTRK3* gene fusion. These tumors account for <0.05% of invasive breast carcinomas [128, 129]. Secretory carcinoma was initially described in children by McDivitt and Stewart and was called "juvenile breast carcinoma" [130] and remains the most common breast cancer of childhood. However, these tumors have subsequently been found to occur predominantly in adults [130–139], and the term juvenile breast carcinoma is not recommended. Unlike other salivary gland-type carcinomas of the breast, secretory carcinoma was first recognized in the breast, with analog tumors that harbor the same *ETV6-NTRK3* fusion (previously termed mammary analog secretory carcinomas [MASC]) subsequently described at other anatomic sites including salivary gland [140–143], sinonasal mucosa [144], skin [145–147], lung [148], vulva [149], and thyroid gland [150–152]. The number of salivary gland secretory carcinomas reported in the literature has now surpassed that of its breast counterpart.

Secretory carcinomas of the breast occur predominantly in women but may also be seen in men [128, 132, 133, 153, 154]. Most of these tumors present in the fourth to seventh decade (range 3–87 years), with a mean patient age of 53 [130–139, 154, 155]. The most common presentation is of a slow-growing, firm, painless, well-circumscribed, mobile breast mass, occasionally with nipple discharge. In women, secretory carcinomas most frequently arise in the upper outer quadrant or near the nipple, but any region of the breast can be involved, including ectopic breast tissue [130–133, 155,

156]. In children or men, the tumors commonly arise in the subareolar region [130, 132, 133].

Gross and Radiologic Features

Gross examination generally reveals a well-circumscribed mass with grayish-white or yellowish-tan, firm cut surfaces. Mean tumor size is approximately 1–2 cm, but a wide range in sizes has been reported (up to 16 cm) [128, 130–135, 137, 138, 157].

On ultrasound, secretory carcinoma presents as a well-circumscribed, round to oval, macrolobulated, isoechoic to hypoechoic, mass mimicking fibroadenoma [158–160] or sometimes as a hypoechoic, irregularly shaped, spiculated mass with heterogeneous internal echoes [161, 162]. Mammographic findings are variable and nonspecific, including a discrete nodular density with irregular margins [158, 159, 162, 163], heterogeneously dense pattern with no evidence of a mass [160], or as an isodensity mass with an obscured margin [161].

Microscopic Features

Secretory carcinomas are composed of polygonal tumor cells with moderate amounts of eosinophilic vacuolated or granular cytoplasm and rounded to oval nuclei, which infiltrate in various growth patterns, including microcystic/honeycomb, papillary, tubular, and solid (Fig. 12.34). Most tumors have mixed growth patterns. The microcystic spaces and tubular lumens are filled with prominent eosinophilic or amphophilic bubbly secretions. Intracellular secretory vacuoles and extracellular secretions stain positively for PASD, mucicarmine, and Alcian blue. The tumor nuclei are usually small to medium in size and rounded to oval with open, vesicular chromatin and small nucleoli (mild to moderate nuclear pleomorphism). Mitotic activity is generally low. Accordingly, the vast majority of secretory carcinomas are histological grade 1 or 2 by modified Scarff-Bloom-Richardson grading. High-grade tumors have been reported but are exceptionally rare [134]. The tumor stroma is often sclerotic. An in situ component may be present, usually with similar secretory features, low- or intermediate-grade nuclei, and cribriform and solid patterns [133, 135, 137, 154]. Distinction of in situ carcinoma from invasive carcinoma with microcystic architecture and rounded contours may be challenging by H&E alone and can be assisted with immunohistochemical stains for myoepithelial markers (Fig. 12.35). Pure secretory carcinoma in situ is exceedingly rare [164].

Immunohistochemistry

The tumor cells typically express S100 protein, CEA (polyclonal), mammaglobin, SOX10, and MUC4, usually in a strong and diffuse staining pattern (Fig. 12.36a–e). GATA3, CK8/18, CD117, and vimentin may also be positive. GCDFP-15 is usually negative or only focally positive (Fig. 12.36f). Most secretory carcinomas show a basal immunophenotype with expression of cytokeratins 5/6, 14, and 17 and EGFR, although positivity may be focal (Fig. 12.37) [132–134, 137, 139]. Secretory carcinomas are often triple negative for ER, PR, and HER2, although weak ER/PR expression is not uncommon [133, 134, 137]. The Ki-67 proliferation index is often <20% but variable across tumors [132, 134, 135].

Most secretory carcinomas show nuclear staining using a pan-TRK antibody [116, 165, 166] (Fig. 12.38). In one study, diffuse (>50% of cells) and/or at least focally strong nuclear staining was found to be sensitive (~83%) and specific (100%) for the diagnosis of breast secretory carcinoma [116]. Cytoplasmic staining is not specific in this context.

Differential Diagnosis

The architectural pattern (microcystic/fenestrated, papillary, tubular, or solid), cytologic features (ample eosinophilic, clear, or vacuolated cytoplasm), and prominent secretory material in secretory carcinoma can mimic several benign and malignant lesions of the breast, especially in a limited CNB sample.

Lactational or lactational-like change: Secretory carcinoma bears superficial resemblance to lactational (or lactational-like) change, as both lesions feature prominent eosinophilic secretions and epithelial cells with vacuolated cytoplasm (Fig. 12.39a, b). However, lactational change is a lobulocentric process and lacks microcystic, papillary, or solid architecture, whereas secretory carcinoma has infiltrative growth with various architectural patterns. In challenging cases with limited material, immunohistochemical stains with myoepithelial markers and pan-TRK antibody can help with the differential diagnosis [116]. The glands of lactational change have intact myoepithelial layers and lack nuclear pan-TRK expression.

Cystic hypersecretory lesions: Secretory carcinoma may also be confused with cystic hypersecretory lesions (including cystic hypersecretory hyperplasia and cystic hypersecretory carcinoma), as these lesions all have densely eosinophilic (thyroid colloid-like) secretions that may retract from the luminal epithelium (Fig. 12.39c, d). However, the tinctorial
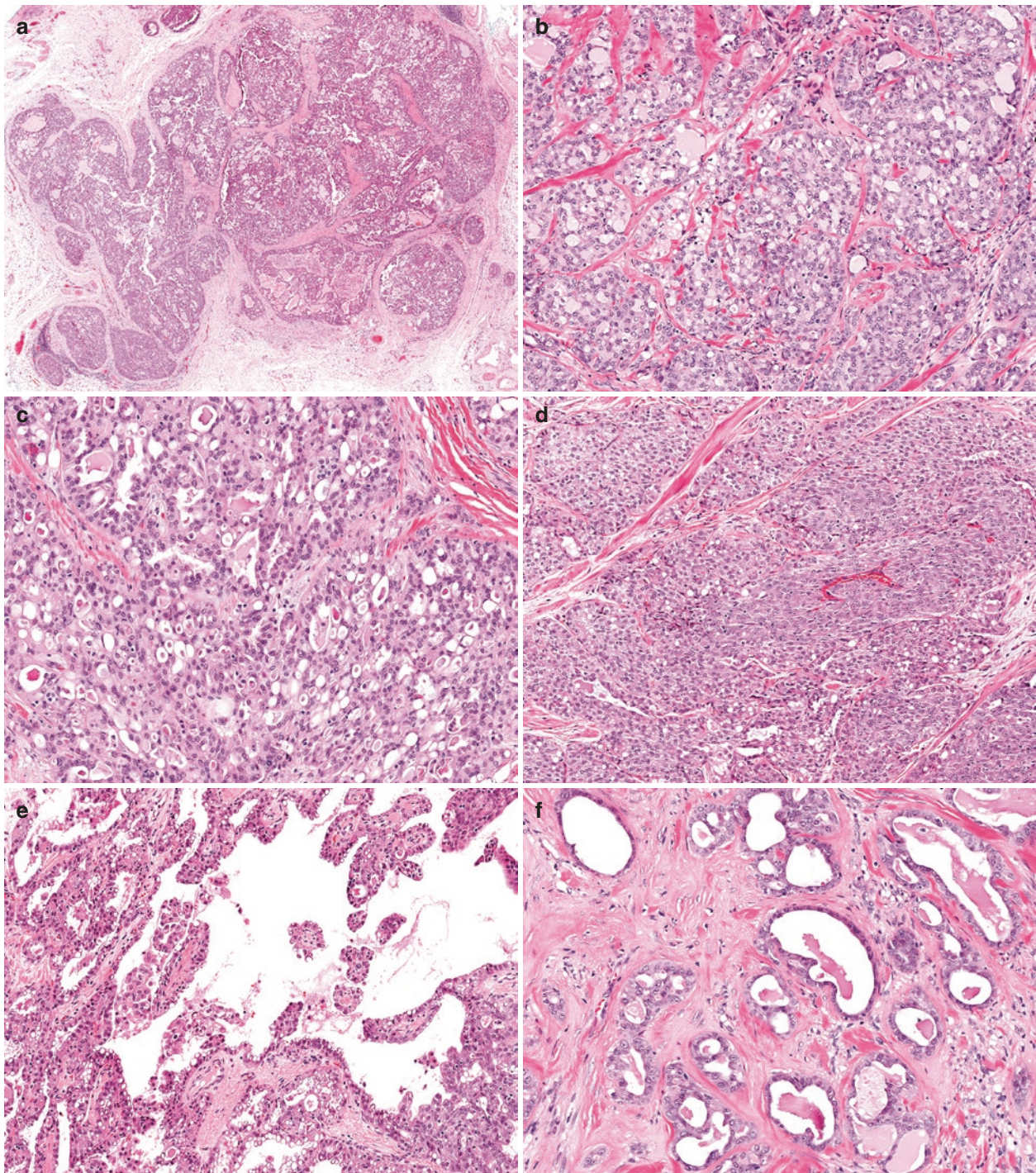
Fig. 12.34 Secretory carcinoma, histologic features. (**a**) Low magnification demonstrates tumor cells arranged in glandular structures and nests of variable size and shape within a fibrotic/sclerotic stroma. The tumor cells are organized in various architectural patterns, including microcystic/fenestrated/honeycomb pattern (**b**, **c**), solid nests (**d**), papillary structures (**e**), and tubular/follicular pattern (**f**). The microcystic pattern is usually the predominant architectural component. However, these patterns are often admixed in various proportions in an individual tumor. Note that the glandular spaces contain prominent secretions, which may be densely eosinophilic (thyroid colloid-like), amphophilic, or basophilic (mucin-like) and often have a bubbling appearance. (**g**, **h**) Cytologically, the tumor cells have moderate to abundant eosinophilic to vacuolated cytoplasm and low-to intermediate-grade nuclei that are usually oval in shape with small nucleoli. Note the vacuolated/bubbly cytoplasm in (**h**). (**i**) In rare examples, scattered tumor cells may have apocrine features, with coarse eosinophilic granules that can be highlighted by GCDFP-15 immunohistochemical stain (*not shown*). (**j**) This tumor shows higher grade nuclear features than is typical, with enlarged nuclei, vesicular chromatin, and prominent nucleoli. Rare tumors with high-grade nuclei, increased mitotic activity and necrosis have been reported and are associated with more aggressive behavior. (**k**, **l**) In this core needle biopsy, the characteristic microcystic glandular pattern with prominent secretions and cytologically bland tumor cells can be appreciated to suggest the diagnosis, which can be confirmed with appropriate immunohistochemical stains and *ETV6* FISH
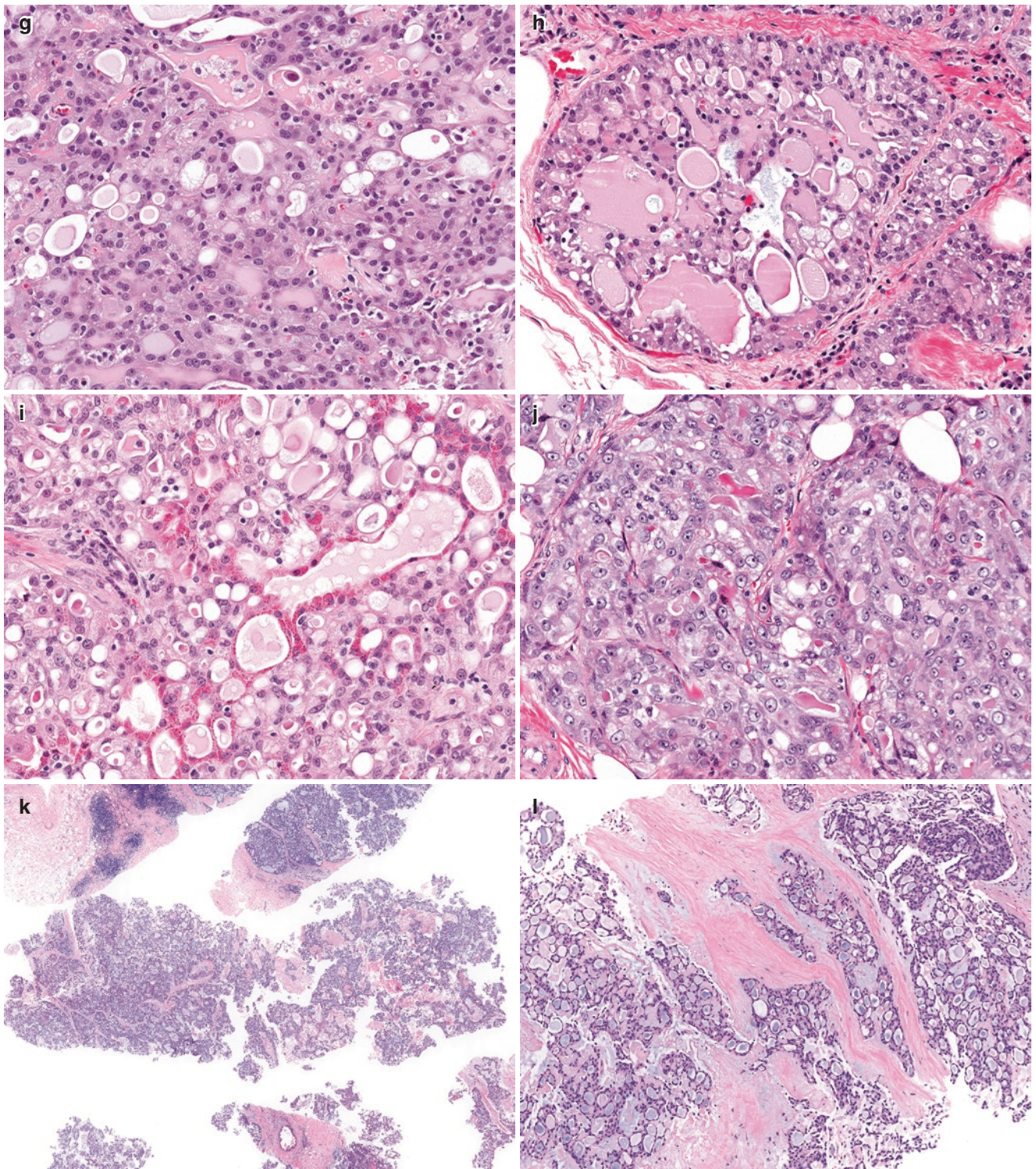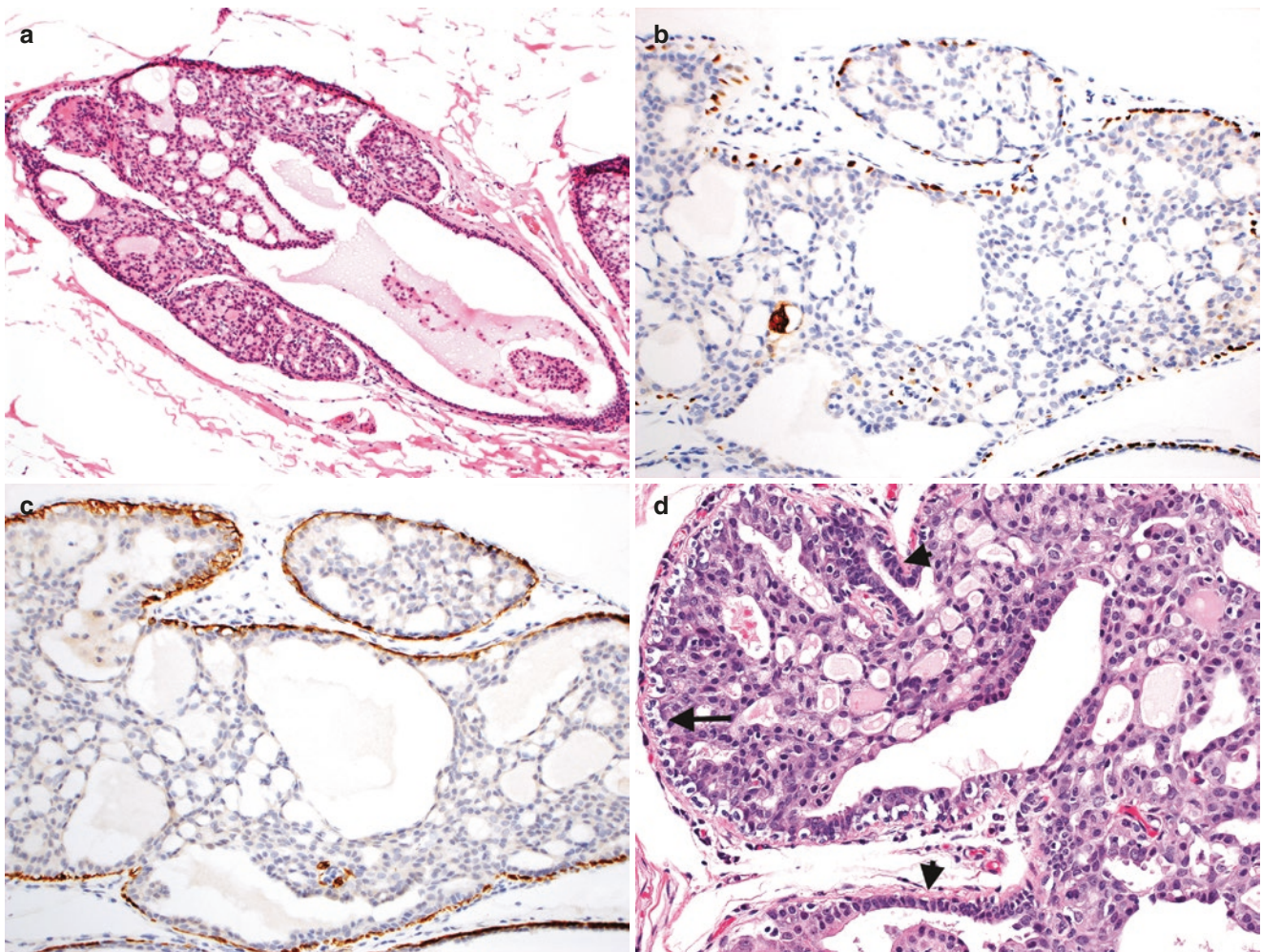
Fig. 12.34 (continued)

Fig. 12.35 Secretory carcinoma, in situ component. (**a–c**) An in situ component may be present in some cases and typically demonstrates a cribriform/fenestrated pattern, prominent eosinophilic secretions in the glandular spaces, and low- to intermediate-grade nuclei, as appreciated on the H&E stain (**a**) in this example. Immunohistochemical stains for myoepithelial markers p63 (**b**) and SMM (**c**) highlight the peripheral myoepithelial layer and support an in situ lesion. (**d**) Another example of secretory carcinoma in situ. Note the layer of myoepithelial cells with clear cytoplasm at the periphery of the duct (*arrows*) and residual normal luminal epithelium (*arrowheads*)

quality of the secretions is different: the secretions in cystic hypersecretory lesions often show parallel linear cracks (but not always), while secretions in secretory carcinoma have an overall bubbling appearance without parallel linear cracks. Cystic hypersecretory lesions are not infiltrative and lack expression of nuclear pan-TRK and basal markers (CK5/6 and EGFR). Most cystic hypersecretory lesions are ER positive (see also Chap. 13).

Usual ductal hyperplasia: In a limited CNB sample, the microcystic/fenestrated pattern, bland cytologic features, and patchy CK5/6 expression of secretory carcinoma may mimic usual ductal hyperplasia (Fig. 12.39e). The prominent luminal secretions and negative (or minimal) ER expression are clues to reconsider the diagnosis.

Low-grade mucoepidermoid carcinoma: A major differential diagnostic consideration for secretory carcinoma is low-grade MEC. These two salivary gland-type carcino-mas share overlapping architectural patterns, PASD-positive secretions, bland cytologic features, and a similar immunophenotype, which includes positive mammaglo-bin, MUC4, and CK5/6 and triple-negative biomarker sta-tus (see also section "Mucoepidermoid Carcinoma" in this chapter and Fig. 12.32). Distinction of the two can be facilitated by FISH using *MAML2* and *ETV6* break-apart probes to identify the hallmark rearrangements of each (Figs. 12.33 and 12.38a), and/or pan-TRK immunohisto-chemistry (Fig. 12.32).

Acinic cell carcinoma: Secretory carcinoma may be confused with acinic cell carcinoma when the latter has follicu-lar and/or solid architecture, luminal secretions, and clear cytoplasm with less conspicuous cytoplasmic granules. Furthermore, both tumor types are strongly S100 positive. However, the large PASD-positive cytoplasmic zymogen-like granules typical of acinic cell carcinoma are absent in
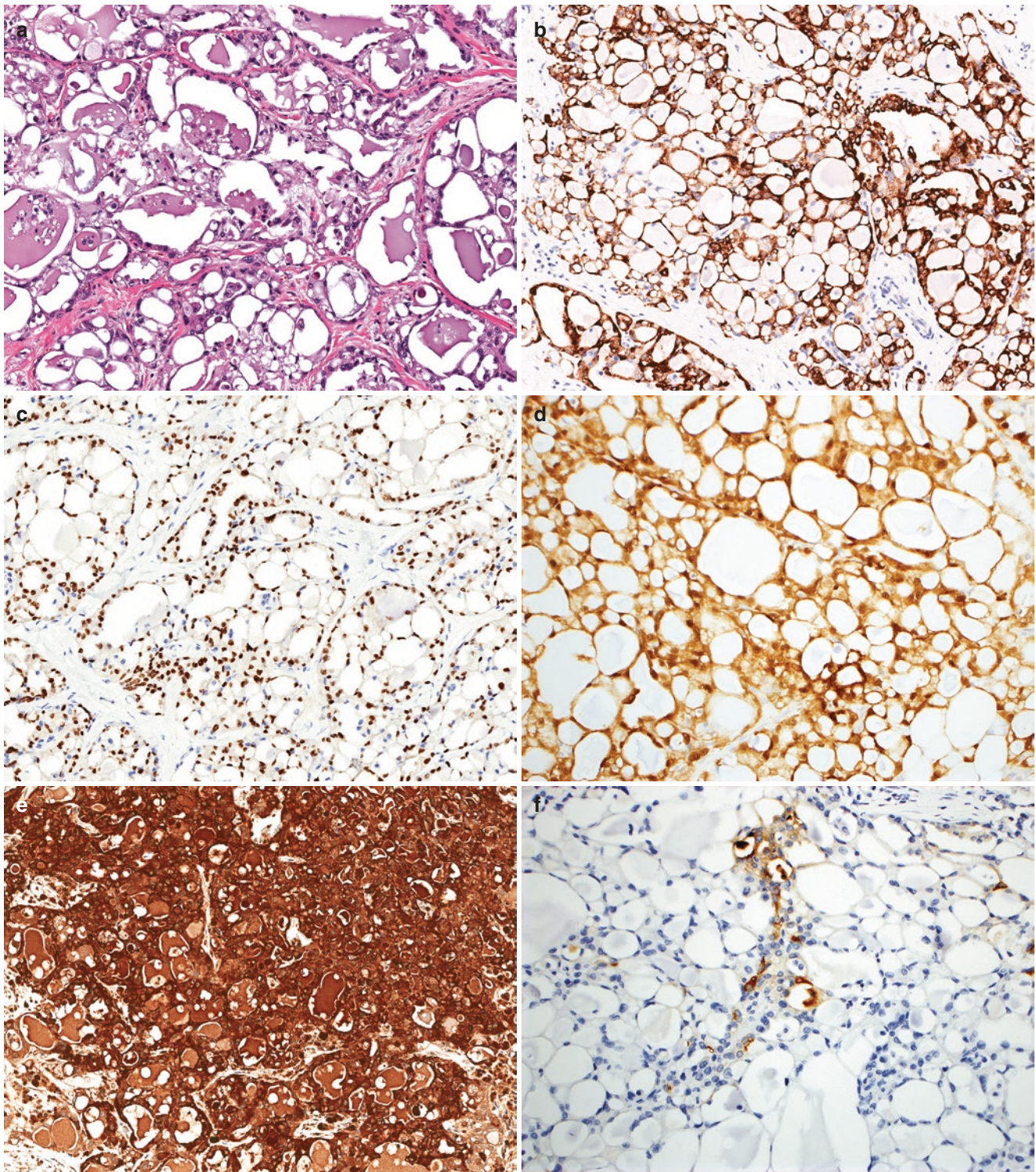
Fig. 12.36 Secretory carcinoma, immunohistochemical profile. Although not specific, secretory carcinoma (**a**) shows a characteristic immunostaining pattern that is helpful in establishing the diagnosis. This includes typically diffuse and strong immunoreactivity to MUC4 (**b**), SOX10 (**c**), S100 protein (**d**), and mammaglobin (**e**). Most tumors are either negative or only focally positive for GCDFP-15 (**f**). However, rare examples with strong GCDFP-15 expression have been noted
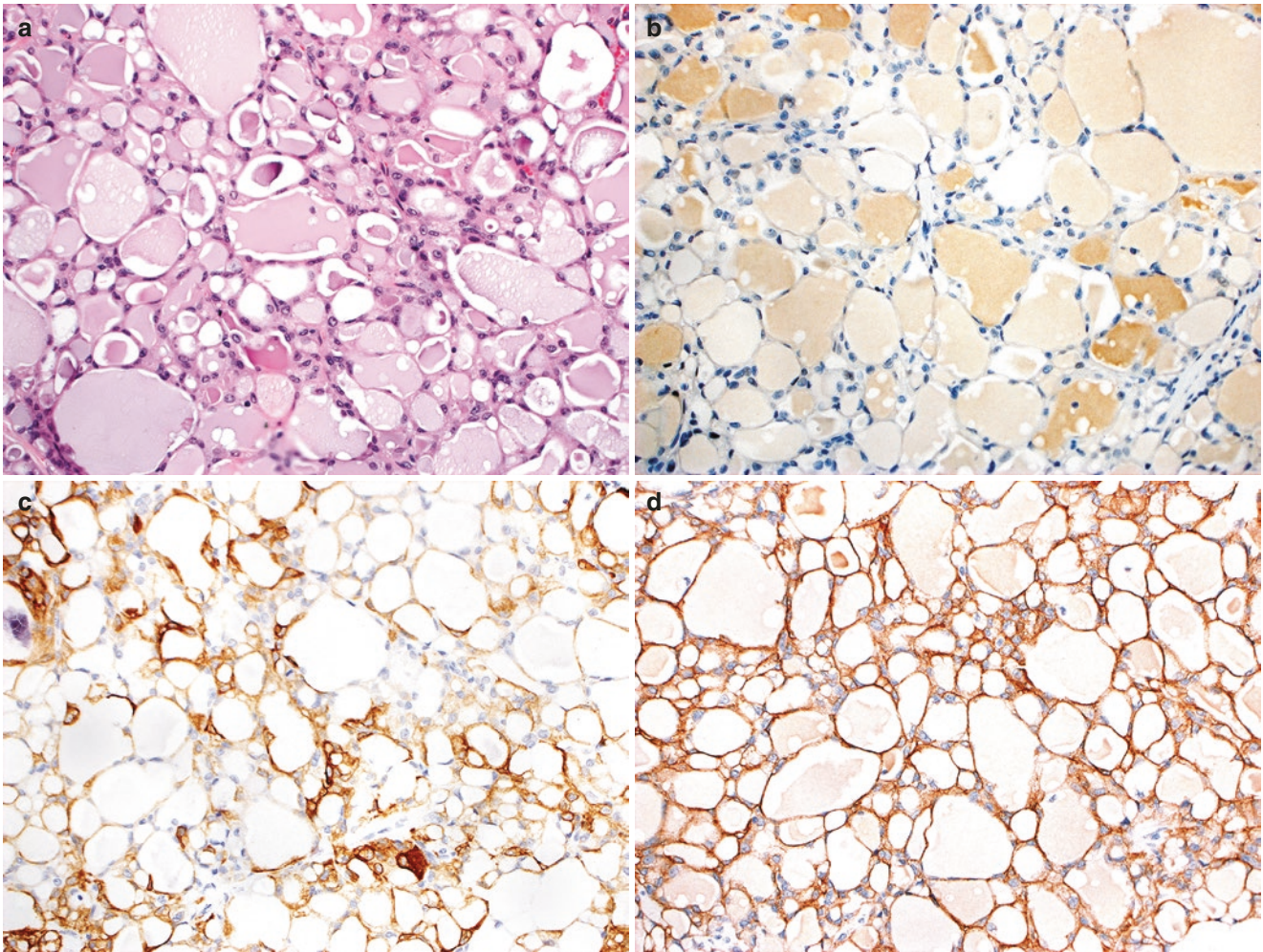
Fig. 12.37 Secretory carcinoma, basal-like immunophenotype. (**a**, **b**) Most secretory carcinomas are negative for ER (**b**), PR (*not shown*) and HER2 (*not shown*). These tumors usually express basal markers, such as CK5/6 (**c**) and EGFR (**d**), although expression may be focal
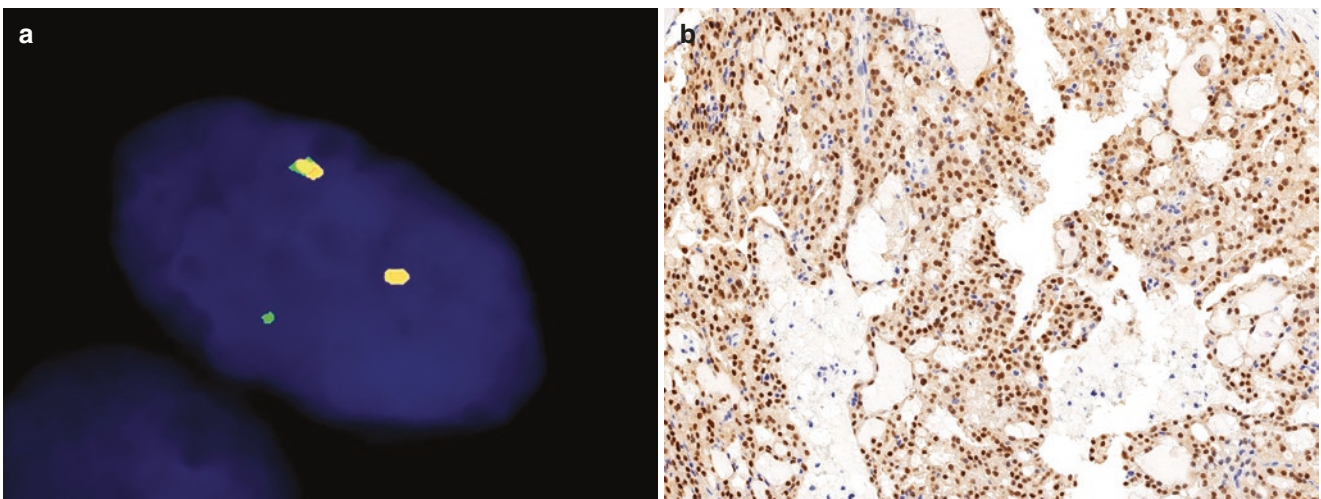

Fig. 12.38 *ETV6-NTRK3* and pan-TRK immunohistochemistry in secretory carcinoma. (**a**) *ETV6* rearrangement can be demonstrated by fluorescence in situ hybridization using an *ETV6* break-apart probe. Note the separate green and orange signals from the rearranged *ETV6* allele and the single fused yellow signal from the other intact *ETV6* allele. The *ETV6-NTRK3* fusion can be directly detected using *ETV6* and *NTRK3* convergence probes (*not shown*) or next-generation sequencing methods. (**b**) Overexpression of the chimeric ETV6-NTRK3 protein can be detected using a pan-TRK antibody, which shows diffuse and/or at least focally strong nuclear staining
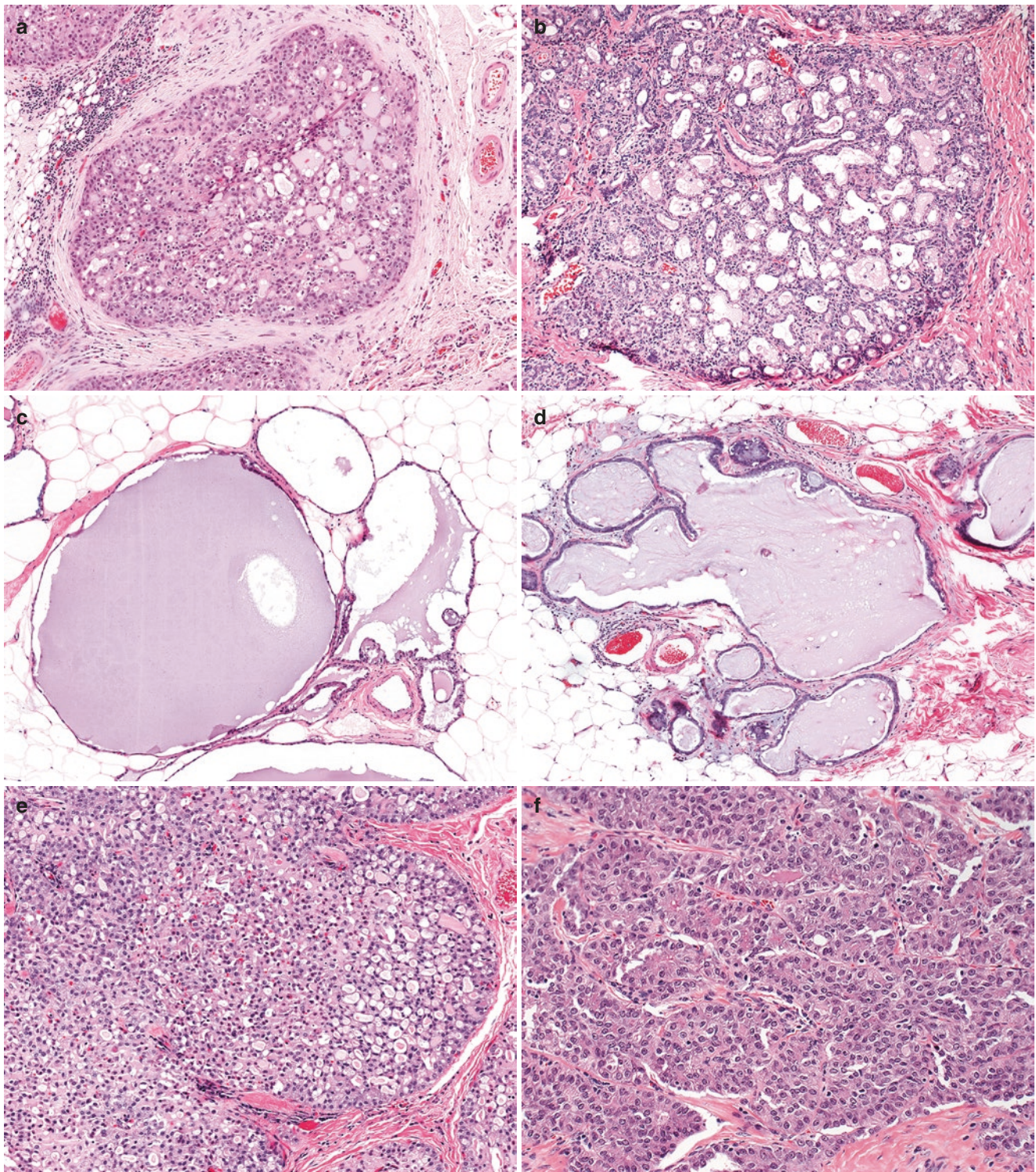
Fig. 12.39 Secretory carcinoma, morphologic mimics. Secretory carcinoma can mimic a number of benign and malignant breast lesions. At low power, the prominent secretions and vacuolated cytoplasm in secretory carcinoma (**a**) can resemble lactational change (**b**). Secretory carcinoma (**c**), especially the follicular pattern, can mimic atypical cystic hypersecretory hyperplasia (**d**). Sometimes, secretory carcinoma with fenestrated pattern and bland cytology (**e**) can be misconstrued as usual ductal hyperplasia. Secretory carcinoma with solid nested pattern and eosinophilic cytoplasm (**f**) may be confused with apocrine carcinoma (**g**). (**h**) The dense eosinophilic secretions in this secretory carcinoma impart a thyroid colloid-like appearance, which could suggest metastatic follicular thyroid carcinoma. The triple-negative biomarker profile may further complicate the issue. Strong mammaglobin expression that is typical of secretory carcinoma would help exclude a metastatic carcinoma
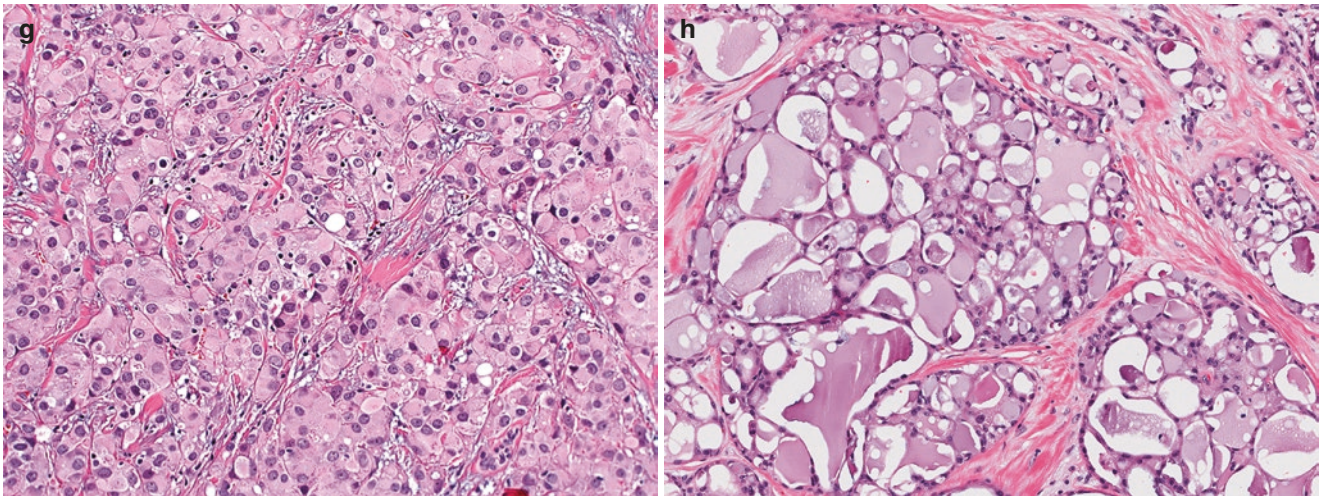
Fig. 12.39 (continued)

secretory carcinoma. Acinic cell carcinoma lacks *ETV6-NTRK3* and is negative for nuclear pan-TRK expression (see also sections "Carcinoma with Apocrine Differentiation" and "Differential Diagnosis" in this chapter).

Carcinoma with apocrine differentiation: Secretory carcinoma can mimic carcinoma with apocrine differentiation, especially when growing in tubular and solid patterns (Figs. 12.34i and 12.39f, g). Carcinoma with apocrine differentiation lacks the typical luminal secretions of secretory carcinoma and the apocrine cells have round nuclei with prominent nucleoli. Immunohistochemically, carcinoma with apocrine differentiation typically shows diffuse and strong expression of GCDFP-15 and AR, and is negative for mammaglobin, S100 protein, and pan-TRK antibody.

Tall cell carcinoma with reversed polarity: TCCRP is another potential consideration in the differential diagnosis of secretory carcinoma, as both tumor types can have papillary and follicular components, eosinophilic colloid-like secretions, and epithelial cells with abundant eosinophilic cytoplasm and low- to intermediate-grade nuclei. Both tumors also share a triple-negative and CK5/6-positive, basal-like immunoprofile. However, TCCRP exhibits distinguishing cytological features, including reverse polarization, nuclear grooves, and cytoplasmic pseudoinclusions. In contrast to secretory carcinoma, TCCRP shows variable and less mammaglobin expression and is negative or only focally positive for S100 protein. Recurrent *IDH2* hotspot mutations of TCCRP can be detected by IDH2 R172 mutant-specific immunohistochemical stain (see also section "Tall Cell Carcinoma with Reversed Polarity" in this chapter).

Pathogenesis

Secretory carcinoma canonically harbors a t(12;15)(p13;q25) chromosomal translocation that results in an *ETV6-NTRK3* fusion gene, which has been identified in both in situ and invasive carcinoma components, consistent with an early oncogenic event [133, 137, 154, 167]. The rearrangement joins the N-terminal dimerization domain of *ETV6* with the C-terminal tyrosine kinase domain of *NTRK3* to produce a ligand-independent, constitutively activated chimeric tyrosine kinase that signals through RAS-mitogen activated protein kinase (MAPK) and PI-3 K pathways and can transform cells of multiple lineages [133, 167–173]. *ETV6-NTRK3* has also been described in secretory carcinomas arising in other anatomic sites [133, 141, 146, 151]. Together, the shared morphologic, immunophenotypic, and genetic features of secretory carcinomas are consistent with a common pathogenesis for these tumors, regardless of anatomic site. Secretory carcinomas with *ETV6* rearrangements lacking *ETV6-NTRK3* fusions have been described in the salivary gland, with identified fusions in these tumors including *ETV6-RET*, *ETV6-MAML3*, and *ETV6-MET* [174–181]. However, such alternate fusions have not been identified in secretory carcinomas of the breast.

Consistent with *ETV6-NTRK3* as the main oncogenic driver of secretory carcinomas, targeted DNA sequencing of primary breast and salivary gland secretory carcinomas did not identify additional driver mutations in these tumors, which were additionally found to have a low exonic mutational burden and quiet genomes with no to few chromo-

somal copy number changes and no focal amplifications or deletions [133]. Accordingly, secretory carcinomas of the breast are genetically distinct from invasive breast carcinomas of no special type (IBC-NST), including common basal-like carcinomas. Instead, akin to other fusion gene-driven salivary gland-like breast carcinomas (AdCC, MEC), secretory carcinomas appear to be genetically more similar to their counterparts at other anatomic sites [45, 100, 133]. A recent study found additional aberrations in distant metastases of two aggressive secretory carcinomas, including amplification of the 16p13.3 locus (containing *PDPK1*), a hotspot *TERT* promotor mutation, and loss of 9p21.3 locus (*CDKN2A, CDKN2B*) [154].

In addition to secretory carcinomas, *ETV6-NTRK3* fusions have been described in a variety of other tumor types, including infantile fibrosarcoma [182], cellular mesoblastic nephroma [183], glioma [165], acute myeloid leukemia [184], ALK-negative inflammatory myofibroblastic tumor [185], Spitz-tumor [186], and radiation-induced thyroid carcinoma [152]. However, *ETV6-NTRK3* appears to be specific for secretory carcinoma in the context of breast cancer and has not been identified in other breast carcinomas [187]. Detection of the hallmark translocation or gene fusion by FISH or next-generation sequencing analysis, respectively, can be used to confirm the diagnosis. *ETV6* break-apart (likely most often used) (Fig. 12.38a), *NTRK3* break-apart, and *ETV6-NTRK3* convergence probes (most specific) are commercially available. In addition, immunohistochemistry using a pan-TRK antibody has been shown to be a highly specific (100%) and slightly less sensitive (~83%) marker for secretory carcinoma in the breast (Fig. 12.38b). In addition to its diagnostic utility, demonstration of the *ETV6-NTRK3* fusion has additional clinical value, as *ETV6-NTRK3* fusions may be targeted for treatment (see sections "Prognosis and Clinical Management").

Prognosis and Clinical Management

Secretory carcinomas generally have an indolent clinical course with favorable outcome, especially in children and young adults and even in the context of axillary nodal metastasis [128, 130, 131, 137]. Five- and ten-year survival rates are 87% and 77%, respectively, and 5- and 10-year cause-specific survival rates are 94% and 91%, respectively [128]. Axillary metastases have been reported in ~20–35% of patients overall [128, 131–134, 154]. Recurrences and distant metastases are uncommon, and

deaths are rare [131, 134, 153, 154, 157]. However, some tumors, often in older adult patients, may be more aggressive [154, 157].

The primary treatment is surgical excision to negative margins with sentinel lymph node sampling [128, 162, 188]. In children, preservation of breast tissue is attempted if possible to ensure normal breast development [188]. The efficacy of adjuvant radiation is uncertain, but radiotherapy has been reported to be increasingly used in adults [128]. Similarly, the role of chemotherapy is unknown, although reports suggest poor responses in patients with metastatic tumors [189]. Small molecule inhibitors (larotrectinib, entrectinib) targeting NTRK3 and other NTRK family members show promising efficacy in patients with TRK fusion cancers [190–192], including breast secretory carcinoma [193].

Carcinoma with Apocrine Differentiation

Overview and Clinical Presentation

Carcinoma with apocrine differentiation is defined as invasive carcinoma with cytologic features of apocrine cells in more than 90% of the tumor cell population [194]. However, recognition of what constitutes apocrine cytology can be subjective, especially at the lower end of the morphologic spectrum, and variable apocrine cytologic features can also be seen in other subtypes of breast carcinomas, including IDC (of no special type), lobular, micropapillary, mucinous, and papillary carcinomas. Furthermore, carcinomas with apocrine morphology can vary in terms of ER and HER2 status and exhibit heterogeneous intrinsic gene expression patterns [37, 195]. Gene expression signatures associated with these tumors (molecular apocrine, luminal androgen receptor [LAR]) lack ER and are enriched for AR expression and hormonally regulated pathways, but do not exclusively correlate with apocrine histology [196, 197]. It is therefore not surprising that different series in the literature have reported variable clinical outcomes for invasive carcinomas with apocrine features. A combination of apocrine cytomorphology and immunophenotype (ER and PR negative, AR positive) has been used to refine the classification. As such, these tumors, which may be triple negative or HER2 positive, have also been referred to as pure apocrine carcinomas, and comprise a subset of the carcinomas identified as LAR or molecular apocrine by gene expression [196–198]. Invasive carcinomas with apocrine morphologic features but lacking the above immunophenotype have been referred to as apocrine-like car-

cinomas [194, 199, 200]. For the purpose of discussion in this chapter, apocrine carcinoma is used synonymously with carcinoma with apocrine differentiation and defined by cytologic features. The term pure apocrine carcinoma is adopted when the tumor is known to also demonstrate an ER- and PR-negative and AR-positive immunophenotype.

Using strict diagnostic criteria, apocrine carcinoma is rare and comprises <1% of all breast cancers [201–203]. The clinical presentation is similar to IBC-NST. Patients may be asymptomatic or present with a hard, palpable, irregular breast lump with or without skin or nipple retraction. Presentation with bloody nipple discharge is uncommon [194]. Apocrine carcinoma is usually unilateral but can be multifocal/multicentric, and rare cases of bilateral tumors considered to be independent primaries have been reported [204]. Overall, patients tend to be postmenopausal and older than patients presenting with IBC-NST [205–214].

Gross and Radiologic Features

Imaging and gross pathologic findings are not distinctive from IBC-NST. Triple-negative apocrine carcinomas (TNAC) have been reported to be smaller than IBC-NST [208, 210, 212, 213, 215].

Microscopic Features

Microscopically, apocrine carcinomas demonstrate architectural growth patterns similar to those of IBC-NST but differ in their cytologic appearance [216] (Fig. 12.40). These tumors are characteristically composed of large cells with abundant cytoplasm, round and/or pleomorphic vesicular nuclei and prominent nucleoli, occasionally associated with apical cytoplasmic "snouts" projecting into the glandular
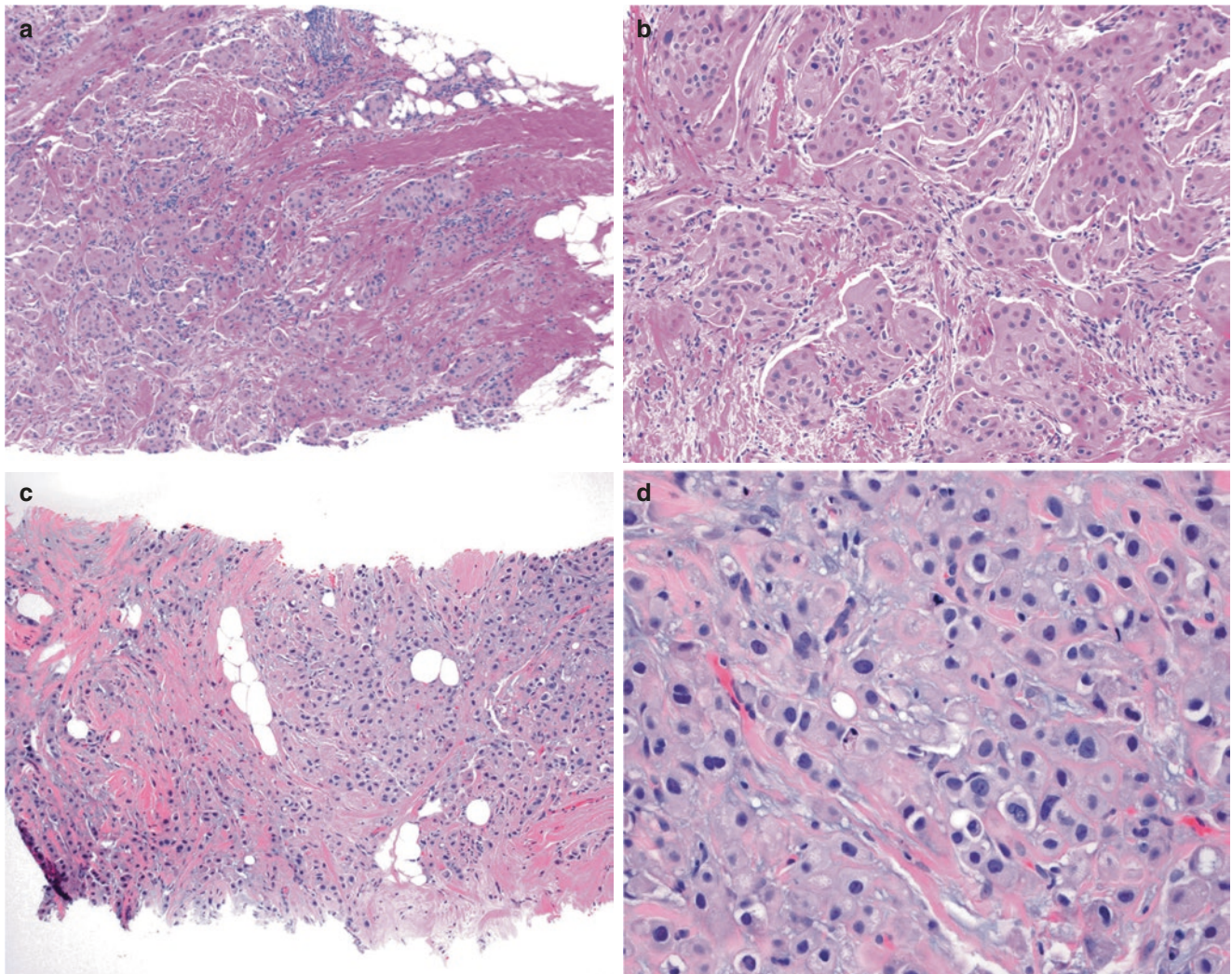

Fig. 12.40 Core needle biopsy showing growth patterns of invasive apocrine carcinoma. (**a–d**) Most apocrine carcinomas invade as irregular nests and small tumor clusters. (**e–g**) In some cases, glandular dif-ferentiation is present, which rarely exceeds 75%. (**h**) Note the apical cytoplasmic snouts projecting into the glandular lumens of this case
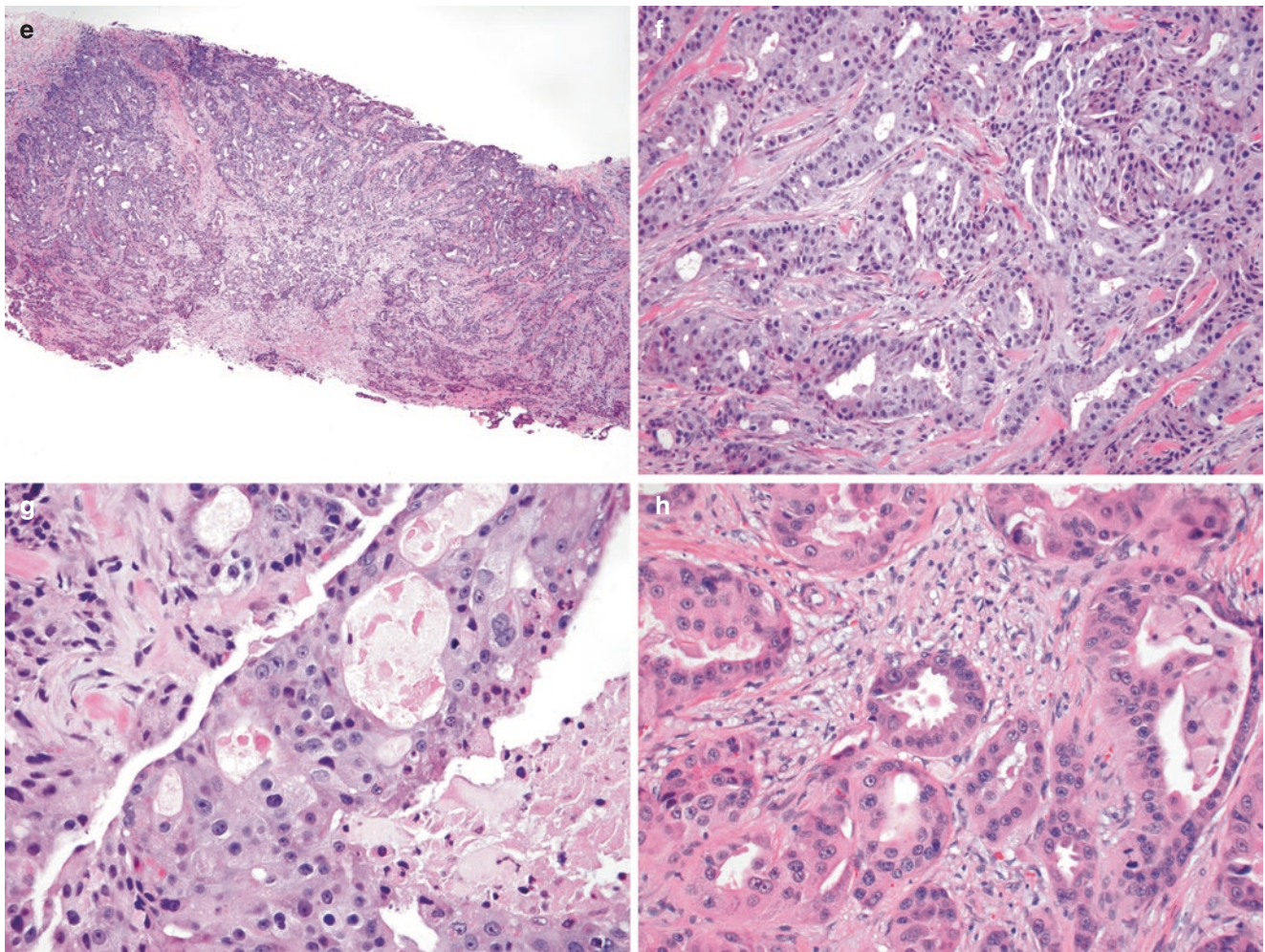
Fig. 12.40 (continued)

lumen (Figs. 12.40h and 12.41). The nuclear chromatin is irregular and often condensed along the periphery of the nuclear membrane. The cell borders are typically sharply defined (Fig. 12.41b) but may be indistinct in some cases (Fig. 12.42h, i). The abundant cytoplasm is eosinophilic, granular, and diastase-resistant periodic-acid-Schiff (PAS) positive (type A cells), vacuolated clear or foamy (type B cells), or a combination of both (Figs. 12.41 and 12.43). Intracytoplasmic lipid, as well as intracytoplasmic and intraluminal mucin, has also been observed (Fig. 12.41b). The majority of these tumors exhibit moderate nuclear pleomorphism, and tubule formation is rarely greater than 75% (Fig. 12.40e–g). Mitotic activity is often moderate or high. Most apocrine carcinomas are graded as modified SBR grade 2 or 3 [217]. TNAC tends to be of lower histological grade (predominantly grade 2) than other TNBC [203, 208, 212,

215]. The in situ component, when present, usually also demonstrates apocrine features, often with intermediate to high nuclear grade with or without comedo necrosis [202] (Fig. 12.44).

Pleomorphic invasive lobular carcinoma may also show apocrine differentiation (Fig. 12.45), and an apocrine variant of pleomorphic lobular carcinoma in situ has been characterized [218–221]. Histiocytoid carcinomas are rare, mostly lobular, invasive carcinomas that may show apocrine features. The neoplastic cells have indistinct borders, abundant foamy or eosinophilic cytoplasm, and regular to slightly pleomorphic nuclei, resembling histiocytes [222]. However, none of these tumors are classified as apocrine carcinomas (see also Chap. 14—Atypical Lobular Hyperplasia and Lobular Carcinoma in Situ and Chap. 15—Invasive Lobular Carcinoma).
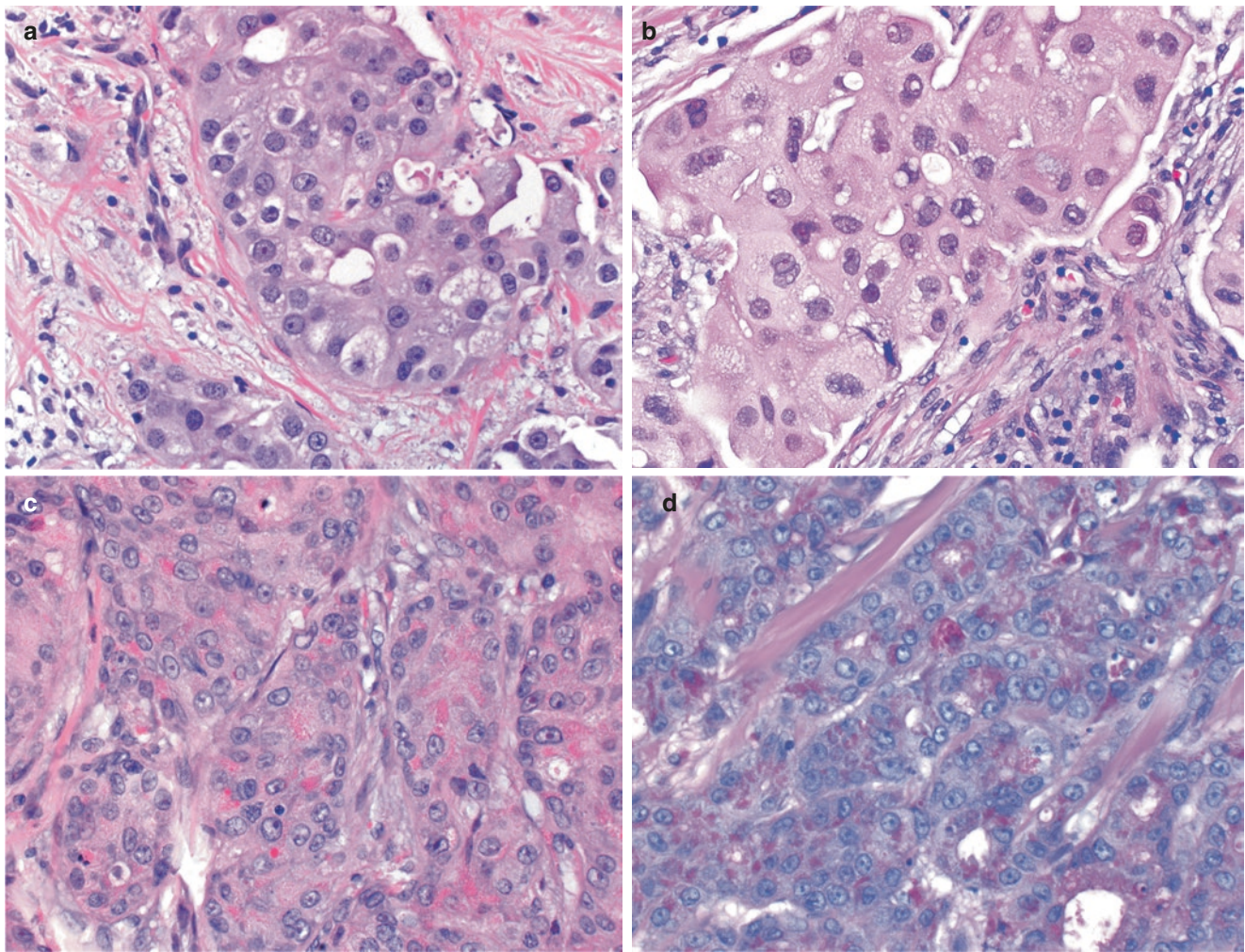
Fig. 12.41 Cytologic features of invasive apocrine carcinoma, granular variant (type A). (**a**) The tumor cells are large with sharply defined borders, abundant eosinophilic granular cytoplasm, and rounded pleomorphic nuclei with vesicular chromatin and prominent nucleoli. (**b**) Rare cases may demonstrate intracytoplasmic mucin. (**c**, **d**) This example shows prominent, coarse, and brightly eosinophilic cytoplasmic granules, which are highlighted by diastase-resistant PAS stain

Immunohistochemistry

ER, PR, AR, and HER2 Biomarkers

The majority of apocrine carcinomas are negative for ER and PR and demonstrate strong AR expression (Fig. 12.46) [199, 223]. Pure apocrine carcinomas are by definition ER negative, PR negative, and AR positive (at least 10% of cells has been suggested) [199]. The ERα isoform ER-α36 was found to be frequently overexpressed in pure apocrine carcinoma [36]. AR expression is much less common in ER-negative carcinomas compared to ER-positive/luminal carcinomas but is not entirely unique to apocrine carcinomas among ER-negative tumors [197, 224, 225]. In contrast to pure apocrine carcinomas, only ~58% of molecular apocrine tumors were found to express AR by immunohistochemistry in one study, despite high AR mRNA expression [197]. AR expression has been associated with HER2 overexpression and/or *ERBB2* amplification [199, 226]. HER2 overexpression and *ERBB2* amplification have been observed in up to 57% of pure apocrine carcinomas [199], which is significantly higher than the incidence of HER2 overexpression in IDC-NST. The remaining pure apocrine carcinomas are triple negative (TNAC) [199, 203]. HER2 overexpression has been inversely correlated with EGFR expression in apocrine carcinomas, with the vast majority of TNAC overexpressing EGFR [199].
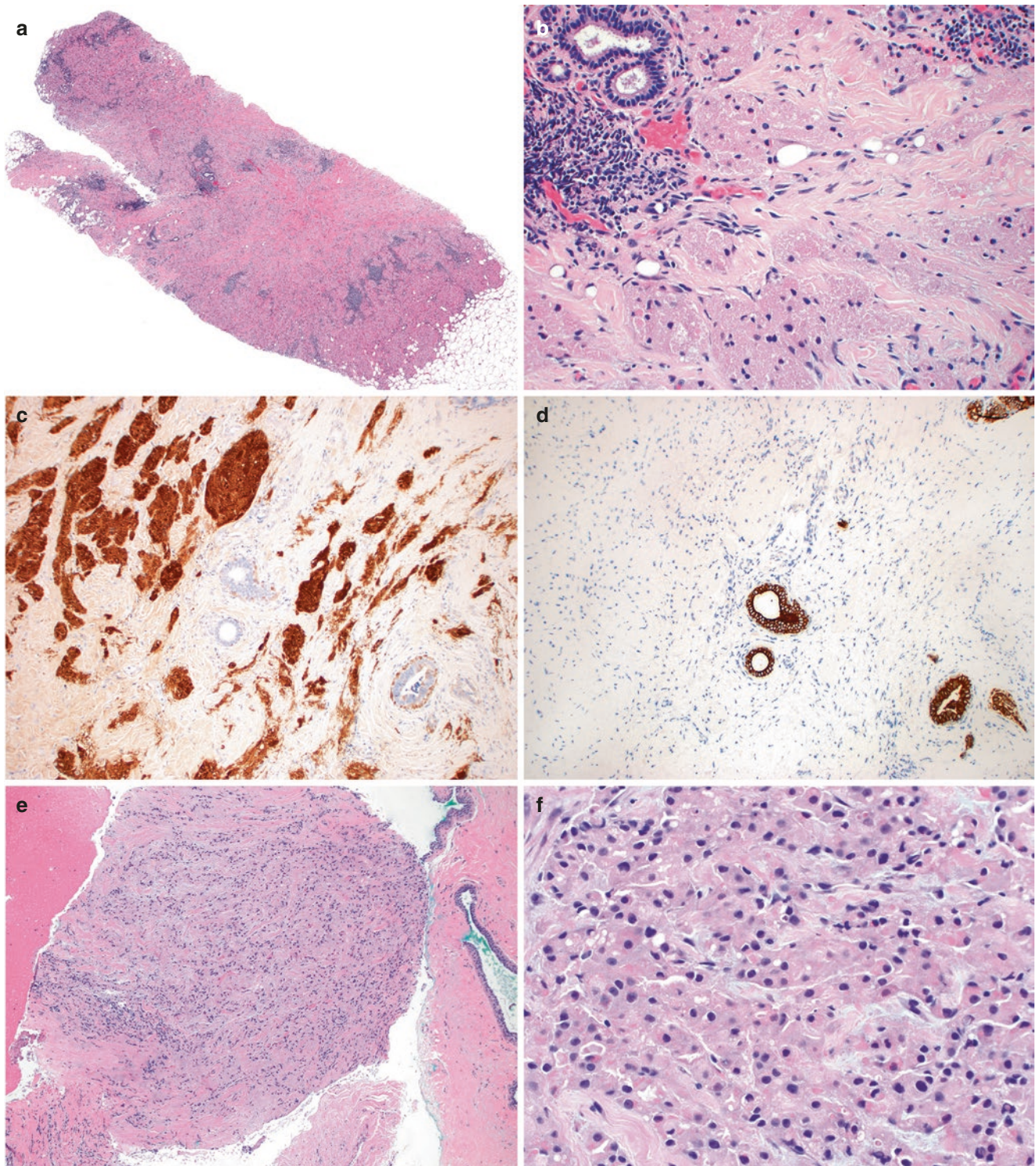
Fig. 12.42 Granular cell tumor may mimic invasive apocrine carcinoma. (**a**, **b**) Granular cell tumor shows infiltrating clusters of epithelioid cells with abundant granular eosinophilic cytoplasm, which may mimic apocrine carcinoma (**e**, **f**). Note the small, bland nuclei of granular cell tumor, in contrast to the larger, more atypical nuclei of apocrine carcinoma. Granular cell tumors (**c**) show strong and diffuse positivity for S100 protein, (**d**) but are negative for keratin, (**g**) in contrast to apo-

crine carcinomas. (**h–k**) The invasive component of this apocrine carcinoma (**h**, **i**) shows infiltrative tumor cell clusters with indistinct cell borders and abundant granular eosinophilic cytoplasm in a dense sclerotic stroma, mimicking granular cell tumor. (**j**) In this case, an associated in situ component shows well-developed apocrine features and is useful to help establish the correct diagnosis. (**k**) An immunostain for ER is negative in invasive apocrine carcinoma (and granular cell tumor)

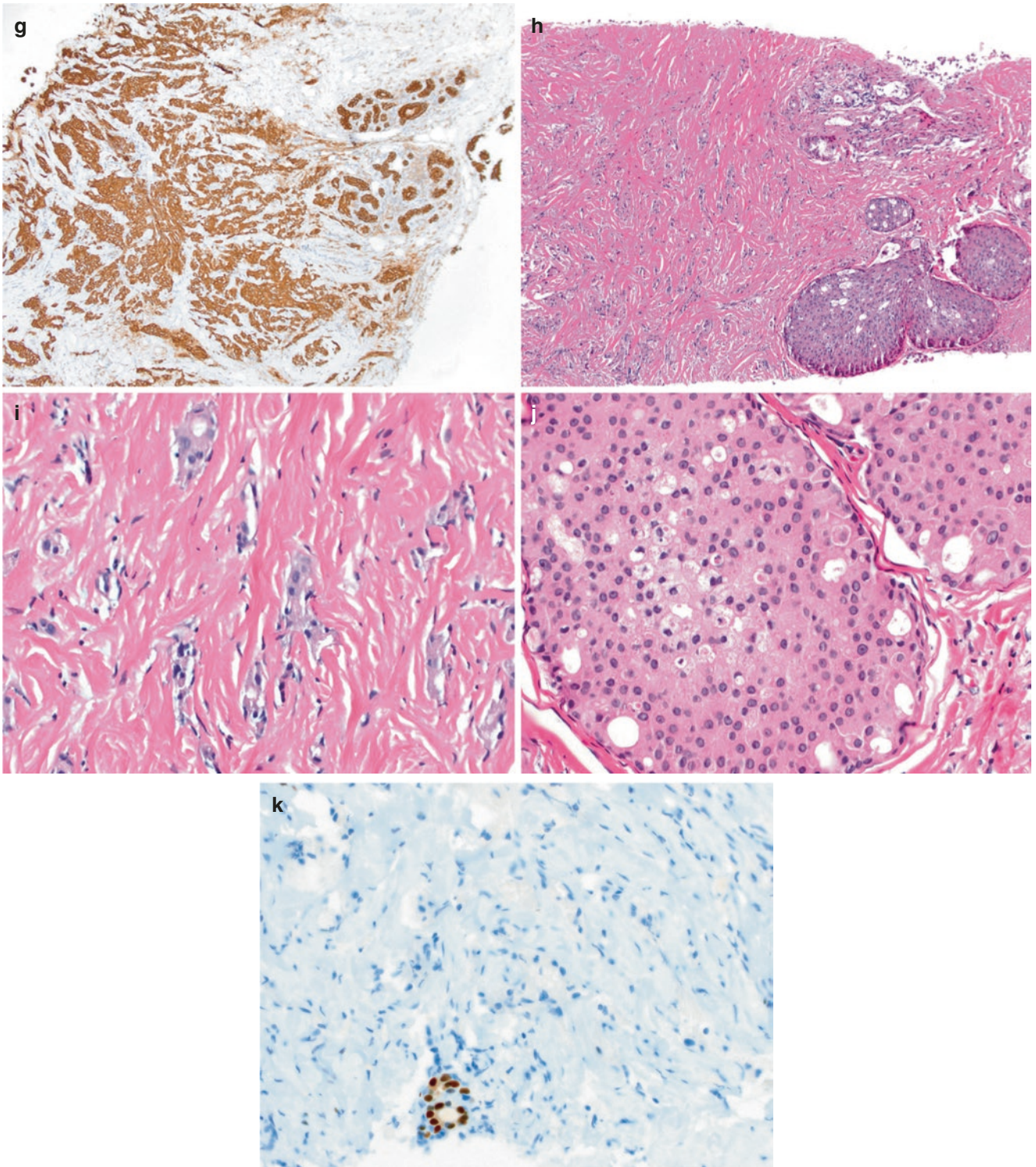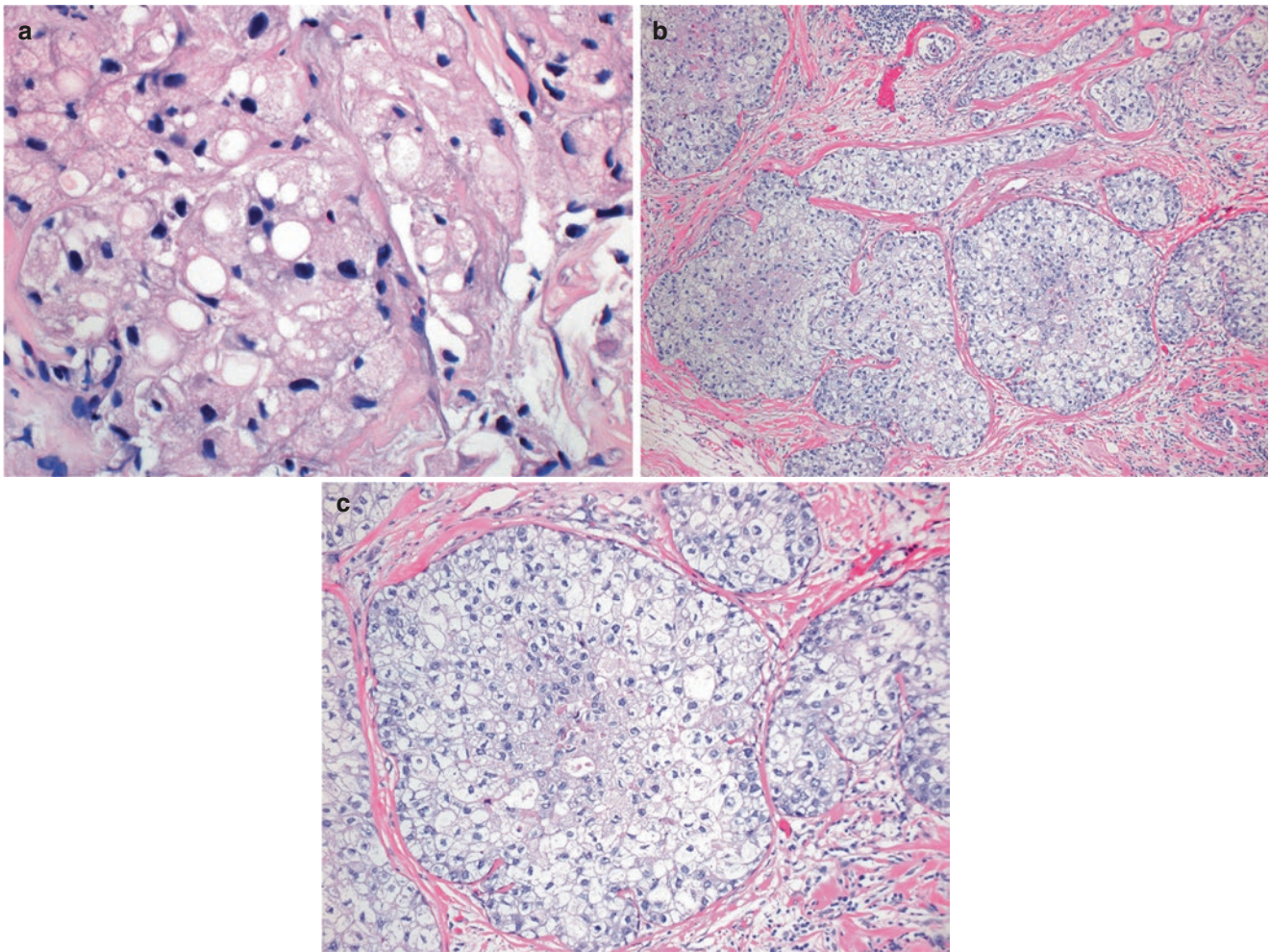**Fig. 12.42** (continued)

Fig. 12.43 Cytologic features of invasive apocrine carcinoma, foamy variant (type B). The tumor cells of this variant have abundant (**a**) foamy to (**b**, **c**) vacuolated clear cytoplasm
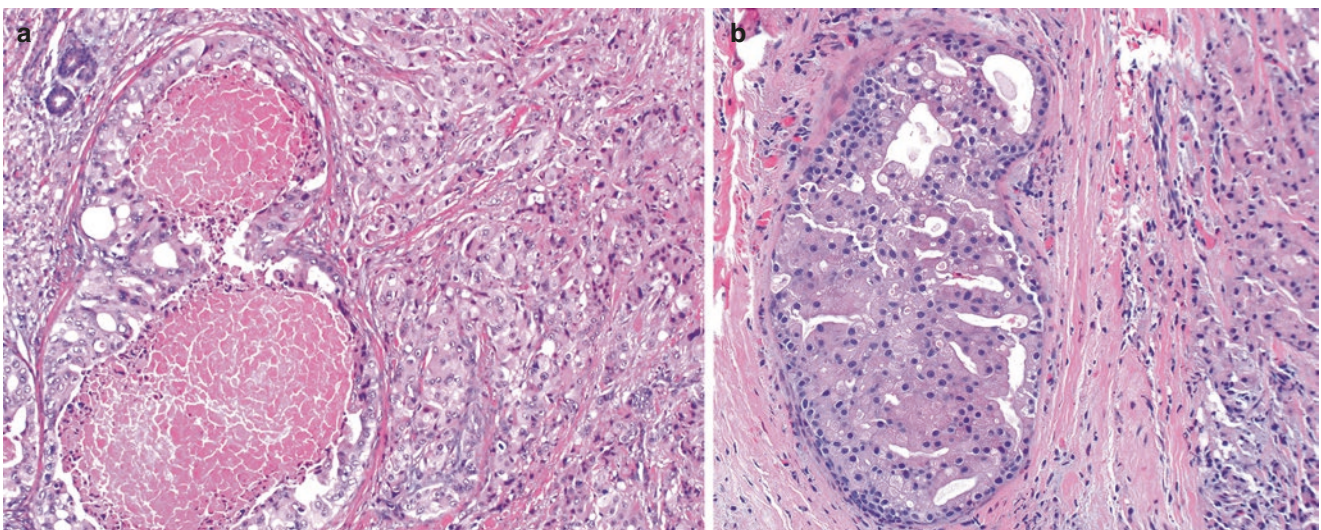

Fig. 12.44 Apocrine ductal carcinoma in situ. (**a**, **b**) The in situ component associated with invasive apocrine carcinoma often displays similar apocrine cytologic features
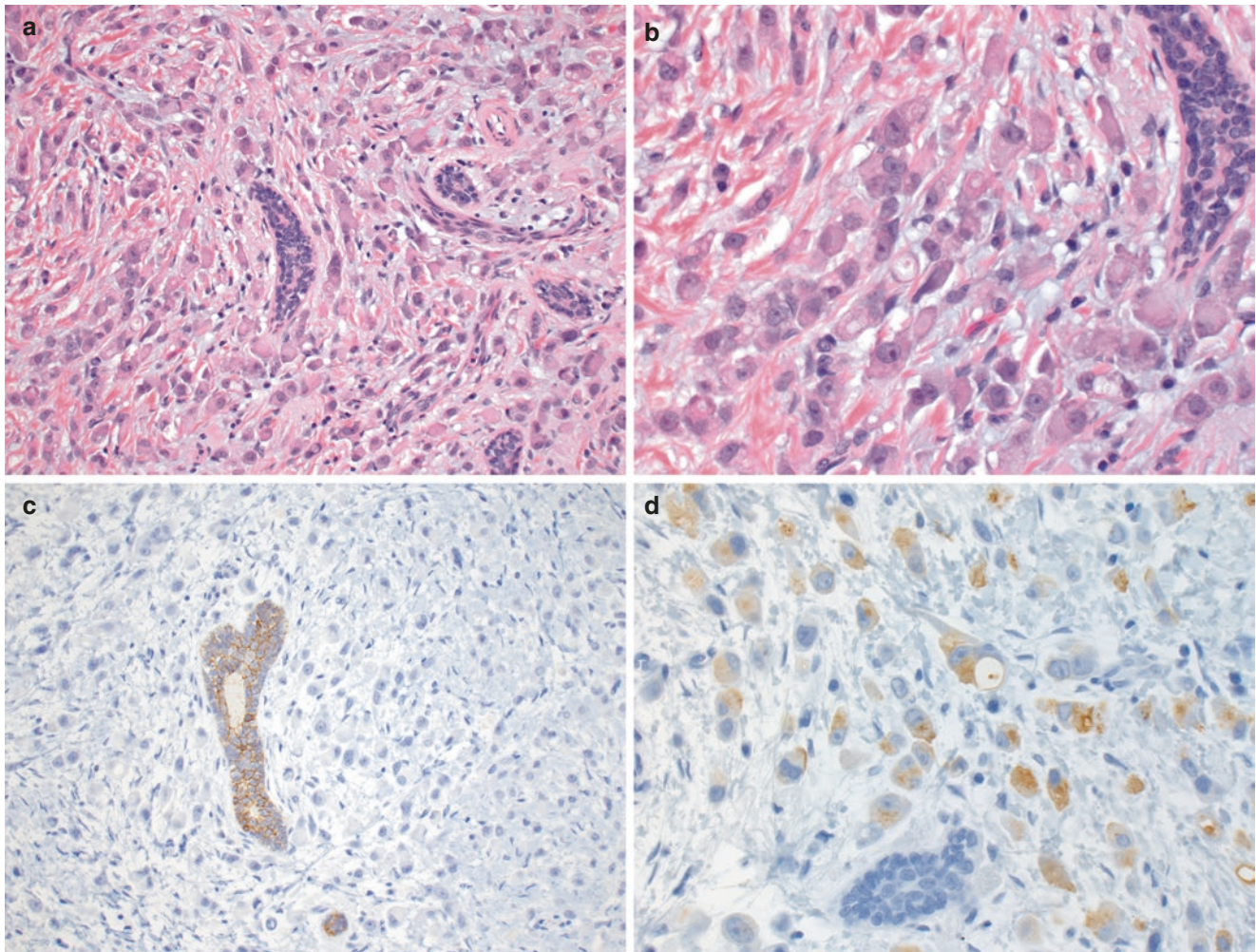
Fig. 12.45 Invasive pleomorphic lobular carcinoma with apocrine features. (**a**) These tumors are characterized by discohesive tumor cells with vacuolated cytoplasm infiltrating as single cells and small cell groups, with permeative and targetoid growth patterns. (**b**) In contrast to classic invasive lobular carcinoma, the tumor cells are large and dem-onstrate abundant eosinophilic granular cytoplasm with pleomorphic nuclei and prominent nucleoli, indicative of apocrine differentiation. (**c**) Negative or aberrant E-cadherin immunostaining supports the lobular phenotype. (**d**) Similar to invasive apocrine carcinomas, in general, these tumors express GCDFP-15

Markers of Apocrine Differentiation

GCDFP-15 is an AR-regulated protein that is often regarded as a functional marker of apocrine differentiation in benign and malignant cells (Fig. 12.46a, b) [227]. GCDFP-15 has been found to strongly correlate with AR expression and with carcinomas showing a surrogate molecular apocrine immunophenotype (ER-, PR-, AR+), and was associated with but not specific for apocrine morphology in the latter group [197, 228]. Pure apocrine carcinomas were positive for GCDFP-15 in ~71% of cases in one study [228]. However, GCDFP-15 has also been positively correlated with HR and HER2 expression and is not limited to apocrine carcinomas [197, 228–230]. With respect to HR-negative carcinomas, one study observed GCDFP-15 expression in molecular apocrine tumors but not in basal-like carcinomas of the control group. However, the vast majority (93%) of molecular apo-crine carcinomas in this study lacked apocrine morphologic features [197]. Decreased GCDFP-15 expression has been demonstrated in lymph node-positive apocrine carcinomas and in advanced disease [229, 231], which also limits its use as a reliable marker for the apocrine phenotype.

Celis et al. defined a specific apocrine protein signature analogous to that of apocrine sweat glands, which included markers consistently expressed in apocrine cells (such as AR, CD24, 15-PDGH [prostaglandin dehydrogenase], ACSMS1 [acyl-CoA synthetase medium-chain family number 1]), as well as markers which are typically not expressed [232]. 5α-Reductase, an enzyme that converts testosterone to dihydrotestosterone, was expressed in approximately 60% of apocrine carcinomas and correlated with adverse prognostic parameters [230]. Other markers reported to be specific for apocrine differentiation include gamma-glutaminyl transfer-
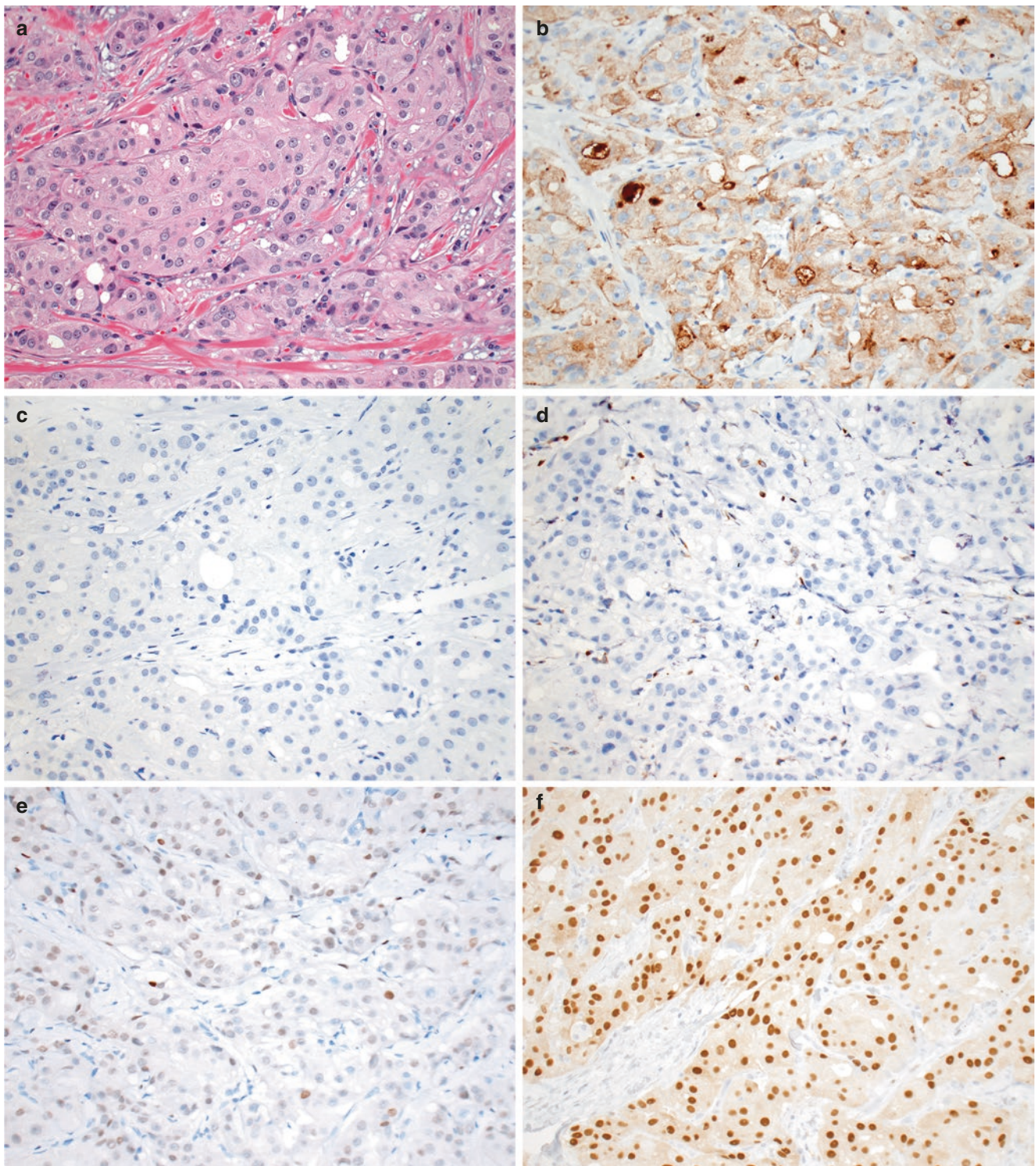
Fig. 12.46 Immunophenotype of invasive apocrine carcinoma. (**a**) Invasive apocrine carcinoma is characterized by strong immunoreactivity to (**b**) GCDFP-15, whereas (**c**) mammaglobin, another commonly utilized breast-specific marker, is typically negative. (**d**) BCL2 is typically negative in these tumors. (**e**, **f**) This invasive apocrine carcinoma shows characteristic immunopositivity for (**e**) GATA3 and (**f**) AR. ER and PR were negative (*not shown*)

ase 1 (GGT-1), tumor-associated glycoprotein-72, HMGCS2, and FAB7 [233–235]. However, none of these markers are currently used for routine clinical application.

Other Immunohistochemical Markers

Apocrine carcinoma cells are immunoreactive for epithelial markers, including EMA and LMWCK (e.g., CK7, CK8, CK18, CK19) [37, 236]. In one study, CK20 reactivity was detected in 50% (4/8) of apocrine carcinomas, while none of the non-apocrine breast carcinomas were CK20 positive [236]. The immunohistochemical profile (expression of luminal CKs, negative for basal cytokeratins CK5/6 and CK14) is consistent with gene expression studies indicating that apocrine carcinomas are generally not basal-like by molecular profiling [37, 196, 198]. CEA positivity has also been observed in apocrine carcinomas [237]. Apocrine cells, both benign and malignant, are usually negative or only

focally positive for the breast marker mammaglobin (Fig. 12.46c). In contrast, GATA3, a sensitive marker for breast carcinomas including TNBC, is usually positive in apocrine carcinomas [114, 238, 239] (Fig. 12.46e) and has also been correlated with AR expression in TNBC [240]. Apocrine carcinomas are typically negative for neuroendocrine markers, such as synaptophysin, chromogranin A, and CD56 [37]. TNAC tend to have a lower Ki-67 proliferation index compared to non-apocrine TNBC [208, 210, 212].

Differential Diagnosis

The most common morphologic mimic of invasive apocrine carcinoma is sclerosing adenosis involved by atypical apocrine cells (atypical apocrine adenosis) or apocrine DCIS (Fig. 12.47). Appreciation of the lobulocentric growth of the
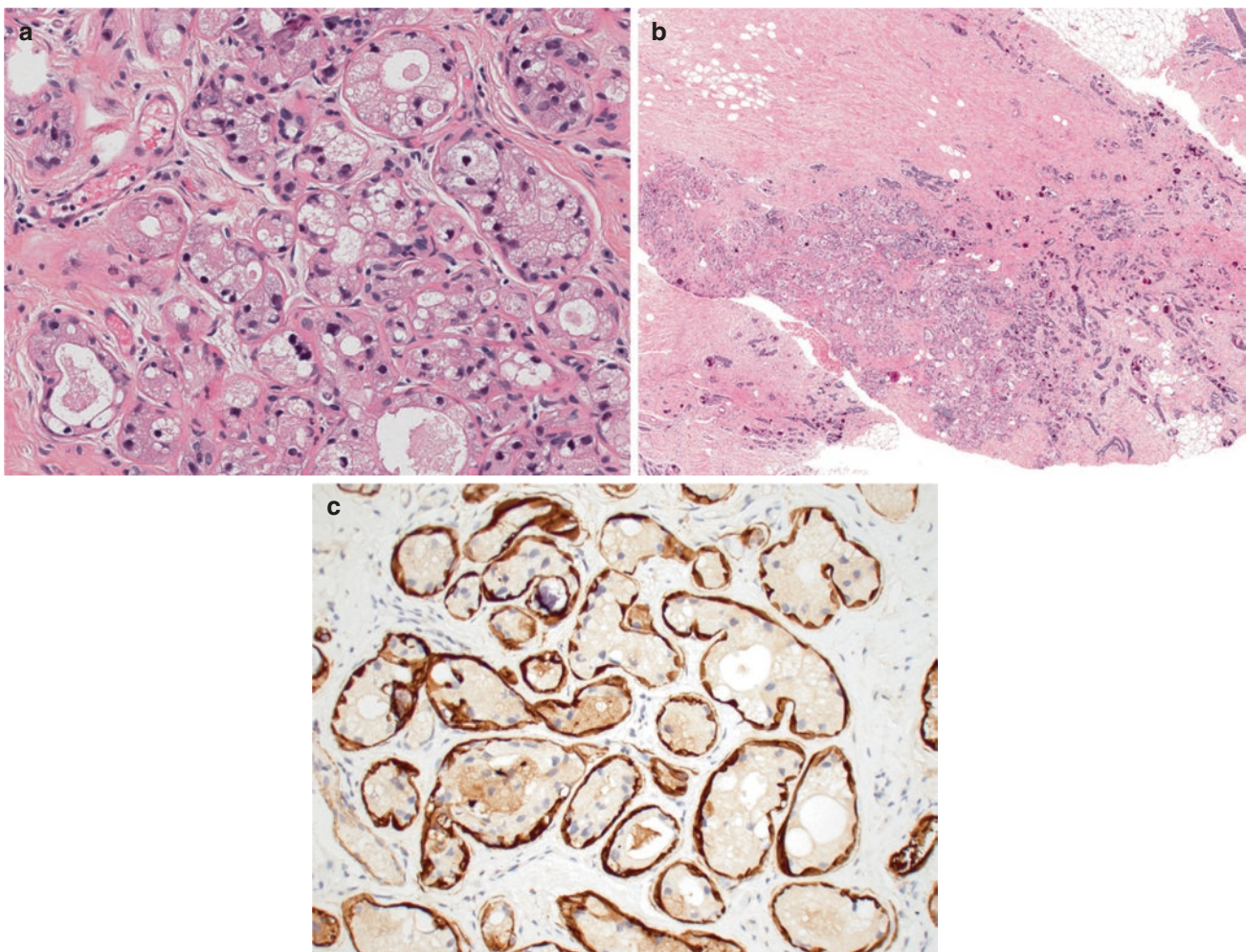
Fig. 12.47 Atypical apocrine adenosis may mimic invasive apocrine carcinoma. (**a**) The nuclei of apocrine cells in atypical apocrine adenosis are enlarged (at least three times the size of normal apocrine cells) and often hyperchromatic. Mitotic figures may be present (*not shown*). The ductules appear crowded and haphazardly arranged on high magnification, which, in combination with the cytologic features, may mimic invasive carcinoma with apocrine differentiation. (**b**) Lower magnification is helpful to appreciate the lobulocentric nature of the lesion, although this may not be well visualized in scant core biopsy specimens. (**c**) Immunohistochemistry for myoepithelial cell markers (SMM in this case) may be helpful to exclude invasive carcinoma and establish the correct diagnosis. Note that myoepithelial cell staining may be attenuated in some apocrine lesions (*not shown here*)

latter lesions on low-power magnification is helpful in making the distinction but may not be apparent in limited core biopsy material. Immunostains can help to highlight the myoepithelial cells of sclerosing lesions in challenging cases. In this context, it should be remembered that myoepithelial cells may be attenuated in non-invasive apocrine and sclerosing lesions [241, 242].

A variety of benign and malignant lesions characterized by large epithelioid cells with abundant eosinophilic or pale vacuolated cytoplasm may be confused with apocrine carcinoma, especially in a limited core biopsy specimen.

Granular cell tumor can rarely arise in the breast and may be misinterpreted as apocrine carcinoma. Contrary to apocrine carcinoma, cells of granular cell tumors have small nuclei with absent to indistinct nucleoli and no to only rare mitotic figures. Cytokeratin immunohistochemistry will stain tumor cells of apocrine carcinoma but is negative in granular cell tumors. Conversely, S100 protein is diffusely and intensely positive in granular cell tumor but is negative or shows only focal weak reactivity in apocrine carcinoma (Fig. 12.42).

An inflammatory process with accumulation of foamy histiocytes may sometimes simulate apocrine carcinoma. However, the histiocytes in such cases have bland cytologic features, in contrast to the atypical nuclei of apocrine carcinomas. Immunohistochemical stains for cytokeratin and histiocytic markers such as CD68 and CD163 can be used to establish the correct diagnosis in cases that are equivocal on H&E (Fig. 12.48a–d).

In addition to apocrine carcinoma, invasive breast carcinoma with oncocytic pattern, acinic cell carcinoma, and neuroendocrine tumors are characterized by eosinophilic

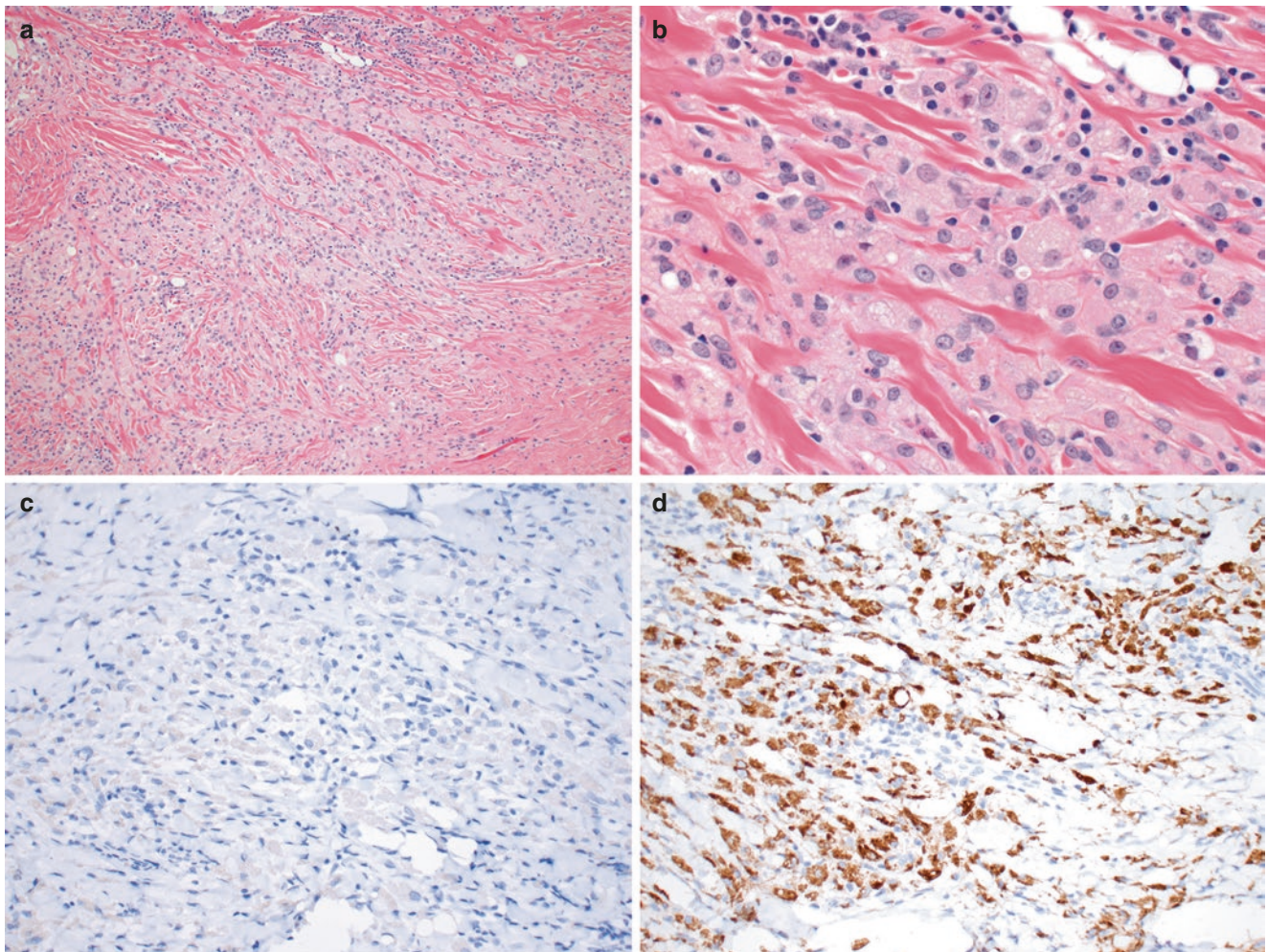**Fig. 12.48** Histiocytic infiltrates may be mistaken for invasive apocrine carcinoma. (**a**, **b**) The cytologic features and nested growth pattern of prominent histiocytic reactions may sometimes mimic invasive apocrine carcinoma, especially in limited core biopsy material. (**d**) CD68 and other histiocytic markers, such as CD163, are positive in such cases, whereas (**c**) keratin is negative

granular cytoplasm. Oncocytic carcinoma was first described by Damiani et al. and characterized by Ragazzi et al. as an invasive carcinoma composed of at least 70% oncocytic cells displaying strong immunoreactivity for anti-mitochondrial antibody [243, 244]. These tumors usually demonstrate a solid growth pattern with pushing margins. The oncocytic cells have well-defined borders and abundant granular eosinophilic cytoplasm, which is due to diffuse accumulation of mitochondria, similar to oncocytes at other anatomic sites. The nuclei range from low grade to pleomorphic. Although apocrine cells and oncocytes share similar morphological features, recognition of a few differences can be helpful to distinguish these tumors. Immunophenotypically, anti-mitochondrial antibody is positive in a diffuse strong granular pattern in invasive breast carcinoma with oncocytic pattern but is negative or focal in apocrine carcinoma. Furthermore, invasive breast carcinoma with oncocytic pattern is often ER positive (~80% of cases) and GCDFP-15 negative (~70%), whereas pure apocrine carcinoma exhibits the reverse immunophenotype [243, 244]. Although considered a rare pattern of invasive breast carcinoma, one study using anti-mitochondrial antibody found that ~20% of 76 consecutive invasive carcinomas were rich in mitochondria [243]. Oncocytic carcinomas or mitochondrion-rich carcinomas of the breast appear to be molecularly heterogeneous, with most classified as luminal or HER2 subtype [245]. A subset of tumors was found to have chromosomal gains of 11q13.1-q13.2 and 19p13, similar to oncocytic tumors of the kidney and thyroid [245]. The clinical features and prognosis of invasive breast carcinoma with oncocytic pattern appear to be similar to other IDC-NST when matched for grade and stage [243, 246, 247].

Acinic cell carcinoma, first described by Roncaroli et al. in 1996 [248], is an exceedingly rare subtype of breast cancer, which displays serous acinar differentiation and is morphologically similar to its salivary gland counterpart. These tumors may present as a palpable mass and show infiltrative growth grossly [249, 250]. The tumor cells exhibit solid, microglandular, or microcystic architectural patterns

and have moderate to abundant, amphophilic to eosinophilic granular cytoplasm and round to oval nuclei. The granules are often large, coarse, and bright red in color, resembling those seen in intestinal Paneth cells (Figs. 12.49 and 12.51). Clear cells with hypernephroid appearance may be observed. The cytoplasm stains with PAS after diastase digestion and may also be focally positive for GCDFP-15, similar to apocrine carcinoma. However, most of the tumor cells are immunoreactive to amylase, alpha-1 antichymotrypsin, lysozyme, S100 protein, and EMA, which confirms the diagnosis (Figs. 12.50 and 12.51). Acinic cell carcinomas are consistently negative for ER, PR, AR, and HER2 [250–252] (Fig. 12.51h). Guerini-Rocco et al. revealed complex genomic patterns of gains and losses in acinic cell carcinoma, similar to other types of high-grade TNBC. Most tumors were also noted to harbor *TP53* mutation [253]. A close relationship has been reported between microglandular adenosis and acinic cell carcinoma [254, 255]. Despite being triple negative, acinic cell carcinomas of the breast have an indolent clinical behavior [250]. A subset of acinic cell carcinomas are found in association with high-grade TNBC of NST (Fig. 12.52), and one study demonstrated shared identical mutations in both components, suggesting that some acinic cell carcinomas might constitute the substrate for the development of a more aggressive form of triple-negative carcinomas [253].

Table 12.7 summarizes the distinguishing features of primary breast carcinomas with granular cytoplasm.

The differential diagnosis of apocrine carcinoma with clear cell features primarily includes metastatic renal cell carcinoma (RCC) of clear cell type, as well as adenomyoepithelioma (Fig. 12.43). Clinical history is critical in suspecting the diagnosis of metastatic RCC. In contrast to apocrine carcinoma, clear cell RCC shows negative immunoreactivity for CK7 and CK20 and is typically positive for PAX2, PAX8, and RCC markers. Lastly, exceedingly rare invasive breast carcinomas with sebaceous, lipid-rich, or glycogen-rich patterns are included in the differential diagnosis (see Chap. 10).

Fig. 12.49 Acinic cell carcinoma of the breast. (**a–c**) Core needle biopsy of an acinic cell carcinoma showing infiltrative microglandular growth of tumor cells with eosinophilic granular cytoplasm and bland rounded nuclei. (**d–f**) Subsequent excision revealed predominantly microglandular and focal solid growth. Note the abundance of distinctive coarse eosinophilic cytoplasmic granules resembling zymogen granules of intestinal Paneth cells (**f**). (*Courtesy of Dr. Jose Jessurun, Department of Pathology and Laboratory Medicine, Weill Cornell Medicine with permission*)
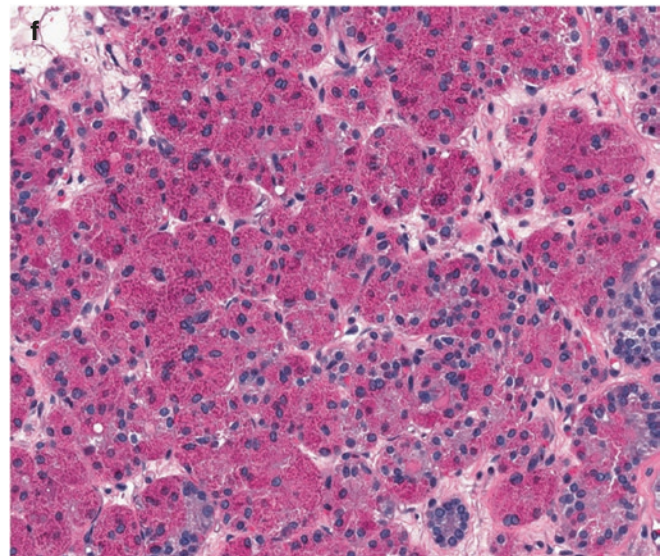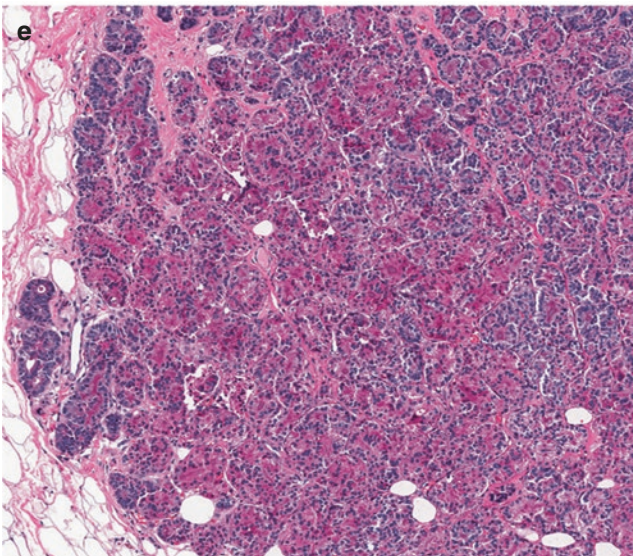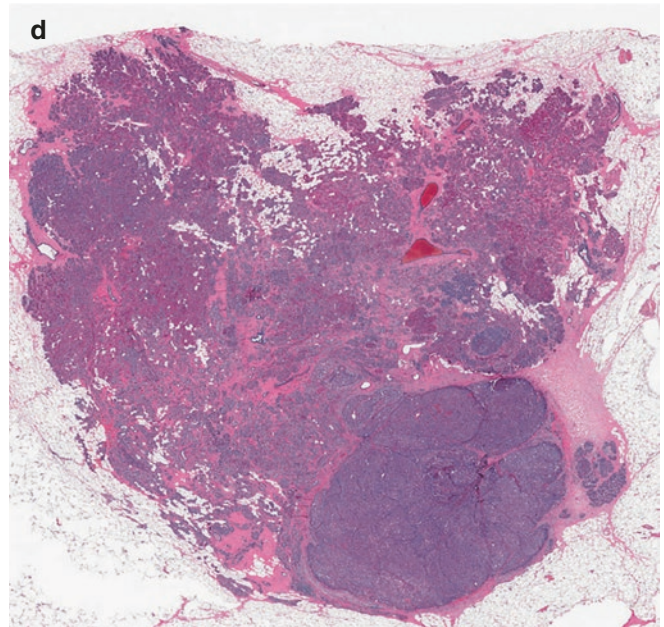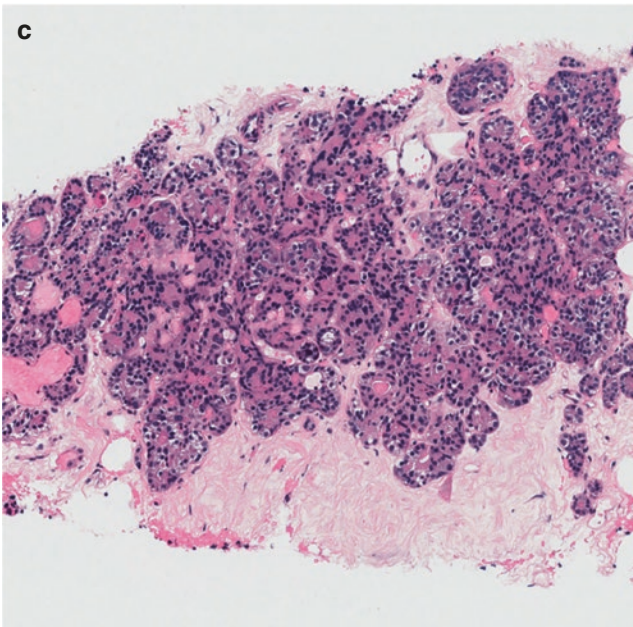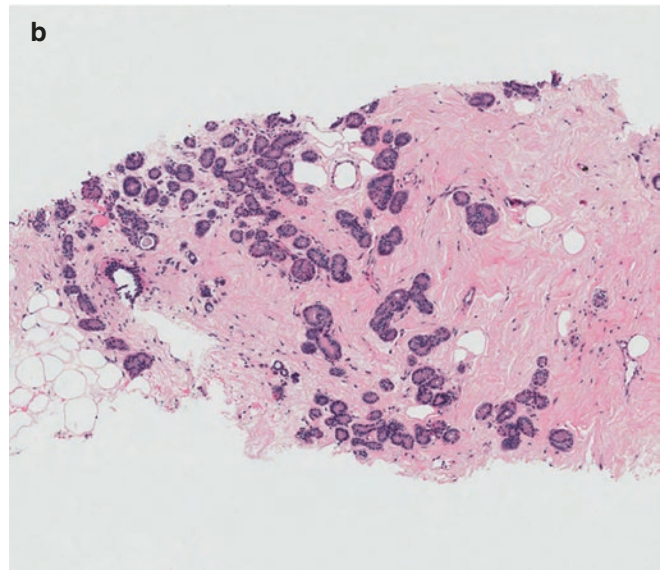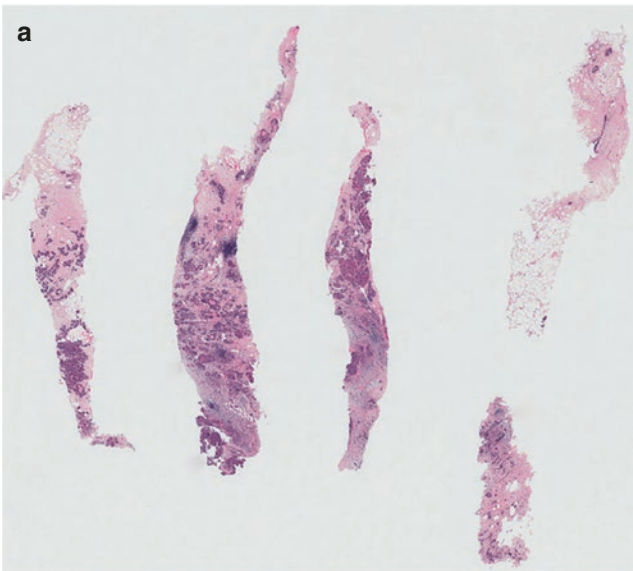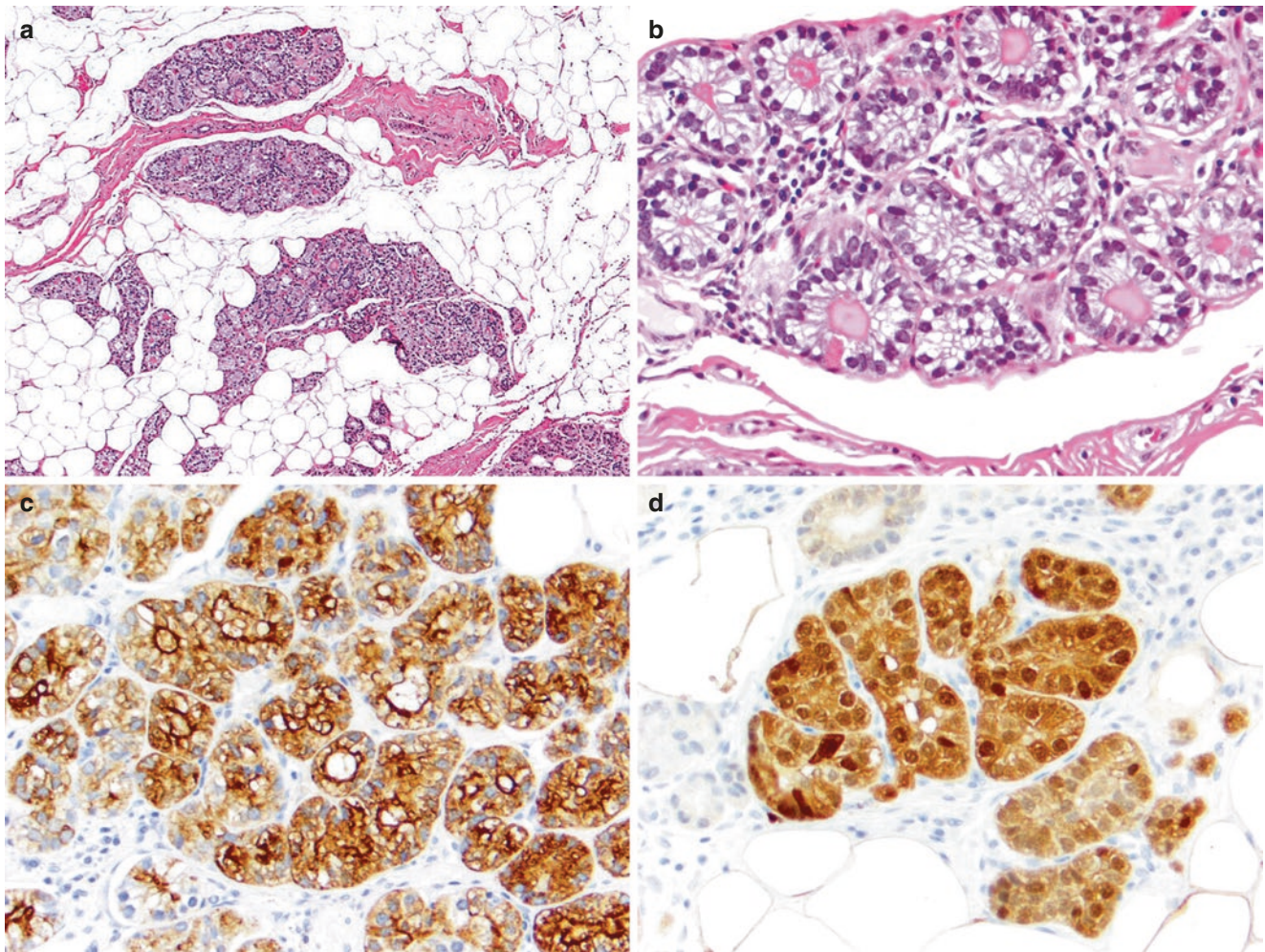
Fig. 12.50 Acinic cell carcinoma of the breast. (**a**, **b**) This example of acinic cell carcinoma demonstrates columnar tumor cells with clear cytoplasm and orderly polarized rounded nuclei arranged in an acinar pattern. Note the presence of large eosinophilic granules in the apical cytoplasm in some tumor cells. The tumor cells are strongly immunoreactive for (**c**) lysozyme and (**d**) S100 protein. (*Courtesy of Dr. Laura C. Collins*, Department of Pathology, Beth Israel Deaconess Medical Center with permission)

Pathogenesis and Risk Factors

The origin and pathogenesis of carcinomas with apocrine differentiation is poorly understood. Using comparative genomic hybridization, one study found evidence of clonality in benign cysts with papillary apocrine hyperplasia, and some of these benign lesions showed chromosomal copy number alterations also identified in apocrine DCIS and invasive apocrine carcinomas (including 2q and 13q gains; 1p, 16q, and 17q losses). These findings suggest that a subset of benign apocrine proliferations may be non-obligate precursors to carcinomas with apocrine differentiation [256]. Given how common apocrine metaplasia and hyperplasia is, such an event would be predicted to be exceedingly rare.

Patients with Cowden disease have germline *PTEN* mutations and an increased risk of breast cancer. Banneau et al.

reported that the gene expression profiles of breast carcinomas in patients with Cowden disease at least partially overlap with the molecular apocrine signature, and many of these tumors show apocrine morphologic and immunophenotypic (AR+, ER-, PR-, HER2+/−) features [234]. Benign breast lesions in patients with Cowden disease also frequently show apocrine differentiation [257, 258]. Together, the observations suggest a possible link between germline *PTEN* mutation and apocrine phenotype. However, most apocrine carcinomas are unrelated to Cowden disease.

Gene expression profiling studies have defined a molecular apocrine signature based on ER-negative breast carcinomas that express high levels of AR, as well as genes typically expressed in ER-positive/luminal tumors. Up to one-half of these tumors are HER2 positive, with the remainder being triple negative. Many but not all of the
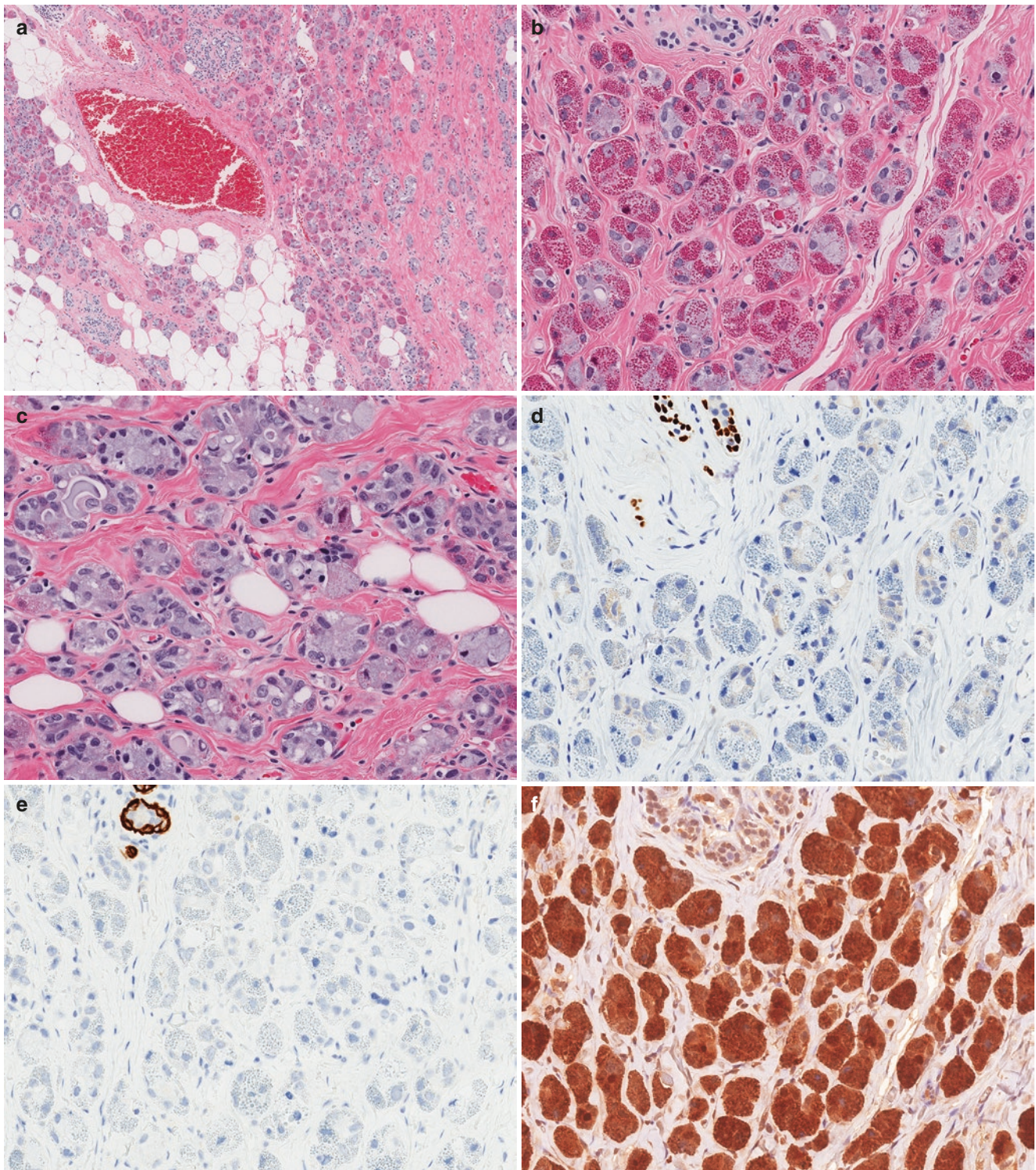
Fig. 12.51 Acinic cell carcinoma of the breast. (**a–c**) Another example of acinic cell carcinoma showing infiltrating small glands in fibrofatty stroma without desmoplastic reaction. The tumor cells forming the microglands have abundant amphophilic cytoplasm, many of which containing large, coarse, and bright eosinophilic granules (**b**, **c**). The small glands lack a myoepithelial layer, as seen with p63 (**d**) and SMM (**e**) immunostains. The neoplastic cells are strongly positive for lysozyme (**f**) and S100 protein (**g**). Acinic cell carcinoma is typically negative for ER (**h**), PR (not shown) and HER2 (not shown)
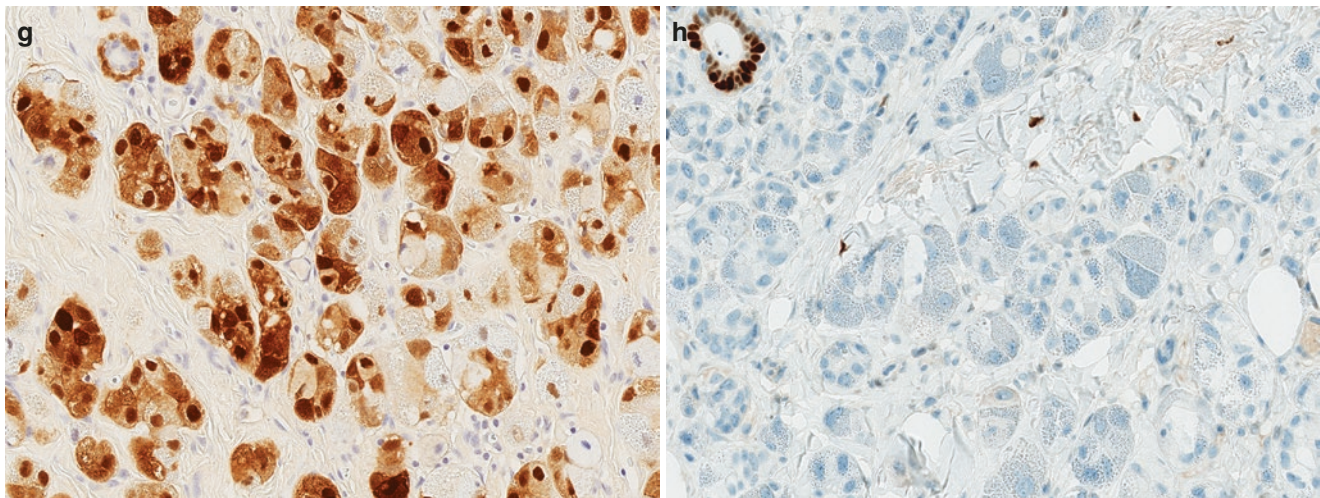
Fig. 12.51 (continued)
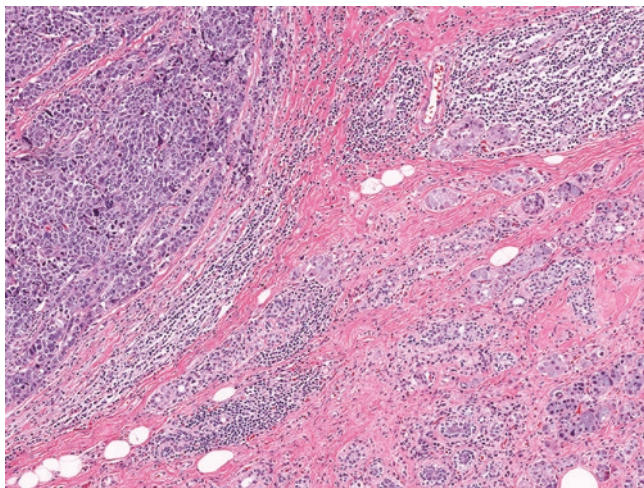
Fig. 12.52 Acinic cell carcinoma (right lower field) with adjacent high-grade, triple-negative IBC-NST (left upper field)

tumors in the combined studies showed morphologic features of apocrine differentiation [198, 259]. Pleomorphic invasive lobular carcinomas with apocrine differentiation have also been found to cluster with the molecular apocrine group [37]. However, in a study that classified molecular apocrine carcinomas based on expression of a targeted subset of genes from the signature, only 7% of tumors had apocrine morphology [197]. Accordingly, apocrine carcinoma shows overlap with but does not always correlate with the molecular apocrine expression signature. Lehmann et al. described an LAR gene expression signature in ~10% of TNBC, which was characterized by increased expression of AR and AR-regulated genes, as well as other features typical of ER-positive luminal carcinomas. This group likely includes the subset of HER2-negative molecular apocrine tumors [196].

Apocrine carcinomas frequently harbor mutations in PI-3K pathway genes, most often *PIK3CA*, as well as *PTEN, PIK3R1,* and *AKT1* [195, 208, 215]. In a study of 18 TNAC, the most frequently mutated genes were *PIK3CA* (~72%), *PTEN* (~33%), and *TP53* (~28%). *TP53* mutations are less common compared to other TNBC [208, 215]. Additional alterations include RAS/RAF/MEK pathway genes, growth factor receptors, and cell cycle genes [208]. A single TNAC with a potentially actionable novel *FGFR2-TACC2* fusion has been reported [208]. Genomic instability of TNAC is low, in contrast to other TNBC [208, 215].

Prognosis and Clinical Management

Data on the prognosis of patients with apocrine carcinoma have been contradictory, which is likely due to retrospective series with relatively low numbers of patients and the lack of uniform defining criteria (morphology alone, versus morphology with ER and/or AR and/or HER2 status, versus molecular subtype without histology). Some studies have reported similar [209, 231, 260–263] or worse [203, 214] outcomes of apocrine carcinomas compared to IDC-NST. These studies have generally included ER-positive or HER2-positive apocrine carcinomas in the analyses, which are likely to drive tumor behavior, treatment, and prognosis. In a SEER study, poor outcomes of patients with apocrine carcinomas compared to IDC-NST improved after correction for demographic and clinicopathologic (grade, stage, ER, PR, HER2, nodal status) factors [214]. A number of studies have observed better outcomes of TNAC compared to other TNBC [207, 210, 211, 264, 265]. This would be consistent with the smaller size, lower grade, and lower Ki-67 indices often associated with TNAC [203, 208, 210–213, 215, 265]. Rates of lymphovascular invasion and lymph node metastasis may be similar

Table 12.7 Distinguishing pathologic features of breast carcinomas with granular cytoplasm

	Apocrine carcinoma	Acinic cell carcinoma	Invasive carcinoma with oncocytic pattern	Neuroendocrine tumor
Growth pattern	Variable (nests, glands, micropapillary, papillary, single cells)	Microglandular, solid, microcystic	Solid growth with pushing margin	Nests (organoid), solid papillary
Cytologic features	Large cells; well-defined cell border; abundant eosinophilic granular to foamy or clear cytoplasm; apical cytoplasmic snouts may be present if glandular	Monotonous cuboidal/columnar to polygonal cells; moderate to abundant, amphophilic to eosinophilic granular or clear cytoplasm	Large round cells; well-defined cell border; abundant eosinophilic granular cytoplasm	Polygonal, plasmacytoid or spindled cells; moderate eosinophilic granular cytoplasm
Nuclear features	Round to pleomorphic; prominent nucleoli	Round to oval	Centrally located; low grade to pleomorphic; prominent nucleoli	Low to intermediate grade
Granules	Electron-dense secretory granules; coarse eosinophilic granules	Zymogen granules; coarse bright red granules	Mitochondria; fine eosinophilic granules	Neurosecretory granules; fine eosinophilic granules
Defining IHC[a] profile	ER−, PR−, AR+	Amylase+, lysozyme+, alpha-1 antichymotrypsin+	Mitochondrial antibody strong staining in ≥70% tumor cells	Synaptophysin+, chromogranin+
Additional IHC profile	GCDFP-15+, BCL2−	ER−, PR−, HER2−, S100+, EMA+	ER+ (~80%), GCDFP-15− (~70%)	ER+, HER2−

[a] Abbreviations: *IHC* immunohistochemical

in TNAC compared to other TNBC [207]. Worse outcomes have been reported in LAR tumors compared to other TNBC and in molecular apocrine carcinomas compared to other molecular subtypes, but these groups defined by either gene expression or immunohistochemistry do not correlate perfectly with apocrine carcinoma [196, 265, 266].

Treatment for apocrine carcinoma is often similar to IBC-NST. The role of adjuvant chemotherapy is limited by paucity of data. Population-based studies have shown that patients with TNAC overall receive chemotherapy at a lower rate than other TNBC, yet outcomes were more favorable [207, 211, 265]. There is little data on the response of apocrine carcinomas to neoadjuvant chemotherapy. Lower rates of pathologic complete response have been observed in apocrine carcinomas, although outcomes remained favorable [262]. Pathologic complete response rates were reported to be variable for LAR tumors [267, 268] and similar to basal-like TNBC for molecular apocrine tumors [266], but apocrine morphology was not considered in these analyses. Apocrine carcinomas with HER2 overexpression are eligible for anti-HER2 targeted therapies.

Given the high frequency of AR expression in apocrine carcinomas or molecularly defined groups (molecular apocrine or LAR tumors), androgen blockade may offer a therapeutic approach for these tumors [269, 270]. The high frequency of PI-3K/mTOR pathway mutations suggests that targeted inhibitors of this pathway may also be therapeutic candidates [271]. Preclinical models have suggested that AR-positive/LAR TNBC are sensitive to CDK4/6 inhibition [272, 273]. A number of clinical trials are examining the utility of PI-3 K and CDK4/6 inhibitors in combination with anti-androgens in TNBC [274].

Metaplastic Carcinoma

Overview and Clinical Presentation

Metaplastic breast carcinomas constitute a heterogeneous group of predominantly triple-negative invasive breast cancers characterized by differentiation of the neoplastic epithelium into squamous and/or mesenchymal-like elements, including spindle cell, chondroid, or osseous components and rarely others [275]. These tumors are uncommon, representing 0.2–1% of all breast carcinomas [275–278]. Differences in the definition of metaplastic carcinoma likely account for the reported variability in prevalence. In general, metaplastic components should comprise >10% of the tumor cells for a diagnosis of metaplastic carcinoma, although some authors have used different cutoffs including <10% or ≥20% [279–281]. IDC-NST may also occasionally show focal metaplastic components.

Various terminologies have been applied in the literature to categorize the different morphologic features that can be seen in metaplastic carcinomas. These tumors have been described as being monophasic, with only one metaplastic component present, or biphasic, with more than one component present. Biphasic tumors may have only metaplastic components or include metaplastic and adenocarcinoma components. Some metaplastic carcinomas are purely epithelial (squamous cell carcinoma, adenosquamous carcinoma) or purely sarcomatoid (spindle cell carcinoma), whereas others are biphasic epithelial and sarcomatoid. The WHO classification uses a practical descriptive system of metaplastic carcinoma patterns based on the histologic type of metaplastic components present: low-grade adenosqua-

mous carcinoma (LGASC), fibromatosis-like metaplastic carcinoma (FLMBC), squamous cell carcinoma (SCC), spindle cell carcinoma, metaplastic carcinoma with heterologous mesenchymal differentiation (MCMD), and mixed metaplastic carcinoma [275]. When a metaplastic carcinoma is composed of multiple different components, it is recommended to report each component and its estimated percentage [275]. LGASC and FLMBC are considered low-grade metaplastic carcinomas and tend to have a favorable prognosis, despite the triple-negative phenotype. The other groups generally have more aggressive behavior and worse outcomes, although retrospective analyses suggest differences in outcomes between some groups [275, 279, 282]. An international study of 364 metaplastic carcinomas from centers in Europe and Asia showed the following frequency distribution: 32% spindle cell carcinoma, 29% matrix-producing carcinoma (mesenchymal differentiation), 21% SCC, 13% mixed squamous and spindle cell carcinoma, and 5% FLMBC [279]. Another study of 347 tumors in the Asia-Pacific Metaplastic Breast Cancer (AP-MBC) consortium found mixed (72%), pure squamous (16%), and pure spindle cell (8%) metaplastic carcinomas to comprise ~96% of cases [282].

The clinical features and patient age distribution of metaplastic carcinomas are overall similar to those of ER-negative IBC-NST, although patients with metaplastic carcinoma tend to present at a higher stage [276, 283]. Most patients (85% in one study) present with a palpable lump [284]. A lower incidence of lymph node involvement has been found compared to IDC-NST [13, 277, 278, 285–287].

Gross and Radiologic Features

Some metaplastic carcinomas display imaging features more often associated with benign lesions, such as round or oval masses with circumscribed margins [288]. However, in a recent series of 71 metaplastic carcinomas, >90% showed imaging features concerning for malignancy, most commonly being an ill-defined mass. Fifteen percent of the tumors in this study were classified as interval cancers [284]. Calcifications are uncommon but may be associated with DCIS or tumors with osseous differentiation [284, 288, 289].

Metaplastic breast carcinomas are often larger than IBC-NST, with a reported mean size of 3.9 cm, ranging from 2 to >10 cm [275, 278, 283, 287]. The gross features are overall not different from those of IBC-NST, with some cases appearing relatively circumscribed and others having irregular, ill-defined borders. Cystic change may be seen, especially in squamous cell carcinomas [290]. Tumors with heterologous cartilaginous differentiation may appear gelati-

nous, and those with osseous differentiation are hard and gritty. Additional features relevant to specific subtypes are discussed in the appropriate sections below.

Low-Grade Adenosquamous Carcinoma

First described by Rosen and Ernsberger in 1987, LGASC is a distinct and uncommon type of metaplastic carcinoma with low-grade features [291]. In contrast to most other metaplastic carcinomas (except FLMBC), LGASC generally have an indolent clinical course, although they can be locally aggressive [292, 293]. The diagnosis can be especially challenging in CNB due to tissue fragmentation, inconsistent sampling of lesional tissue, and variable staining with epithelial and myoepithelial markers [291, 294]. Familiarity with the morphologic features and unique immunophenotype is thus important for diagnosis [292].

These tumors are overall smaller than other types of metaplastic carcinoma, with a median size of 2–2.8 cm (ranging from 0.5 to 8.6 cm). Grossly, LGASC has a stellate configuration with irregular borders and a firm to hard yellow cut surface [291].

Microscopic Features

Microscopically, LGASC are composed of infiltrating small glands intermixed with solid nests of squamous cells in a spindle cell background (Fig. 12.53a). The growth pattern is occasionally centrifugal and can resemble a radial scar on low magnification. The glands are usually small, elongated, and compressed, forming slender extensions suggestive of syringomatous differentiation [291, 293]. The glands are lined by biphasic luminal epithelial cells and myoepithelial cells, with variable degrees of squamous differentiation of the luminal epithelial cells (Fig. 12.53b–e). The glandular lumens may contain eosinophilic amorphous material with a condensed, inspissated appearance. The squamous nests are of various sizes and shapes, including thin strands and single cells. Squamous pearls or squamous cysts may also be present (Fig. 12.53f). Both the glandular and squamous cells exhibit low-grade cytology, low mitotic activity, and a lack of necrosis, which correlates with the indolent clinical course [291–293]. The stroma of LGASC is typically composed of cellular spindle cells but may be fibrotic and paucicellular. The stromal cells are often arranged in a concentric fashion around the epithelial elements, from which they appear to emanate. A prominent lymphocytic response is often observed at the periphery of the tumor, sometimes in a "cannon ball" pattern. Osteocartilaginous metaplasia may rarely be seen in the stroma [293]. LGASC are highly infiltrative, with the small tumor glands and squamous nests insinuating between and into normal undistorted lobules (Fig. 12.54c).
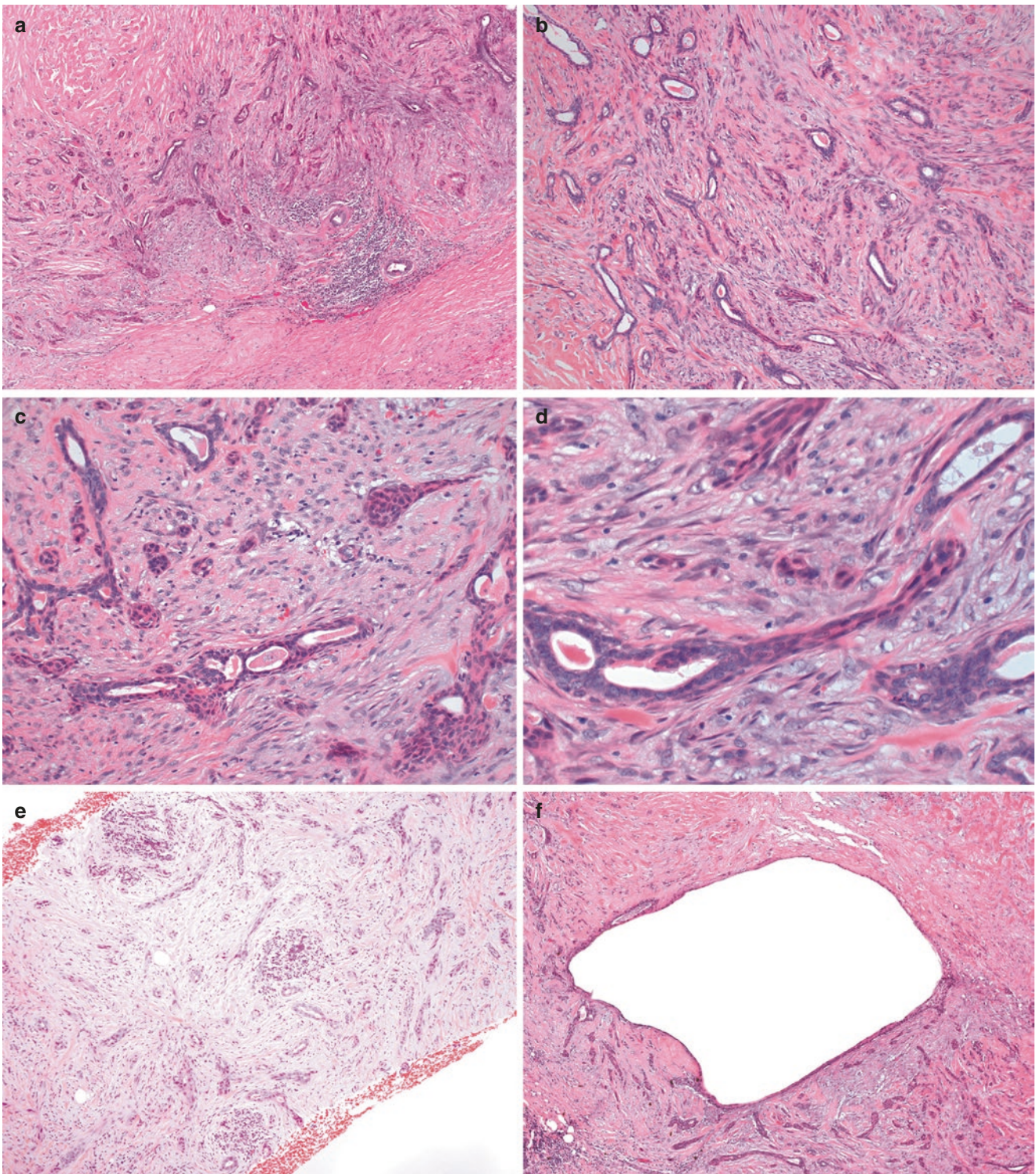
Fig. 12.53 Low-grade adenosquamous carcinoma. (**a**) LGASC showing infiltrating small glands and nests of squamous cells within a desmoplastic to focally fibrotic stroma. Note the lymphoid aggregates, which are usually present at the periphery of the tumor. (**b–d**) Higher power views highlighting the infiltrative glands, which are typically elongated and/or compressed and show variable squamous differentiation. Note some of the cell nests with tear-drop extensions, suggestive of syringomatous differentiation. (**e**) These features can be appreciated on core biopsy. (**f**) Squamous cysts may be seen in some cases
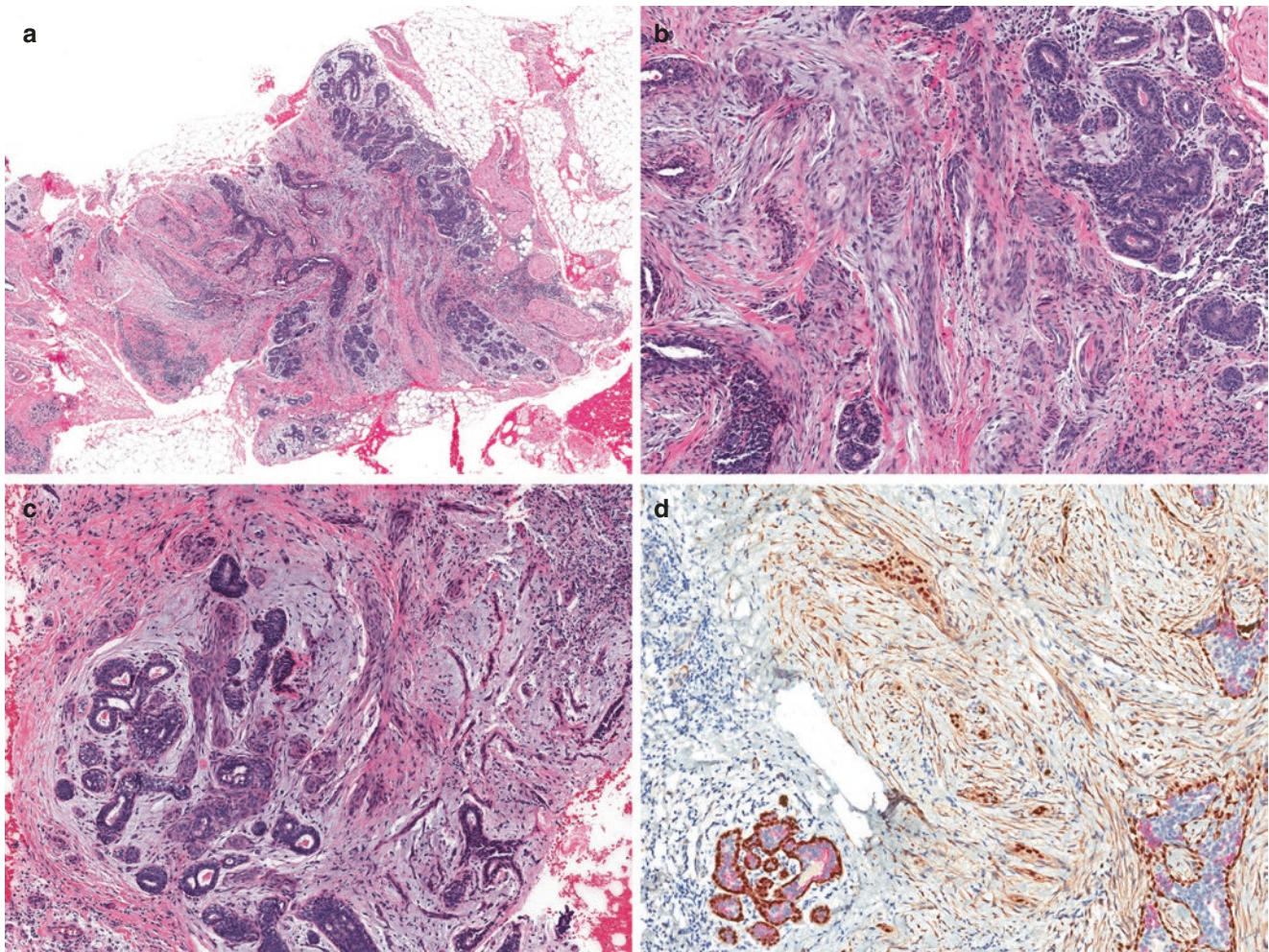
Fig. 12.54 Low-grade adenosquamous carcinoma mimicking sclerosing lesion. (**a**) The low-power architecture of this LGASC is suggestive of a sclerosing lesion. (**b**) On medium power, slender compressed glands are present within a cellular stroma, which is accentuated around the tumor nests. Note the lymphocytic infiltrates at the tumor periphery (right side of images **a** and **b**). (**c**) The neoplastic glands show squamous differentiation and infiltrate between and within the benign lobules. (**d**) Immunohistochemical triple stain (p63 and calponin in brown chromogen and CAM5.2 in red) shows that the tumor cell nests are positive for p63 and negative for both calponin and CAM5.2

Rare cases may demonstrate coexisting DCIS or IDC-NST or show transition to higher grade metaplastic components [292, 295, 296].

LGASC may arise in association with a central sclerosing proliferative lesion, such as radial scar, sclerosing adenosis, or sclerosing papilloma [292, 293, 297]. Association with adenomyoepithelioma has also been reported [298]. In these settings, the small glands and squamous nests of LGASC surround and intermingle with the background distorted ducts and can be easily overlooked and misinterpreted as part of the entrapped epithelial structures characteristic of these sclerosing lesions. However, the stroma of LGASC is desmoplastic rather than fibroelastotic, and the morphologic features of the epithelium, including squamous cell nests, should alert the pathologist to the possibility of LGASC mimicking a benign sclerosing lesion (Fig. 12.54a–d).

Immunohistochemistry

Immunophenotypically, LGASC demonstrate an unusual "consistently variable" staining pattern with myoepithelial markers. In a study of a large series of LGASC, myoepithelial markers (p63, SMM, calponin, SMA, CD10) were found to exhibit a spectrum of complete, discontinuous, or absent staining around the epithelial nests within the same tumor in over one-third of the cases, with 11% of tumors demonstrating complete circumferential staining (Fig. 12.55f, g) [294]. No tumor showed complete absence of staining by any of the myoepithelial markers. Glandular luminal staining for p63 was observed in approximately 75% of LGASC, further supporting squamous differentiation of these glandular structures. In addition, a distinctive lamellar (concentric) staining pattern of stromal cells surrounding glands was noted with

SMM and/or calponin in more than half of the lesions, which can complicate interpretation of true myoepithelial staining (Fig. 12.55e). Another feature is the core staining pattern observed with various cytokeratins, in which the luminally located epithelial cells of neoplastic glands stained stronger than the adjacent basal cells within the same glands (Fig. 12.55d). These unique inconsistent staining patterns with epithelial and myoepithelial markers may be diagnostically valuable in problematic cases to support the suspicion of LGASC (Fig. 12.55a–g). LGASC are triple negative for ER, PR, and HER2 (Fig. 12.55h) and show consistent expression of basal cytokeratins (CK5/6, CK14, CK17) [295, 296, 299–302], indicative of a basal-like immunophenotype. EGFR is variably expressed [295, 299, 302].

Differential Diagnosis

The differential diagnosis of LGASC includes benign fibrosclerosing lesions (sclerosing adenosis, radial scar/complex sclerosing lesion), reactive squamous metaplasia, tubular carcinoma, and syringomatous adenoma of the nipple [292, 294]. Fibrosclerosing lesions usually do not demonstrate squamous differentiation, and the associated stroma is typically fibroelastic and hypocellular. These lesions also lack infiltrative growth of glands between and into normal lobules, and the glands are often surrounded by a complete myoepithelial layer (Fig. 12.54a–d). However, rare squamous metaplasia may be observed in fibrosclerosing lesions, and decreased or focal lack of myoepithelial marker expression can be seen [241]. Early cellular sclerosing lesions can
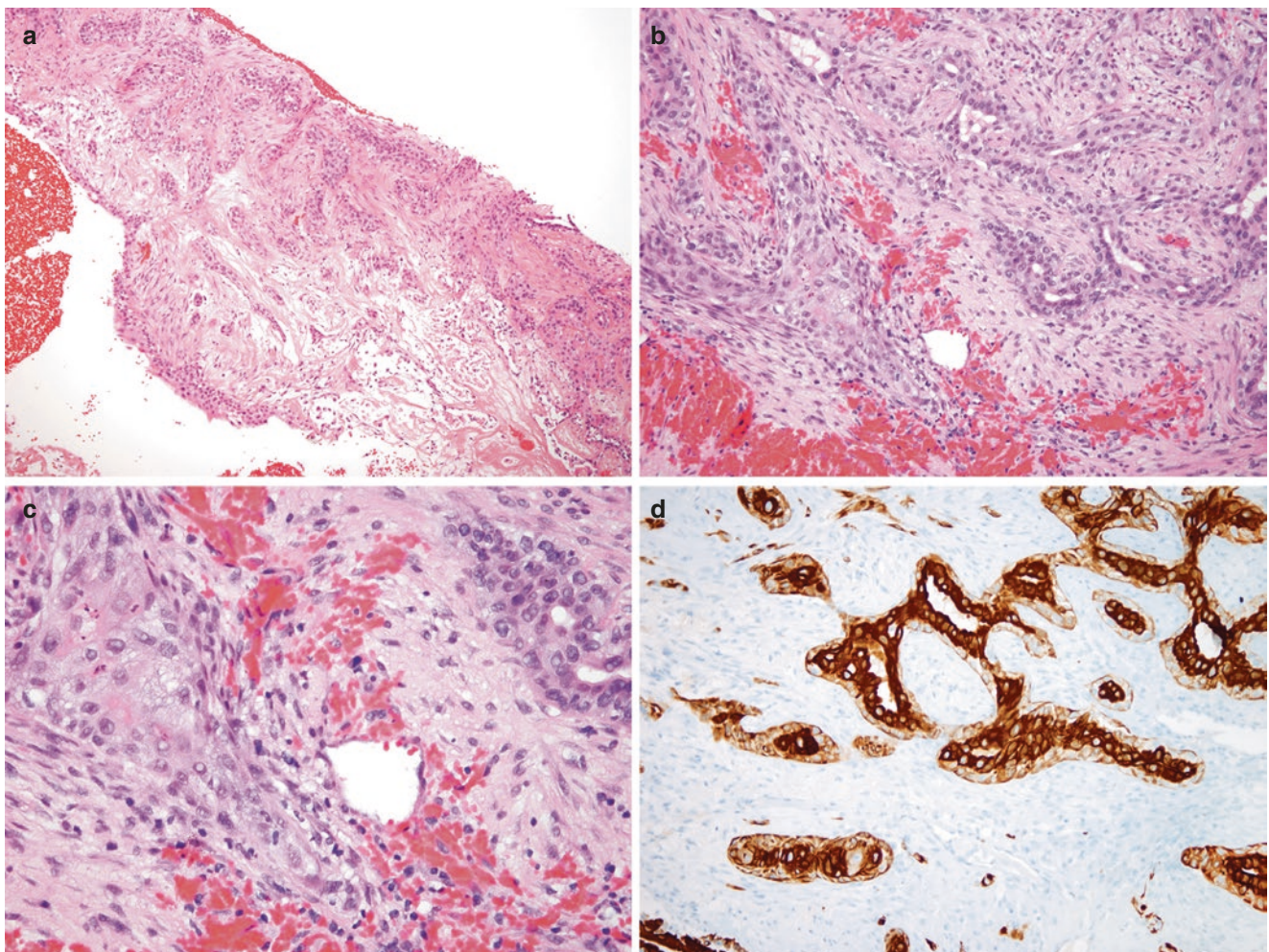
Fig. 12.55 Core needle biopsy of low-grade adenosquamous carcinoma. (**a–c**) This CNB shows nests and glands of tumor cells with squamous features embedded within a cellular spindle cell stroma. (**d**) Immunohistochemical staining for CK7 demonstrates characteristic "core staining" pattern, with stronger staining of luminal epithelial cells than surrounding basally located cells. (**e**) SMM immunostain highlights stromal cell cuffing around lesional cells giving characteristic "lamellar" staining pattern. (**f, g**) p63 and calponin immunostains show the consistently variable staining pattern, with a spectrum of complete, discontinuous, and absent staining pattern around the tumor nests within the same lesion. (**h**) The tumor cells lack ER expression
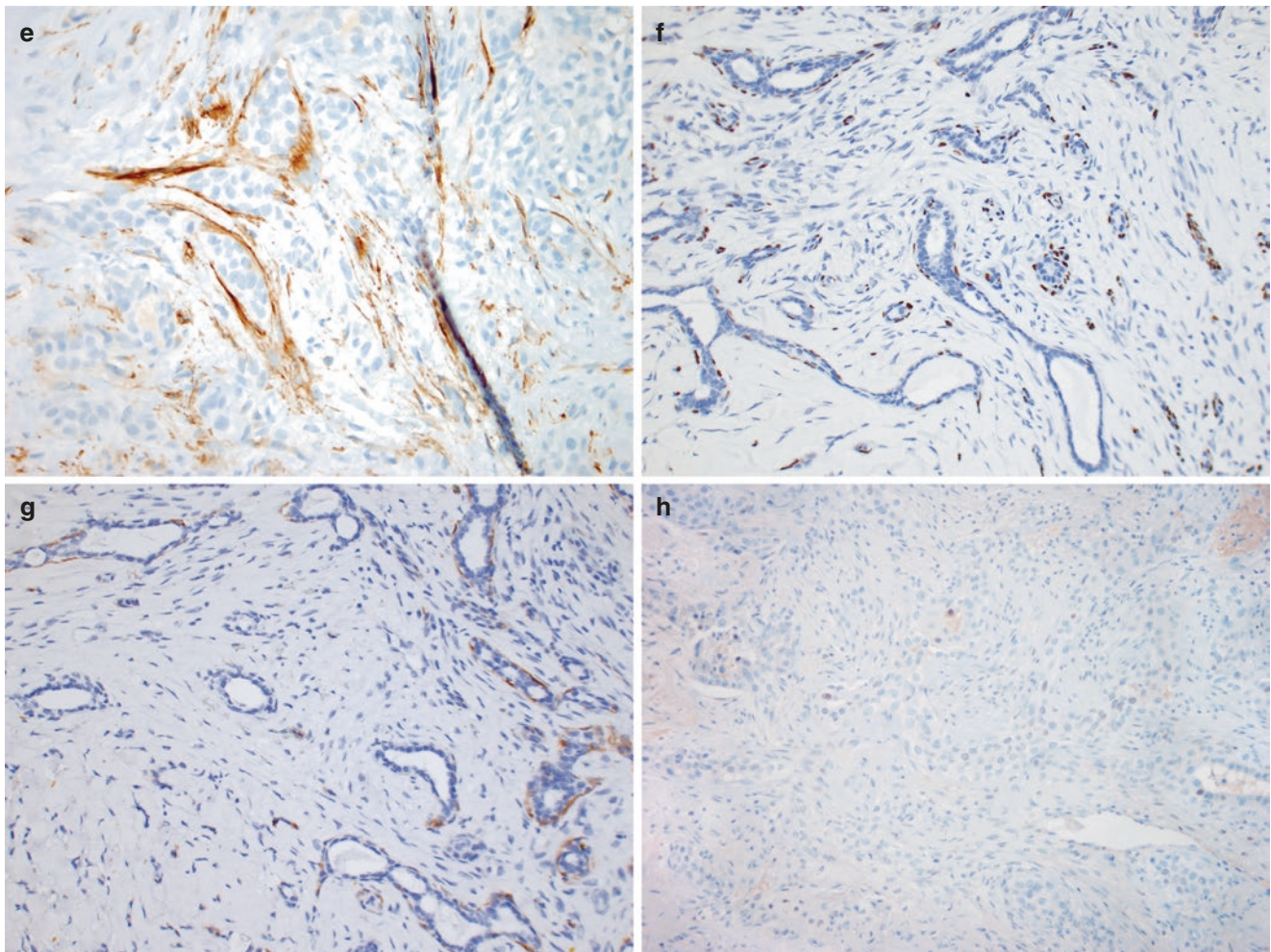
Fig. 12.55 (continued)

harbor adenosquamous-like areas in the central nidus, raising consideration for LGASC [303]. Therefore, the distinction between LGASC and benign fibrosclerosing lesions may be difficult even with immunohistochemical stains in a core biopsy specimen. In such challenging cases, a descriptive diagnosis of "atypical sclerosing lesion" with a comment to recommend excision can be considered.

Tubular carcinomas feature angulated glands in a cellular desmoplastic stroma, which may be confused with LGASC. However, tubular carcinomas do not show squamous differentiation. Furthermore, LGASCs demonstrate inconsistent staining patterns with myoepithelial markers, whereas the neoplastic glands of tubular carcinomas lack myoepithelial staining altogether. Lastly, tubular carcinomas are strongly positive for ER, in sharp contrast to the negative ER immunophenotype of LGASC.

The most difficult differential diagnosis of LGASC is with syringomatous tumor of the nipple, as both lesions share identical or nearly identical morphologic and immuno-

histochemical features, and both have a propensity for local recurrence [275, 292, 301]. Tumor location is also not a strong discriminating feature, as both can occur in the retroareolar region [294]. Syringomatous tumor of the nipple may exhibit a similar inconsistent staining pattern with myoepithelial markers as is typical of LGASC, although the "lamellar" myoepithelial and core "cytokeratin" staining patterns are not likely to be seen in the former [294].

LGASC should be distinguished from high-grade adenosquamous carcinoma (SCC mixed with IBC-NST), due to the often-aggressive behavior of the latter.

Fibromatosis-Like Metaplastic Carcinoma

FLMBC was first described by Gobbi et al. in 1999 as a low-grade variant of metaplastic carcinoma that mimics fibromatosis [304]. Compared to other metaplastic carcinomas, these tumors are associated with unique clinical behavior

characterized by low malignant potential, a high incidence of local recurrence, and very rare distant metastases. FLMBC has shown predilection for older women and the left breast [305].

Grossly, FLMBC appears as a hard mass with homogenous gritty, gray white cut surfaces, ranging in size from 1 to 7 cm. Some lesions are circumscribed, whereas others have irregular borders or may even be cystic in appearance [305].

Microscopic Features

Histologically, FLMBC exhibit an infiltrative, fibromatosis-like growth pattern [304, 306]. The tumors comprise bland spindle cells arranged as interlacing fascicles and embedded in a collagenized stroma, comprising at least 95% of the total tumor area [307] (Figs. 12.56, 12.57, 12.58a–c, and 12.59a–c). Tumor cell nuclei are slender with tapered edges and finely distributed chromatin [275]. Nuclear atypia is absent or mild. Scattered foci of more plump and polygonal (epithelioid) cells with rounded nuclei, eosinophilic cytoplasm, and foci of glandular or squamous elements may be seen but should comprise <5% of the lesion [304, 306] (Figs. 12.57b, 12.59c, and 12.60). Not infrequently, the epithelioid cells are arranged in a perivascular pattern (Fig. 12.59b) [297, 304]. Mitotic activity is absent to low (<2/10 HPF). The majority of tumors have a mild chronic inflammatory infiltrate admixed with the neoplastic spindle cells [306] (Fig. 12.58a–c). It should be noted that these tumors demonstrate significant intertumoral and even intratumoral variation in the degree of cellularity and amount of stromal collagen. Tumors with extensive collagenous stroma and scant spindle cells
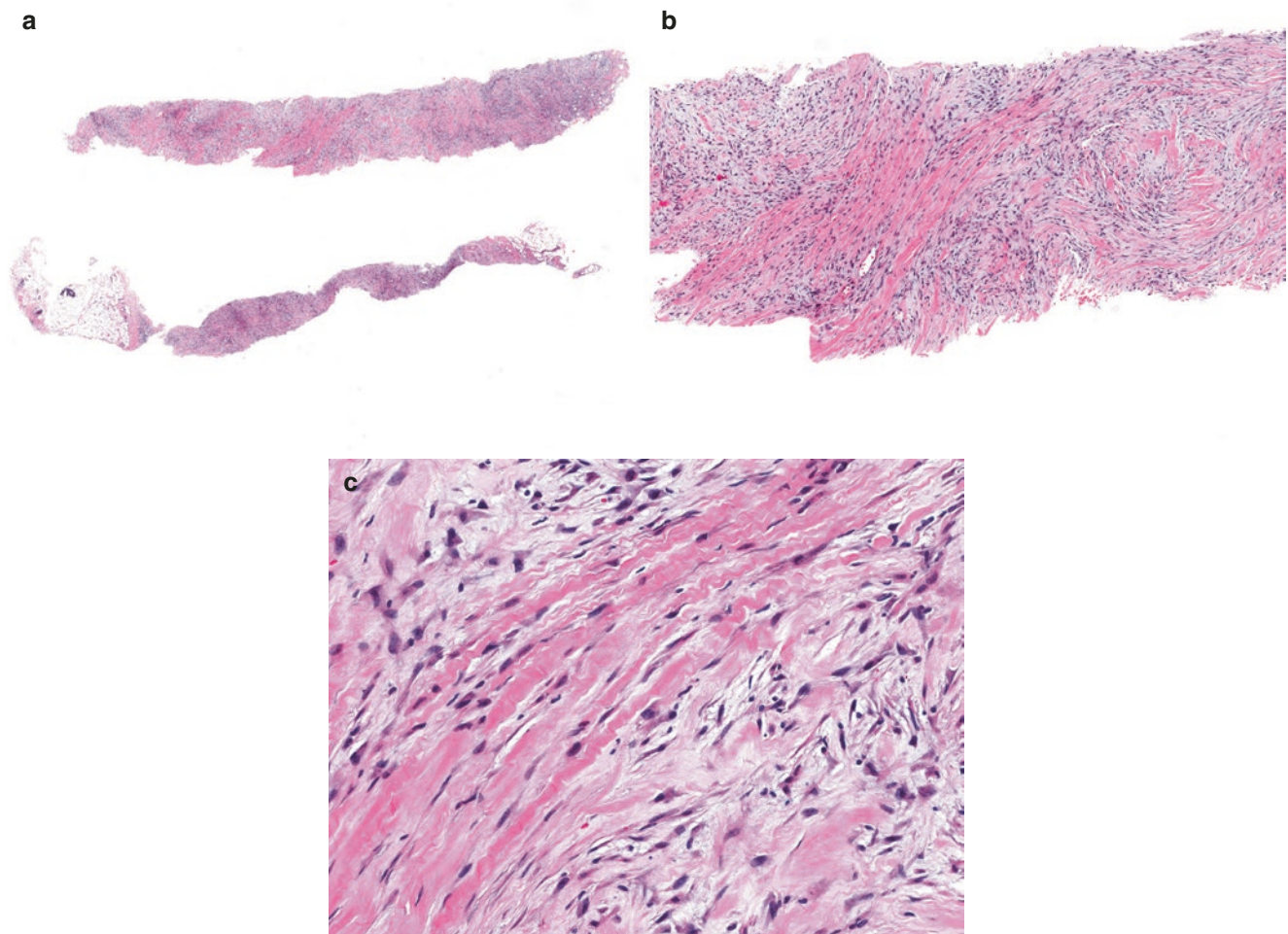
Fig. 12.56 Fibromatosis-like metaplastic carcinoma. (**a**, **b**) Core needle biopsy demonstrates spindled tumor cells arranged in long fascicles mimicking fibromatosis. (**c**) On higher magnification, the spindled cells demonstrate pale eosinophilic cytoplasm and bland, slender nuclei with tapered edges, and finely distributed chromatin. Note the abundant stromal collagen in the background
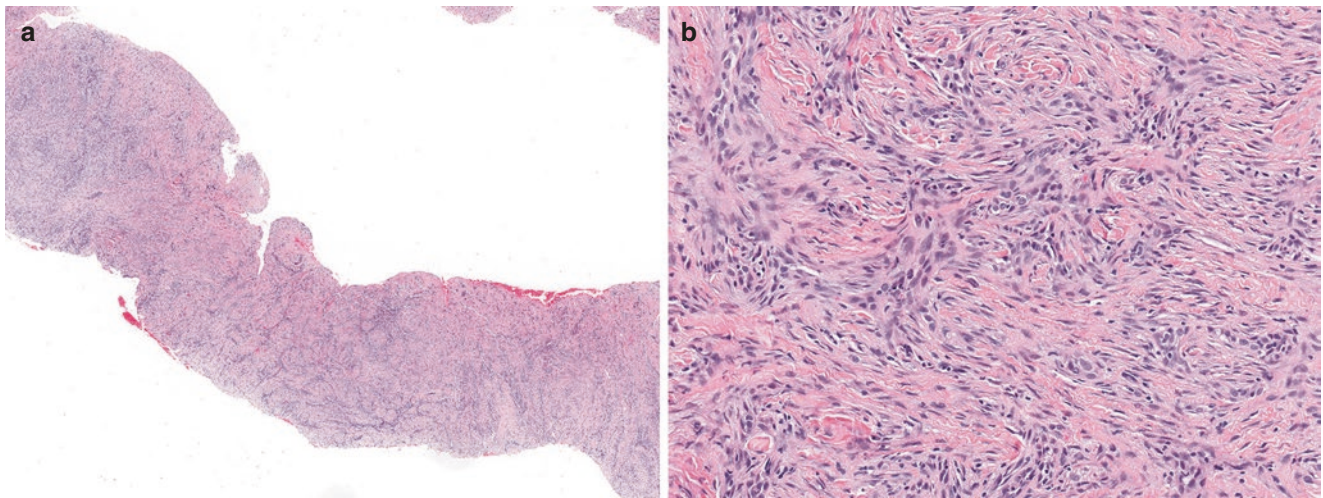
Fig. 12.57 Fibromatosis-like metaplastic carcinoma (FLMBC). (**a**, **b**) FLMBC showing higher cellularity and foci of epithelioid tumor cells with more rounded nuclei. Nuclear features are bland, and mitotic activity is low
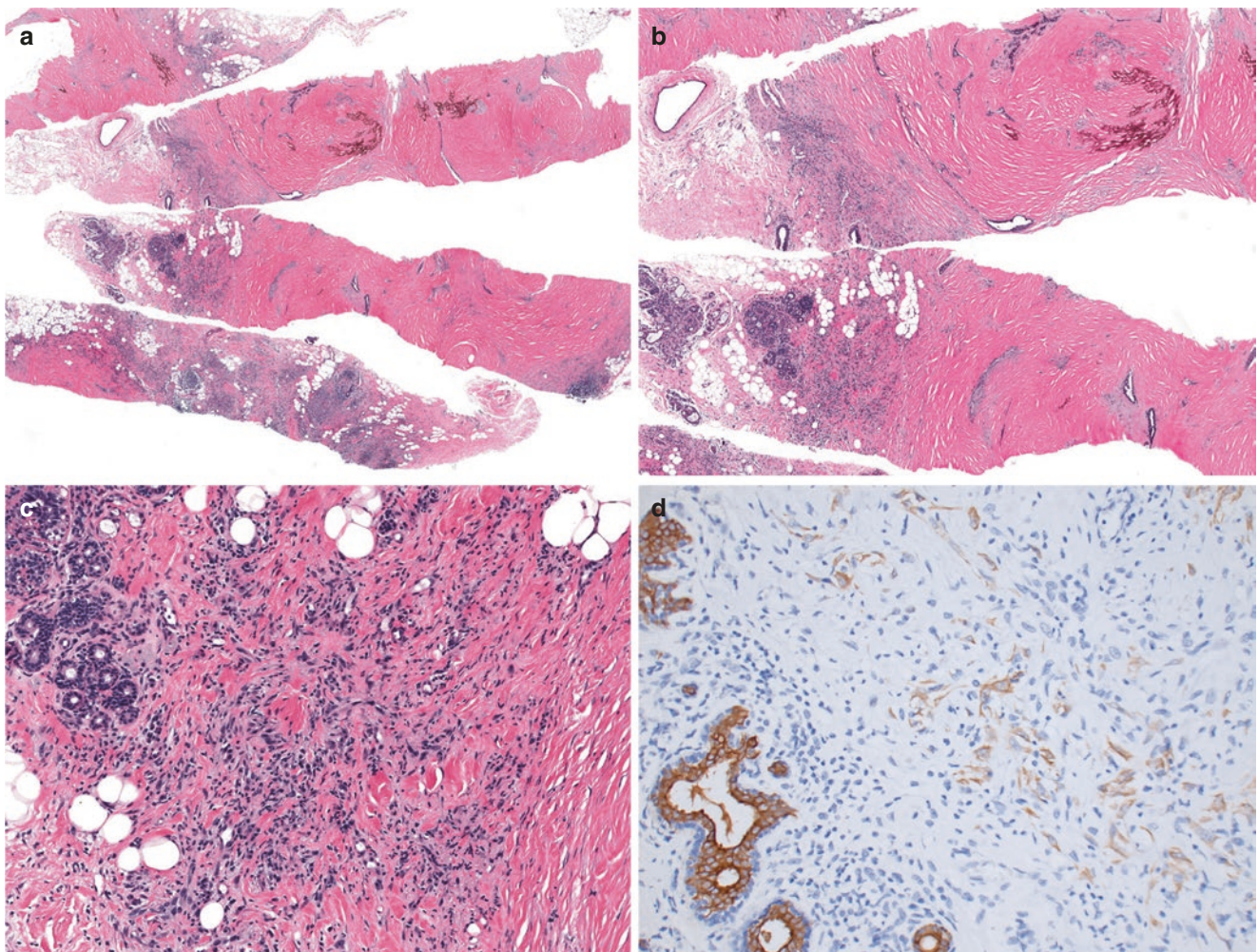
Fig. 12.58 Fibromatosis-like metaplastic carcinoma (FLMBC). (**a**, **b**) This FLMBC shows extensive sclerotic and hypocellular stroma involving multiple core fragments, with peripheral inflammatory foci noted on low power. This case could easily be mistaken for a fibroinflammatory process. (**c**) Higher magnification reveals the subtle presence of atypical spindle cells in association with the inflammatory lymphohistiocytic infiltrates. Immunostains for (**d**) keratin AE1/AE3 and (**e**) p63 highlight the infiltrative growth of the atypical spindle cells and confirm the diagnosis
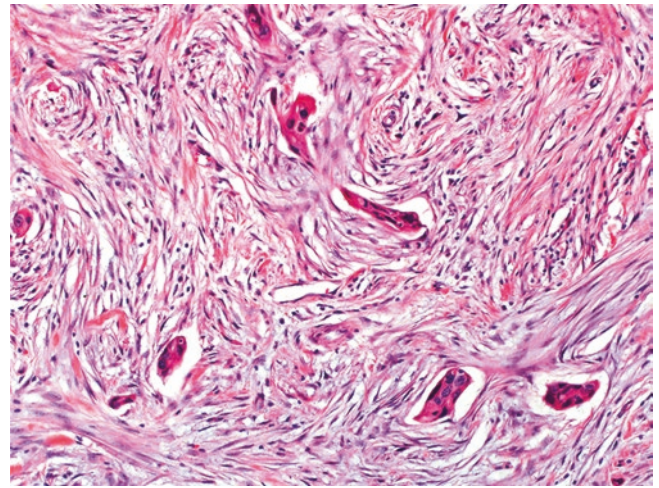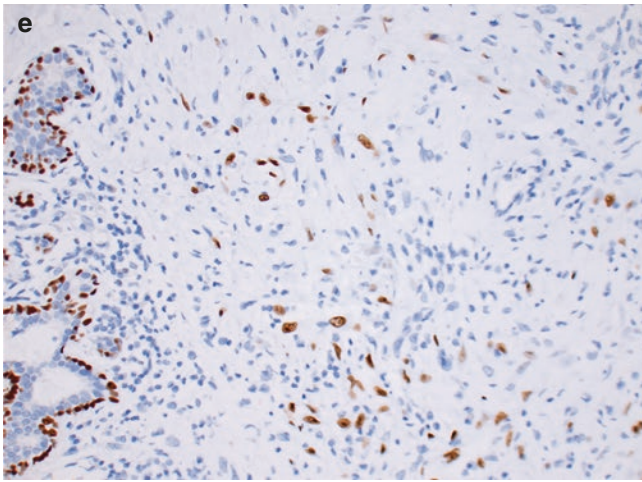
Fig. 12.58 (continued)

Fig. 12.60 Fibromatosis-like metaplastic carcinoma (FLMBC) with squamous tumor cells. Small clusters of squamous cells are embedded within the spindle cell proliferation of this FLMBC. These squamous cells should comprise <5% of the tumor
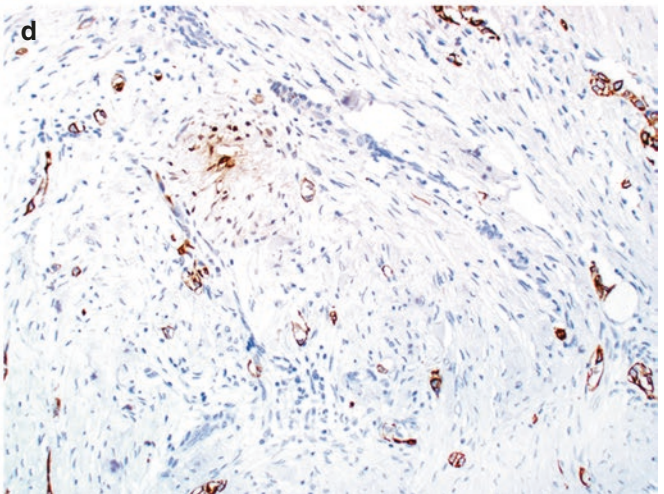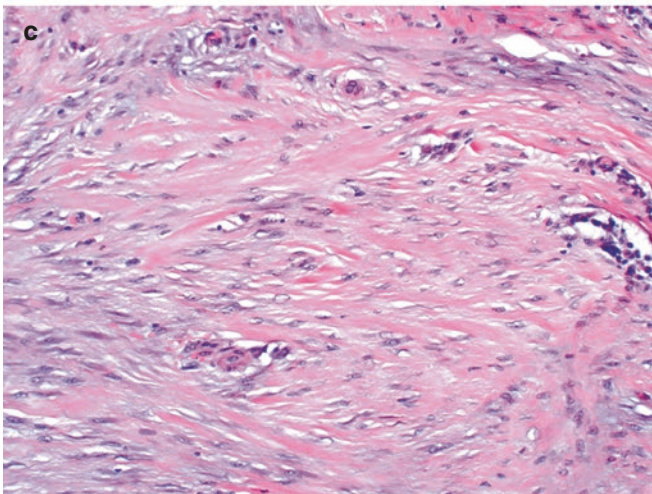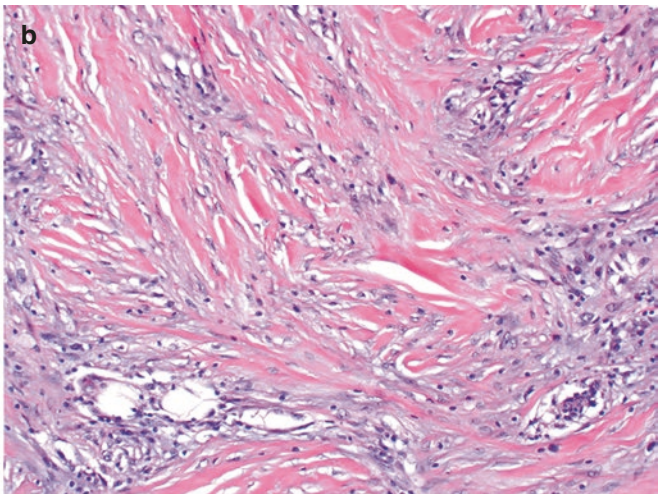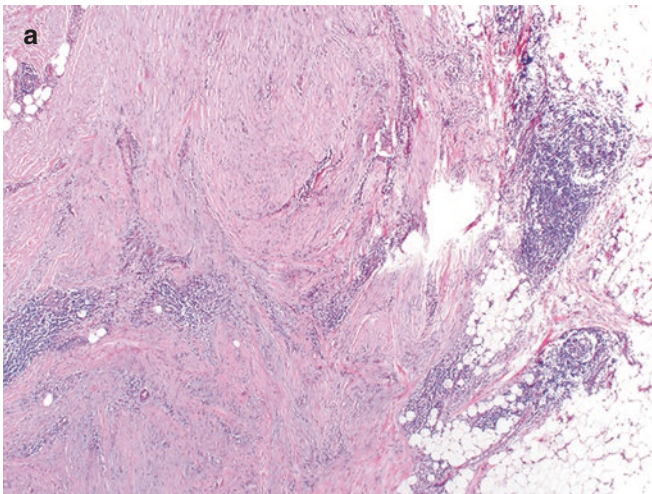
Fig. 12.59 Fibromatosis-like metaplastic carcinoma (FLMBC) mimicking scar tissue. (**a**) This FLMBC demonstrates low-power features suggestive of scar tissue. (**b**) High-power examination reveals abundant dense collagen with associated bland spindle cells and a mild inflamma-tory infiltrate. (**c**) Rare single and small clusters of epithelioid cells with squamoid features are identified after thorough searching. (**d**) HMWCK (34βE12) immunostain highlights the neoplastic cells

have been mistaken as a scar or fibroinflammatory process (Figs. 12.58 and 12.59).

Immunohistochemistry

FLMBC are consistently p63 and cytokeratin positive, which is useful to establish the diagnosis (Figs. 12.58d, e and 12.59d) [282, 302, 304, 308]. However, the immunoreactivity may be focal and sometimes largely restricted to areas with epithelioid cells. The spindle cells express vimentin and may be EMA or SMA positive [302]. Like other types of metaplastic carcinoma, FLMBC are triple negative for ER, PR, and HER2 [302, 306] (see additional discussion in section "Spindle Cell Carcinoma" and Table 12.8 for immunohistochemical markers useful in the diagnosis of metaplastic carcinoma).

Differential Diagnosis

FLMBC should always be considered in a breast core biopsy of a bland spindle cell proliferation. The differential diagnosis of FLMBC encompasses various bland spindle cell lesions, including scar, fibromatosis, nodular fasciitis, myofibroblastoma, and inflammatory myofibroblastic tumor. These lesions can be all distinguished from FLMBC by lack of epithelioid clusters and cytokeratin and p63 expression

Table 12.8 Useful immunohistochemical markers in the diagnostic workup of spindle cell metaplastic carcinoma

Markers	Utility and interpretation
CK (MNF116, AE1/3, 34βE12, CAM5.2, CK5/6, CK14, CK19)	Positive in metaplastic carcinoma, especially AE1/3 and MNF116 (~80%) and basal keratins (34βE12, CK5/6, CK14, CK19) (~70%); luminal keratins (CK7, CK8/18, CK19) less frequently positive (~30–60%) May be positive in phyllodes tumors[a]
p63	Positive in metaplastic carcinoma, especially FLMBC, but also other types May be positive in phyllodes tumors[a], as well as benign and malignant mesenchymal tumors
CD34	Positive in fibroadenoma, phyllodes tumor, PASH, myofibroblastoma, angiosarcoma and dermatofibrosarcoma protuberans Negative in metaplastic carcinoma, fibromatosis, and nodular fasciitis
β-Catenin	Aberrant nuclear expression in fibromatosis, but not specific (also in some phyllodes tumors and metaplastic carcinomas)
SOX10	Sensitive marker for melanoma and nerve-sheath-derived tumors May be positive in metaplastic carcinoma
Other markers	Based on morphologic features and history: S100 protein, SOX10, HMB-45 (melanoma); SMA, desmin, myogenin (muscle tumor); RB loss (myofibroblastoma); ERG, CD31, MYC (vascular tumor), etc.

[a]CK and p63 reactivity, when detected in phyllodes tumors, is often focal

[304]. CD34 shows strong positivity in myofibroblastoma but is negative in metaplastic carcinoma. Of note, aberrant nuclear staining for beta-catenin is characteristic of fibromatosis but can also be observed in some metaplastic carcinomas and phyllodes tumors [309]. FLMBC should be distinguished from metaplastic spindle cell carcinoma, which is not associated with the same indolent clinical behavior as FLMBC. Spindle cell carcinomas are higher grade tumors with moderate or marked nuclear pleomorphism and higher mitotic activity.

Spindle Cell Carcinoma

Microscopic Features

Spindle cell carcinomas are composed of atypical elongated to plump spindled cells arranged in cellular fascicular, herringbone, fasciitis-like, vaguely storiform, or patternless growth patterns (Fig. 12.61a–d). The spindle cells can entrap native ducts and lobules or obliterate the normal breast architecture. Microcystic or pseudovascular spaces may occasionally be seen and can mimic angiosarcoma. Nuclear pleomorphism is typically moderate or marked. The mitotic rate is variable, and markedly atypical mitotic figures are common in higher grade tumors [310]. The tumor cells may be focally more epithelioid or squamous, which can be a clue to the diagnosis. A chronic inflammatory infiltrate is often present, and scattered multinucleated osteoclast-like giant cells may be seen (Figs. 12.62, 12.63a, b, and 12.64a–d). Focal myxoid change or stromal hyalinization may be seen. Small foci of chondroid or osseous differentiation may also be present but should be focal. Most spindle cell carcinomas have infiltrative borders, but some may show a rounded pushing edge. DCIS may occasionally be seen in association with the invasive spindle cell component, which supports the epithelial nature of the tumor and can facilitate the diagnosis [311] (Fig. 12.65).

Immunohistochemistry

Immunohistochemistry is essential to demonstrate epithelial differentiation of the spindle cells in spindle cell carcinoma, especially in cases lacking associated DCIS. A panel of epithelial markers is recommended and should include broad spectrum keratins (MNF116, AE1/AE3), high-molecular-weight keratins (34βE12, CK5/6, CK14), and p63 [312] (Figs. 12.61e, f, 12.63c, d, and 12.64e). In general, the spindle cells are more likely to express high-molecular-weight keratins, whereas luminal keratins (CAM5.2, CK7, CK19) are more often negative [302, 313]. It should be emphasized that no single keratin is consistently positive in metaplastic
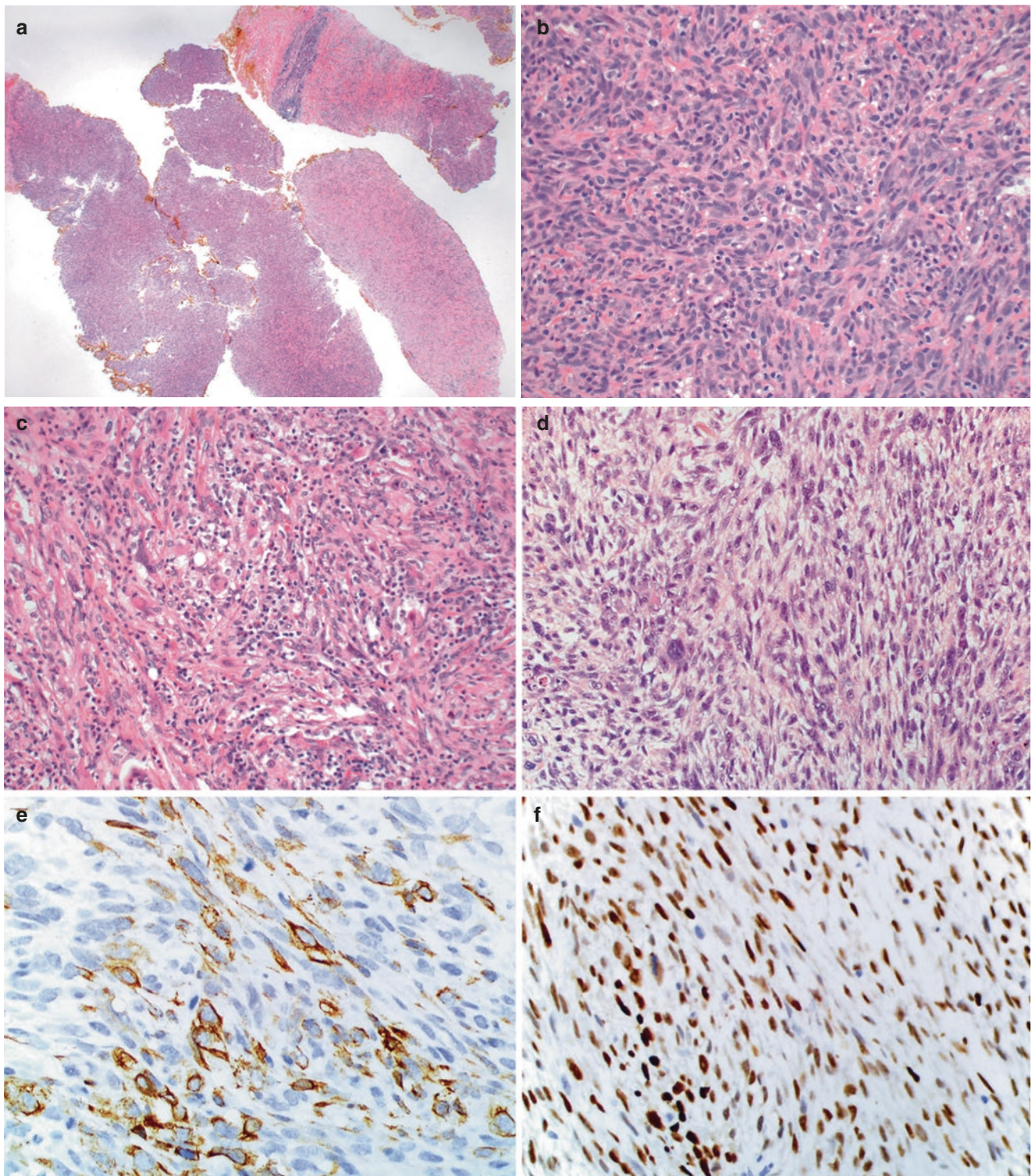
Fig. 12.61 Spindle cell carcinoma. (**a**, **b**) Core needle biopsy of this breast mass reveals a hypercellular spindle cell neoplasm with a stori-form growth pattern, moderate nuclear atypia, and scattered mitotic figures. (**c**, **d**) Other examples showing a more sarcomatoid appearance, featuring fascicles of spindled tumor cells with severe cytologic atypia. (**e**, **f**) Immunostains for keratins (in this case, MNF116) and p63 are helpful to confirm the epithelial nature of the spindle cells
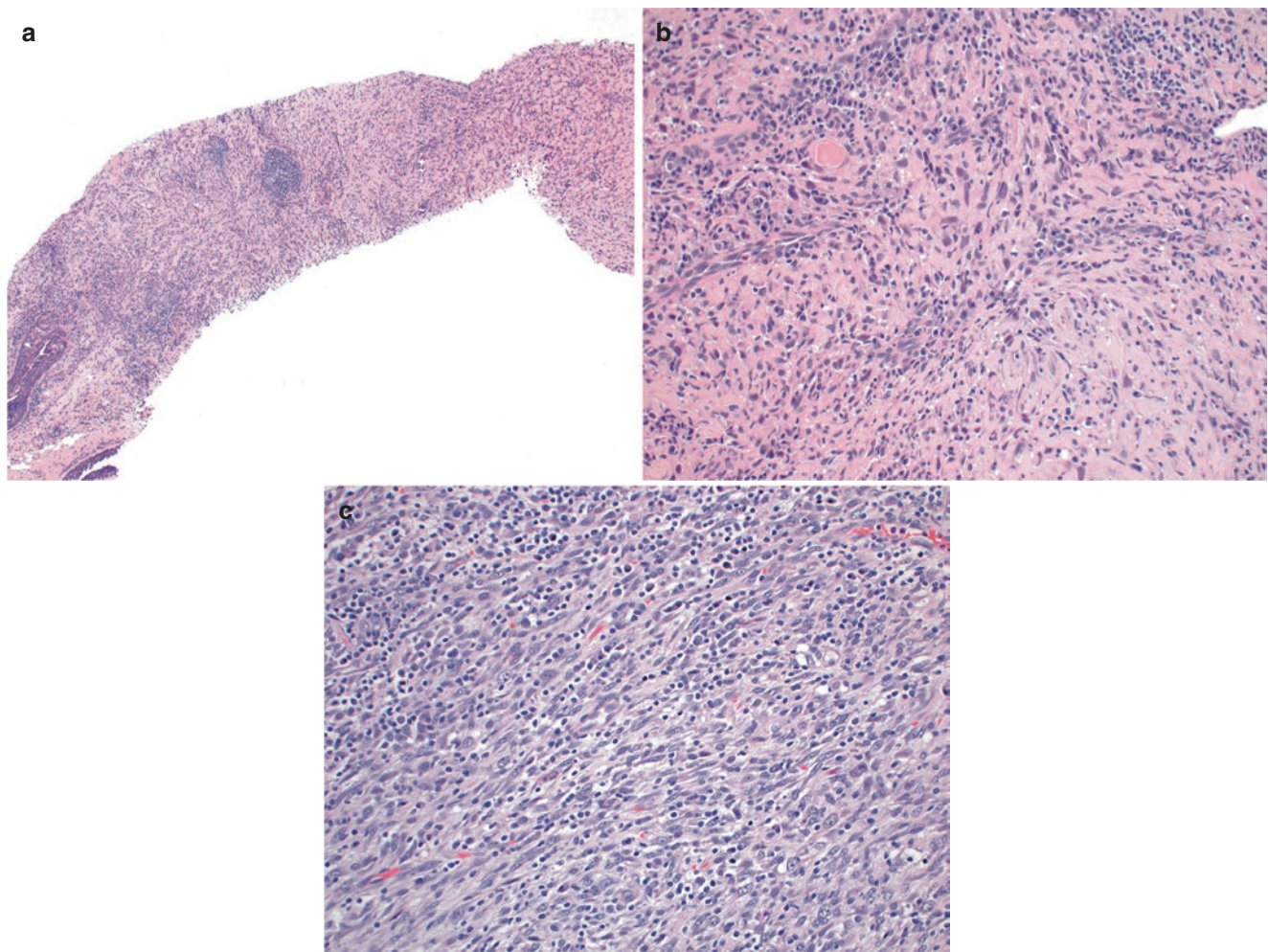
Fig. 12.62 Spindle cell carcinoma with prominent lymphoplasmacytic inflammation. (**a–c**) These two cases of spindle cell carcinoma show prominent associated lymphoplasmacytic infiltrates associated with the tumor cells

carcinoma. In addition, keratin positivity may be very focal [314]. Therefore, negative keratin staining in a core biopsy specimen does not exclude the diagnosis of metaplastic carcinoma. Immunohistochemical testing of multiple blocks of a surgical excision specimen may be required to reveal keratin reactivity in some cases. P63 is a sensitive marker for metaplastic carcinoma but is not specific and can be expressed in a variety of benign and malignant mesenchymal lesions, notably including malignant phyllodes tumors, which are often high in the differential diagnosis, especially in a core biopsy [315–318] (see section "Differential Diagnosis"). In addition to p63, other markers expressed by myoepithelial cells, such as SOX10, SMA, S100 protein, CD10, and maspin, can also be positive in spindle cell (and other) metaplastic carcinomas, supporting the notion that some of these tumors have myoepithelial-like differentiation and are on a spectrum with myoepithelial carcinoma [302, 319].

Metaplastic carcinomas may exhibit aberrant nuclear staining for beta-catenin, a feature traditionally regarded as

characteristic of fibromatosis [309]. GATA3 may also be positive in metaplastic carcinomas (~20–50%), including spindle cell carcinomas, with most positive cases showing weak staining [319–321]. A recent immunohistochemical study found overexpression of TRPS1, a GATA transcription factor and regulator of mammary epithelial cell growth and differentiation, in 86% of metaplastic carcinomas, including spindle cell carcinoma, SCC, and MCMD. Additional studies will be required to validate these results and their diagnostic utility [321]. CD34, a marker expressed in several mesenchymal tumors of the breast including phyllodes tumors, is typically negative in spindle cell carcinoma. Table 12.8 summarizes useful immunohistochemical markers that can be used in the diagnostic workup of spindle cell carcinoma.

Like other metaplastic carcinomas, spindle cell carcinomas are triple negative for ER, PR, and HER2. EGFR overexpression is frequent, with EGFR gene amplification described in a subset of cases [322, 323].
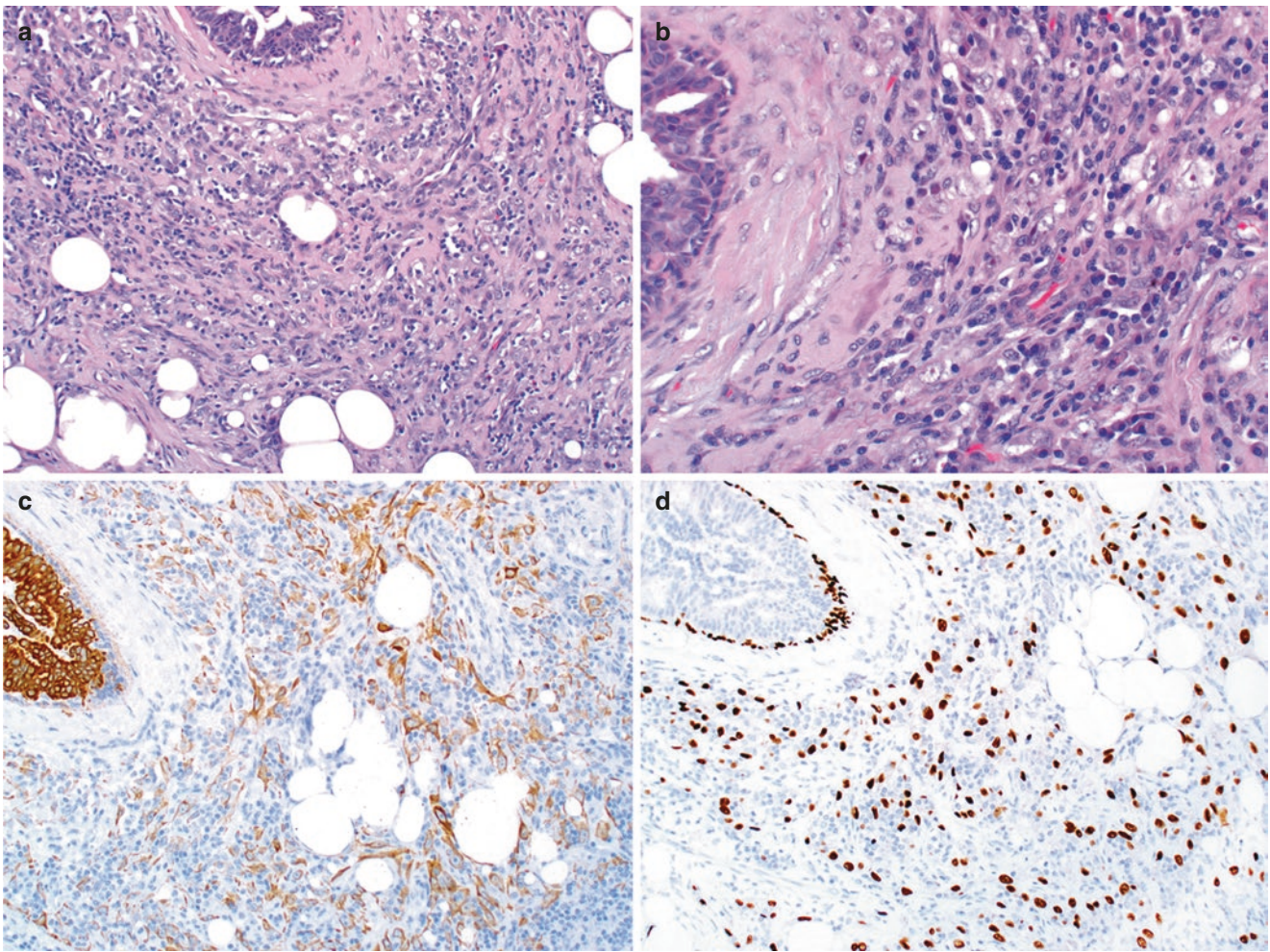
Fig. 12.63 Spindle cell carcinoma mimicking mastitis. (**a**) In this example, marked inflammatory infiltrates obscure the underlying neoplastic spindle cells and impart an appearance of mastitis on lower power evaluation. (**b**) Higher power magnification reveals the atypical spindle and epithelioid cells dispersed within the inflammation. (**c**, **d**) Broad spectrum cytokeratin antibody MNF116 and p63 demonstrate positive staining in the tumor cells, respectively. Note the lace-like pattern of the numerous tumor cells highlighted by MNF116

Differential Diagnosis

Despite a long list of differential diagnoses, metaplastic carcinoma is by far the most common spindle cell lesion of the breast (~45%), followed by phyllodes tumor, fibromatosis, and myofibroblastoma (each ~10%) [324]. Primary or metastatic sarcomas, including angiosarcoma, must also be included in the differential, but these tumors are rare in the breast. Accordingly, metaplastic carcinoma with a spindle cell component should always be considered when encountering a spindle cell proliferation arising in the breast. Identification of associated DCIS or small squamous foci helps support the epithelial nature of the tumor to facilitate the diagnosis. Therefore, adequate tumor sampling with careful evaluation for DCIS or epithelioid/squamous foci is critical in an excision specimen. However, DCIS may be scant or absent and not sampled by core biopsy. A panel of immunohistochemical markers is often required to demonstrate the epithelial nature of the spindle cells and establish the correct diagnosis (Table 12.8).

Distinction of spindle cell metaplastic carcinoma from malignant phyllodes tumor with stromal overgrowth is often problematic, especially in core biopsies. Like metaplastic carcinomas, the stromal cells of malignant phyllodes tumors can be p63 or keratin positive, although staining in phyllodes tumors is usually focal [317, 318] (Fig. 12.66). The ΔN p63 isoform p40 was suggested in one study to be more specific but less sensitive than p63 for the diagnosis of spindle cell carcinoma, although this requires further validation [317]. Focal expression of keratin, p63, and/or p40 in a spindle cell neoplasm of the breast therefore does not exclude phyllodes tumor, especially in a core biopsy specimen. CD34 may be helpful in this setting, as a subset of malig-
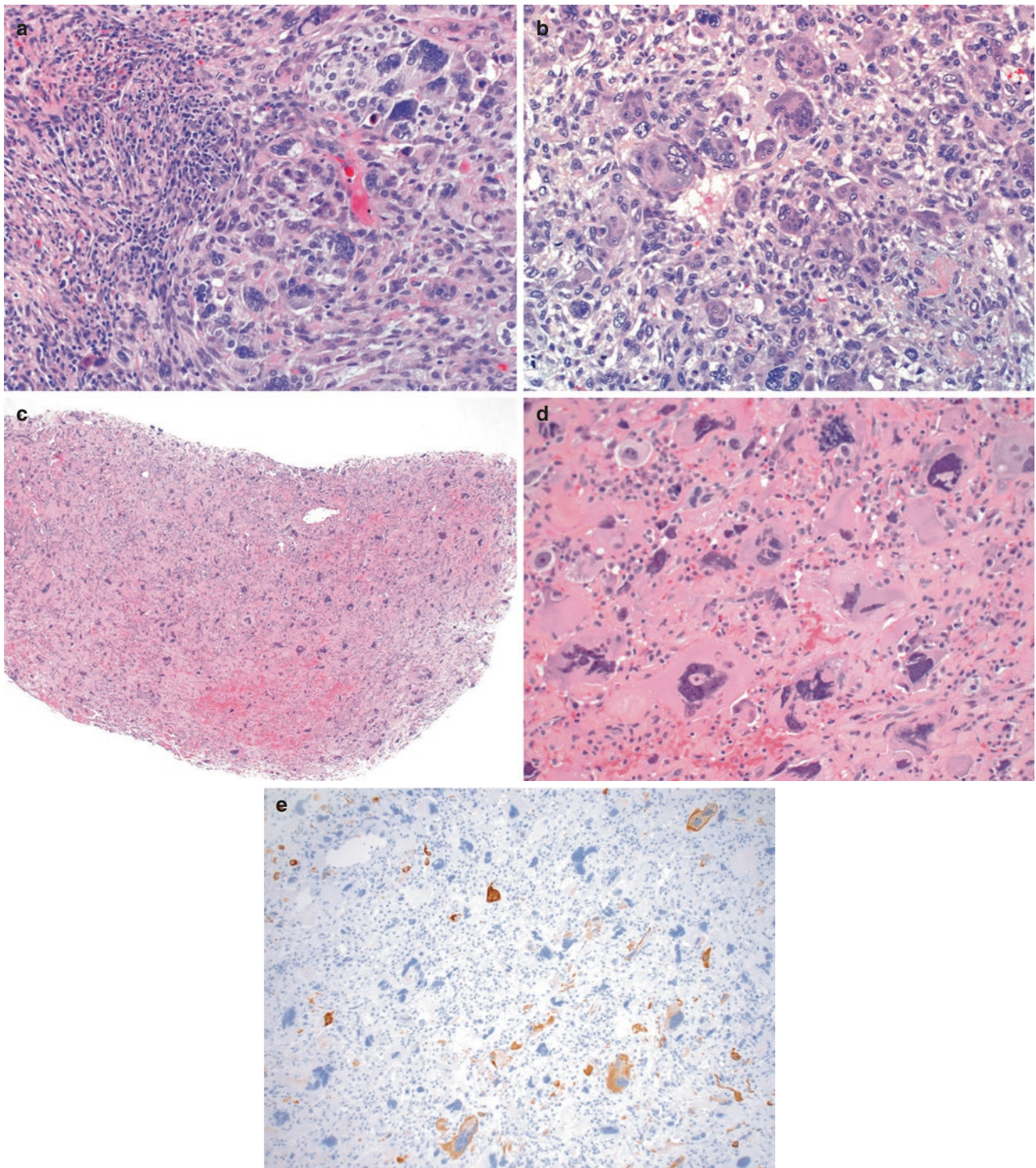
Fig. 12.64 Spindle cell carcinoma with giant cells. (**a, b**) Spindle cell carcinoma with osteoclastic-like giant cells. The tumor-associated giant cells demonstrate abundant eosinophilic cytoplasm and multiple small bland oval clustered nuclei, typical of osteoclastic-like giant cells. These cells are benign and are considered to belong to the histiocytic lineage. (**c–e**) In contrast, this spindle cell carcinoma is composed of markedly pleomorphic neoplastic epithelial cells, supported by positive keratin immunostain
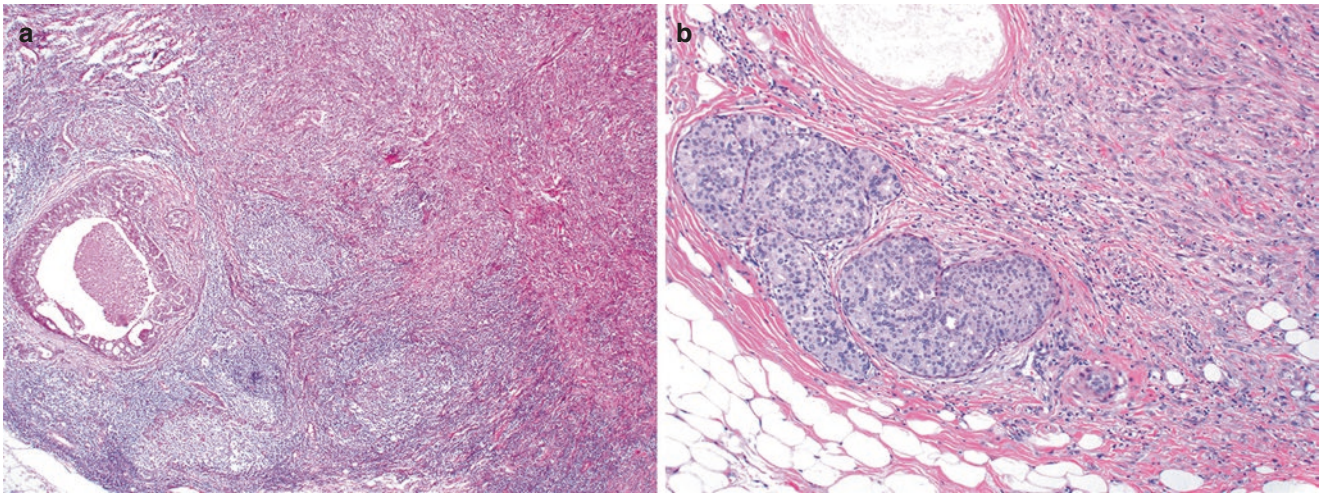
Fig. 12.65 Conventional ductal carcinoma in situ (DCIS) associated with spindle cell carcinoma. (**a**, **b**) The presence of DCIS associated with a spindle cell neoplasm helps support a diagnosis of metaplastic carcinoma, even if immunohistochemical stains for keratin are negative
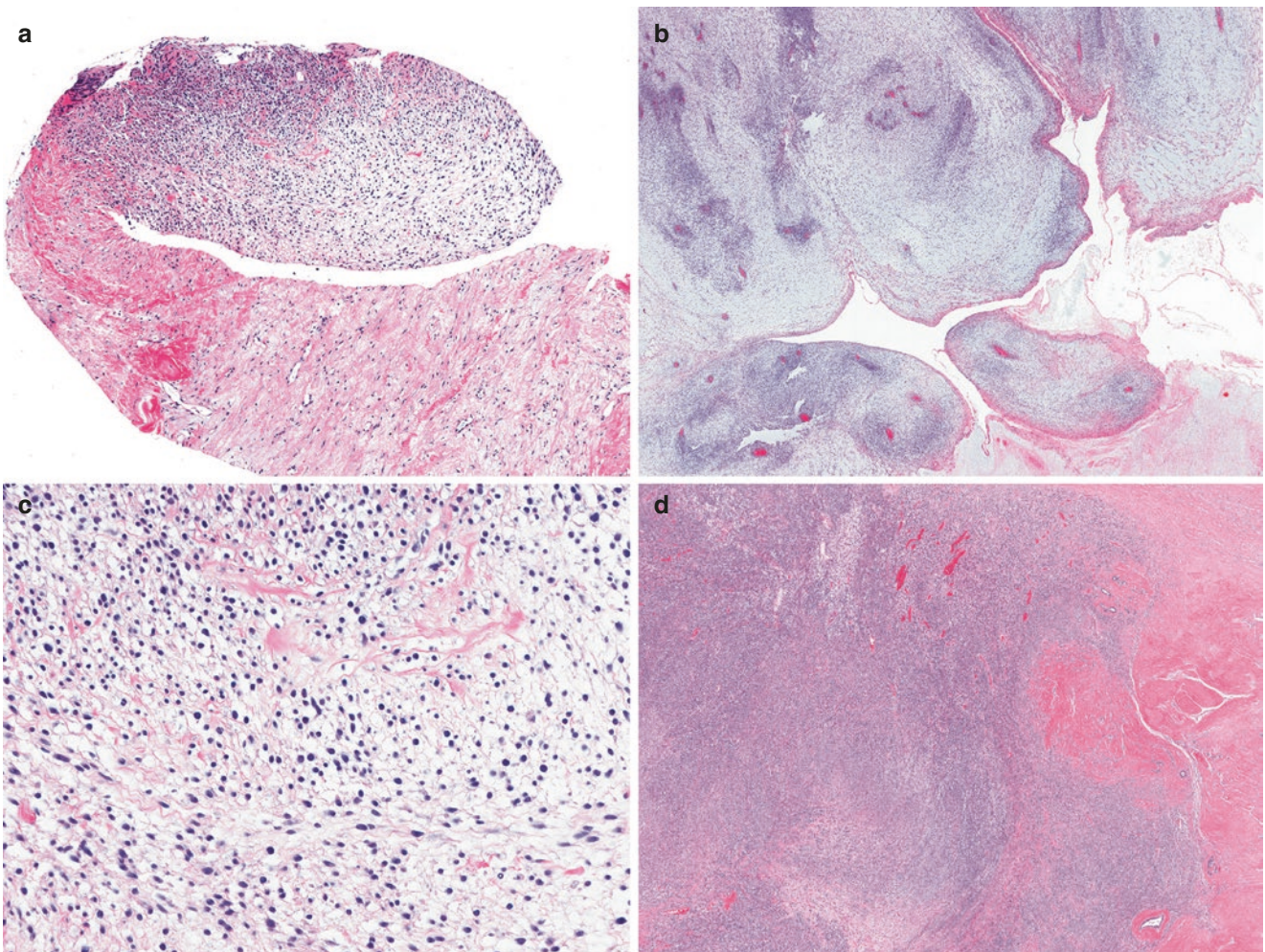
Fig. 12.66 Cytokeratin expression in a spindle cell neoplasm of the breast does not exclude phyllodes tumor. (**a**, **c**) This CNB demonstrates a spindle cell neoplasm with epithelioid features, including areas of cytoplasmic clearing and rounded hyperchromatic nuclei, but no glandular or ductal component. (**e**) An immunostain for pancytokeratin is positive in <5% of the spindle cells. (**b**, **d**) Excision revealed a malignant phyllodes tumor (**b**) with hypercellular areas of characteristic leaf-like growth, as well as (**d**) abundant stromal overgrowth. Note the presence of a residual hyalinized fibroepithelial area at the right of the image. (**f**) Immunohistochemistry also revealed focal (<5%) cytokeratin positivity of the phyllodes tumor stromal cells in the excision specimen
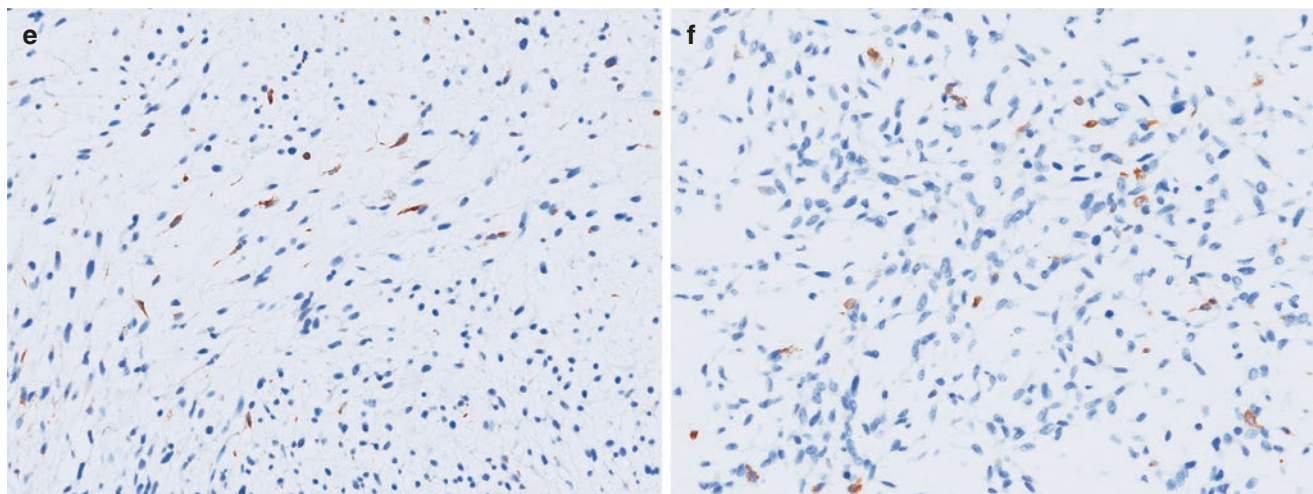
Fig. 12.66 (continued)

nant phyllodes tumors express this marker, which is negative in spindle cell carcinoma [313, 325]. Strong and diffuse keratin and p63 staining favors spindle cell carcinoma. Conversely, negative staining p63 and keratin staining in a core biopsy does not exclude metaplastic carcinoma, as expression can be focal (see also Chap. 7, sections "Phyllodes Tumor—Immunohistochemistry" and "Differential Diagnosis"). In the absence of histologic or immunophenotypic evidence for epithelial differentiation, it may not be possible to differentiate metaplastic carcinoma from phyllodes tumor or sarcoma on core biopsy. In such cases, a descriptive diagnosis such as "atypical spindle cell proliferation" or "spindle cell neoplasm" should be rendered, with recommendation for surgical excision. Indeed, unless epithelial differentiation is obvious and/or keratin immunopositivity is diffuse, a spindle cell neoplasm in the breast should be excised for definitive classification. In challenging cases, targeted sequencing could be useful in distinguishing metaplastic carcinoma from malignant PT. Specifically, the identification of a hotspot *MED12* mutation would confirm a fibroepithelial tumor and essentially exclude metaplastic carcinoma [282, 311, 326–332].

Squamous Cell Carcinoma

Primary squamous cell carcinoma (SCC) of the breast is a rare type of metaplastic carcinoma, accounting for <0.1% of all breast tumors [333, 334]. Pure SCC is almost entirely (>90%) composed of squamous cell carcinoma [335], but SCC may also be mixed with other types of metaplastic carcinoma, most commonly with a spindle cell pattern, or with IBC-NST, the latter of which is classified as high-grade ade-

nosquamous carcinoma. Primary cutaneous or metastatic SCC must be excluded prior to making a diagnosis of metaplastic SCC.

The etiology of metaplastic SCC is not known. It has been hypothesized that these tumors can arise from squamous metaplasia associated with either benign breast lesions or ductal carcinoma [336–339]. Rare SCC have been identified in association with inflammatory lesions, such as abscesses, chronic cysts, chronic mastitis, or implant capsules, suggesting that chronic inflammation may be a contributing factor to tumor development in some cases [337, 338, 340–343].

### Microscopic Features

SCC of the breast can present with various histomorphologic patterns of the invasive squamous cells, including keratinizing, non-keratinizing, cystic, papillary, clear cell, and acantholytic [344]. In most cases, the squamous cells are keratinized with eosinophilic glassy cytoplasm, intercellular bridges, and keratin debris accompanied by necrosis, desmoplastic stromal reaction, and prominent inflammation (Figs. 12.67a–c and 12.68). Cystic degeneration is common, with portions of the tumor composed of squamous lined cysts with variable nuclear pleomorphism [345] (Fig. 12.69). Acantholytic change in SCC is characterized by the presence of vascular like channels and pseudoglandular structures that can mimic angiosarcoma [344, 346]. The following pathological criteria are required to establish a diagnosis of metaplastic SCC of the breast: (1) the tumor is not derived from the overlying skin or nipple; (2) the infiltrative component is predominantly (>90%) of squamous type; (3) no other invasive neoplastic elements (ductal, mesenchymal, or other) are present in significant
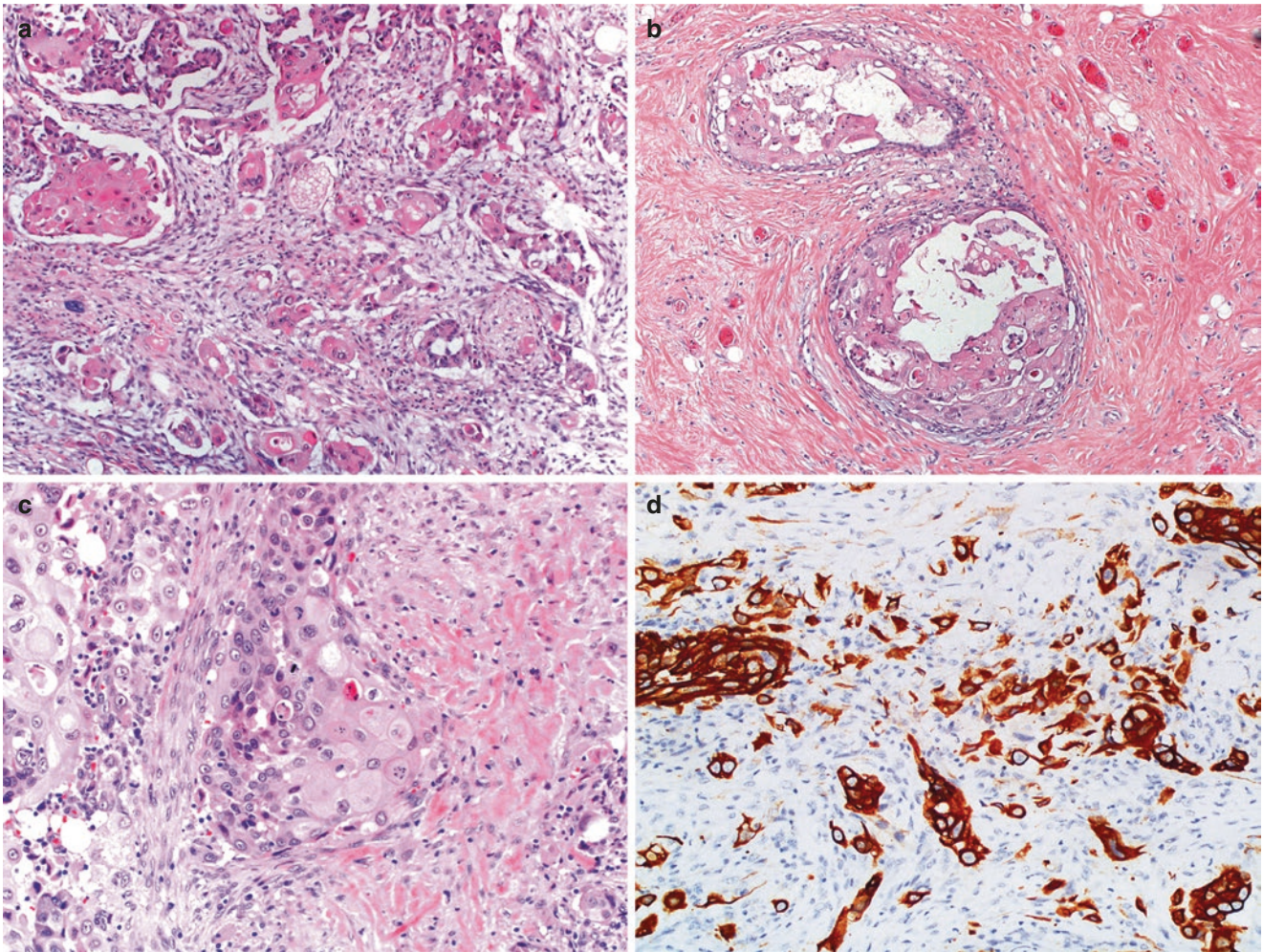
Fig. 12.67 Metaplastic squamous cell carcinoma. (**a**) This metaplastic carcinoma demonstrates infiltrating nests of squamous carcinoma cells with well-developed cytoplasmic keratinization. (**b**) Associated carcinoma in situ in this case also shows prominent squamous differentiation. (**c**) Another case of metaplastic SCC showing clusters of pleomorphic squamous cells, characterized by well-defined cell borders and glassy eosinophilic cytoplasm indicative of keratinization. (**d**) An immunostain for CK5/6 shows strong and diffuse positivity in the tumor cells
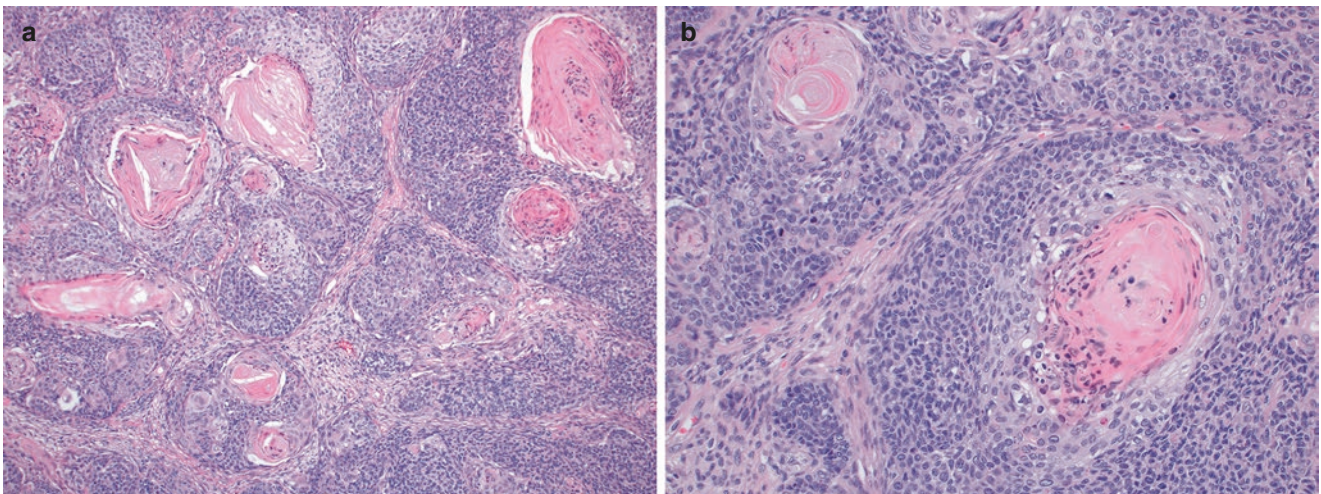
Fig. 12.68 Metaplastic squamous cell carcinoma. (**a**, **b**) Another example of metaplastic SCC showing keratin pearl formation. Note the presence of intercellular bridges in the malignant squamous cells surrounding the keratin pearls on high magnification
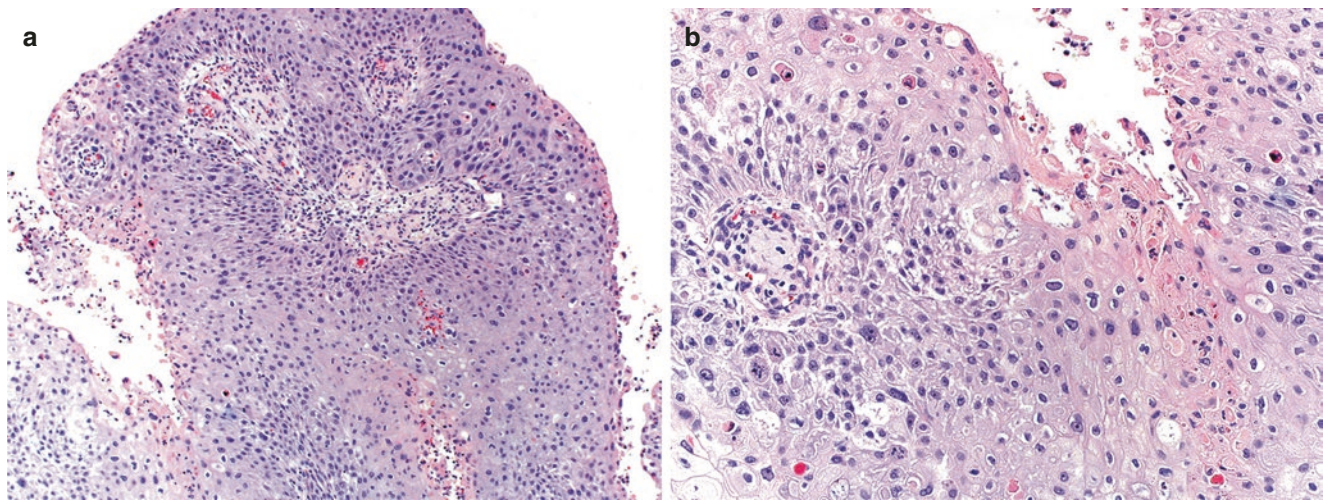
Fig. 12.69 Metaplastic squamous cell carcinoma with cystic degeneration. (**a**) CNB of this metaplastic SCC demonstrates foci of cystic degeneration, which may mimic sampling of an epidermal inclusion cyst. (**b**) Higher magnification illustrates distinct cytologic atypia, mitotic figures, and apoptotic cells

amounts (<10% total) after thorough sampling; and (4) metastatic SCC from another primary site has been excluded [337, 344].

Immunohistochemistry

The diagnosis of SCC is established primarily based on the cytologic features of squamous differentiation and not by immunohistochemical staining, although the latter can help support the diagnosis. SCC express basal keratins (CK5/6, CK14), p63, and p40 (Fig. 12.67d). These tumors are usually triple negative for ER, PR, and HER2, although, like other metaplastic carcinoma types, some SCC may be ER or HER2 positive [302, 311, 335, 347]. EGFR is frequently expressed [302, 335].

Differential Diagnosis

High-grade invasive ductal carcinomas, particularly those with abundant eosinophilic cytoplasm, may exhibit cytologic features suggestive of SCC. Strict morphologic criteria should be adopted when assessing a carcinoma for squamous differentiation. These include well-developed intercellular bridges, unequivocal keratinized cells, or squamous pearls. Necrotic and degenerating cells can mimic keratinized cells, as both may have hyperchromatic pyknotic nuclei and dense eosinophilic cytoplasm. The presence of perinuclear halos can help favor keratinized cells. Immunohistochemistry may not be helpful, because reactivity to CK5/6, p63, and p40 is not specific for SCC but is also noted in basal-like triple-negative IDC-NST.

Diagnosis of metaplastic SCC requires exclusion of cutaneous or metastatic SCC. In the absence of associated DCIS or overlying skin with dysplasia, this distinction can usually not be made based on histologic review of a core biopsy specimen alone and requires correlation with clinical history and tumor location (deep versus superficial).

Mucoepidermoid carcinoma (MEC) of the breast may also be mistaken for SCC. In contrast to SCC, MEC is composed of a mixture of intermediate, epidermoid, and mucinous cells (Figs. 12.28 and 12.70a–c). Focal squamous differentiation may be observed in the epidermoid cells. However, true keratinization with formation of squamous pearls excludes the diagnosis of MEC and favors SCC. Immunohistochemistry of MEC demonstrates a "zoning phenomenon," in which high-molecular-weight keratin (such as CK14) highlights the intermediate and epidermoid cells at the periphery of the tumor nests and cysts, and low-molecular-weight keratin (such as CAM5.2) decorates mucinous cells in the central regions of the nests [348] (Fig. 12.30). This unique staining pattern is not seen in SCC. Immunohistochemical stain p63 shows differential expression in the various components of MEC, with consistent expression in the intermediate cells, variable reactivity in epidermoid cells, and lack of expression in the mucinous areas (Figs. 12.28 and 12.70d). Intra- and extracellular mucin is PASD and mucicarmine positive, which can also be helpful in the differential diagnosis with SCC, which is PASD and mucicarmine negative (Figs. 12.27b and 12.70e). In contrast to SCC, MEC harbors *MAML2* rearrangement [100, 105, 111, 112] (see also section "Mucoepidermoid Carcinoma" in this chapter).
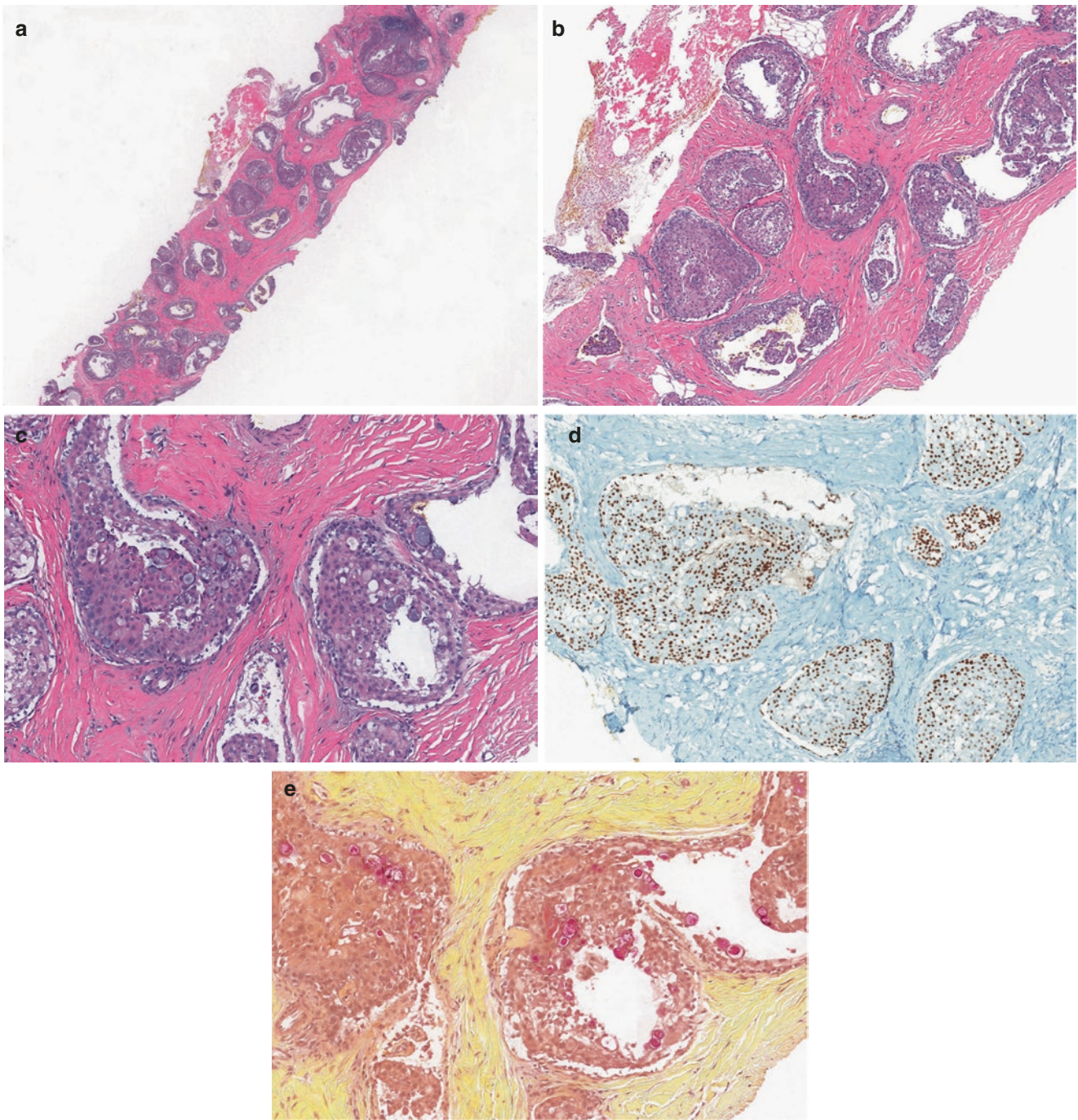
Fig. 12.70 Mucoepidermoid carcinoma of the breast, core needle biopsy. (**a**, **b**) This MEC shows a predominantly nested growth pattern with admixed microcystic spaces. (**c**) Higher magnification reveals the presence of epidermoid, intermediate, and mucinous tumor cells, which is diagnostic. (**d**) Immunohistochemistry for p63 is positive in the intermediate and epidermoid cells, whereas the mucinous cells are p63 negative. (**e**) In contrast, mucicarmine stain highlights the mucinous cells

Metaplastic Carcinoma with Heterologous Mesenchymal Differentiation

Microscopic Features

MCMD are invasive carcinomas composed of heterologous mesenchymal-like elements often admixed with carcinomatous areas. The mesenchymal-like component is often chondroid (Figs. 12.71, 12.72, 12.73, and 12.74), osseous (Fig. 12.75), or less frequently rhabdomyoid (Fig. 12.76), and the carcinomatous component is typically akin to moderately or poorly differentiated IDC-NST or squamous. The mesenchymal component may appear differentiated or frankly malignant, resembling chondrosarcoma and osteosarcoma of soft tissue [280]. Wargotz and Norris originally described a group of "matrix-producing carcinomas," which are characterized by direct transition from ductal carcinoma

to areas with cartilaginous or osseous matrix deposition, without an intervening spindle cell component [349] (Figs. 12.71 and 12.74). Matrix-producing carcinomas with chondroid differentiation tend to have circumscribed borders and large areas of central necrosis, with viable tumor cells concentrated near the peripheral rim of the tumor (Fig. 12.71). The stromal matrix, which can range from chondroid to chondromyxoid, is composed of acid mucopolysaccharides that stain metachromatically with Alcian blue and aldehyde fuchsin and are resistant to hyaluronidase and diastase digestion. A conventional adenocarcinoma component is often present to variable extent, but in some cases extensive sampling may be required to identify these areas, which help to differentiate these tumors from soft tissue chondrosarcoma or osteosarcoma. Associated DCIS is identified in a subset of cases, and when present, can be of NST or rarely show lumi-
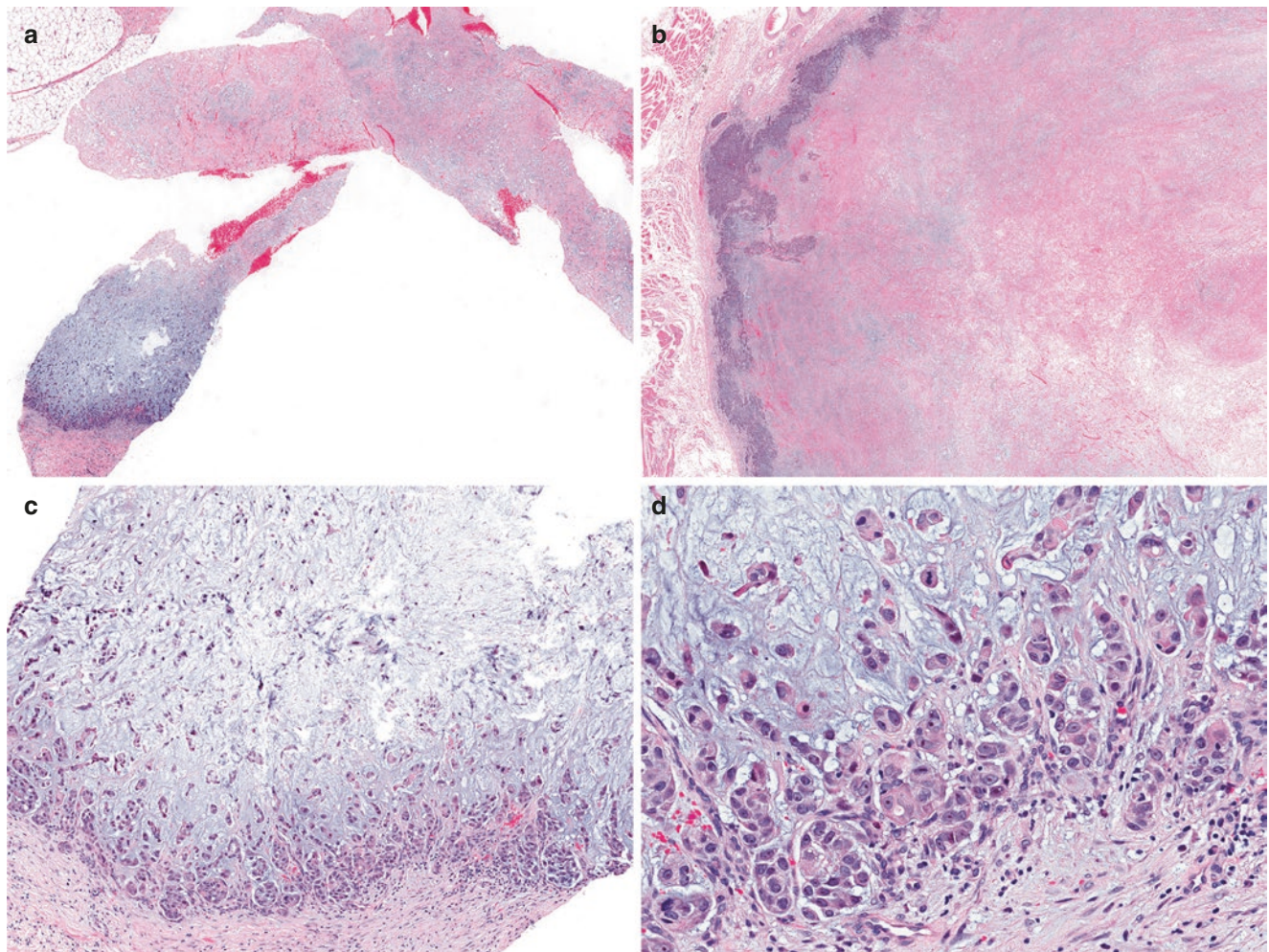
Fig. 12.71 Metaplastic carcinoma with heterologous mesenchymal (chondroid) differentiation, matrix-producing carcinoma. (**a**, **c**) On CNB, the chondroid matrix of this metaplastic carcinoma is obvious at low magnification, with increased cellularity noted at the tumor periphery and other areas being hypocellular and necrotic. (**b**) On excision, these tumors are often relatively well circumscribed at low power, with large areas of central necrosis and the bulk of tumor cellularity concentrated at the tumor periphery. (**d**) High-power evaluation reveals moderate cytologic atypia and scattered mitotic figures
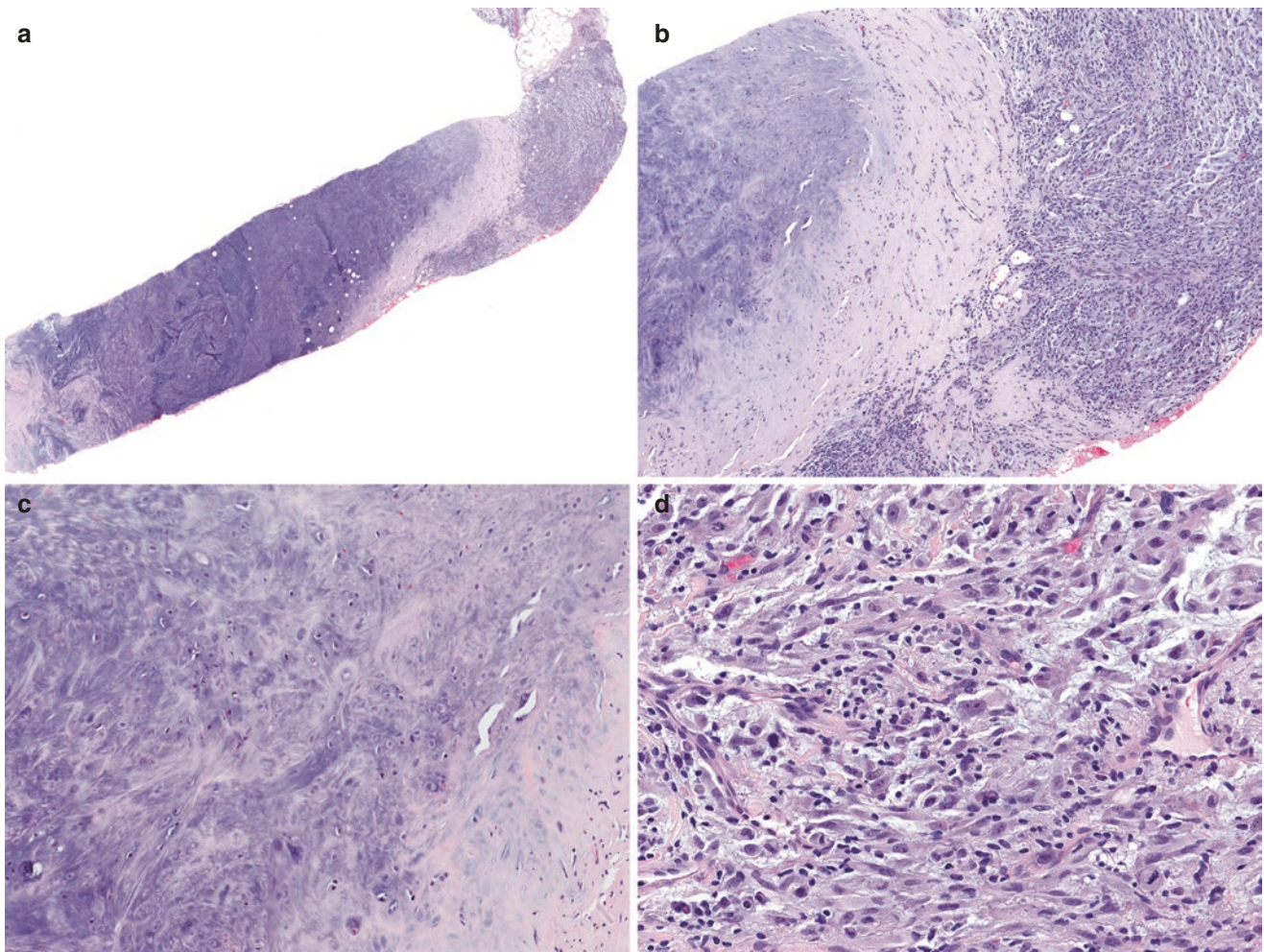
Fig. 12.72 Metaplastic carcinoma with heterologous mesenchymal (chondroid) differentiation. (**a**, **b**) On CNB, an area of hypocellular chondroid matrix is appreciated adjacent to a focal hypercellular spindle cell area. (**c**) The chondroid area is distinctly hypocellular with well-formed lacunae but no significant cytologic atypia. (**d**) In contrast, higher magnification of the hypercellular focus reveals malignant spindle cells with moderate nuclear atypia and prominent mitotic activity within myxoid stroma. Focal spindle cells are allowable in a tumor that otherwise meets criteria for matrix-producing carcinoma

nal matrix secretion (Fig. 12.77). Metaplastic carcinomas with chondroid differentiation can arise in association with microglandular adenosis [25, 350–352].

Immunohistochemistry

As for other metaplastic carcinomas, immunohistochemistry is essential to demonstrate epithelial differentiation of MCMD, especially in cases lacking a histologically recognizable invasive carcinomatous/ductal component or associated DCIS. A panel of epithelial markers including broad spectrum keratins (MNF116, AE1/AE3), high-molecular-weight keratins (34βE12, CK5/6, CK14), luminal keratins (CAM5.2, CK7), and p63 is suggested, as it is not possible to predict which marker(s) will be positive and staining may be focal. Keratin and p63 may be positive in epithelial and/or spindle cell components. MCMD may also express myoepithelial markers in addition to p63, such as SMA, CD10, SOX10, and S100 protein [302, 319] (Figs. 12.75d, e and 12.78). Like other metaplastic carcinomas, these tumors are usually triple negative for ER, PR, and HER2. EGFR can be positive in a subset [302].

Differential Diagnosis

MCMD should be distinguished from other lesions that have chondroid or osseous matrix. On the malignant end of the spectrum, this includes malignant phyllodes tumor with heterologous differentiation and primary or metastatic sarcoma (chondrosarcoma or osteosarcoma). In the absence of a
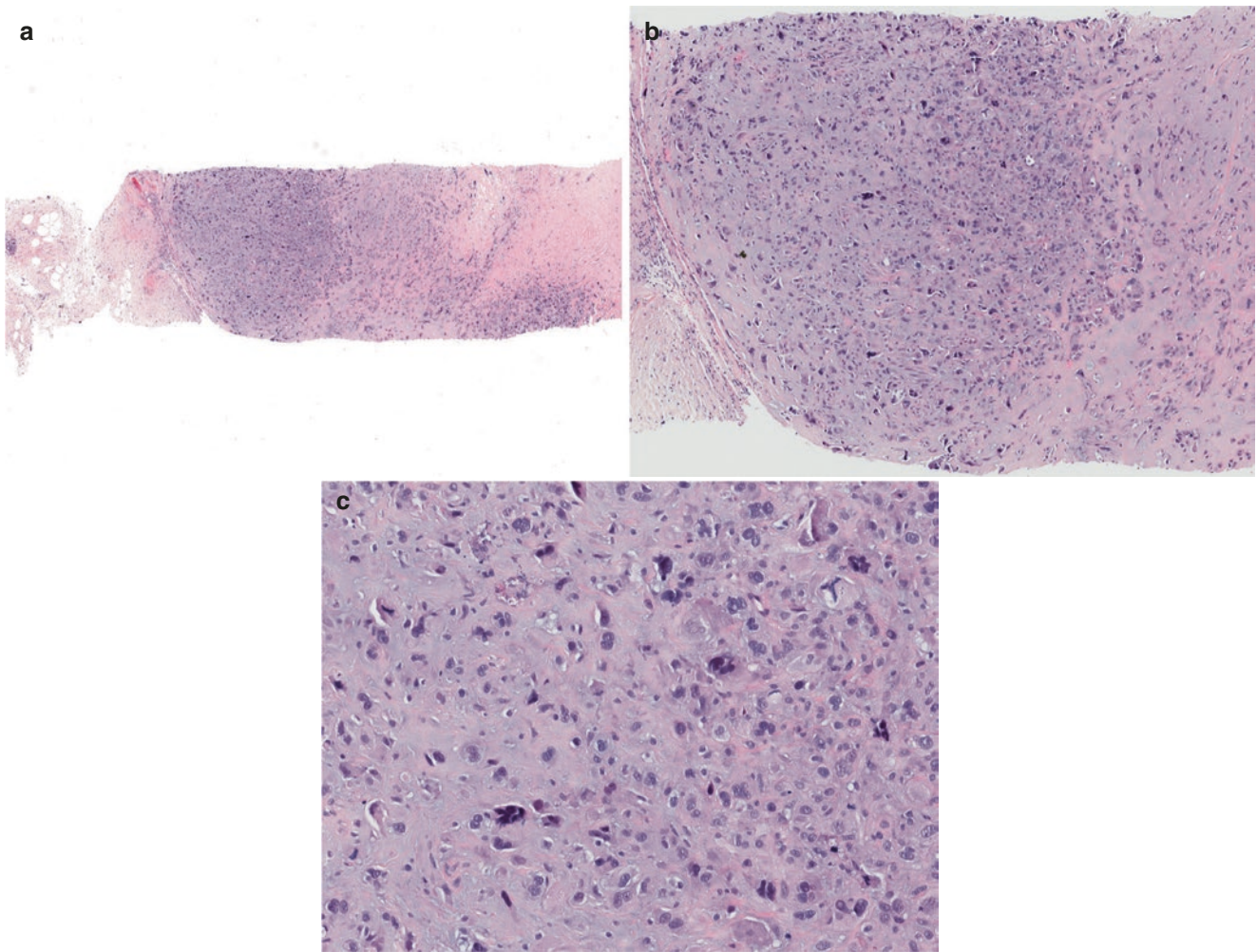
Fig. 12.73 Metaplastic carcinoma with heterologous mesenchymal (chondroid) differentiation. (**a–c**) On CNB, metaplastic carcinoma with chondroid differentiation and high-grade cytologic features may be indistinguishable from primary or metastatic soft tissue chondrosarcoma. Keratin immunopositivity or the presence of a diagnostic epithelial component can make this distinction (not shown)
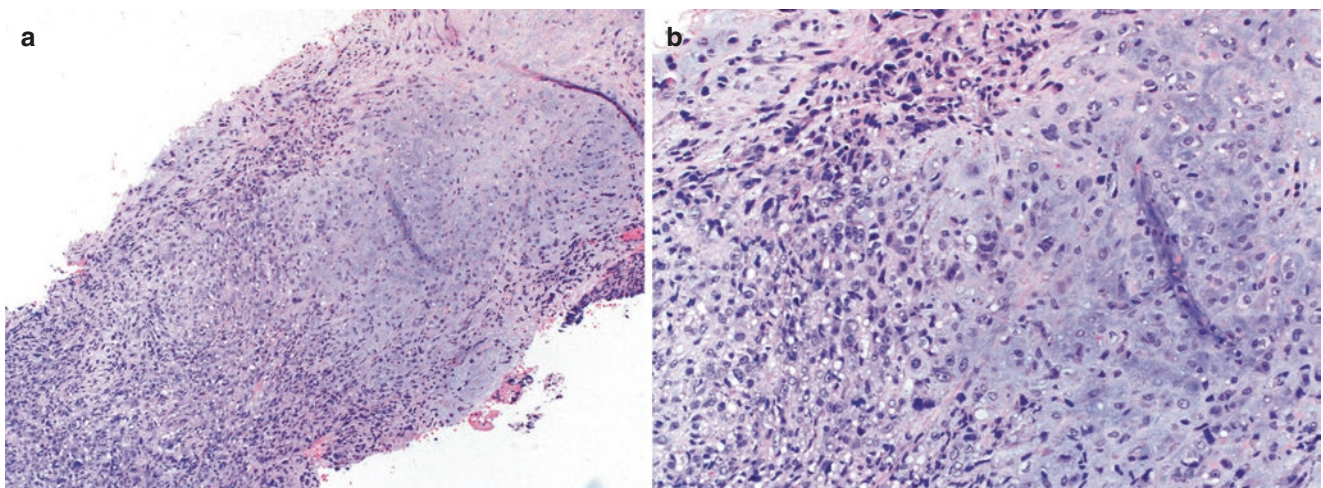
Fig. 12.74 Metaplastic carcinoma with heterologous mesenchymal (chondroid) differentiation. (**a**, **b**) Another example of chondroid matrix-producing carcinoma with prominent cytological atypia on core needle biopsy
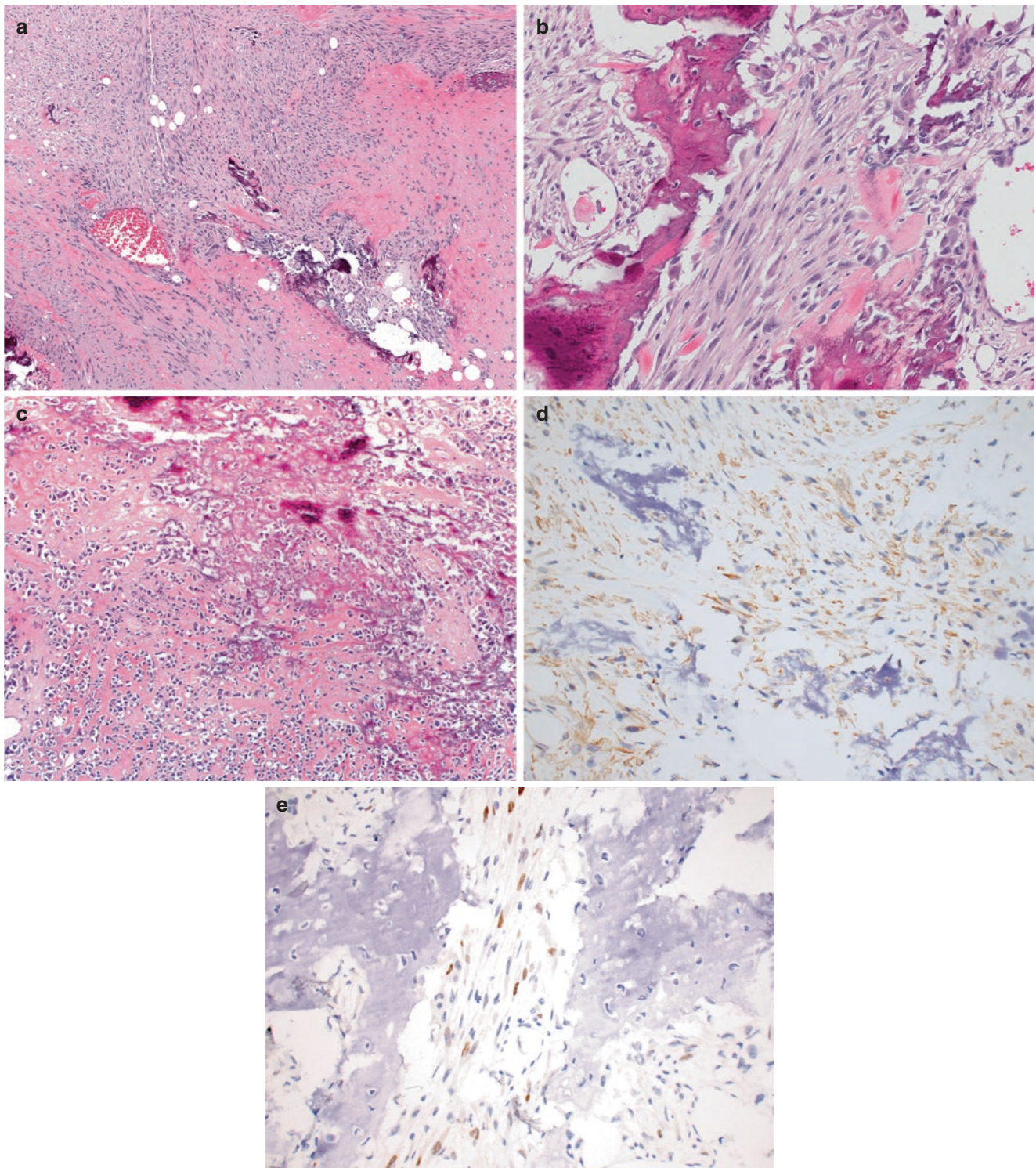
Fig. 12.75 Metaplastic carcinoma with heterologous mesenchymal (osseous) differentiation. (**a**, **b**) This metaplastic carcinoma shows areas of malignant spindle cells admixed with areas of osteoid and bone formation. (**c**) Another example of metaplastic carcinoma with osseous differentiation. Positive immunohistochemistry for (**d**) keratins (in this case CK14) and/or (**e**) p63 is useful in such cases to support the epithelial nature of the malignant tumor cells
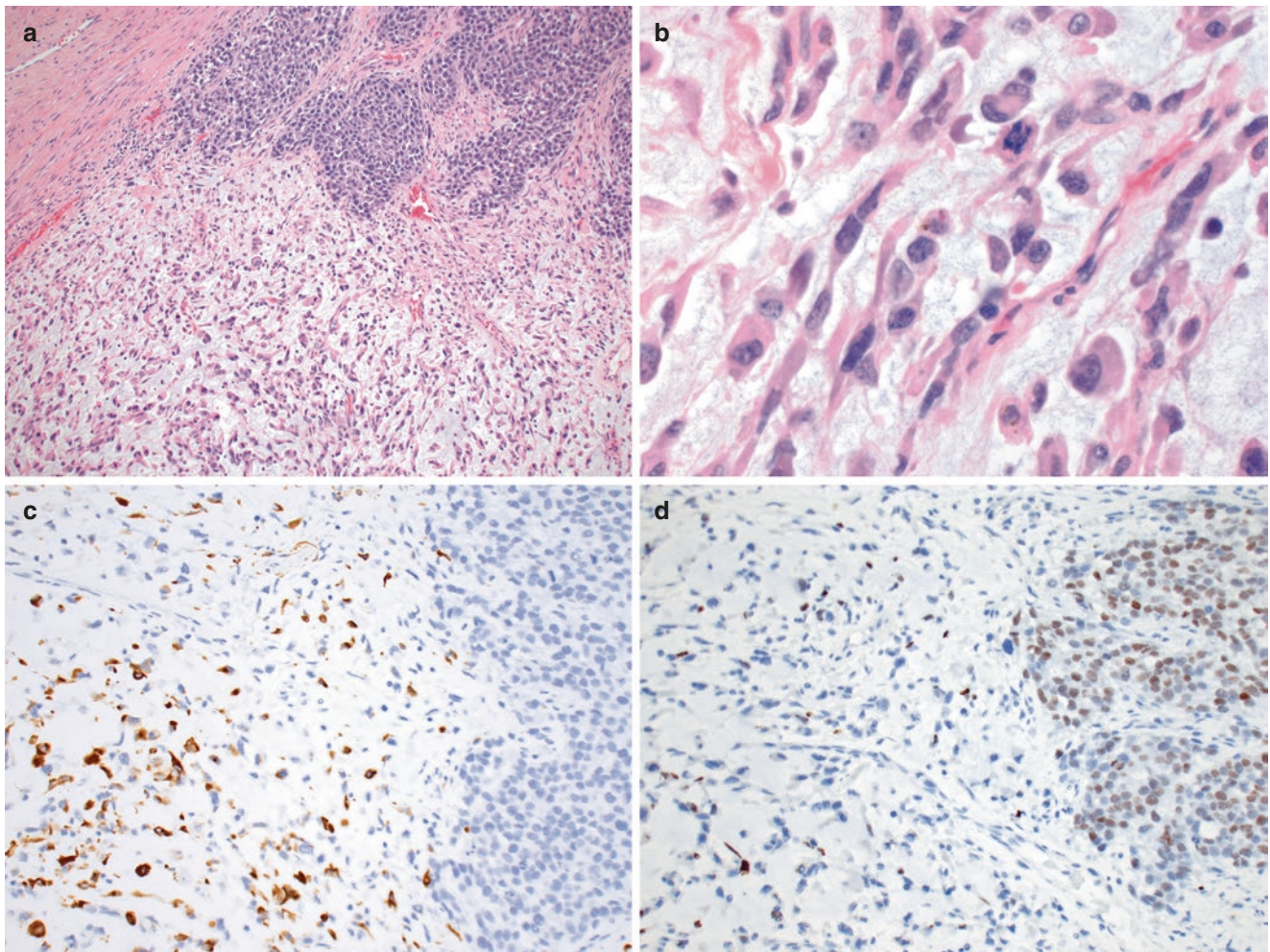
Fig. 12.76 Metaplastic carcinoma with rhabdomyoid differentiation. (**a**) This metaplastic carcinoma shows an abrupt transition between areas of cohesive epithelioid carcinoma cells (upper right) and discohesive spindled tumor cells. (**b**) Higher magnification reveals pleomorphic spindled tumor cells with rhabdoid features, including prominent eosinophilic cytoplasm and eccentrically located nuclei. (**c**) Immunohistochemistry for desmin is positive in the spindled tumor cells, further supporting the muscle phenotype. The spindle cells are also positive for myogenin (not shown). (**d**) In contrast, immunohistochemistry for p63 is diffusely positive in the epithelioid cells but only decorates rare spindled tumor cells
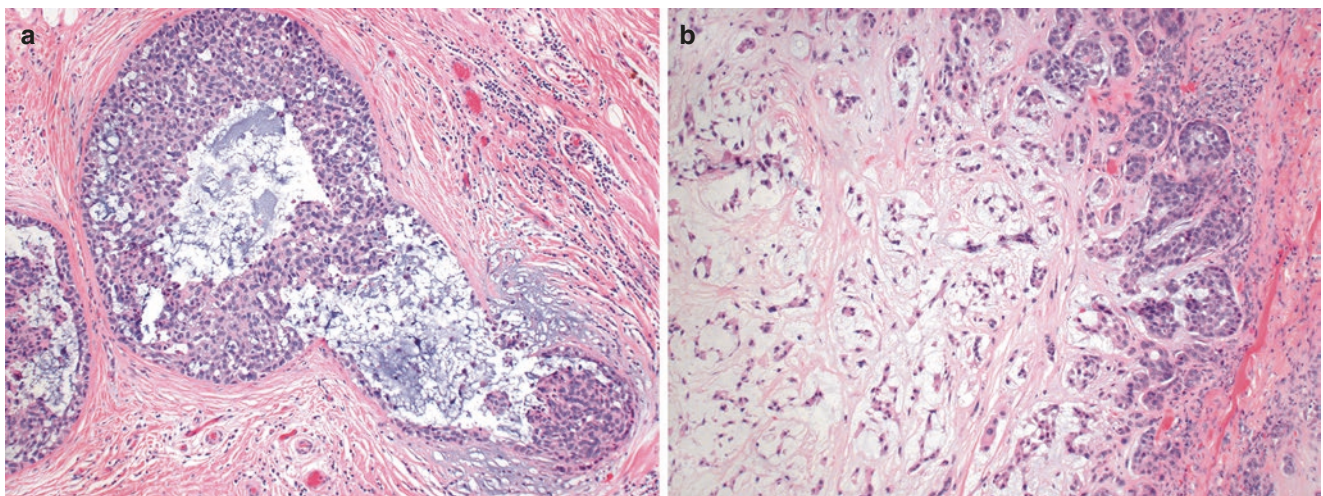
Fig. 12.77 Ductal carcinoma in situ with chondromyxoid features. (**a**) The in situ component of this carcinoma shows chondromyxoid features similar to that of (**b**) the associated matrix-producing carcinoma
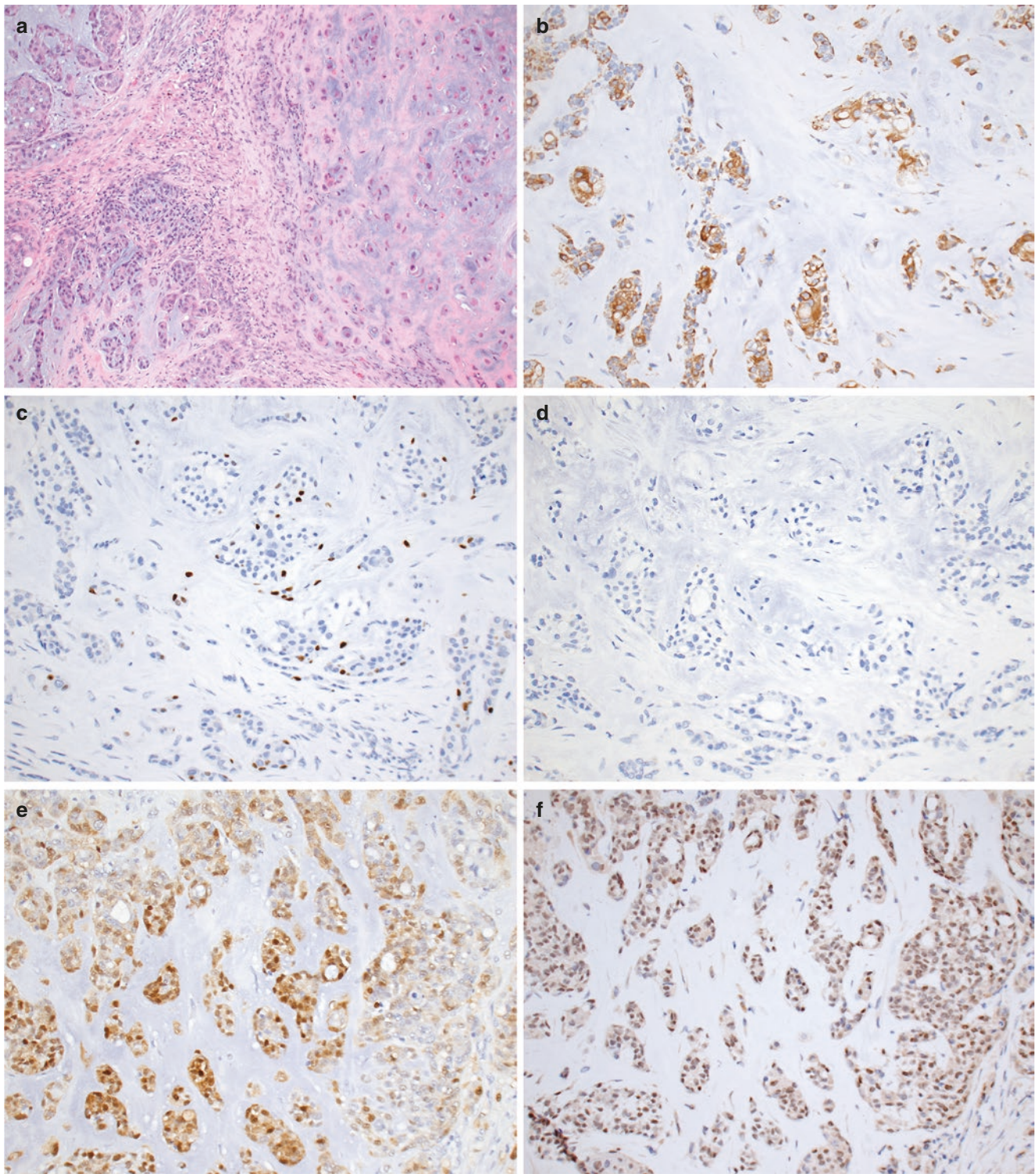
Fig. 12.78 Immunohistochemistry of metaplastic carcinoma with heterologous chondroid differentiation. (**a**) Immunohistochemistry of this metaplastic carcinoma shows positive staining of the chondroid matrix-associated tumor cells for (**b**) keratin AE1/AE3 and (**c**) patchy staining for p63, whereas (**d**) low-molecular-weight keratin CAM5.2 is negative. Metaplastic carcinoma, especially those with chondroid differentiation, often demonstrate expression of (**e**) S100 protein and (**f**) SOX10

conventional invasive carcinoma component or DCIS, the distinction from malignant phyllodes tumor rests on the identification of an associated benign epithelial component with intracanalicular architecture or embedded elongated and compressed ducts in phyllodes tumor, which may be absent in a core biopsy. A panel of immunohistochemical stains for keratins, p63, and CD34 may be useful, with the caveat that some phyllodes tumors can express keratins and p63 and may be CD34 negative (see sections "Spindle Cell Carcinoma" and "Differential Diagnosis," and Chap. 7, section "Phyllodes Tumor—Immunohistochemistry" and "Differential Diagnosis") [313, 317, 318, 325]. Chondrosarcoma or osteosarcoma, either primary or metastatic to the breast, is exceedingly rare and is a diagnosis of exclusion which can only be made after extensive tumor sampling and thorough immunohistochemical workup to exclude epithelial differentiation, as well as review of the clinical history.

MCMD with loose chondromyxoid matrix may also be confused with mucinous carcinoma in small biopsy specimens. Mucinous carcinomas do not show large areas of zonal necrosis, and the neoplastic cells usually exhibit less cytologic atypia and are more evenly distributed throughout the mucin. In addition, mucinous carcinomas are strongly positive for ER and luminal cytokeratins, whereas metaplastic carcinoma is ER negative.

Benign entities with chondromyxoid matrix are in the differential diagnosis on limited core biopsy material, including sclerosing papilloma with chondroid metaplasia and pleo-

morphic adenoma (Figs. 12.79 and 12.80a, b). In comparison to metaplastic carcinomas, pleomorphic adenomas lack necrosis and consist of biphasic epithelial and myoepithelial cells with bland cytology and no to rare mitotic figures (Fig. 12.80a–d).
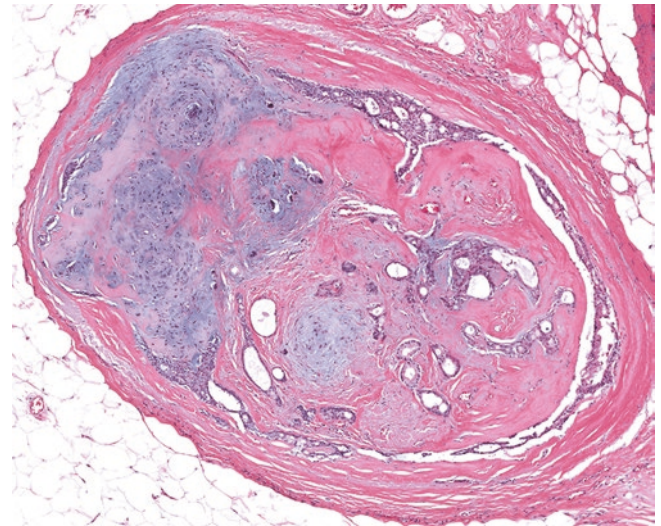
Fig. 12.79 Sclerosing papilloma with chondroid stroma. Chondroid metaplasia involving a sclerosed papilloma may raise the differential diagnosis of metaplastic carcinoma with chondroid differentiation. This may be especially challenging on core needle biopsy. The presence of associated sclerosed benign epithelial elements, lack of cytologic atypia, hypocellularity, and overall circumscription can be useful to make the distinction
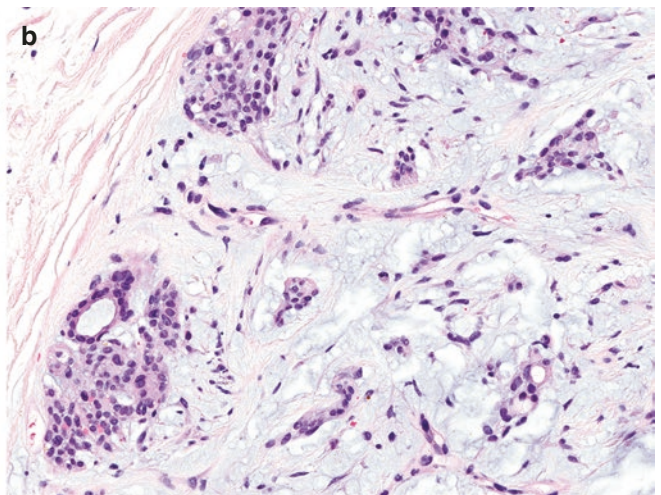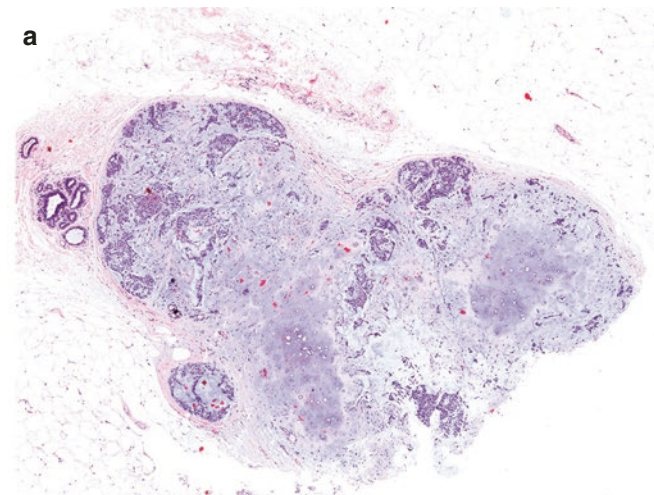
Fig. 12.80 Metaplastic carcinoma with heterologous chondroid differentiation versus pleomorphic adenoma. The distinction of these lesions can be challenging, especially on limited core needle biopsy material. (**a**) Low-power view of pleomorphic adenoma shows a well-circumscribed lobulated nodule composed of chondromyxoid matrix with associated cellular proliferation and without areas of necrosis. Note the benign breast lobule in the upper left corner. (**b**) High-power magnification reveals the characteristic biphasic tubule-forming epithelial and admixed myoepithelial proliferation, each with bland cytology and lack of mitotic activity. (**c**) In contrast, metaplastic carcinoma with heterologous chondroid differentiation displays central necrosis (right) with subtle infiltrative growth (left) into fat. (**d**) On high power, the cells are more atypical with larger hyperchromatic nuclei and scattered mitoses
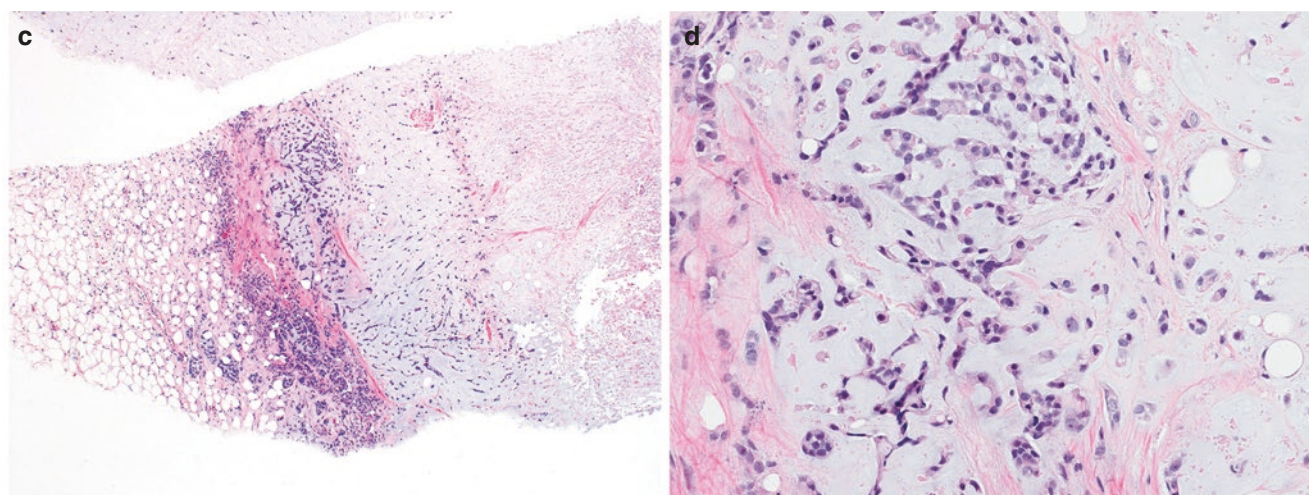
Fig. 12.80 (continued)

Mixed Metaplastic Carcinomas

A significant proportion of metaplastic carcinomas harbor a mixture of different metaplastic elements or metaplastic elements with conventional carcinoma (Fig. 12.81). These cases are classified as mixed metaplastic carcinoma. Each of the various components present should be recorded in the pathology report [275].

Pathogenesis and Risk Factors

The cell of origin of metaplastic carcinomas is unknown. It has been postulated that this heterogeneous group of tumors may develop from dedifferentiation events later during carcinogenesis, rather than malignant transformation of a particular cancer stem cell [353]. Regardless, genetic studies have confirmed a shared monoclonal origin of the various heterologous and conventional carcinomatous components, as well as associated DCIS [311, 354–358]. Metaplastic carcinomas show stem cell-like features, with enrichment for markers of tumor-initiating cells (ALDH1, CD44+/CD42−/low) and characteristics of epithelial-mesenchymal transition (EMT), such as increased expression of vimentin and E-cadherin repressors (ZEB1, SLUG, TWIST) and decreased cell-cell adhesion proteins, including E-cadherin and claudins [359–361]. Consistent with this, these tumors generally cluster with the basal-like and claudin-low intrinsic gene expression subgroups, the latter of which is enriched for EMT and cancer stem cell-like features [360–364]. The stem cell-like and EMT features of metaplastic carcinomas may explain their relative chemoresistance [365]. Transcriptomic heterogeneity between morphological types has been

described, with spindle cell carcinomas being claudin-low, and SCC and metaplastic carcinomas with chondroid differentiation being enriched for basal-like profiles. Using the TNBC gene expression classifier, metaplastic carcinomas with chondroid differentiation were all mesenchymal-like, whereas other types showed variable or unstable phenotypes [366].

Genetic studies have begun to elucidate the mutational landscape of metaplastic carcinomas. As a group (excluding LGASC and FLMBC), these tumors are enriched for mutations in *TP53*, PI-3 K pathway (*PIK3CA*, *PIK3R1*, *PTEN*), MAPK pathway (*KRAS*, *HRAS*, *NF1*), and Wnt pathway (*FAT1*, *CCN6*) genes, as well as *TERT* promoter. Chromatin remodeling genes are also frequently mutated (*ARID1A*, *KMT2C*, *KMT2D*) [282, 311, 331, 363, 367–370]. Metaplastic carcinomas and associated DCIS share identical sets of mutations, including in PI-3 K (*PIK3CA*, *PIK3R1*, *AKT1*, *PTEN*) and MAPK (*KRAS*, *HRAS*) pathway genes, highlighting an early role for these pathways in tumor development [311]. Overall, mutations in PI-3 K (*PIK3CA*, *PIK3R1*, *PTEN*) and MAPK (*NF1*, *HRAS*, *KRAS*) pathway genes are significantly more frequent in metaplastic carcinomas compared to other TNBC [311, 331]. However, differences in the mutational repertoire have been identified in morphologic types. Metaplastic carcinomas with chondroid differentiation (matrix-producing carcinomas) lack *PIK3CA* mutations, which are enriched in carcinomas with spindle cell and/or squamous differentiation [311, 331]. Similarly, *TERT* promoter mutations were found to be enriched in spindle cell carcinomas, SCC, and mixed metaplastic carcinomas with spindle and squamous differentiation, but absent in matrix-producing carcinomas [311]. *TP53* mutations appear to be less common in spindle cell carcinomas compared to
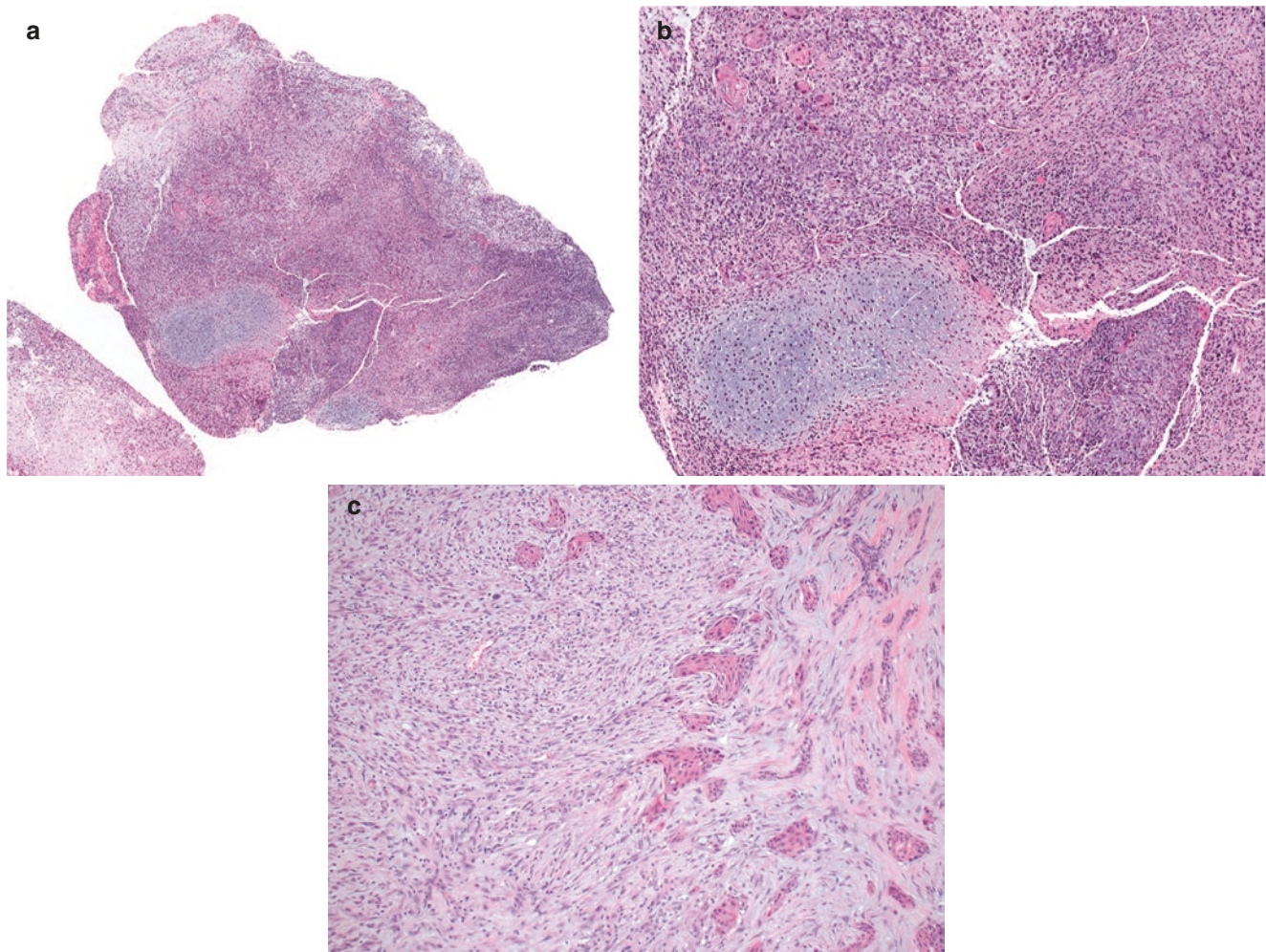
Fig. 12.81 Mixed metaplastic carcinoma with chondroid, squamous and spindle cell differentiation. (**a–c**) This metaplastic carcinoma shows mixed differentiation, with admixed chondroid and squamous differentiation and adjacent spindle cell areas

the other groups [311, 371]. Aside from LGASC and FLMBC, metaplastic carcinomas have complex genomes, including a subset with chromosomal alterations characteristically associated with *BRCA1/2* inactivation (BRCAness) [311, 331, 360, 366].

Case reports of metaplastic carcinoma arising in patients with neurofibromatosis suggest a possible, albeit rare, association [372–374]. Loss of heterozygosity at the variant germline *NF1* allele was described in one case arising in a 41-year-old woman [372].

The molecular features of low-grade metaplastic carcinomas (LGASC and FLMBC) have been characterized in less detail than high-grade metaplastic carcinomas. LGASC are basal-like carcinomas by surrogate immunohistochemical profiling (triple negative, CK5/6/14/17 positive, EGFR positive) [295, 299]. These tumors frequently have hotspot *PIK3CA* mutations and lack *TP53* mutations [295]. Chromosomal copy number analysis revealed a simple genome with few gains and losses in one tumor and a firestorm pattern with EGFR ampli-

fication in another [299]. Case reports describe rare LGASC arising in a patient with germline *BRCA1* mutation [375] and in another with germline *BRIP1* mutation [376], although genetic analysis of the tumors was not performed. It has been postulated that LGASC arise from adenosquamous proliferations associated with radial sclerosing lesions, which could explain the histologic association of these entities. Like LGASC, adenosquamous proliferations have been found to be clonal with *PIK3CA* mutations [303].

FLMBC are basal-like carcinomas with a claudin-low phenotype by immunohistochemistry, exhibiting low expression of adhesion molecules, a tumor-initiating cell phenotype (CD44+/CD24-), and features of EMT (vimentin expression with lack of E-cadherin) [307]. A limited number of tumors have been analyzed genetically. *PIK3CA* and *TERT* promoter hotspot mutations were each identified in three of four tumors analyzed by targeted DNA sequencing, akin to metaplastic spindle cell carcinomas [377]. Chromosomal copy number analysis of three tumors identified very few alterations, with

9p21.3 loss (including *CDKN2A*, which encodes p16) identified in two of the cases [378].

Prognosis and Clinical Management

With the exception of LGASC and FLMBC, metaplastic carcinomas are aggressive tumors with 3-year, 5-year, and 10-year survival rates of approximately 77%, 62%, and 53%, respectively [276, 277, 379, 380]. Outcome analyses have been overall limited by retrospective study design with selection bias, population-based or local studies without central pathology review, and lack of matching for stage in some cases. Nonetheless, patient outcomes are generally considered to be worse for metaplastic carcinoma than for other TNBC, with increased local recurrence risk and shorter disease-free and overall survival in the former, despite low rates of nodal involvement [279, 283, 310, 381–383]. On the other hand, metaplastic carcinomas tend to present with higher stage than IDC-NST [276, 278, 283, 379], and a large multi-institutional study found similar outcomes to IDC-NST matched for age, grade, ER, and HER2 status if analysis was limited to early stage (pT1/pT2) tumors [279]. Others have found similar results [384–386]. Distant metastases are common, even in the absence of nodal metastasis [278, 283, 381, 383, 387], with brain and lung being frequent sites.

Regarding conventional breast cancer prognostic factors in metaplastic carcinoma, inferior outcomes have been associated with older patient age [276, 278, 382, 388], nodal involvement, [278, 279, 383, 387, 388], lymphovascular invasion [279], and large tumor size [278, 282, 379, 389, 390]. Others have found no prognostic association with tumor size [279]. In a population-based study using SEER data, there were no differences in 5-year survival between hormone receptor positive and negative metaplastic carcinoma [277]. HER2-positive metaplastic carcinomas may have more favorable outcomes than triple-negative metaplastic carcinomas [276].

Intriguingly, there are data to suggest that different morphologic types of metaplastic carcinoma may have different outcomes. Mixed metaplastic carcinomas have been associated with worse outcomes compared to other morphologic types in several studies [279, 282, 388, 389]. In a large international consortium study of metaplastic carcinomas (AP-MBC), mixed metaplastic carcinomas and spindle cell carcinomas had worse 10-year breast cancer-specific survival (BCSS) than SCC. Moreover, mixed metaplastic carcinomas with more than three morphological components had worse outcomes than those with only two or three components [282]. Accordingly, the number and percentage of morphologic components in a metaplastic carcinoma should be reported by the pathologist [275]. In another international study, Rakha et al. observed longest BCSS for patients

with matrix-producing carcinomas, and shortest BCSS for those with spindle cell carcinomas or mixed spindle and squamous cell carcinomas. These associations were maintained even after exclusion of locally advanced tumors [279]. In contrast to these studies, others have found no significant associations between morphologic type and outcome [383, 388]. EGFR overexpression and lack of keratin expression (CK AE1/3) have been correlated with poor outcomes [282]. The prognostic significance of histologic grade is uncertain [275, 279, 282].

There are no specific NCCN guidelines for the treatment of metaplastic carcinoma, and these tumors are in general treated like other IBC-NST/TNBC [391]. Chemotherapy is routinely offered, although metaplastic carcinomas appear to have poor responses [262, 275, 278, 333, 335, 379, 383, 385, 386, 388, 389, 392–396]. Response rates to neoadjuvant chemotherapy are low, with complete pathologic responses of 0–17% across studies [262, 335, 379, 383, 386, 388, 389, 396]. There is evidence to suggest that matrix-producing carcinomas may achieve better responses to neoadjuvant chemotherapy than other types [388, 396]. Radiation therapy may provide survival benefit for patients undergoing breast-conserving surgery and for high-risk patients with large (>5 cm) tumors or extensive nodal disease [277, 278, 380, 390, 395, 397, 398].

Given the high rate of PI-3K pathway aberrations in metaplastic carcinomas, these patients are potential candidates for *PIK3CA* or mTOR inhibitors. In a study of 52 women with advanced metaplastic carcinoma, a 21% objective response rate was reported for a regimen consisting of the mTOR inhibitors temsirolimus or everolimus in combination with doxorubicin and bevacizumab. *PIK3CA* mutations were significantly associated with improved objective response rate (31 versus 0%) but not clinical benefit rate [399]. Patients with metaplastic carcinoma treated with this regimen had better long-term outcomes compared to patients with TNBC treated with the same regimen [399]. Given the high rate of homologous recombination repair deficiency signatures in metaplastic carcinomas [400], one could postulate that these patients may benefit from PARP inhibitor therapy [397].

Variable PD-L1 tumor cell and immune cell expression has been reported in metaplastic carcinomas, with staining being more frequent than in other TNBC [367, 401–404]. In one study, positive PD-L1 expression was observed in 95% of metaplastic carcinomas using the FDA-approved SP142 antibody and scoring criteria used in the Impassion130 trial (≥1% immune cell staining), which is significantly higher than the positivity of TNBC in the trial (41%) [404, 405]. These findings suggest that most advanced metaplastic carcinomas are potentially eligible for anti-PD-L1 therapy. Indeed, case reports have described durable responses to Pembrolizumab (anti-PD-1)/nab-paclitaxel and durvalumab (anti-PD-L1)/paclitaxel in metaplastic spindle cell carci-

noma and metaplastic carcinoma with squamous elements, respectively [406, 407].

FLMBC and LGASC are low-grade metaplastic carcinoma subtypes that are recognized to have more indolent clinical behavior with overall favorable prognosis [293, 297]. The incidence of nodal or distant metastasis is extremely low. However, both FLMBC and LGASC exhibit potentially locally aggressive behavior with high risk of recurrence. Accordingly, these tumors are generally treated by excision to clear margins. The role of chemotherapy is undetermined. The NCCN guidelines note that limited data support local excision only for these tumors, with consideration of systemic or targeted therapy only in node-positive disease [391].

Invasive Breast Carcinoma with Medullary Pattern

Overview and Clinical Presentation

Medullary carcinoma of the breast (MC) was previously described as a rare subtype of breast cancer with distinct morphology and favorable prognosis, despite its high-grade histopathologic features and often triple-negative immunophenotype. However, classification was notoriously complicated by poor interobserver and intraobserver diagnostic reproducibility [408–414]. MC and related tumors have undergone multiple rounds of reclassification over the years. In the first formal definition of MC in 1945, Moore and Foote described a unique tumor with well-circumscribed borders, poorly differentiated cells, and a prominent lymphoid infiltrate [415]. Based on strict diagnostic criteria initially proposed by Ridolfi et al. that correlated with favorable outcomes, the first three editions of the WHO classification included MC as a breast cancer subtype with circumscribed borders, syncytial architecture, pleomorphic nuclei, and a prominent lymphoplasmacytic inflammatory infiltrate [408]. In recognition of the poor reproducibility of the diagnosis and challenges in consistent reporting, the fourth edition introduced the category of "carcinomas with medullary features" to include MC, atypical medullary carcinomas (AMC), and a subset of IDC-NST [416]. However, aside from poor diagnostic reproducibility, these tumors as a group were found to show broad histopathologic overlap with basal-like carcinomas and carcinomas arising in *BRCA1* carriers. In addition, it has been recognized that the favorable prognosis of MC and other invasive carcinomas not meeting strict MC criteria is likely explained by the presence of large numbers of tumor infiltrating lymphocytes (TILs), which is associated with better outcomes in TNBC [275, 417–421]. This recognition has reduced the necessity of diagnostically differentiating these tumors. Accordingly, invasive carcinomas with medullary features are considered in the fifth edition to represent one end of the histopathologic spectrum of TIL-rich IBC-NST and classified as a morphologic pattern, rather than a separate subtype [422]. A descriptive modifier indicating the medullary pattern or basal-like features should be included with the diagnosis.

Invasive carcinomas meeting the previous criteria for MC are rare and account for <1% of invasive breast cancers. A higher prevalence can be expected if other invasive carcinomas with medullary pattern are included (up to 7% in some studies) [423–427]. The average age at presentation typically ranges from 45 to 54 years across various series, although patients tend to be relatively younger compared to those with other invasive breast carcinomas, with one study showing higher numbers of patients with MC in the 35 years or younger group [409, 412, 415, 426, 428–431]. These tumors are rare in men [424].

The clinical presentation is similar to other IBC-NST, with most tumors presenting as a palpable mass. Average size of tumors previously classified as MC ranged from 2 to 3.2 cm [409, 411, 424, 431, 432]. Ipsilateral lymphadenopathy is not uncommon and is reactive in many cases [433].

Gross and Radiologic Features

Grossly, invasive carcinomas with medullary pattern are well-circumscribed, soft to moderately firm tumors, and may show a characteristic shiny, pearly white appearance that bulges above the cut surfaces [434]. Foci of hemorrhage or necrosis may be present, the latter of which may cause cystic degeneration. Prominent cystic degeneration is seen usually in larger tumors [221]. Some tumors may be poorly circumscribed, due to irregular extension of the inflammatory infiltrate beyond the margins of tumor [408].

On mammography, invasive carcinomas with medullary pattern are well circumscribed round, oval, or lobulated with smooth borders and without calcifications. Ultrasound shows a well-circumscribed hypoechoic mass. Given their circumscription, these tumors may be mistaken radiographically for fibroadenomas [435]. On MRI, invasive carcinomas with medullary pattern are also round or lobular with well-circumscribed smooth margins. Peripheral rim enhancement with or without enhancing internal septations is often noted [436, 437].

Microscopic Features

Histologic features of invasive carcinoma with medullary pattern include circumscribed tumor borders, syncytial growth, high Nottingham/SBR grade, and a prominent lymphoplasmacytic inflammatory infiltrate, features which overlap with basal-like carcinomas and carcinomas associated with *BRCA1* mutations.

Although the WHO no longer classifies tumors as MC, AMC, or invasive carcinomas with medullary features, the previously used diagnostic criteria for these tumors are included here for reference and context. Ridolfi et al. defined MC as an invasive carcinoma with a well-circumscribed rounded tumor border without infiltration into adjacent tissue, >75% syncytial growth, associated moderate to marked diffuse lymphocytic infiltrate, intermediate or high nuclear grade, absence of glandular features, and lack of an intraductal component (Figs. 12.82, 12.83, 12.84, and 12.85). AMC referred to tumors with at least 75% syncytial growth but lacking one or two of the other features, and non-medullary carcinomas lacked at least 75% syncytial growth or three or more medullary features [408]. Using the Ridolfi classification, studies showed 10-year MC survival rates of 84–95%, compared to 53–80% for AMC and 51–70% for

non-medullary carcinomas [408, 424, 438]. Tumors classified as AMC only due to the presence of an intraductal component had outcomes similar to MC [408]. Wargotz and Silverberg used similar criteria but allowed for intraductal carcinoma, focal marginal infiltration, or a sparse lymphocytic infiltrate and observed similarly favorable outcome for MC [409]. Pedersen et al. proposed a simplified classification system that defined MC as having syncytial growth, diffuse stromal lymphocytic inflammation, <25% necrosis, and lack of tubular growth [428]. This was further simplified by Marginean et al., who required only 30% anastomosing growth and prominent inflammation, which also correlated well with survival outcomes [439]. Overall, the Ridolfi criteria were most commonly applied and correlated well with outcomes but are the strictest with the worst interobserver reproducibility [411]. It is now recognized that invasive car-
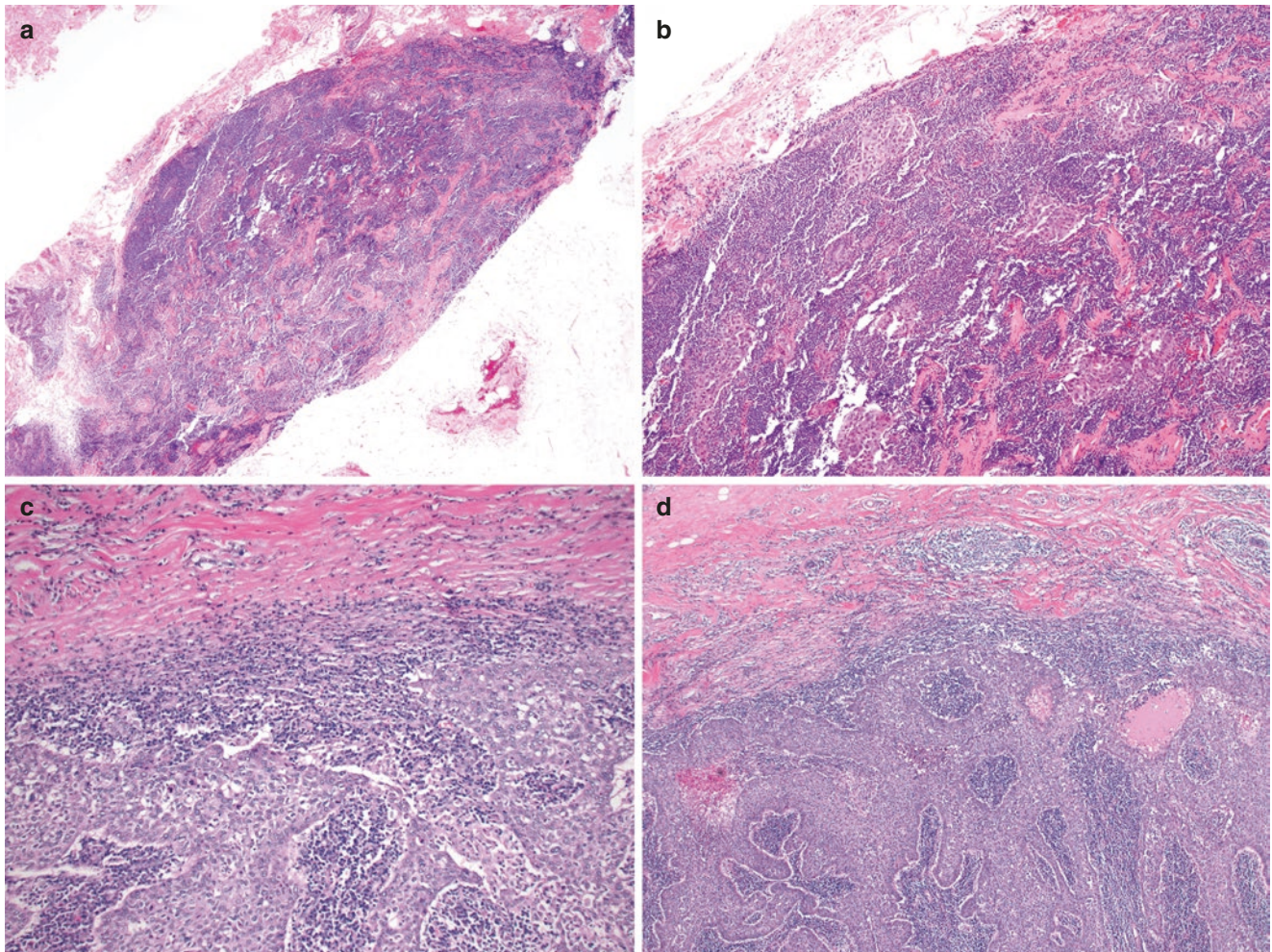
Fig. 12.82 Invasive breast carcinoma with medullary pattern, with well-circumscribed borders. (**a**, **b**) Core needle biopsy of this invasive breast carcinoma with medullary pattern reveals a rounded circumscribed border, without infiltration of tumor syncytium into adjacent fat. (**c**, **d**) Another example of invasive breast carcinoma with medullary pattern with well-circumscribed borders and a pushing-type of invasion. Note that the associated lymphoplasmacytic infiltrate is present throughout the tumor and at the periphery, where it may infiltrate the adjacent tissue
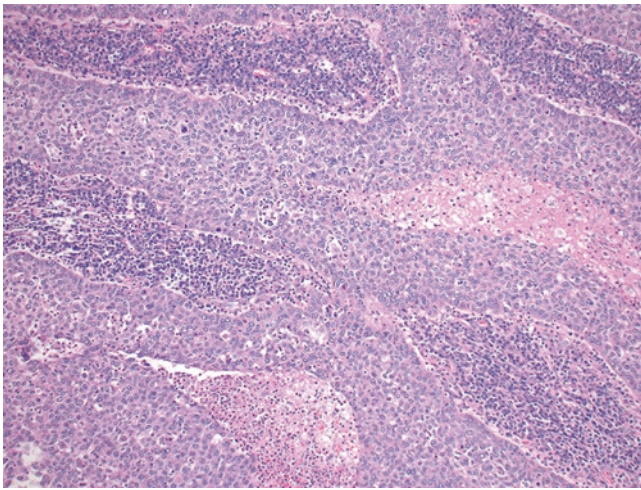
Fig. 12.83 Syncytial growth pattern of invasive breast carcinoma with medullary pattern. Syncytial growth is characterized by interanastomosing sheets of pleomorphic tumor cells with ill-defined cell membranes and borders. The typical lymphoplasmacytic infiltrate with scant collagenous stroma is present between areas of tumor syncytium. Note the presence of tumor necrosis in this case

cinomas with a medullary pattern exist along a morphologic continuum, with outcomes likely explained by their association with TILs, and discrete separation is no longer suggested.

Syncytial growth of invasive breast carcinomas with medullary pattern is characterized by broad interanastomosing sheets of tumor cells with indistinct cell borders (Figs. 12.83 and 12.84). The features may sometimes impart a squamoid appearance. Well-circumscribed tumors have rounded peripheral contours with a pushing-type convex border and lack of tumor infiltration into adjacent tissue. The inflammatory infiltrate is lymphoplasmacytic and often diffuse (Fig. 12.82). TILs can be quantitated in these tumors if clinically indicated, using the international consensus scoring recommendations [440]. A practical guide to TILs evaluation can be accessed online: https://www.tilsinbreastcancer.org. Lymphoid follicles with germinal center formation may be present. The inflammatory infiltrate may percolate among adjacent ducts and lobules at the tumor edge (Fig. 12.82d). Benign lobules distant from the tumor may show a similar
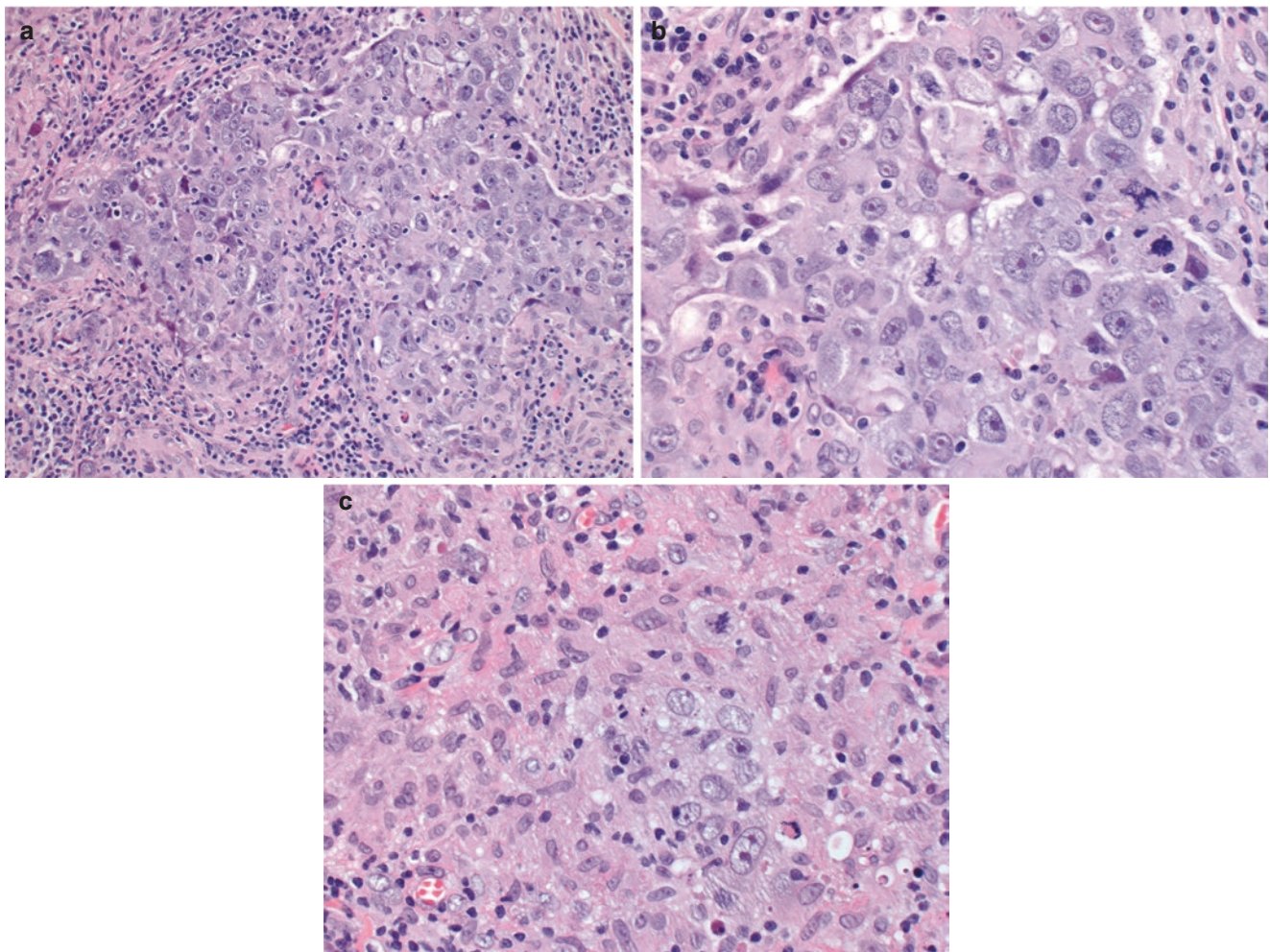
Fig. 12.84 Cytologic features of invasive breast carcinoma with medullary pattern. (**a–c**) The tumor cells are markedly pleomorphic, with grade 3 nuclei that have vesicular chromatin and prominent nucleoli. Mitotic activity is robust. Note also the syncytial appearance of the tumor cells and associated lymphoplasmacytic inflammatory infiltrate
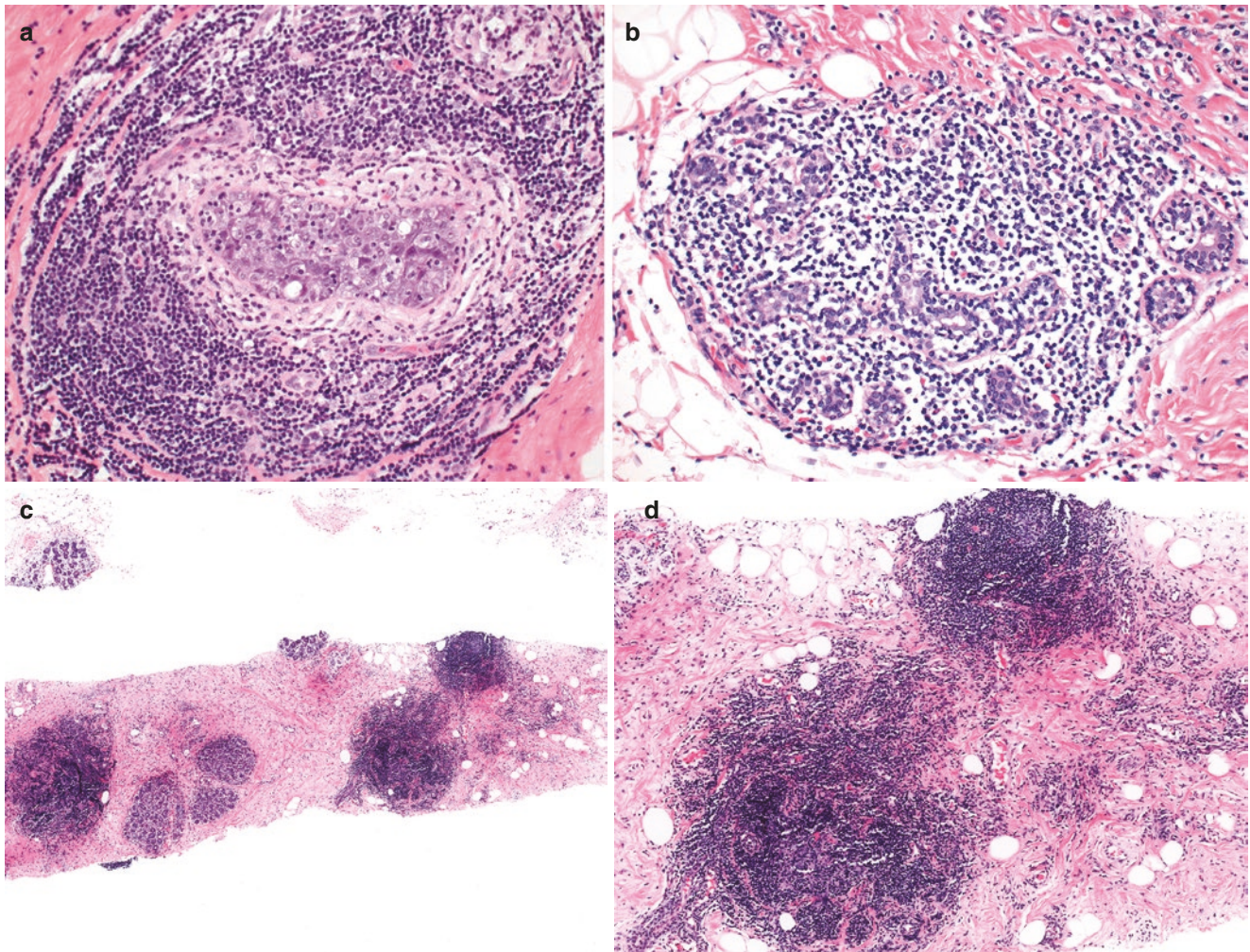
Fig. 12.85 Perilobular inflammatory infiltrates of invasive breast carcinoma with medullary pattern. (**a**) Intraductal carcinoma associated with invasive breast carcinoma with medullary pattern is characteristically high grade, in this example with a solid growth pattern. Note the associated perilobular lymphoplasmacytic infiltrate, which is typical. (**b**) Benign lobules may also demonstrate a similar prominent lymphoplasmacytic infiltrate, which may be seen at some distance from the carcinoma. (**c**, **d**) This CNB targeted for a breast mass demonstrates benign breast tissue with prominent lymphoplasmacytic infiltrates associated with some lobules and no carcinoma. The findings in the CNB were interpreted as lymphocytic mastitis. Excision revealed invasive breast carcinoma with medullary pattern (*not shown*). This case illustrates prominent perilobular lymphoplasmacytic infiltrate that is often observed in benign tissue adjacent to these tumors and also highlights the importance of radiological-pathological correlation in evaluating a breast CNB specimen

infiltrate (Fig. 12.85b–d). The tumor cells are enlarged and pleomorphic, with abundant cytoplasm and grade 2 or 3 nuclei with coarse or vesicular chromatin and often one or several prominent nucleoli (Fig. 12.84). Atypical giant cells with bizarre nuclei may be present. Focal squamous differentiation can be seen [408, 441]. Frequent mitotic figures, including abnormal forms, are common, as are pyknotic nuclei and smudged cells [434]. Areas of necrosis can lead to cystic degeneration. An intraductal component is not uncommon, usually with identical cytologic features and solid or comedo pattern, with or without lobular extension. A lymphoplasmacytic infiltrate is also often present surrounding the in situ carcinoma (Fig. 12.85a).

Immunohistochemistry

Invasive breast carcinomas with medullary pattern are usually triple (ER, PR, HER2) negative, although some tumors can be ER and PR positive [413, 417, 442–446]. HER2 overexpression is uncommon [417, 442, 443, 447–449]. These tumors express LMWCK (CK8/18 and CK7), with variable expression of HMWCK (such as CK5/6, CK14, and CK17) and other basal markers (EGFR, p-cadherin) [411, 417, 442, 443, 447, 450, 451]. In one series, a basal-like immunophenotype (triple negative with expression of either CK5/6 or EGFR) was demonstrated in ~63% of invasive carcinomas with medullary features compared to ~19% of matched IBC-

NST [442]. SMA, S100 protein, and p53 may be positive [417, 418, 442, 443, 452, 453], with p53 overexpression generally being due to *TP53* mutation [418, 443]. Ki-67 is usually >50% (~50–90%) [417, 442].

The lymphoplasmacytic infiltrate is predominantly composed of CD3+, CD8+, TIA-1+, and granzyme B+ lymphocytes [454–456].

Invasive breast carcinomas with medullary pattern may be positive for the immune checkpoint protein PD-L1 using either SP142 or 22C3 companion assays [457].

Differential Diagnosis

With the understanding that invasive breast carcinomas with medullary pattern belong to a morphologic continuum and that clinical behavior and outcomes are likely linked to TILs in these tumors, there is less necessity to categorically differentiate these tumors. Instead, the medullary pattern should be used as a descriptor for IBC-NST.

Some authors have described lymphoepithelioma-like carcinoma (LEC) of the breast, which is morphologically similar to LEC arising at other sites and tends to lack circumscribed borders and syncytial growth [458]. In contrast to extramammary LEC, LEC is generally negative for Epstein–Barr virus (EBV) by immunohistochemistry, in situ hybridization, and polymerase chain reaction [459]. LEC is not recognized as a breast cancer subtype in the WHO classification, and it is unclear if these tumors represent morphologic variants along the spectrum of invasive breast carcinomas with medullary pattern.

Due to the prominence of the lymphoplasmacytic infiltrate in some invasive breast carcinomas with medullary pattern, the differential diagnosis may include lymphoma, especially in scant CNB material. Immunohistochemical stains for cytokeratin can be helpful in these cases (Fig. 12.86).

Invasive breast carcinomas with medullary pattern can mimic metastatic carcinoma within a lymph node, especially in tumors presenting as an axillary mass, and this can be particularly problematic in CNB or fine needle aspiration. The presence of germinal centers is not helpful, as these may be seen in invasive breast carcinomas with medullary pattern. Identification of a lymph node capsule and/or subcapsular sinus is useful if present (Fig. 12.87).

The differential diagnosis may also include a variety of reactive processes, including diabetic mastopathy, granulomatous mastitis, and mammary Rosai–Dorfman disease (RDD), all of which can be associated with a prominent lymphoplasmacytic inflammatory infiltrate. Attention to cytomorphologic features helps to distinguish the histiocytes of granulomatous mastitis and RDD from high-grade carcinoma cells, although limited sampling in CNB material may be problematic. Cytokeratin immunohistochemistry is helpful in challenging cases. The histiocytes of granulomatous mastitis and RDD are positive for histiocytic markers, including CD68 and CD163. Immunohistochemistry for S100 protein is less useful, as RDD histiocytes and invasive carcinoma cells may both be positive [417].

Pathogenesis and Risk Factors

Invasive breast carcinomas with medullary pattern share many features with *BRCA1*-associated breast cancers, including younger age at presentation, high-grade histopathologic features with high mitotic activity, prominent lymphoplasmacytic infiltration, pushing borders, triple negative or basal phenotype, and frequent *TP53* mutations. Indeed, a high proportion of germline *BRCA1*-associated breast carcinomas demonstrate medullary-like features [460–466]. Conversely, carcinomas with medullary-like features harbor higher rates of *BRCA1* mutations than other IBC-NST, and often show *BRCA1* promoter hypermethylation [462, 467]. These tumors are also genomically unstable with high large-scale state transition (LST) status, indicative of a BRCAness phenotype due to deficient DNA repair [443]. *TP53* mutations are common [443].

The vast majority of tumors previously classified as MC are basal-like by gene expression profiling and surrogate immunohistochemistry [37, 442, 443, 468]. Using the original 6-group TNBC classification developed by Lehmann et al. (TNBCtype), most of these tumors belonged to the immunomodulatory (IM) group, which is enriched for gene ontologies in immune cell processes [196, 469]. Immune signaling genes in the IM subgroup overlap with a previously identified gene expression signature for MC, which includes genes related to the immune response, antigen processing and apoptosis [468]. Using a refined 4-group TNBC molecular classification, the tumors belong to the basal-like 1 (BL1) group, which is enriched for cell cycle and DNA damage response genes [196]. Teschendorff et al. similarly found that invasive carcinomas previously classified as MC clustered with a prognostically favorable ER-negative group enriched for genes in cell cycle and immune response genes [470]. Together, gene expression studies and association of these tumors with *BRCA1* aberrations and a BRCAness phenotype highlight the importance of immune regulation and DNA repair deregulation in pathogenesis.

Prognosis and Clinical Management

Despite the basal-like and triple-negative phenotype, the prognosis of MC has been historically favorable, with most studies finding improved 5- and 10-year survival rates compared to non-medullary invasive carcinomas, although out-
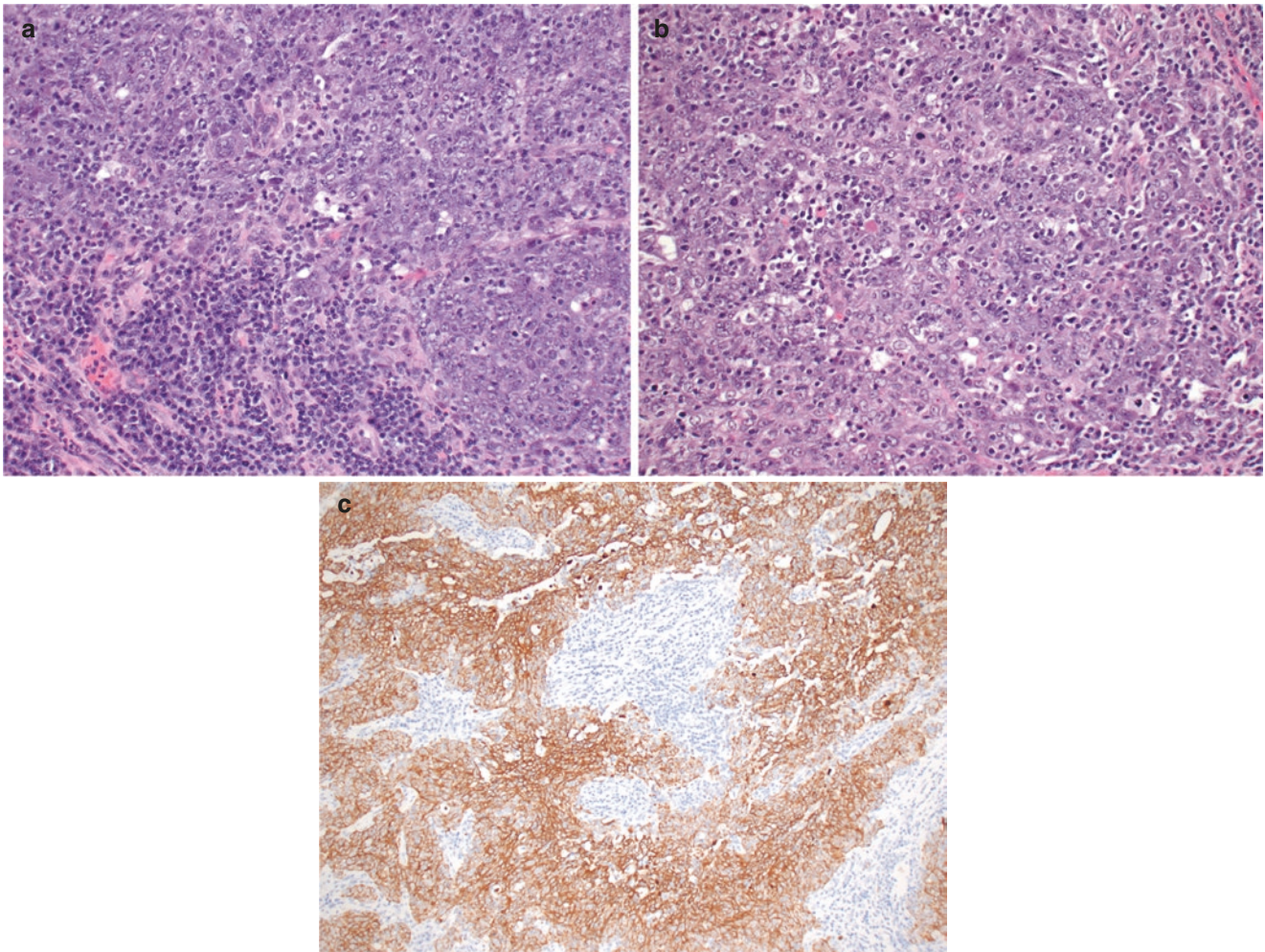
Fig. 12.86 Lymphoplasmacytic infiltrate of invasive breast carcinoma with medullary pattern may mask carcinoma cells. (**a**, **b**) In some cases, the inflammatory infiltrate may be very pronounced and mask the associated carcinoma cells, raising consideration for lymphoma. (**c**) Keratin immunostain is helpful in such cases to highlight the epithelial nature of the malignant cells. Note the interanastomosing sheets of syncytial epithelial cells
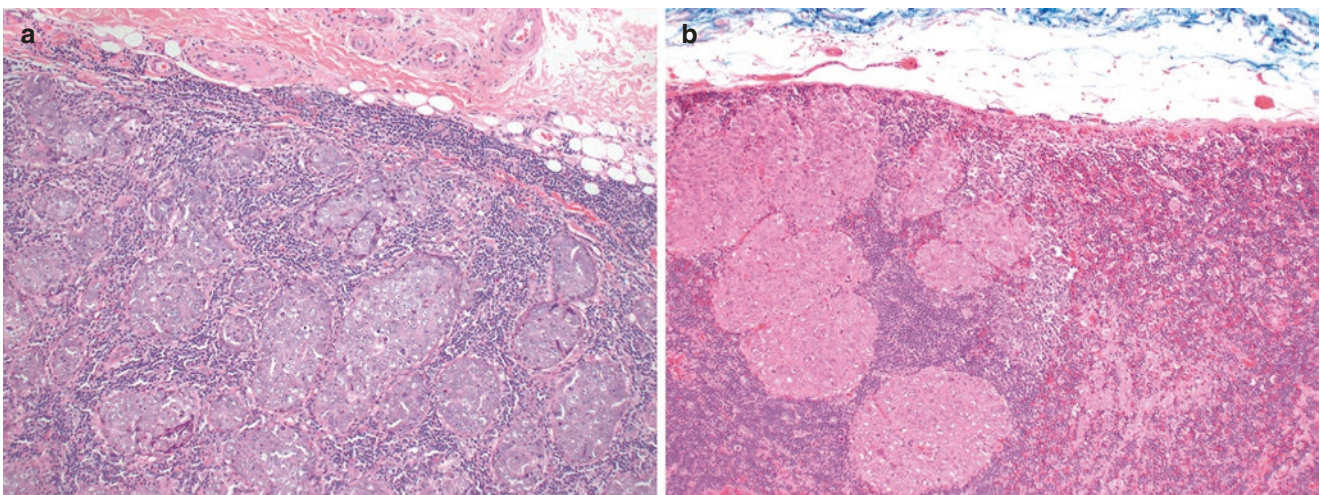
Fig. 12.87 Invasive breast carcinoma with medullary pattern may mimic metastatic carcinoma in a lymph node. (**a**) The prominent lymphoplasmacytic infiltrate and well-circumscribed tumor border of invasive breast carcinoma with medullary pattern may mimic metastatic carcinoma in a lymph node. The lack of a capsule and/or subcapsular sinus may be helpful in such cases. (**b**) In contrast, this lymph node with metastatic carcinoma demonstrates a distinct albeit compressed capsule

comes were generally dependent on strict and poorly reproducible diagnostic criteria. Most studies also observed decreased rates of axillary lymph node metastasis in patients with MC, and these patients had excellent long-term prognosis. Survival of patients with AMC were found to be intermediate between MC and non-medullary carcinomas, similar to non-medullary carcinomas, or similar to MC, depending on the study [408–412, 425, 431, 471, 472].

More recently, the prognostic impact of TILs has been discovered in high-grade carcinomas with and without medullary histologic features. High numbers of TILs are associated with improved response to neoadjuvant chemotherapy and longer disease-free survival in TNBC [419, 420, 472]. Moreover, survival in MC was not found to be significantly different from grade 3 IDC with prominent inflammation, but survival in both was significantly better than grade 3 IDC without prominent lymphocytic inflammation. There were no survival differences between MC and AMC in this study [472]. In another study, superior outcomes observed in invasive carcinomas with medullary features compared to other TNBC were lost once TILs were included in multivariate analysis [473]. Consistent with these findings, a gene expression signature for MC that is enriched for immune response genes was able to identify a prognostically favorable subgroup of basal-like carcinomas [474]. The data together suggest that the favorable outcomes ascribed to invasive breast carcinomas with medullary pattern are related to the prominent lymphoplasmacytic infiltrates in these tumors.

Rates of local tumor recurrence following breast conservation therapy are similar for patients with tumors previously classified as MC and IDC-NST [431, 475, 476]. Treatment of invasive breast carcinomas with medullary features is generally similar to other IBC-NST. Given the prominence of TILs in these tumors, immune checkpoint inhibitor therapy with PD-L1 (atezolizumab) or PD-1 (pembrolizumab) inhibitors can be an option for eligible patients [457].

References

1. Geschickter CF. Diseases of the breast: diagnosis, pathology, treatment. 2nd ed. Philadelphia, PA: JB Lippincott; 1945.
2. Arpino G, Clark GM, Mohsin S, Bardou VJ, Elledge RM. Adenoid cystic carcinoma of the breast: molecular markers, treatment, and clinical outcome. Cancer. 2002;94(8):2119–27.
3. Da Silva L, Buck L, Simpson PT, Reid L, McCallum N, Madigan BJ, et al. Molecular and morphological analysis of adenoid cystic carcinoma of the breast with synchronous tubular adenosis. Virchows Arch. 2009;454(1):107–14.
4. Miyai K, Schwartz MR, Divatia MK, Anton RC, Park YW, Ayala AG, et al. Adenoid cystic carcinoma of breast: recent advances. World J Clin Cases. 2014;2(12):732–41.
5. Ferlito A, Di Bonito L. Adenoid cystic carcinoma of the male breast: report of a case. Am Surg. 1974;40(1):72–6.
6. Hjorth S, Magnusson PH, Blomquist P. Adenoid cystic carcinoma of the breast. Report of a case in a male and review of the literature. Acta Chir Scand. 1977;143(3):155–8.
7. Santamaria G, Velasco M, Zanon G, Farrus B, Molina R, Sole M, et al. Adenoid cystic carcinoma of the breast: mammographic appearance and pathologic correlation. AJR Am J Roentgenol. 1998;171(6):1679–83.
8. Rosen PP. Adenoid cystic carcinoma of the breast. A morphologically heterogeneous neoplasm. Pathol Annu. 1989;24(Pt 2):237–54.
9. Tavassoli FA, Norris HJ. Mammary adenoid cystic carcinoma with sebaceous differentiation. A morphologic study of the cell types. Arch Pathol Lab Med. 1986;110(11):1045–53.
10. Tsuboi N, Ogawa Y, Inomata T, Nishioka A, Yoshida D, Yoshida S, et al. Dynamic MR appearance of adenoid cystic carcinoma of the breast in a 67-year-old female. Radiat Med. 1998;16(3):225–8.
11. Glazebrook KN, Reynolds C, Smith RL, Gimenez EI, Boughey JC. Adenoid cystic carcinoma of the breast. AJR Am J Roentgenol. 2010;194(5):1391–6.
12. Sheen-Chen SM, Eng HL, Chen WJ, Cheng YF, Ko SF. Adenoid cystic carcinoma of the breast: truly uncommon or easily overlooked? Anticancer Res. 2005;25(1B):455–8.
13. Foschini MPGF, Hayes MM, Marchio C, Nishimura R. Adenoid cystic carcinoma. In: WHO Classification of Tumours. Editorial Board, editors. WHO Classification of Breast Tumours. 5th ed. Lyon: International Agency for Research on Cancer (IARC); 2019. p. 142–5.
14. Kasami M, Olson SJ, Simpson JF, Page DL. Maintenance of polarity and a dual cell population in adenoid cystic carcinoma of the breast: an immunohistochemical study. Histopathology. 1998;32(3):232–8.
15. Shin SJ, Rosen PP. Solid variant of mammary adenoid cystic carcinoma with basaloid features: a study of nine cases. Am J Surg Pathol. 2002;26(4):413–20.
16. Lamovec J, Us-Krasovec M, Zidar A, Kljun A. Adenoid cystic carcinoma of the breast: a histologic, cytologic, and immunohistochemical study. Semin Diagn Pathol. 1989;6(2):153–64.
17. Foschini MP, Rizzo A, De Leo A, Laurino L, Sironi M, Rucco V. Solid variant of adenoid cystic carcinoma of the breast: a case series with proposal of a new grading system. Int J Surg Pathol. 2016;24(2):97–102.
18. Masse J, Truntzer C, Boidot R, Khalifa E, Perot G, Velasco V, et al. Solid-type adenoid cystic carcinoma of the breast, a distinct molecular entity enriched in NOTCH and CREBBP mutations. Mod Pathol. 2020;33(6):1041–55.
19. Righi A, Lenzi M, Morandi L, Flamminio F, De Biase D, Farnedi A, et al. Adenoid cystic carcinoma of the breast associated with invasive duct carcinoma: a case report. Int J Surg Pathol. 2011;19(2):230–4.
20. Fusco N, Geyer FC, De Filippo MR, Martelotto LG, Ng CK, Piscuoglio S, et al. Genetic events in the progression of adenoid cystic carcinoma of the breast to high-grade triple-negative breast cancer. Mod Pathol. 2016;29(11):1292–305.
21. Cabibi D, Cipolla C, Maria Florena A, Fricano S, Barresi E, Vieni S, et al. Solid variant of mammary "adenoid cystic carcinoma with basaloid features" merging with "small cell carcinoma". Pathol Res Pract. 2005;201(10):705–11.
22. Noske A, Schwabe M, Pahl S, Fallenberg E, Richter-Ehrenstein C, Dietel M, et al. Report of a metaplastic carcinoma of the breast with multi-directional differentiation: an adenoid cystic carcinoma, a spindle cell carcinoma and melanoma. Virchows Arch. 2008;452(5):575–9.
23. Acs G, Simpson JF, Bleiweiss IJ, Hugh J, Reynolds C, Olson S, et al. Microglandular adenosis with transition into adenoid cystic carcinoma of the breast. Am J Surg Pathol. 2003;27(8):1052–60.

24. James BA, Cranor ML, Rosen PP. Carcinoma of the breast arising in microglandular adenosis. Am J Clin Pathol. 1993;100(5):507–13.

25. Khalifeh IM, Albarracin C, Diaz LK, Symmans FW, Edgerton ME, Hwang RF, et al. Clinical, histopathologic, and immunohistochemical features of microglandular adenosis and transition into in situ and invasive carcinoma. Am J Surg Pathol. 2008;32(4):544–52.

26. McClenathan JH, de la Roza G. Adenoid cystic breast cancer. Am J Surg. 2002;183(6):646–9.

27. Peters GN, Wolff M. Adenoid cystic carcinoma of the breast. Report of 11 new cases: review of the literature and discussion of biological behavior. Cancer. 1983;52(4):680–6.

28. Ro JY, Silva EG, Gallager HS. Adenoid cystic carcinoma of the breast. Hum Pathol. 1987;18(12):1276–81.

29. Kleer CG, Oberman HA. Adenoid cystic carcinoma of the breast: value of histologic grading and proliferative activity. Am J Surg Pathol. 1998;22(5):569–75.

30. D'Alfonso TM, Mosquera JM, MacDonald TY, Padilla J, Liu YF, Rubin MA, et al. MYB-NFIB gene fusion in adenoid cystic carcinoma of the breast with special focus paid to the solid variant with basaloid features. Hum Pathol. 2014;45(11):2270–80.

31. Vranic S, Bender R, Palazzo J, Gatalica Z. A review of adenoid cystic carcinoma of the breast with emphasis on its molecular and genetic characteristics. Hum Pathol. 2013;44(3):301–9.

32. Poling JS, Yonescu R, Subhawong AP, Sharma R, Argani P, Ning Y, et al. MYB labeling by immunohistochemistry is more sensitive and specific for breast adenoid cystic carcinoma than MYB labeling by FISH. Am J Surg Pathol. 2017;41(7):973–9.

33. Kim M, Lee DW, Im J, Suh KJ, Keam B, Moon HG, et al. Adenoid cystic carcinoma of the breast: a case series of six patients and literature review. Cancer Res Treat. 2014;46(1):93–7.

34. Yang C, Zhang L, Sanati S. SOX10 is a sensitive marker for breast and salivary gland adenoid cystic carcinoma: immunohistochemical characterization of adenoid cystic carcinomas. Breast Cancer (Auckl). 2019;13:1178223419842185.

35. Trendell-Smith NJ, Peston D, Shousha S. Adenoid cystic carcinoma of the breast: a tumour commonly devoid of oestrogen receptors and related proteins. Histopathology. 1999;35(3):241–8.

36. Vranic S, Gatalica Z, Deng H, Frkovic-Grazio S, Lee LM, Gurjeva O, et al. ER-alpha36, a novel isoform of ER-alpha66, is commonly over-expressed in apocrine and adenoid cystic carcinomas of the breast. J Clin Pathol. 2011;64(1):54–7.

37. Weigelt B, Horlings HM, Kreike B, Hayes MM, Hauptmann M, Wessels LF, et al. Refinement of breast cancer classification by molecular characterization of histological special types. J Pathol. 2008;216(2):141–50.

38. Vranic S, Frkovic-Grazio S, Lamovec J, Serdarevic F, Gurjeva O, Palazzo J, et al. Adenoid cystic carcinomas of the breast have low Topo IIalpha expression but frequently overexpress EGFR protein without EGFR gene amplification. Hum Pathol. 2010;41(11):1617–23.

39. Wetterskog D, Lopez-Garcia MA, Lambros MB, A'Hern R, Geyer FC, Milanezi F, et al. Adenoid cystic carcinomas constitute a genomically distinct subgroup of triple-negative and basal-like breast cancers. J Pathol. 2012;226(1):84–96.

40. Pastolero G, Hanna W, Zbieranowski I, Kahn HJ. Proliferative activity and p53 expression in adenoid cystic carcinoma of the breast. Mod Pathol. 1996;9(3):215–9.

41. Albores-Saavedra J, Heard SC, McLaren B, Kamino H, Witkiewicz AK. Cylindroma (dermal analog tumor) of the breast: a comparison with cylindroma of the skin and adenoid cystic carcinoma of the breast. Am J Clin Pathol. 2005;123(6):866–73.

42. Mahmoud A, Hill DH, O'Sullivan MJ, Bennett MW. Cylindroma of the breast: a case report and review of the literature. Diagn Pathol. 2009;4:30.

43. Azoulay S, Lae M, Freneaux P, Merle S, Al Ghuzlan A, Chnecker C, et al. KIT is highly expressed in adenoid cystic carcinoma of the breast, a basal-like carcinoma associated with a favorable outcome. Mod Pathol. 2005;18(12):1623–31.

44. Persson M, Andren Y, Mark J, Horlings HM, Persson F, Stenman G. Recurrent fusion of MYB and NFIB transcription factor genes in carcinomas of the breast and head and neck. Proc Natl Acad Sci U S A. 2009;106(44):18740–4.

45. Martelotto LG, De Filippo MR, Ng CK, Natrajan R, Fuhrmann L, Cyrta J, et al. Genomic landscape of adenoid cystic carcinoma of the breast. J Pathol. 2015;237(2):179–89.

46. Drier Y, Cotton MJ, Williamson KE, Gillespie SM, Ryan RJ, Kluk MJ, et al. An oncogenic MYB feedback loop drives alternate cell fates in adenoid cystic carcinoma. Nat Genet. 2016;48(3):265–72.

47. Hudson JB, Collins BT. MYB gene abnormalities t(6;9) in adenoid cystic carcinoma fine-needle aspiration biopsy using fluorescence in situ hybridization. Arch Pathol Lab Med. 2014;138(3):403–9.

48. Kim J, Geyer FC, Martelotto LG, Ng CK, Lim RS, Selenica P, et al. MYBL1 rearrangements and MYB amplification in breast adenoid cystic carcinomas lacking the MYB-NFIB fusion gene. J Pathol. 2018;244(2):143–50.

49. Rooper LM, Lombardo KA, Oliai BR, Ha PK, Bishop JA. MYB RNA in situ hybridization facilitates sensitive and specific diagnosis of adenoid cystic carcinoma regardless of translocation status. Am J Surg Pathol. 2021;45(4):488–97.

50. Butcher MRL, Argani P, White M, Cimino-Mathews A. MYB RNA in situ hybridization is a useful tool to distinguish breast adenoid cystic carcinoma from other triple negative breast carcinomas (abstract). US Can Acad Pathol (USCAP). 2021;101:87.

51. Mastropasqua MG, Maiorano E, Pruneri G, Orvieto E, Mazzarol G, Vento AR, et al. Immunoreactivity for c-kit and p63 as an adjunct in the diagnosis of adenoid cystic carcinoma of the breast. Mod Pathol. 2005;18(10):1277–82.

52. Idowu MO, Kmieciak M, Dumur C, Burton RS, Grimes MM, Powers CN, et al. CD44(+)/CD24(-/low) cancer stem/progenitor cells are more abundant in triple-negative invasive breast carcinoma phenotype and are associated with poor outcome. Hum Pathol. 2012;43(3):364–73.

53. Millar BA, Kerba M, Youngson B, Lockwood GA, Liu FF. The potential role of breast conservation surgery and adjuvant breast radiation for adenoid cystic carcinoma of the breast. Breast Cancer Res Treat. 2004;87(3):225–32.

54. Vranic S, Bilalovic N, Lee LM, Kruslin B, Lilleberg SL, Gatalica Z. PIK3CA and PTEN mutations in adenoid cystic carcinoma of the breast metastatic to kidney. Hum Pathol. 2007;38(9):1425–31.

55. Page DL. Adenoid cystic carcinoma of breast, a special histopathologic type with excellent prognosis. Breast Cancer Res Treat. 2005;93(3):189–90.

56. Sumpio BE, Jennings TA, Merino MJ, Sullivan PD. Adenoid cystic carcinoma of the breast. Data from the Connecticut Tumor Registry and a review of the literature. Ann Surg. 1987;205(3):295–301.

57. Hodgson NC, Lytwyn A, Bacopulos S, Elavathil L. Adenoid cystic breast carcinoma: high rates of margin positivity after breast conserving surgery. Am J Clin Oncol. 2010;33(1):28–31.

58. Coates JM, Martinez SR, Bold RJ, Chen SL. Adjuvant radiation therapy is associated with improved survival for adenoid cystic carcinoma of the breast. J Surg Oncol. 2010;102(4):342–7.

59. Khanfir K, Kallel A, Villette S, Belkacemi Y, Vautravers C, Nguyen T, et al. Management of adenoid cystic carcinoma of the breast: a Rare Cancer Network study. Int J Radiat Oncol Biol Phys. 2012;82(5):2118–24.

60. Goldhirsch A, Wood WC, Coates AS, Gelber RD, Thurlimann B, Senn HJ, et al. Strategies for subtypes--dealing with the diversity of breast cancer: highlights of the St. Gallen International Expert

Consensus on the Primary Therapy of Early Breast Cancer 2011. Ann Oncol. 2011;22(8):1736–47.

61. Moore G, Annett S, McClements L, Robson T. Top notch targeting strategies in cancer: a detailed overview of recent insights and current perspectives. Cells. 2020;9(6):1503.

62. Eusebi V, Damiani S, Ellis IO, Azzopardi JG, Rosai J. Breast tumor resembling the tall cell variant of papillary thyroid carcinoma: report of 5 cases. Am J Surg Pathol. 2003;27(8):1114–8.

63. Chiang S, Weigelt B, Wen HC, Pareja F, Raghavendra A, Martelotto LG, et al. IDH2 mutations define a unique subtype of breast cancer with altered nuclear polarity. Cancer Res. 2016;76(24):7118–29.

64. Foschini MP, Asioli S, Foreid S, Cserni G, Ellis IO, Eusebi V, et al. Solid papillary breast carcinomas resembling the tall cell variant of papillary thyroid neoplasms: a unique invasive tumor with indolent behavior. Am J Surg Pathol. 2017;41(7):887–95.

65. Bhargava R, Florea AV, Pelmus M, Jones MW, Bonaventura M, Wald A, et al. Breast tumor resembling tall cell variant of papillary thyroid carcinoma: a solid papillary neoplasm with characteristic immunohistochemical profile and few recurrent mutations. Am J Clin Pathol. 2017;147(4):399–410.

66. Tosi AL, Ragazzi M, Asioli S, Del Vecchio M, Cavalieri M, Eusebi LH, et al. Breast tumor resembling the tall cell variant of papillary thyroid carcinoma: report of 4 cases with evidence of malignant potential. Int J Surg Pathol. 2007;15(1):14–9.

67. Colella R, Guerriero A, Giansanti M, Sidoni A, Bellezza G. An additional case of breast tumor resembling the tall cell variant of papillary thyroid carcinoma. Int J Surg Pathol. 2015;23(3):217–20.

68. Chang SY, Fleiszer DM, Mesurolle B, El Khoury M, Omeroglu A. Breast tumor resembling the tall cell variant of papillary thyroid carcinoma. Breast J. 2009;15(5):531–5.

69. Cameselle-Teijeiro J, Abdulkader I, Barreiro-Morandeira F, Ruiz-Ponte C, Reyes-Santias R, Chavez E, et al. Breast tumor resembling the tall cell variant of papillary thyroid carcinoma: a case report. Int J Surg Pathol. 2006;14(1):79–84.

70. Pitino A, Squillaci S, Spairani C, Rassu PC, Cosimi MF. Tall cell variant of papillary breast carcinoma: an additional case with review of the literature. Pathologica. 2017;109(3):162–7.

71. Jassim M, Premalata CS, Okaly G, Srinivas C. Tall cell carcinoma with reverse polarity of breast: report of a case with unique morphologic and molecular features. Turk Patoloji Derg. 2021;37(2):183–8.

72. Lozada JR, Basili T, Pareja F, Alemar B, Paula ADC, Gularte-Merida R, et al. Solid papillary breast carcinomas resembling the tall cell variant of papillary thyroid neoplasms (solid papillary carcinomas with reverse polarity) harbour recurrent mutations affecting IDH2 and PIK3CA: a validation cohort. Histopathology. 2018;73(2):339–44.

73. Haefliger S, Muenst S, Went P, Bihl M, Dellas S, Weber WP, et al. Tall cell carcinoma of the breast with reversed polarity (TCCRP) with mutations in the IDH2 and PIK3CA genes: a case report. Mol Biol Rep. 2020;47(6):4917–21.

74. Gai L, Done SJ, Cook D, Denic N, Erivwo P, Voisey K, et al. Breast tumour resembling tall cell variant of papillary thyroid carcinoma: case presentation (in a patient with Lynch syndrome). J Clin Pathol. 2018;71(11):1031–2.

75. Alsadoun N, MacGrogan G, Truntzer C, Lacroix-Triki M, Bedgedjian I, Koeb MH, et al. Solid papillary carcinoma with reverse polarity of the breast harbors specific morphologic, immunohistochemical and molecular profile in comparison with other benign or malignant papillary lesions of the breast: a comparative study of 9 additional cases. Mod Pathol. 2018;31(9):1367–80.

76. Toss MS, Billingham K, Egbuniwe IU, Moreno F, Abass A, Rakha EA. Breast tumours resembling the tall cell variant of thyroid papillary carcinoma: are they part of the papillary carcinoma spectrum or a distinct entity? Pathobiology. 2019;86(2-3):83–91.

77. Masood S, Davis C, Kubik MJ. Changing the term "breast tumor resembling the tall cell variant of papillary thyroid carcinoma" to "tall cell variant of papillary breast carcinoma". Adv Anat Pathol. 2012;19(2):108–10.

78. Zhong E, Scognamiglio T, D'Alfonso T, Song W, Tran H, Baek I, et al. Breast tumor resembling the tall cell variant of papillary thyroid carcinoma: molecular characterization by next-generation sequencing and histopathological comparison with tall cell papillary carcinoma of thyroid. Int J Surg Pathol. 2019;27(2):134–41.

79. Hameed O, Perry A, Banerjee R, Zhu X, Pfeifer JD. Papillary carcinoma of the breast lacks evidence of RET rearrangements despite morphological similarities to papillary thyroid carcinoma. Mod Pathol. 2009;22(9):1236–42.

80. Yang WTBH, Foschini MP, Schnitt SJ. Tall cell carcinoma with reversed polarity. In: WHO Classification of Tumours. Editorial Board, editors. WHO Classification of Breast Tumours. 5th ed. Lyon: International Agency for Research on Cancer (IARC); 2019. p. 153–4.

81. Ding LM, Hu HX, Wang YJ, Ji D, Ni LY, Sun ZH, et al. Tall cell variant of papillary breast carcinoma: report of a case. Zhonghua Bing Li Xue Za Zhi. 2019;48(10):815–7.

82. Pareja F, da Silva EM, Frosina D, Geyer FC, Lozada JR, Basili T, et al. Immunohistochemical analysis of IDH2 R172 hotspot mutations in breast papillary neoplasms: applications in the diagnosis of tall cell carcinoma with reverse polarity. Mod Pathol. 2020;33(6):1056–64.

83. Agoumi M, Giambattista J, Hayes MM. Practical considerations in breast papillary lesions: a review of the literature. Arch Pathol Lab Med. 2016;140(8):770–90.

84. Fiche M, Cassagnau E, Aillet G, Bailly J, Chupin M, Classe JM, et al. Breast metastasis from a "tall cell variant" of papillary thyroid carcinoma. Ann Pathol. 1998;18(2):130–2.

85. Eusebi V, Millis RR. Epitheliosis, infiltrating epitheliosis, and radial scar. Semin Diagn Pathol. 2010;27(1):5–12.

86. Eberle CA, Piscuoglio S, Rakha EA, Ng CK, Geyer FC, Edelweiss M, et al. Infiltrating epitheliosis of the breast: characterization of histological features, immunophenotype and genomic profile. Histopathology. 2016;68(7):1030–9.

87. Yan H, Parsons DW, Jin G, McLendon R, Rasheed BA, Yuan W, et al. IDH1 and IDH2 mutations in gliomas. N Engl J Med. 2009;360(8):765–73.

88. Green A, Beer P. Somatic mutations of IDH1 and IDH2 in the leukemic transformation of myeloproliferative neoplasms. N Engl J Med. 2010;362(4):369–70.

89. Dogan S, Chute DJ, Xu B, Ptashkin RN, Chandramohan R, Casanova-Murphy J, et al. Frequent IDH2 R172 mutations in undifferentiated and poorly-differentiated sinonasal carcinomas. J Pathol. 2017;242(4):400–8.

90. Amary MF, Bacsi K, Maggiani F, Damato S, Halai D, Berisha F, et al. IDH1 and IDH2 mutations are frequent events in central chondrosarcoma and central and periosteal chondromas but not in other mesenchymal tumours. J Pathol. 2011;224(3):334–43.

91. Borger DR, Tanabe KK, Fan KC, Lopez HU, Fantin VR, Straley KS, et al. Frequent mutation of isocitrate dehydrogenase (IDH)1 and IDH2 in cholangiocarcinoma identified through broad-based tumor genotyping. Oncologist. 2012;17(1):72–9.

92. Yang H, Ye D, Guan KL, Xiong Y. IDH1 and IDH2 mutations in tumorigenesis: mechanistic insights and clinical perspectives. Clin Cancer Res. 2012;18(20):5562–71.

93. Lu C, Ward PS, Kapoor GS, Rohle D, Turcan S, Abdel-Wahab O, et al. IDH mutation impairs histone demethylation and results in a block to cell differentiation. Nature. 2012;483(7390):474–8.

94. Xu W, Yang H, Liu Y, Yang Y, Wang P, Kim SH, et al. Oncometabolite 2-hydroxyglutarate is a competitive inhibitor

of alpha-ketoglutarate-dependent dioxygenases. Cancer Cell. 2011;19(1):17–30.

95. Ciriello G, Gatza ML, Beck AH, Wilkerson MD, Rhie SK, Pastore A, et al. Comprehensive molecular portraits of invasive lobular breast cancer. Cell. 2015;163(2):506–19.

96. Pereira B, Chin SF, Rueda OM, Vollan HK, Provenzano E, Bardwell HA, et al. The somatic mutation profiles of 2,433 breast cancers refines their genomic and transcriptomic landscapes. Nat Commun. 2016;7:11479.

97. The Cancer Genome Atlas N. Comprehensive molecular portraits of human breast tumours. Nature. 2012;490(7418):61–70.

98. Foschini MPGF, Marchio C, Nishimura R. Mucoepidermoid carcinoma. In: WHO Classification of Tumours. Editorial Board, editors. WHO Classification of Breast Tumours. 5th ed. Lyon: International Agency for Reseasrch on Cancer (IARC); 2019. p. 149–50.

99. Di Tommaso L, Foschini MP, Ragazzini T, Magrini E, Fornelli A, Ellis IO, et al. Mucoepidermoid carcinoma of the breast. Virchows Arch. 2004;444(1):13–9.

100. Bean GR, Krings G, Otis CN, Solomon DA, Garcia JJ, van Zante A, et al. CRTC1-MAML2 fusion in mucoepidermoid carcinoma of the breast. Histopathology. 2019;74(3):463–73.

101. Fisher ER, Palekar AS, Gregorio RM, Paulson JD. Mucoepidermoid and squamous cell carcinomas of breast with reference to squamous metaplasia and giant cell tumors. Am J Surg Pathol. 1983;7(1):15–27.

102. Cheng M, Geng C, Tang T, Song Z. Mucoepidermoid carcinoma of the breast: four case reports and review of the literature. Medicine (Baltimore). 2017;96(51):e9385.

103. Patchefsky AS, Frauenhoffer CM, Krall RA, Cooper HS. Low-grade mucoepidermoid carcinoma of the breast. Arch Pathol Lab Med. 1979;103(4):196–8.

104. Ye RP, Liao YH, Xia T, Kuang R, Long HA, Xiao XL. Breast mucoepidermoid carcinoma: a case report and review of literature. Int J Clin Exp Pathol. 2020;13(12):3192–9.

105. Yan M, Gilmore H, Harbhajanka A. Mucoepidermoid carcinoma of the breast with MAML2 rearrangement: a case report and literature review. Int J Surg Pathol. 2020;28(7):787–92.

106. Hornychova H, Ryska A, Betlach J, Bohac R, Cizek T, Tomsova M, et al. Mucoepidermoid carcinoma of the breast. Neoplasma. 2007;54(2):168–72.

107. Fujino M, Mori D, Akashi M, Yamamoto H, Aibe H, Matake K, et al. Mucoepidermoid carcinoma of the breast found during treatment of lymphoma. Case Rep Oncol. 2016;9(3):806–14.

108. Horii R, Akiyama F, Ikenaga M, Iwase T, Sakamoto G. Muco-epidermoid carcinoma of the breast. Pathol Int. 2006;56(9):549–53.

109. Sherwell-Cabello S, Maffuz-Aziz A, Rios-Luna NP, Pozo-Romero M, Lopez-Jimenez PV, Rodriguez-Cuevas S. Primary mucoepidermoid carcinoma of the breast. Breast J. 2017;23(6):753–5.

110. Basbug M, Akbulut S, Arikanoglu Z, Sogutcu N, Firat U, Kucukoner M. Mucoepidermoid carcinoma in a breast affected by burn scars: comprehensive literature review and case report. Breast Care (Basel). 2011;6(4):293–7.

111. Camelo-Piragua SI, Habib C, Kanumuri P, Lago CE, Mason HS, Otis CN. Mucoepidermoid carcinoma of the breast shares cytogenetic abnormality with mucoepidermoid carcinoma of the salivary gland: a case report with molecular analysis and review of the literature. Hum Pathol. 2009;40(6):887–92.

112. Pareja F, Da Cruz PA, Gularte-Merida R, Vahdatinia M, Li A, Geyer FC, et al. Pleomorphic adenomas and mucoepidermoid carcinomas of the breast are underpinned by fusion genes. NPJ Breast Cancer. 2020;6:20.

113. Cipriani NA, Lusardi JJ, McElherne J, Pearson AT, Olivas AD, Fitzpatrick C, et al. Mucoepidermoid carcinoma: a comparison of histologic grading systems and relationship to MAML2 rearrangement and prognosis. Am J Surg Pathol. 2019;43(7):885–97.

114. Krings G, Nystrom M, Mehdi I, Vohra P, Chen YY. Diagnostic utility and sensitivities of GATA3 antibodies in triple-negative breast cancer. Hum Pathol. 2014;45(11):2225–32.

115. Hung YP, Jo VY, Hornick JL. Immunohistochemistry with a pan-TRK antibody distinguishes secretory carcinoma of the salivary gland from acinic cell carcinoma. Histopathology. 2019;75(1):54–62.

116. Harrison BT, Fowler E, Krings G, Chen YY, Bean GR, Vincent-Salomon A, et al. Pan-TRK immunohistochemistry: a useful diagnostic adjunct for secretory carcinoma of the Breast. Am J Surg Pathol. 2019;43(12):1693–700.

117. Kyrpychova L, Kacerovska D, Vanecek T, Grossmann P, Michal M, Kerl K, et al. Cutaneous hidradenoma: a study of 21 neoplasms revealing neither correlation between the cellular composition and CRTC1-MAML2 fusions nor presence of CRTC3-MAML2 fusions. Ann Diagn Pathol. 2016;23:8–13.

118. Kuma Y, Yamada Y, Yamamoto H, Kohashi K, Ito T, Furue M, et al. A novel fusion gene CRTC3-MAML2 in hidradenoma: histopathological significance. Hum Pathol. 2017;70:55–61.

119. Kazakov DV, Vanecek T, Belousova IE, Mukensnabl P, Kollertova D, Michal M. Skin-type hidradenoma of the breast parenchyma with t(11;19) translocation: hidradenoma of the breast. Am J Dermatopathol. 2007;29(5):457–61.

120. Hsieh MS, Lien HC, Hua SF, Kuo WH, Lee YH. Clear cell hidradenoma of the breast with MAML2 gene rearrangement. Pathology. 2017;49(1):84–7.

121. Memon RA, Prieto Granada CN, Wei S. Clear cell papillary neoplasm of the breast with MAML2 gene rearrangement: clear cell hidradenoma or low-grade mucoepidermoid carcinoma? Pathol Res Pract. 2020;216(10):153140.

122. Yan M, Gilmore H, Harbhajanka A. Low-grade mucoepidermoid carcinoma versus nodular hidradenoma: potential diagnostic challenge in breast pathology. Int J Surg Pathol. 2021;29(3):346–7.

123. Fehr A, Roser K, Heidorn K, Hallas C, Loning T, Bullerdiek J. A new type of MAML2 fusion in mucoepidermoid carcinoma. Genes Chromosomes Cancer. 2008;47(3):203–6.

124. Lennerz JK, Perry A, Dehner LP, Pfeifer JD, Lind AC. CRTC1 rearrangements in the absence of t(11;19) in primary cutaneous mucoepidermoid carcinoma. Br J Dermatol. 2009;161(4):925–9.

125. Tonon G, Modi S, Wu L, Kubo A, Coxon AB, Komiya T, et al. t(11;19)(q21;p13) translocation in mucoepidermoid carcinoma creates a novel fusion product that disrupts a Notch signaling pathway. Nat Genet. 2003;33(2):208–13.

126. Komiya T, Park Y, Modi S, Coxon AB, Oh H, Kaye FJ. Sustained expression of Mect1-Maml2 is essential for tumor cell growth in salivary gland cancers carrying the t(11;19) translocation. Oncogene. 2006;25(45):6128–32.

127. Chen Z, Ni W, Li JL, Lin S, Zhou X, Sun Y, et al. The CRTC1-MAML2 fusion is the major oncogenic driver in mucoepidermoid carcinoma. JCI Insight. 2021;6(7):e139497.

128. Horowitz DP, Sharma CS, Connolly E, Gidea-Addeo D, Deutsch I. Secretory carcinoma of the breast: results from the survival, epidemiology and end results database. Breast. 2012;21(3):350–3.

129. Botta G, Fessia L, Ghiringhello B. Juvenile milk protein secreting carcinoma. Virchows Arch A Pathol Anat Histol. 1982;395(2):145–52.

130. McDivitt RW, Stewart FW. Breast carcinoma in children. JAMA. 1966;195(5):388–90.

131. Tavassoli FA, Norris HJ. Secretory carcinoma of the breast. Cancer. 1980;45(9):2404–13.

132. Li D, Xiao X, Yang W, Shui R, Tu X, Lu H, et al. Secretory breast carcinoma: a clinicopathological and immunophenotypic

study of 15 cases with a review of the literature. Mod Pathol. 2012;25(4):567–75.

133. Krings G, Joseph NM, Bean GR, Solomon D, Onodera C, Talevich E, et al. Genomic profiling of breast secretory carcinomas reveals distinct genetics from other breast cancers and similarity to mammary analog secretory carcinomas. Mod Pathol. 2017;30(8):1086–99.

134. Del Castillo M, Chibon F, Arnould L, Croce S, Ribeiro A, Perot G, et al. Secretory breast carcinoma: a histopathologic and genomic spectrum characterized by a joint specific ETV6-NTRK3 gene fusion. Am J Surg Pathol. 2015;39(11):1458–67.

135. Diallo R, Schaefer KL, Bankfalvi A, Decker T, Ruhnke M, Wülfing P, et al. Secretory carcinoma of the breast: a distinct variant of invasive ductal carcinoma assessed by comparative genomic hybridization and immunohistochemistry. Hum Pathol. 2003;34(12):1299–305.

136. Din NU, Idrees R, Fatima S, Kayani N. Secretory carcinoma of breast: clinicopathologic study of 8 cases. Ann Diagn Pathol. 2013;17(1):54–7.

137. Laé M, Fréneaux P, Sastre-Garau X, Chouchane O, Sigal-Zafrani B, Vincent-Salomon A. Secretory breast carcinomas with ETV6-NTRK3 fusion gene belong to the basal-like carcinoma spectrum. Mod Pathol. 2009;22(2):291–8.

138. Oberman HA. Secretory carcinoma of the breast in adults. Am J Surg Pathol. 1980;4(5):465–70.

139. Rosen PP, Cranor ML. Secretory carcinoma of the breast. Arch Pathol Lab Med. 1991;115(2):141–4.

140. Bishop JA. Unmasking MASC: bringing to light the unique morphologic, immunohistochemical and genetic features of the newly recognized mammary analogue secretory carcinoma of salivary glands. Head Neck Pathol. 2013;7(1):35–9.

141. Skálová A, Vanecek T, Sima R, Laco J, Weinreb I, Perez-Ordonez B, et al. Mammary analogue secretory carcinoma of salivary glands, containing the ETV6-NTRK3 fusion gene: a hitherto undescribed salivary gland tumor entity. Am J Surg Pathol. 2010;34(5):599–608.

142. Connor A, Perez-Ordoñez B, Shago M, Skálová A, Weinreb I. Mammary analog secretory carcinoma of salivary gland origin with the ETV6 gene rearrangement by FISH: expanded morphologic and immunohistochemical spectrum of a recently described entity. Am J Surg Pathol. 2012;36(1):27–34.

143. Majewska H, Skálová A, Stodulski D, Klimková A, Steiner P, Stankiewicz C, et al. Mammary analogue secretory carcinoma of salivary glands: a new entity associated with ETV6 gene rearrangement. Virchows Arch. 2015;466(3):245–54.

144. Wu B, Loh TKS, Vanecek T, Michal M, Petersson F. (Mammary Analogue) Secretory carcinoma of the nasal cavity: report of a rare case with p63 and DOG1 expression and uncommon exon 4-exon 14 ETV6-NTRK3 fusion diagnosed with next generation sequencing. Head Neck Pathol. 2020;14(2):542–9.

145. Amin SM, Beattie A, Ling X, Jennings LJ, Guitart J. Primary cutaneous mammary analog secretory carcinoma with ETV6-NTRK3 translocation. Am J Dermatopathol. 2016;38(11):842–5.

146. Bishop JA, Taube JM, Su A, Binder SW, Kazakov DV, Michal M, et al. Secretory carcinoma of the skin harboring ETV6 gene fusions: a cutaneous analogue to secretory carcinomas of the breast and salivary glands. Am J Surg Pathol. 2017;41(1):62–6.

147. Chang MD, Arthur AK, García JJ, Sukov WR, Shon W. ETV6 rearrangement in a case of mammary analogue secretory carcinoma of the skin. J Cutan Pathol. 2016;43(11):1045–9.

148. Huang T, McHugh JB, Berry GJ, Myers JL. Primary mammary analogue secretory carcinoma of the lung: a case report. Hum Pathol. 2018;74:109–13.

149. Nguyen JK, Bridge JA, Joshi C, McKenney JK. Primary mammary analog secretory carcinoma (MASC) of the vulva with

ETV6-NTRK3 fusion: a case report. Int J Gynecol Pathol. 2019;38(3):283–7.

150. Dettloff J, Seethala RR, Stevens TM, Brandwein-Gensler M, Centeno BA, Otto K, et al. Mammary analog secretory carcinoma (MASC) involving the thyroid gland: a report of the first 3 cases. Head Neck Pathol. 2017;11(2):124–30.

151. Dogan S, Wang L, Ptashkin RN, Dawson RR, Shah JP, Sherman EJ, et al. Mammary analog secretory carcinoma of the thyroid gland: a primary thyroid adenocarcinoma harboring ETV6-NTRK3 fusion. Mod Pathol. 2016;29(9):985–95.

152. Leeman-Neill RJ, Kelly LM, Liu P, Brenner AV, Little MP, Bogdanova TI, et al. ETV6-NTRK3 is a common chromosomal rearrangement in radiation-associated thyroid cancer. Cancer. 2014;120(6):799–807.

153. Arce C, Cortes-Padilla D, Huntsman DG, Miller MA, Dueñas-Gonzalez A, Alvarado A, et al. Secretory carcinoma of the breast containing the ETV6-NTRK3 fusion gene in a male: case report and review of the literature. World J Surg Oncol. 2005;3:35.

154. Hoda RS, Brogi E, Pareja F, Nanjangud G, Murray MP, Weigelt B, et al. Secretory carcinoma of the breast: clinicopathologic profile of 14 cases emphasising distant metastatic potential. Histopathology. 2019;75(2):213–24.

155. Krings GCY, Sorensen PHB, Yang WT. Secretory carcinoma. In: WHO Classification of Tumours. Editorial Board, editors. WHO Classification of Breast Tumours. 5th ed. Lyon: International Agency for Research on Cancer (IARC); 2019. p. 146–8.

156. Shin SJ, Sheikh FS, Allenby PA, Rosen PP. Invasive secretory (juvenile) carcinoma arising in ectopic breast tissue of the axilla. Arch Pathol Lab Med. 2001;125(10):1372–4.

157. Krausz T, Jenkins D, Grontoft O, Pollock DJ, Azzopardi JG. Secretory carcinoma of the breast in adults: emphasis on late recurrence and metastasis. Histopathology. 1989;14(1):25–36.

158. Siegel JR, Karcnik TJ, Hertz MB, Gelmann H, Baker SR. Secretory carcinoma of the breast. Breast J. 1999;5(3):204–7.

159. Mun SH, Ko EY, Han BK, Shin JH, Kim SJ, Cho EY. Secretory carcinoma of the breast: sonographic features. J Ultrasound Med. 2008;27(6):947–54.

160. Paeng MH, Choi HY, Sung SH, Moon BI, Shim SS. Secretory carcinoma of the breast. J Clin Ultrasound. 2003;31(8):425–9.

161. Wu IK, Lai YC, Chiou HJ, Hsu CY. Secretory carcinoma of the breast: a case report and literature review. J Med Ultrasound. 2021;29(1):57–9.

162. Lee SG, Jung SP, Lee HY, Kim S, Kim HY, Kim I, et al. Secretory breast carcinoma: a report of three cases and a review of the literature. Oncol Lett. 2014;8(2):683–6.

163. Montalvo N, Posso V, Redrobán L. Secretory carcinoma in a 79-year-old woman: an exceptionally rare type of breast carcinoma. Rare Tumors. 2016;8(4):6650.

164. Yang Y, Wang Z, Pan G, Li S, Wu Y, Liu L. Pure secretory carcinoma in situ: a case report and literature review. Diagn Pathol. 2019;14(1):95.

165. Gatalica Z, Xiu J, Swensen J, Vranic S. Molecular characterization of cancers with NTRK gene fusions. Mod Pathol. 2019;32(1):147–53.

166. Hechtman JF, Benayed R, Hyman DM, Drilon A, Zehir A, Frosina D, et al. Pan-Trk Immunohistochemistry Is an Efficient and Reliable Screen for the Detection of NTRK Fusions. Am J Surg Pathol. 2017;41(11):1547–51.

167. Tognon C, Knezevich SR, Huntsman D, Roskelley CD, Melnyk N, Mathers JA, et al. Expression of the ETV6-NTRK3 gene fusion as a primary event in human secretory breast carcinoma. Cancer Cell. 2002;2(5):367–76.

168. Tognon C, Garnett M, Kenward E, Kay R, Morrison K, Sorensen PH. The chimeric protein tyrosine kinase ETV6-NTRK3 requires both Ras-Erk1/2 and PI3-kinase-Akt signaling for fibroblast transformation. Cancer Res. 2001;61(24):8909–16.

169. Lannon CL, Sorensen PH. ETV6-NTRK3: a chimeric protein tyrosine kinase with transformation activity in multiple cell lineages. Semin Cancer Biol. 2005;15(3):215–23.

170. Jin W, Yun C, Hobbie A, Martin MJ, Sorensen PH, Kim SJ. Cellular transformation and activation of the phosphoinositide-3-kinase-Akt cascade by the ETV6-NTRK3 chimeric tyrosine kinase requires c-Src. Cancer Res. 2007;67(7):3192–200.

171. Wai DH, Knezevich SR, Lucas T, Jansen B, Kay RJ, Sorensen PH. The ETV6-NTRK3 gene fusion encodes a chimeric protein tyrosine kinase that transforms NIH3T3 cells. Oncogene. 2000;19(7):906–15.

172. Cetinbas N, Huang-Hobbs H, Tognon C, Leprivier G, An J, McKinney S, et al. Mutation of the salt bridge-forming residues in the ETV6-SAM domain interface blocks ETV6-NTRK3-induced cellular transformation. J Biol Chem. 2013;288(39):27940–50.

173. Tognon CE, Mackereth CD, Somasiri AM, McIntosh LP, Sorensen PH. Mutations in the SAM domain of the ETV6-NTRK3 chimeric tyrosine kinase block polymerization and transformation activity. Mol Cell Biol. 2004;24(11):4636–50.

174. Skálová A, Vanecek T, Simpson RH, Laco J, Majewska H, Baneckova M, et al. Mammary analogue secretory carcinoma of salivary glands: molecular analysis of 25 ETV6 gene rearranged tumors with lack of detection of classical ETV6-NTRK3 fusion transcript by standard RT-PCR: report of 4 cases harboring ETV6-X gene fusion. Am J Surg Pathol. 2016;40(1):3–13.

175. Ito Y, Ishibashi K, Masaki A, Fujii K, Fujiyoshi Y, Hattori H, et al. Mammary analogue secretory carcinoma of salivary glands: a clinicopathologic and molecular study including 2 cases harboring ETV6-X fusion. Am J Surg Pathol. 2015;39(5):602–10.

176. Skálová A, Stenman G, Simpson RHW, Hellquist H, Slouka D, Svoboda T, et al. The role of molecular testing in the differential diagnosis of salivary gland carcinomas. Am J Surg Pathol. 2018;42(2):e11–27.

177. Skalova A, Vanecek T, Martinek P, Weinreb I, Stevens TM, Simpson RHW, et al. Molecular profiling of mammary analog secretory carcinoma revealed a subset of tumors harboring a novel ETV6-RET translocation: report of 10 cases. Am J Surg Pathol. 2018;42(2):234–46.

178. Rooper LM, Karantanos T, Ning Y, Bishop JA, Gordon SW, Kang H. Salivary secretory carcinoma with a novel ETV6-MET fusion: expanding the molecular spectrum of a recently described entity. Am J Surg Pathol. 2018;42(8):1121–6.

179. Guilmette J, Dias-Santagata D, Nosé V, Lennerz JK, Sadow PM. Novel gene fusions in secretory carcinoma of the salivary glands: enlarging the ETV6 family. Hum Pathol. 2019;83:50–8.

180. Black M, Liu CZ, Onozato M, Iafrate AJ, Darvishian F, Jour G, et al. Concurrent identification of novel EGFR-SEPT14 fusion and ETV6-RET fusion in secretory carcinoma of the salivary gland. Head Neck Pathol. 2020;14(3):817–21.

181. Salgado CM, Alaggio R, Reyes-Múgica M, Zin A, de Vito R. Clinicopathologic and Molecular Characterization of Four Cases of Pediatric Salivary Secretory Carcinoma (SSC), One with ETV6-RET Fusion. Head Neck Pathol. 2021;15(3):796–802.

182. Knezevich SR, McFadden DE, Tao W, Lim JF, Sorensen PH. A novel ETV6-NTRK3 gene fusion in congenital fibrosarcoma. Nat Genet. 1998;18(2):184–7.

183. Knezevich SR, Garnett MJ, Pysher TJ, Beckwith JB, Grundy PE, Sorensen PH. ETV6-NTRK3 gene fusions and trisomy 11 establish a histogenetic link between mesoblastic nephroma and congenital fibrosarcoma. Cancer Res. 1998;58(22):5046–8.

184. De Braekeleer E, Douet-Guilbert N, Morel F, Le Bris MJ, Basinko A, De Braekeleer M. ETV6 fusion genes in hematological malignancies: a review. Leuk Res. 2012;36(8):945–61.

185. Alassiri AH, Ali RH, Shen Y, Lum A, Strahlendorf C, Deyell R, et al. ETV6-NTRK3 is expressed in a subset of ALK-negative

186. inflammatory myofibroblastic tumors. Am J Surg Pathol. 2016;40(8):1051–61.

186. Yeh I, Tee MK, Botton T, Shain AH, Sparatta AJ, Gagnon A, et al. NTRK3 kinase fusions in Spitz tumours. J Pathol. 2016;240(3):282–90.

187. Makretsov N, He M, Hayes M, Chia S, Horsman DE, Sorensen PH, et al. A fluorescence in situ hybridization study of ETV6-NTRK3 fusion gene in secretory breast carcinoma. Genes Chromosomes Cancer. 2004;40(2):152–7.

188. Costa NM, Rodrigues H, Pereira H, Pardal F, Matos E. Secretory breast carcinoma--case report and review of the medical literature. Breast. 2004;13(4):353–5.

189. Herz H, Cooke B, Goldstein D. Metastatic secretory breast cancer. Non-responsiveness to chemotherapy: case report and review of the literature. Ann Oncol. 2000;11(10):1343–7.

190. Drilon A, Li G, Dogan S, Gounder M, Shen R, Arcila M, et al. What hides behind the MASC: clinical response and acquired resistance to entrectinib after ETV6-NTRK3 identification in a mammary analogue secretory carcinoma (MASC). Ann Oncol. 2016;27(5):920–6.

191. Drilon A, Laetsch TW, Kummar S, DuBois SG, Lassen UN, Demetri GD, et al. Efficacy of larotrectinib in TRK fusion-positive cancers in adults and children. N Engl J Med. 2018;378(8):731–9.

192. Kheder ES, Hong DS. Emerging targeted therapy for tumors with NTRK fusion proteins. Clin Cancer Res. 2018;24(23):5807–14.

193. Shukla N, Roberts SS, Baki MO, Mushtaq Q, Goss PE, Park BH, et al. Successful targeted therapy of refractory pediatric ETV6-NTRK3 fusion-positive secretory breast carcinoma. JCO Precis Oncol. 2017;2017:PO.17.00034.

194. Provenzano EGZ, Vranic S. Carcinoma with apocrine differentiation. In: WHO Classification of Tumours. Editorial Board, editors. WHO Classification of Breast Tumours. 5th ed. Lyon: International Agency for Research on Cancer (IARC); 2019. p. 131–3.

195. Vranic S, Marchio C, Castellano I, Botta C, Scalzo MS, Bender RP, et al. Immunohistochemical and molecular profiling of histologically defined apocrine carcinomas of the breast. Hum Pathol. 2015;46(9):1350–9.

196. Lehmann BD, Bauer JA, Chen X, Sanders ME, Chakravarthy AB, Shyr Y, et al. Identification of human triple-negative breast cancer subtypes and preclinical models for selection of targeted therapies. J Clin Invest. 2011;121(7):2750–67.

197. Lehmann-Che J, Hamy AS, Porcher R, Barritault M, Bouhidel F, Habuellelah H, et al. Molecular apocrine breast cancers are aggressive estrogen receptor negative tumors overexpressing either HER2 or GCDFP15. Breast Cancer Res. 2013;15(3):R37.

198. Farmer P, Bonnefoi H, Becette V, Tubiana-Hulin M, Fumoleau P, Larsimont D, et al. Identification of molecular apocrine breast tumours by microarray analysis. Oncogene. 2005;24(29):4660–71.

199. Vranic S, Tawfik O, Palazzo J, Bilalovic N, Eyzaguirre E, Lee LM, et al. EGFR and HER-2/neu expression in invasive apocrine carcinoma of the breast. Mod Pathol. 2010;23(5):644–53.

200. D'Arcy C, Quinn CM. Apocrine lesions of the breast: part 2 of a two-part review. Invasive apocrine carcinoma, the molecular apocrine signature and utility of immunohistochemistry in the diagnosis of apocrine lesions of the breast. J Clin Pathol. 2019;72(1):7–11.

201. Yamazaki M, Nagata Y, Monji S, Shigematsu Y, Baba T, Shimokawa H, et al. Apocrine carcinoma of the breast. J UOEH. 2011;33(4):293–301.

202. Vranic S, Schmitt F, Sapino A, Costa JL, Reddy S, Castro M, et al. Apocrine carcinoma of the breast: a comprehensive review. Histol Histopathol. 2013;28(11):1393–409.

203. Dellapasqua S, Maisonneuve P, Viale G, Pruneri G, Mazzarol G, Ghisini R, et al. Immunohistochemically defined subtypes

and outcome of apocrine breast cancer. Clin Breast Cancer. 2013;13(2):95–102.

204. Schmitt FC, Soares R, Seruca R. Bilateral apocrine carcinoma of the breast. Molecular and immunocytochemical evidence for two independent primary tumours. Virchows Arch. 1998;433(6):505–9.

205. Mossler JA, Barton TK, Brinkhous AD, McCarty KS, Moylan JA, McCarty KS Jr. Apocrine differentiation in human mammary carcinoma. Cancer. 1980;46(11):2463–71.

206. Gerhard R, Costa JL, Schmitt F. Benign and malignant apocrine lesions of the breast. Expert Rev Anticancer Ther. 2012;12(2):215–21.

207. Arciero CA, Diehl AH 3rd, Liu Y, Sun Q, Gillespie T, Li X, et al. Triple-negative apocrine carcinoma: a rare pathologic subtype with a better prognosis than other triple-negative breast cancers. J Surg Oncol. 2020;122(6):1232–9.

208. Sun X, Zuo K, Yao Q, Zhou S, Shui R, Xu X, et al. Invasive apocrine carcinoma of the breast: clinicopathologic features and comprehensive genomic profiling of 18 pure triple-negative apocrine carcinomas. Mod Pathol. 2020;33(12):2473–82.

209. Imamovic D, Bilalovic N, Skenderi F, Beslagic V, Ceric T, Hasanbegovic B, et al. A clinicopathologic study of invasive apocrine carcinoma of the breast: a single-center experience. Breast J. 2018;24(6):1105–8.

210. Meattini I, Pezzulla D, Saieva C, Bernini M, Orzalesi L, Sanchez LJ, et al. Triple negative apocrine carcinomas as a distinct subtype of triple negative breast cancer: a case-control study. Clin Breast Cancer. 2018;18(5):e773–e80.

211. Montagna E, Cancello G, Pagan E, Bagnardi V, Munzone E, Dellapasqua S, et al. Prognosis of selected triple negative apocrine breast cancer patients who did not receive adjuvant chemotherapy. Breast. 2020;53:138–42.

212. Mills AM, Gottlieb CE, Wendroth SM, Brenin CM, Atkins KA. Pure apocrine carcinomas represent a clinicopathologically distinct androgen receptor-positive subset of triple-negative breast cancers. Am J Surg Pathol. 2016;40(8):1109–16.

213. Zhao S, Ma D, Xiao Y, Jiang YZ, Shao ZM. Clinicopathologic features and prognoses of different histologic types of triple-negative breast cancer: a large population-based analysis. Eur J Surg Oncol. 2018;44(4):420–8.

214. Zhang N, Zhang H, Chen T, Yang Q. Dose invasive apocrine adenocarcinoma has worse prognosis than invasive ductal carcinoma of breast: evidence from SEER database. Oncotarget. 2017;8(15):24579–92.

215. Weisman PS, Ng CK, Brogi E, Eisenberg RE, Won HH, Piscuoglio S, et al. Genetic alterations of triple negative breast cancer by targeted next-generation sequencing and correlation with tumor morphology. Mod Pathol. 2016;29(5):476–88.

216. Ogiya A, Horii R, Osako T, Ito Y, Iwase T, Eishi Y, et al. Apocrine metaplasia of breast cancer: clinicopathological features and predicting response. Breast Cancer. 2010;17(4):290–7.

217. Durham JR, Fechner RE. The histologic spectrum of apocrine lesions of the breast. Am J Clin Pathol. 2000;113(suppl_1):S3–18.

218. Shamir ER, Chen YY, Krings G. Genetic analysis of pleomorphic and florid lobular carcinoma in situ variants: frequent ERBB2/ERBB3 alterations and clonal relationship to classic lobular carcinoma in situ and invasive lobular carcinoma. Mod Pathol. 2020;33(6):1078–91.

219. Chen YY, Hwang ES, Roy R, DeVries S, Anderson J, Wa C, et al. Genetic and phenotypic characteristics of pleomorphic lobular carcinoma in situ of the breast. Am J Surg Pathol. 2009;33(11):1683–94.

220. Zhong E, Solomon JP, Cheng E, Baum J, Song W, Hoda SA. Apocrine variant of pleomorphic lobular carcinoma in situ: further clinical, histopathologic, immunohistochemical, and molecular characterization of an emerging entity. Am J Surg Pathol. 2020;44(8):1092–103.

221. Hoda SA, Brogi E, Koerner FC, Rosen PP. Rosen's breast pathology. Philadelphia, PA: Lippincott Williams and Williams; 2014.

222. Hood CI, Font RL, Zimmerman LE. Metastatic mammary carcinoma in the eyelid with histiocytoid appearance. Cancer. 1973;31(4):793–800.

223. Astvatsaturyan K, Yue Y, Walts AE, Bose S. Androgen receptor positive triple negative breast cancer: clinicopathologic, prognostic, and predictive features. PLoS One. 2018;13(6):e0197827.

224. Collins LC, Cole KS, Marotti JD, Hu R, Schnitt SJ, Tamimi RM. Androgen receptor expression in breast cancer in relation to molecular phenotype: results from the Nurses' Health Study. Mod Pathol. 2011;24(7):924–31.

225. Niemeier LA, Dabbs DJ, Beriwal S, Striebel JM, Bhargava R. Androgen receptor in breast cancer: expression in estrogen receptor-positive tumors and in estrogen receptor-negative tumors with apocrine differentiation. Mod Pathol. 2010;23(2):205–12.

226. Daemen A, Manning G. HER2 is not a cancer subtype but rather a pan-cancer event and is highly enriched in AR-driven breast tumors. Breast Cancer Res. 2018;20(1):8.

227. Loos S, Schulz KD, Hackenberg R. Regulation of GCDFP-15 expression in human mammary cancer cells. Int J Mol Med. 1999;4(2):135–40.

228. Darb-Esfahani S, von Minckwitz G, Denkert C, Ataseven B, Hogel B, Mehta K, et al. Gross cystic disease fluid protein 15 (GCDFP-15) expression in breast cancer subtypes. BMC Cancer. 2014;14:546.

229. Honma N, Takubo K, Akiyama F, Sawabe M, Arai T, Younes M, et al. Expression of GCDFP-15 and AR decreases in larger or node-positive apocrine carcinomas of the breast. Histopathology. 2005;47(2):195–201.

230. Kasashima S, Kawashima A, Ozaki S, Nakanuma Y. Expression of 5alpha-reductase in apocrine carcinoma of the breast and its correlation with clinicopathological aggressiveness. Histopathology. 2012;60(6B):E51–7.

231. Tanaka K, Imoto S, Wada N, Sakemura N, Hasebe K. Invasive apocrine carcinoma of the breast: clinicopathologic features of 57 patients. Breast J. 2008;14(2):164–8.

232. Celis JE, Cabezon T, Moreira JM, Gromov P, Gromova I, Timmermans-Wielenga V, et al. Molecular characterization of apocrine carcinoma of the breast: validation of an apocrine protein signature in a well-defined cohort. Mol Oncol. 2009;3(3):220–37.

233. Honma N, Takubo K, Arai T, Younes M, Kasumi F, Akiyama F, et al. Comparative study of monoclonal antibody B72.3 and gross cystic disease fluid protein-15 as markers of apocrine carcinoma of the breast. APMIS. 2006;114(10):712–9.

234. Banneau G, Guedj M, MacGrogan G, de Mascarel I, Velasco V, Schiappa R, et al. Molecular apocrine differentiation is a common feature of breast cancer in patients with germline PTEN mutations. Breast Cancer Res. 2010;12(4):R63.

235. Gromov P, Espinoza JA, Talman ML, Honma N, Kroman N, Timmermans Wielenga V, et al. FABP7 and HMGCS2 are novel protein markers for apocrine differentiation categorizing apocrine carcinoma of the breast. PLoS One. 2014;9(11):e112024.

236. Shao MM, Chan SK, Yu AM, Lam CC, Tsang JY, Lui PC, et al. Keratin expression in breast cancers. Virchows Arch. 2012;461(3):313–22.

237. Shousha S, Bull TB, Southall PJ, Mazoujian G. Apocrine carcinoma of the breast containing foam cells. An electron microscopic and immunohistological study. Histopathology. 1987;11(6):611–20.

238. Defteros G, Sanguino Ramirez AM, Silverman JF, Krishnamurti U. GATA3 immunohistochemistry expression in histologic subtypes of primary breast carcinoma and metastatic breast carcinoma cytology. Am J Surg Pathol. 2015;39(9):1282–9.

239. Wendroth SM, Mentrikoski MJ, Wick MR. GATA3 expression in morphologic subtypes of breast carcinoma: a comparison with gross cystic disease fluid protein 15 and mammaglobin. Ann Diagn Pathol. 2015;19(1):6–9.

240. Kim S, Moon BI, Lim W, Park S, Cho MS, Sung SH. Expression patterns of GATA3 and the androgen receptor are strongly correlated in patients with triple-negative breast cancer. Hum Pathol. 2016;55:190–5.

241. Hilson JB, Schnitt SJ, Collins LC. Phenotypic alterations in myoepithelial cells associated with benign sclerosing lesions of the breast. Am J Surg Pathol. 2010;34(6):896–900.

242. Tramm T, Kim JY, Tavassoli FA. Diminished number or complete loss of myoepithelial cells associated with metaplastic and neoplastic apocrine lesions of the breast. Am J Surg Pathol. 2011;35(2):202–11.

243. Ragazzi M, de Biase D, Betts CM, Farnedi A, Ramadan SS, Tallini G, et al. Oncocytic carcinoma of the breast: frequency, morphology and follow-up. Hum Pathol. 2011;42(2):166–75.

244. Damiani S, Eusebi V, Losi L, D'Adda T, Rosai J. Oncocytic carcinoma (malignant oncocytoma) of the breast. Am J Surg Pathol. 1998;22(2):221–30.

245. Geyer FC, de Biase D, Lambros MB, Ragazzi M, Lopez-Garcia MA, Natrajan R, et al. Genomic profiling of mitochondrion-rich breast carcinoma: chromosomal changes may be relevant for mitochondria accumulation and tumour biology. Breast Cancer Res Treat. 2012;132(1):15–28.

246. Pia-Foschini M, Reis-Filho JS, Eusebi V, Lakhani SR. Salivary gland-like tumours of the breast: surgical and molecular pathology. J Clin Pathol. 2003;56(7):497–506.

247. Costa MJ, Silverberg SG. Oncocytic carcinoma of the male breast. Arch Pathol Lab Med. 1989;113(12):1396–9.

248. Roncaroli F, Lamovec J, Zidar A, Eusebi V. Acinic cell-like carcinoma of the breast. Virchows Arch. 1996;429(1):69–74.

249. Foschini MPGF, Marchio C, Nishimura R. Acinic cell carcinoma. In: WHO Classification of Tumours. Editorial Board, editors. WHO Classification of Breast Tumours. 5th ed. Lyon: International Agency for Research on Cancer (IARC); 2019. p. 139–41.

250. Limite G, Di Micco R, Esposito E, Sollazzo V, Cervotti M, Pettinato G, et al. Acinic cell carcinoma of the breast: review of the literature. Int J Surg. 2014;12(Suppl 1):S35–9.

251. Foschini MP, Eusebi V. Carcinomas of the breast showing myoepithelial cell differentiation. A review of the literature. Virchows Arch. 1998;432(4):303–10.

252. Peintinger F, Leibl S, Reitsamer R, Moinfar F. Primary acinic cell carcinoma of the breast: a case report with long-term follow-up and review of the literature. Histopathology. 2004;45(6):645–8.

253. Guerini-Rocco E, Hodi Z, Piscuoglio S, Ng CK, Rakha EA, Schultheis AM, et al. The repertoire of somatic genetic alterations of acinic cell carcinomas of the breast: an exploratory, hypothesis-generating study. J Pathol. 2015;237(2):166–78.

254. Kahn R, Holtveg H, Nissen F, Holck S. Are acinic cell carcinoma and microglandular carcinoma of the breast related lesions? Histopathology. 2003;42(2):195–6.

255. Geyer FC, Lacroix-Triki M, Colombo PE, Patani N, Gauthier A, Natrajan R, et al. Molecular evidence in support of the neoplastic and precursor nature of microglandular adenosis. Histopathology. 2012;60(6B):E115–30.

256. Jones C, Damiani S, Wells D, Chaggar R, Lakhani SR, Eusebi V. Molecular cytogenetic comparison of apocrine hyperplasia and apocrine carcinoma of the breast. Am J Pathol. 2001;158(1):207–14.

257. Schrager CA, Schneider D, Gruener AC, Tsou HC, Peacocke M. Clinical and pathological features of breast disease in Cowden's syndrome: an underrecognized syndrome with an increased risk of breast cancer. Hum Pathol. 1998;29(1):47–53.

258. Schrager CA, Schneider D, Gruener AC, Tsou HC, Peacocke M. Similarities of cutaneous and breast pathology in Cowden's syndrome. Exp Dermatol. 1998;7(6):380–90.

259. Doane AS, Danso M, Lal P, Donaton M, Zhang L, Hudis C, et al. An estrogen receptor-negative breast cancer subset characterized by a hormonally regulated transcriptional program and response to androgen. Oncogene. 2006;25(28):3994–4008.

260. d'Amore ES, Terrier-Lacombe MJ, Travagli JP, Friedman S, Contesso G. Invasive apocrine carcinoma of the breast: a long term follow-up study of 34 cases. Breast Cancer Res Treat. 1988;12(1):37–44.

261. Abati AD, Kimmel M, Rosen PP. Apocrine mammary carcinoma. A clinicopathologic study of 72 cases. Am J Clin Pathol. 1990;94(4):371–7.

262. Nagao T, Kinoshita T, Hojo T, Tsuda H, Tamura K, Fujiwara Y. The differences in the histological types of breast cancer and the response to neoadjuvant chemotherapy: the relationship between the outcome and the clinicopathological characteristics. Breast. 2012;21(3):289–95.

263. Cha YJ, Jung WH, Koo JS. The clinicopathologic features of molecular apocrine breast cancer. Korean J Pathol. 2012;46(2):169–76.

264. Liao HY, Zhang WW, Sun JY, Li FY, He ZY, Wu SG. The clinicopathological features and survival outcomes of different histological subtypes in triple-negative breast cancer. J Cancer. 2018;9(2):296–303.

265. Wu W, Wu M, Peng G, Shi D, Zhang J. Prognosis in triple-negative apocrine carcinomas of the breast: a population-based study. Cancer Med. 2019;8(18):7523–31.

266. Bonnefoi H, MacGrogan G, Poncet C, Iggo R, Pommeret F, Grellety T, et al. Molecular apocrine tumours in EORTC 10994/BIG 1-00 phase III study: pathological response after neoadjuvant chemotherapy and clinical outcomes. Br J Cancer. 2019;120(9):913–21.

267. Masuda H, Baggerly KA, Wang Y, Zhang Y, Gonzalez-Angulo AM, Meric-Bernstam F, et al. Differential response to neoadjuvant chemotherapy among 7 triple-negative breast cancer molecular subtypes. Clin Cancer Res. 2013;19(19):5533–40.

268. Lehmann BD, Jovanovic B, Chen X, Estrada MV, Johnson KN, Shyr Y, et al. Refinement of triple-negative breast cancer molecular subtypes: implications for neoadjuvant chemotherapy selection. PLoS One. 2016;11(6):e0157368.

269. Grellety T, Callens C, Richard E, Briaux A, Velasco V, Pulido M, et al. Enhancing abiraterone acetate efficacy in androgen receptor-positive triple-negative breast cancer: Chk1 as a potential target. Clin Cancer Res. 2019;25(2):856–67.

270. Gucalp A, Traina TA. Androgen receptor-positive, triple-negative breast cancer. Cancer. 2017;123(10):1686–8.

271. Pascual J, Turner NC. Targeting the PI3-kinase pathway in triple-negative breast cancer. Ann Oncol. 2019;30(7):1051–60.

272. Asghar US, Barr AR, Cutts R, Beaney M, Babina I, Sampath D, et al. Single-cell dynamics determines response to CDK4/6 inhibition in triple-negative breast cancer. Clin Cancer Res. 2017;23(18):5561–72.

273. Christenson JL, O'Neill KI, Williams MM, Spoelstra NS, Jones KL, Trahan GD, et al. Activity of combined androgen receptor antagonism and cell cycle inhibition in androgen receptor positive triple negative breast cancer. Mol Cancer Ther. 2021;20(6):1062–71.

274. Marra A, Trapani D, Viale G, Criscitiello C, Curigliano G. Practical classification of triple-negative breast cancer: intra-

tumoral heterogeneity, mechanisms of drug resistance, and novel therapies. NPJ Breast Cancer. 2020;6:54.

275. Reis-Filho JSGH, McCart Read AE, Rakha EA, Shin SJ, Sotiriou C, Vincent-Salomon A. Metaplastic carcinoma. In: WHO Classification of Tumours. Editorial Board, editors. WHO Classification of Breast Tumours. 5th ed. Lyon: International Agency for Research on Cancer (IARC); 2019. p. 134–8.

276. Schroeder MC, Rastogi P, Geyer CE Jr, Miller LD, Thomas A. Early and locally advanced metaplastic breast cancer: presentation and survival by receptor status in surveillance, epidemiology, and end results (SEER) 2010-2014. Oncologist. 2018;23(4):481–8.

277. Paul Wright G, Davis AT, Koehler TJ, Melnik MK, Chung MH. Hormone receptor status does not affect prognosis in metaplastic breast cancer: a population-based analysis with comparison to infiltrating ductal and lobular carcinomas. Ann Surg Oncol. 2014;21(11):3497–503.

278. Nelson RA, Guye ML, Luu T, Lai LL. Survival outcomes of metaplastic breast cancer patients: results from a US population-based analysis. Ann Surg Oncol. 2015;22(1):24–31.

279. Rakha EA, Tan PH, Varga Z, Tse GM, Shaaban AM, Climent F, et al. Prognostic factors in metaplastic carcinoma of the breast: a multi-institutional study. Br J Cancer. 2015; 112(2):283–9.

280. Downs-Kelly E, Nayeemuddin KM, Albarracin C, Wu Y, Hunt KK, Gilcrease MZ. Matrix-producing carcinoma of the breast: an aggressive subtype of metaplastic carcinoma. Am J Surg Pathol. 2009;33(4):534–41.

281. Gwin K, Wheeler DT, Bossuyt V, Tavassoli FA. Breast carcinoma with chondroid differentiation: a clinicopathologic study of 21 triple negative (ER-, PR-, Her2/neu-) cases. Int J Surg Pathol. 2010;18(1):27–35.

282. McCart Reed AE, Kalaw E, Nones K, Bettington M, Lim M, Bennett J, et al. Phenotypic and molecular dissection of metaplastic breast cancer and the prognostic implications. J Pathol. 2019;247(2):214–27.

283. El Zein D, Hughes M, Kumar S, Peng X, Oyasiji T, Jabbour H, et al. Metaplastic carcinoma of the breast is more aggressive than triple-negative breast cancer: a study from a single institution and review of literature. Clin Breast Cancer. 2017;17(5):382–91.

284. Langlands F, Cornford E, Rakha E, Dall B, Gutteridge E, Dodwell D, et al. Imaging overview of metaplastic carcinomas of the breast: a large study of 71 cases. Br J Radiol. 2016;89(1064):20140644.

285. Oberman HA. Metaplastic carcinoma of the breast. A clinicopathologic study of 29 patients. Am J Surg Pathol. 1987;11(12):918–29.

286. Tse GM, Tan PH, Putti TC, Lui PC, Chaiwun B, Law BK. Metaplastic carcinoma of the breast: a clinicopathological review. J Clin Pathol. 2006;59(10):1079–83.

287. Pezzi CM, Patel-Parekh L, Cole K, Franko J, Klimberg VS, Bland K. Characteristics and treatment of metaplastic breast cancer: analysis of 892 cases from the National Cancer Data Base. Ann Surg Oncol. 2007;14(1):166–73.

288. Yang WT, Hennessy B, Broglio K, Mills C, Sneige N, Davis WG, et al. Imaging differences in metaplastic and invasive ductal carcinomas of the breast. AJR Am J Roentgenol. 2007;189(6):1288–93.

289. Kashyap R, Vellathussery Chakkalakkoombil S, Ch Toi P, Satheesan D. Metaplastic breast carcinoma with osseous differentiation presenting as calcified breast mass-Radio-pathological correlation. Breast J. 2020;26(9):1825–7.

290. Cardoso F, Leal C, Meira A, Azevedo R, Mauricio MJ, Leal da Silva JM, et al. Squamous cell carcinoma of the breast. Breast. 2000;9(6):315–9.

291. Rosen PP, Ernsberger D. Low-grade adenosquamous carcinoma. A variant of metaplastic mammary carcinoma. Am J Surg Pathol. 1987;11(5):351–8.

292. Soo K, Tan PH. Low-grade adenosquamous carcinoma of the breast. J Clin Pathol. 2013;66(6):506–11.

293. Van Hoeven KH, Drudis T, Cranor ML, Erlandson RA, Rosen PP. Low-grade adenosquamous carcinoma of the breast. A clinicopathologic study of 32 cases with ultrastructural analysis. Am J Surg Pathol. 1993;17(3):248–58.

294. Kawaguchi K, Shin SJ. Immunohistochemical staining characteristics of low-grade adenosquamous carcinoma of the breast. Am J Surg Pathol. 2012;36(7):1009–20.

295. Bataillon G, Fuhrmann L, Girard E, Menet E, Lae M, Capovilla M, et al. High rate of PIK3CA mutations but no TP53 mutations in low-grade adenosquamous carcinoma of the breast. Histopathology. 2018;73(2):273–83.

296. Denley H, Pinder SE, Tan PH, Sim CS, Brown R, Barker T, et al. Metaplastic carcinoma of the breast arising within complex sclerosing lesion: a report of five cases. Histopathology. 2000;36(3):203–9.

297. Gobbi H, Simpson JF, Jensen RA, Olson SJ, Page DL. Metaplastic spindle cell breast tumors arising within papillomas, complex sclerosing lesions, and nipple adenomas. Mod Pathol. 2003;16(9):893–901.

298. Foschini MP, Pizzicannella G, Peterse JL, Eusebi V. Adenomyoepithelioma of the breast associated with low-grade adenosquamous and sarcomatoid carcinomas. Virchows Arch. 1995;427(3):243–50.

299. Geyer FC, Lambros MB, Natrajan R, Mehta R, Mackay A, Savage K, et al. Genomic and immunohistochemical analysis of adenosquamous carcinoma of the breast. Mod Pathol. 2010;23(7):951–60.

300. Tan QT, Chuwa EW, Chew SH, Lim-Tan SK, Lim SH. Low-grade adenosquamous carcinoma of the breast: a diagnostic and clinical challenge. Int J Surg. 2015;19:22–6.

301. Boecker W, Stenman G, Loening T, Andersson MK, Sinn HP, Barth P, et al. Differentiation and histogenesis of syringomatous tumour of the nipple and low-grade adenosquamous carcinoma: evidence for a common origin. Histopathology. 2014;65(1):9–23.

302. Rakha EA, Coimbra ND, Hodi Z, Juneinah E, Ellis IO, Lee AH. Immunoprofile of metaplastic carcinomas of the breast. Histopathology. 2017;70(6):975–85.

303. Wilsher MJ, Owens TW, Allcock RJ. Next generation sequencing of the nidus of early (adenosquamous proliferation rich) radial sclerosing lesions of the breast reveals evidence for a neoplastic precursor lesion. J Pathol Clin Res. 2017;3(2):115–22.

304. Gobbi H, Simpson JF, Borowsky A, Jensen RA, Page DL. Metaplastic breast tumors with a dominant fibromatosis-like phenotype have a high risk of local recurrence. Cancer. 1999;85(10):2170–82.

305. Nonnis R, Paliogiannis P, Giangrande D, Marras V, Trignano M. Low-grade fibromatosis-like spindle cell metaplastic carcinoma of the breast: a case report and literature review. Clin Breast Cancer. 2012;12(2):147–50.

306. Sneige N, Yaziji H, Mandavilli SR, Perez ER, Ordonez NG, Gown AM, et al. Low-grade (fibromatosis-like) spindle cell carcinoma of the breast. Am J Surg Pathol. 2001;25(8):1009–16.

307. Rito M, Schmitt F, Pinto AE, Andre S. Fibromatosis-like metaplastic carcinoma of the breast has a claudin-low immunohistochemical phenotype. Virchows Arch. 2014;465(2):185–91.

308. Koker MM, Kleer CG. p63 expression in breast cancer: a highly sensitive and specific marker of metaplastic carcinoma. Am J Surg Pathol. 2004;28(11):1506–12.

309. Lacroix-Triki M, Geyer FC, Lambros MB, Savage K, Ellis IO, Lee AH, et al. beta-catenin/Wnt signalling pathway in fibromato-

sis, metaplastic carcinomas and phyllodes tumours of the breast. Mod Pathol. 2010;23(11):1438–48.

310. Carter MR, Hornick JL, Lester S, Fletcher CD. Spindle cell (sarcomatoid) carcinoma of the breast: a clinicopathologic and immunohistochemical analysis of 29 cases. Am J Surg Pathol. 2006;30(3):300–9.

311. Krings G, Chen YY. Genomic profiling of metaplastic breast carcinomas reveals genetic heterogeneity and relationship to ductal carcinoma. Mod Pathol. 2018;31(11):1661–74.

312. Dunne B, Lee AH, Pinder SE, Bell JA, Ellis IO. An immunohistochemical study of metaplastic spindle cell carcinoma, phyllodes tumor and fibromatosis of the breast. Hum Pathol. 2003;34(10):1009–15.

313. Lee AH. Recent developments in the histological diagnosis of spindle cell carcinoma, fibromatosis and phyllodes tumour of the breast. Histopathology. 2008;52(1):45–57.

314. Rakha EA, Quinn CM, Foschini MP, Munoz Martin M, Dabbs DJ, Lakhani S, et al. Metaplastic carcinomas of the breast without evidence of epithelial differentiation: a diagnostic approach for management. Histopathology. 2021;78(5):759–71.

315. Jo VY, Fletcher CD. p63 immunohistochemical staining is limited in soft tissue tumors. Am J Clin Pathol. 2011;136(5): 762–6.

316. Bishop JA, Montgomery EA, Westra WH. Use of p40 and p63 immunohistochemistry and human papillomavirus testing as ancillary tools for the recognition of head and neck sarcomatoid carcinoma and its distinction from benign and malignant mesenchymal processes. Am J Surg Pathol. 2014;38(2):257–64.

317. Cimino-Mathews A, Sharma R, Illei PB, Vang R, Argani P. A subset of malignant phyllodes tumors express p63 and p40: a diagnostic pitfall in breast core needle biopsies. Am J Surg Pathol. 2014;38(12):1689–96.

318. Bansal M, Chen J, Wang X. Focal anomalous expression of cytokeratin and p63 in malignant phyllodes tumor: a comparison with spindle cell metaplastic carcinoma. Appl Immunohistochem Mol Morphol. 2018;26(3):198–201.

319. Cimino-Mathews A, Subhawong AP, Elwood H, Warzecha HN, Sharma R, Park BH, et al. Neural crest transcription factor Sox10 is preferentially expressed in triple-negative and metaplastic breast carcinomas. Hum Pathol. 2013;44(6):959–65.

320. Jin C, Hacking S, Sajjan S, Kamanda S, Bhuiya T, Nasim M. GATA binding protein 3 (GATA3) as a marker for metaplastic spindle cell carcinoma of the breast. Pathol Res Pract. 2021;221:153413.

321. Ai D, Yao J, Yang F, Huo L, Chen H, Lu W, et al. TRPS1: a highly sensitive and specific marker for breast carcinoma, especially for triple-negative breast cancer. Mod Pathol. 2021;34(4):710–9.

322. Leibl S, Moinfar F. Metaplastic breast carcinomas are negative for Her-2 but frequently express EGFR (Her-1): potential relevance to adjuvant treatment with EGFR tyrosine kinase inhibitors? J Clin Pathol. 2005;58(7):700–4.

323. Reis-Filho JS, Milanezi F, Carvalho S, Simpson PT, Steele D, Savage K, et al. Metaplastic breast carcinomas exhibit EGFR, but not HER2, gene amplification and overexpression: immunohistochemical and chromogenic in situ hybridization analysis. Breast Cancer Res. 2005;7(6):R1028–35.

324. Varma S, Shin SJ. An algorithmic approach to spindle cell lesions of the breast. Adv Anat Pathol. 2013;20(2):95–109.

325. Moore T, Lee AH. Expression of CD34 and bcl-2 in phyllodes tumours, fibroadenomas and spindle cell lesions of the breast. Histopathology. 2001;38(1):62–7.

326. Md Nasir ND, Ng CCY, Rajasegaran V, Wong SF, Liu W, Ng GXP, et al. Genomic characterisation of breast fibroepithelial lesions in an international cohort. J Pathol. 2019;249(4):447–60.

327. Piscuoglio S, Ng CK, Murray M, Burke KA, Edelweiss M, Geyer FC, et al. Massively parallel sequencing of phyllodes tumours of the breast reveals actionable mutations, and TERT promoter hotspot mutations and TERT gene amplification as likely drivers of progression. J Pathol. 2016;238(4):508–18.

328. Tan J, Ong CK, Lim WK, Ng CC, Thike AA, Ng LM, et al. Genomic landscapes of breast fibroepithelial tumors. Nat Genet. 2015;47(11):1341–5.

329. Liu SY, Joseph NM, Ravindranathan A, Stohr BA, Greenland NY, Vohra P, et al. Genomic profiling of malignant phyllodes tumors reveals aberrations in FGFR1 and PI-3 kinase/RAS signaling pathways and provides insights into intratumoral heterogeneity. Mod Pathol. 2016;29(9):1012–27.

330. Nozad S, Sheehan CE, Gay LM, Elvin JA, Vergilio JA, Suh J, et al. Comprehensive genomic profiling of malignant phyllodes tumors of the breast. Breast Cancer Res Treat. 2017;162(3):597–602.

331. Ng CKY, Piscuoglio S, Geyer FC, Burke KA, Pareja F, Eberle CA, et al. The landscape of somatic genetic alterations in metaplastic breast carcinomas. Clin Cancer Res. 2017;23(14):3859–70.

332. Yeong J, Thike AA, Young Ng CC, Md Nasir ND, Loh K, Teh BT, et al. A genetic mutation panel for differentiating malignant phyllodes tumour from metaplastic breast carcinoma. Pathology. 2017;49(7):786–9.

333. Menes T, Schachter J, Morgenstern S, Fenig E, Lurie H, Gutman H. Primary squamous cell carcinoma (SqCC) of the breast. Am J Clin Oncol. 2003;26(6):571–3.

334. Grabowski J, Saltzstein SL, Sadler G, Blair S. Squamous cell carcinoma of the breast: a review of 177 cases. Am Surg. 2009;75(10):914–7.

335. Hennessy BT, Krishnamurthy S, Giordano S, Buchholz TA, Kau SW, Duan Z, et al. Squamous cell carcinoma of the breast. J Clin Oncol. 2005;23(31):7827–35.

336. Stevenson JT, Graham DJ, Khiyami A, Mansour EG. Squamous cell carcinoma of the breast: a clinical approach. Ann Surg Oncol. 1996;3(4):367–74.

337. Behranwala KA, Nasiri N, Abdullah N, Trott PA, Gui GP. Squamous cell carcinoma of the breast: clinico-pathologic implications and outcome. Eur J Surg Oncol. 2003;29(4):386–9.

338. Olsen DL, Keeney GL, Chen B, Visscher DW, Carter JM. Breast implant capsule-associated squamous cell carcinoma: a report of 2 cases. Hum Pathol. 2017;67:94–100.

339. Huws AM, Semkin L, Moalla A, Udayasankar S, Holt SDH, Sharaiha YM. Primary squamous cell carcinoma of the breast in association with Zuska's disease. Breast Cancer. 2018;25(3):365–9.

340. Tan YM, Yeo A, Chia KH, Wong CY. Breast abscess as the initial presentation of squamous cell carcinoma of the breast. Eur J Surg Oncol. 2002;28(1):91–3.

341. Gupta C, Malani AK, Weigand RT, Rangineni G. Pure primary squamous cell carcinoma of the breast: a rare presentation and clinicopathologic comparison with usual ductal carcinoma of the breast. Pathol Res Pract. 2006;202(6):465–9.

342. Wrightson WR, Edwards MJ, McMasters KM. Primary squamous cell carcinoma of the breast presenting as a breast abscess. Am Surg. 1999;65(12):1153–5.

343. Goldberg MT, Llaneras J, Willson TD, Boyd JB, Venegas RJ, Dauphine C, et al. Squamous cell carcinoma arising in breast implant capsules. Ann Plast Surg. 2021;86(3):268–72.

344. Nayak A, Wu Y, Gilcrease MZ. Primary squamous cell carcinoma of the breast: predictors of locoregional recurrence and overall survival. Am J Surg Pathol. 2013;37(6):867–73.

345. Wargotz ES, Norris HJ. Metaplastic carcinomas of the breast. IV. Squamous cell carcinoma of ductal origin. Cancer. 1990;65(2):272–6.

346. Eusebi V, Lamovec J, Cattani MG, Fedeli F, Millis RR. Acantholytic variant of squamous-cell carcinoma of the breast. Am J Surg Pathol. 1986;10(12):855–61.

347. Lei T, Pu T, Wei B, Fan Y, Yang L, Shen M, et al. Clinicopathologic characteristics of HER2-positive metaplastic squamous cell carcinoma of the breast. J Clin Pathol. 2022;75(1):18–23.

348. Foschini MP, Marucci G, Eusebi V. Low-grade mucoepidermoid carcinoma of salivary glands: characteristic immunohistochemical profile and evidence of striated duct differentiation. Virchows Arch. 2002;440(5):536–42.

349. Wargotz ES, Norris HJ. Metaplastic carcinomas of the breast. I. Matrix-producing carcinoma. Hum Pathol. 1989;20(7):628–35.

350. Rosenblum MK, Purrazzella R, Rosen PP. Is microglandular adenosis a precancerous disease? A study of carcinoma arising therein. Am J Surg Pathol. 1986;10(4):237–45.

351. Kim GE, Kim NI, Lee JS, Park MH. Metaplastic carcinoma with chondroid differentiation arising in microglandular adenosis. J Pathol Transl Med. 2017;51(4):418–21.

352. Schwartz CJ, Dolgalev I, Yoon E, Osman I, Heguy A, Vega-Saenz de Miera EC, et al. Microglandular adenosis is an advanced precursor breast lesion with evidence of molecular progression to matrix-producing metaplastic carcinoma. Hum Pathol. 2019;85:65–71.

353. van Deurzen CH, Lee AH, Gill MS, Menke-Pluijmers MB, Jager A, Ellis IO, et al. Metaplastic breast carcinoma: tumour histogenesis or dedifferentiation? J Pathol. 2011;224(4):434–7.

354. Teixeira MR, Qvist H, Bohler PJ, Pandis N, Heim S. Cytogenetic analysis shows that carcinosarcomas of the breast are of monoclonal origin. Genes Chromosomes Cancer. 1998;22(2):145–51.

355. Geyer FC, Weigelt B, Natrajan R, Lambros MB, de Biase D, Vatcheva R, et al. Molecular analysis reveals a genetic basis for the phenotypic diversity of metaplastic breast carcinomas. J Pathol. 2010;220(5):562–73.

356. Lien HC, Lin CW, Mao TL, Kuo SH, Hsiao CH, Huang CS. p53 overexpression and mutation in metaplastic carcinoma of the breast: genetic evidence for a monoclonal origin of both the carcinomatous and the heterogeneous sarcomatous components. J Pathol. 2004;204(2):131–9.

357. Avigdor BE, Beierl K, Gocke CD, Zabransky DJ, Cravero K, Kyker-Snowman K, et al. Whole-exome sequencing of metaplastic breast carcinoma indicates monoclonality with associated ductal carcinoma component. Clin Cancer Res. 2017;23(16):4875–84.

358. Zhuang Z, Lininger RA, Man YG, Albuquerque A, Merino MJ, Tavassoli FA. Identical clonality of both components of mammary carcinosarcoma with differential loss of heterozygosity. Mod Pathol. 1997;10(4):354–62.

359. Zhang Y, Toy KA, Kleer CG. Metaplastic breast carcinomas are enriched in markers of tumor-initiating cells and epithelial to mesenchymal transition. Mod Pathol. 2012;25(2):178–84.

360. Hennessy BT, Gonzalez-Angulo AM, Stemke-Hale K, Gilcrease MZ, Krishnamurthy S, Lee JS, et al. Characterization of a naturally occurring breast cancer subset enriched in epithelial-to-mesenchymal transition and stem cell characteristics. Cancer Res. 2009;69(10):4116–24.

361. Gerhard R, Ricardo S, Albergaria A, Gomes M, Silva AR, Logullo AF, et al. Immunohistochemical features of claudin-low intrinsic subtype in metaplastic breast carcinomas. Breast. 2012;21(3):354–60.

362. Weigelt B, Ng CK, Shen R, Popova T, Schizas M, Natrajan R, et al. Corrigendum: metastatic breast carcinomas display genomic and transcriptomic heterogeneity. Mod Pathol. 2015;28(4):607.

363. Piscuoglio S, Ng CKY, Geyer FC, Burke KA, Cowell CF, Martelotto LG, et al. Genomic and transcriptomic heterogeneity in metaplastic carcinomas of the breast. NPJ Breast Cancer. 2017;3:48.

364. Prat A, Parker JS, Karginova O, Fan C, Livasy C, Herschkowitz JI, et al. Phenotypic and molecular characterization of the claudin-low intrinsic subtype of breast cancer. Breast Cancer Res. 2010;12(5):R68.

365. May CD, Sphyris N, Evans KW, Werden SJ, Guo W, Mani SA. Epithelial-mesenchymal transition and cancer stem cells: a dangerously dynamic duo in breast cancer progression. Breast Cancer Res. 2011;13(1):202.

366. Weigelt B, Ng CK, Shen R, Popova T, Schizas M, Natrajan R, et al. Metaplastic breast carcinomas display genomic and transcriptomic heterogeneity [corrected]. Mod Pathol. 2015;28(3):340–51.

367. Joneja U, Vranic S, Swensen J, Feldman R, Chen W, Kimbrough J, et al. Comprehensive profiling of metaplastic breast carcinomas reveals frequent overexpression of programmed death-ligand 1. J Clin Pathol. 2017;70(3):255–9.

368. Edenfield J, Schammel C, Collins J, Schammel D, Edenfield WJ. Metaplastic breast cancer: molecular typing and identification of potential targeted therapies at a single institution. Clin Breast Cancer. 2017;17(1):e1–e10.

369. Pareja F, Ferrando L, Lee SSK, Beca F, Selenica P, Brown DN, et al. The genomic landscape of metastatic histologic special types of invasive breast cancer. NPJ Breast Cancer. 2020;6:53.

370. Hayes MJ, Thomas D, Emmons A, Giordano TJ, Kleer CG. Genetic changes of Wnt pathway genes are common events in metaplastic carcinomas of the breast. Clin Cancer Res. 2008;14(13):4038–44.

371. Ross JS, Badve S, Wang K, Sheehan CE, Boguniewicz AB, Otto GA, et al. Genomic profiling of advanced-stage, metaplastic breast carcinoma by next-generation sequencing reveals frequent, targetable genomic abnormalities and potential new treatment options. Arch Pathol Lab Med. 2015;139(5):642–9.

372. Suarez-Kelly LP, Akagi K, Reeser JW, Samorodnitsky E, Reeder M, Smith A, et al. Metaplastic breast cancer in a patient with neurofibromatosis type 1 and somatic loss of heterozygosity. Cold Spring Harb Mol Case Stud. 2018;4(2):a002352.

373. Lee HS, Jung EJ, Kim JY, Song EJ, Jeong CY, Ju YT, et al. Metaplastic spindle cell carcinoma of the breast in a patient with neurofibromatosis type 1. Breast J. 2018;24(3):391–4.

374. Natsiopoulos I, Chatzichristou A, Stratis I, Skordalaki A, Makrantonakis N. Metaplastic breast carcinoma in a patient with Von Recklinghausen's disease. Clin Breast Cancer. 2007;7(7):573–5.

375. Noel JC, Buxant F, Engohan-Aloghe C. Low-grade adenosquamous carcinoma of the breast--A case report with a BRCA1 germline mutation. Pathol Res Pract. 2010;206(7):511–3.

376. Nam G, Strenger R, Cutitar M, Wang Y. Low-grade adenosquamous carcinoma of the breast: a case with pathogenic germline mutation in the BRIP1 gene. Case Reports. 2020;22:200444.

377. Zhong S, Zhou S, Li A, Lv H, Li M, Tang S, et al. High frequency of PIK3CA and TERT promoter mutations in fibromatosis-like spindle cell carcinomas. J Clin Pathol. 2022;75(7):477–82.

378. Takano EA, Hunter SM, Campbell IG, Fox SB. Low-grade fibromatosis-like spindle cell carcinomas of the breast are molecularly exiguous. J Clin Pathol. 2015;68(5):362–7.

379. Hennessy BT, Giordano S, Broglio K, Duan Z, Trent J, Buchholz TA, et al. Biphasic metaplastic sarcomatoid carcinoma of the breast. Ann Oncol. 2006;17(4):605–13.

380. Tseng WH, Martinez SR. Metaplastic breast cancer: to radiate or not to radiate? Ann Surg Oncol. 2011;18(1):94–103.

381. Jung SY, Kim HY, Nam BH, Min SY, Lee SJ, Park C, et al. Worse prognosis of metaplastic breast cancer patients than other patients with triple-negative breast cancer. Breast Cancer Res Treat. 2010;120(3):627–37.

382. Lester TR, Hunt KK, Nayeemuddin KM, Bassett RL Jr, Gonzalez-Angulo AM, Feig BW, et al. Metaplastic sarcomatoid carcinoma of the breast appears more aggressive than other triple receptor-negative breast cancers. Breast Cancer Res Treat. 2012;131(1):41–8.

383. Zhang Y, Lv F, Yang Y, Qian X, Lang R, Fan Y, et al. Clinicopathological features and prognosis of metaplastic breast

carcinoma: experience of a major chinese cancer center. PLoS One. 2015;10(6):e0131409.

384. Beatty JD, Atwood M, Tickman R, Reiner M. Metaplastic breast cancer: clinical significance. Am J Surg. 2006;191(5): 657–64.

385. Bae SY, Lee SK, Koo MY, Hur SM, Choi MY, Cho DH, et al. The prognoses of metaplastic breast cancer patients compared to those of triple-negative breast cancer patients. Breast Cancer Res Treat. 2011;126(2):471–8.

386. Corso G, Frassoni S, Girardi A, De Camilli E, Montagna E, Intra M, et al. Metaplastic breast cancer: prognostic and therapeutic considerations. J Surg Oncol. 2021;123(1):61–70.

387. Lee H, Jung SY, Ro JY, Kwon Y, Sohn JH, Park IH, et al. Metaplastic breast cancer: clinicopathological features and its prognosis. J Clin Pathol. 2012;65(5):441–6.

388. Han M, Salamat A, Zhu L, Zhang H, Clark BZ, Dabbs DJ, et al. Metaplastic breast carcinoma: a clinical-pathologic study of 97 cases with subset analysis of response to neoadjuvant chemotherapy. Mod Pathol. 2019;32(6):807–16.

389. Cimino-Mathews A, Verma S, Figueroa-Magalhaes MC, Jeter SC, Zhang Z, Argani P, et al. A clinicopathologic analysis of 45 patients with metaplastic breast carcinoma. Am J Clin Pathol. 2016;145(3):365–72.

390. Takala S, Heikkilä P, Nevanlinna H, Blomqvist C, Mattson J. Metaplastic carcinoma of the breast: prognosis and response to systemic treatment in metastatic disease. Breast J. 2019;25(3):418–24.

391. Gradishar WJ, Moran MS, Abraham J, Aft R, Agnese D, Allison KH, et al. NCCN guidelines(R) insights: breast cancer, version 4.2021. J Natl Compr Canc Netw. 2021;19(5):484–93.

392. Honda M, Saji S, Horiguchi S, Suzuki E, Aruga T, Horiguchi K, et al. Clinicopathological analysis of ten patients with metaplastic squamous cell carcinoma of the breast. Surg Today. 2011;41(3):328–32.

393. Liu J, Yu Y, Sun JY, He SS, Wang X, Yin J, et al. Clinicopathologic characteristics and prognosis of primary squamous cell carcinoma of the breast. Breast Cancer Res Treat. 2015;149(1):133–40.

394. Lan T, Lu Y, Zheng R, Shao X, Luo H, He J, et al. The Role of adjuvant chemotherapy in metaplastic breast carcinoma: a competing risk analysis of the SEER database. Front Oncol. 2021;11:572230.

395. He X, Ji J, Dong R, Liu H, Dai X, Wang C, et al. Prognosis in different subtypes of metaplastic breast cancer: a population-based analysis. Breast Cancer Res Treat. 2019;173(2):329–41.

396. Wong W, Brogi E, Reis-Filho JS, Plitas G, Robson M, Norton L, et al. Poor response to neoadjuvant chemotherapy in metaplastic breast carcinoma. NPJ Breast Cancer. 2021;7(1):96.

397. Tray N, Taff J, Adams S. Therapeutic landscape of metaplastic breast cancer. Cancer Treat Rev. 2019;79:101888.

398. Haque W, Verma V, Naik N, Butler EB, Teh BS. Metaplastic breast cancer: practice patterns, outcomes, and the role of radiotherapy. Ann Surg Oncol. 2018;25(4):928–36.

399. Basho RK, Gilcrease M, Murthy RK, Helgason T, Karp DD, Meric-Bernstam F, et al. Targeting the PI3K/AKT/mTOR pathway for the treatment of mesenchymal triple-negative breast cancer: evidence from a phase 1 trial of mTOR inhibition in combination with liposomal doxorubicin and bevacizumab. JAMA Oncol. 2017;3(4):509–15.

400. Moukarzel LA, Ferrando L, Da Cruz PA, Brown DN, Geyer FC, Pareja F, et al. The genetic landscape of metaplastic breast cancers and uterine carcinosarcomas. Mol Oncol. 2021;15(4):1024–39.

401. Lien HC, Lee YH, Chen IC, Lin CH, Chen TW, Lu YT, et al. Tumor-infiltrating lymphocyte abundance and programmed death-ligand 1 expression in metaplastic breast carcinoma: implications for distinct immune microenvironments in different metaplastic components. Virchows Arch. 2021;478(4):669–78.

402. Morgan E, Suresh A, Ganju A, Stover DG, Wesolowski R, Sardesai S, et al. Assessment of outcomes and novel immune biomarkers in metaplastic breast cancer: a single institution retrospective study. World J Surg Oncol. 2020;18(1):11.

403. Chao X, Liu L, Sun P, Yang X, Li M, Luo R, et al. Immune parameters associated with survival in metaplastic breast cancer. Breast Cancer Res. 2020;22(1):92.

404. Grabenstetter A, Jungbluth AA, Frosina D, Hoda R, Dos Anjos CH, Patil S, et al. PD-L1 expression in metaplastic breast carcinoma using the PD-L1 SP142 assay and concordance among PD-L1 immunohistochemical assays. Am J Surg Pathol. 2021;45(9):1274–81.

405. Schmid P, Adams S, Rugo HS, Schneeweiss A, Barrios CH, Iwata H, et al. Atezolizumab and Nab-paclitaxel in advanced triple-negative breast cancer. N Engl J Med. 2018;379(22): 2108–21.

406. Adams S. Dramatic response of metaplastic breast cancer to chemo-immunotherapy. NPJ Breast Cancer. 2017;3:8.

407. Al Sayed AD, Elshenawy MA, Tulbah A, Al-Tweigeri T, Ghebeh H. Complete response of chemo-refractory metastatic metaplastic breast cancer to paclitaxel-immunotherapy combination. Am J Case Rep. 2019;20:1630–5.

408. Ridolfi RL, Rosen PP, Port A, Kinne D, Mike V. Medullary carcinoma of the breast: a clinicopathologic study with 10 year follow-up. Cancer. 1977;40(4):1365–85.

409. Wargotz ES, Silverberg SG. Medullary carcinoma of the breast: a clinicopathologic study with appraisal of current diagnostic criteria. Hum Pathol. 1988;19(11):1340–6.

410. Pedersen L, Zedeler K, Holck S, Schiodt T, Mouridsen HT. Medullary carcinoma of the breast, proposal for a new simplified histopathological definition. Based on prognostic observations and observations on inter- and intraobserver variability of 11 histopathological characteristics in 131 breast carcinomas with medullary features. Br J Cancer. 1991;63(4):591–5.

411. Jensen ML, Kiaer H, Andersen J, Jensen V, Melsen F. Prognostic comparison of three classifications for medullary carcinomas of the breast. Histopathology. 1997;30(6):523–32.

412. Pedersen L, Zedeler K, Holck S, Schiodt T, Mouridsen HT. Medullary carcinoma of the breast. Prevalence and prognostic importance of classical risk factors in breast cancer. Eur J Cancer. 1995;31A(13-14):2289–95.

413. Pedersen L, Holck S, Schiodt T, Zedeler K, Mouridsen HT. Inter- and intraobserver variability in the histopathological diagnosis of medullary carcinoma of the breast, and its prognostic implications. Breast Cancer Res Treat. 1989;14(1):91–9.

414. Gaffey MJ, Mills SE, Frierson HF Jr, Zarbo RJ, Boyd JC, Simpson JF, et al. Medullary carcinoma of the breast: interobserver variability in histopathologic diagnosis. Mod Pathol. 1995;8(1):31–8.

415. Moore OS Jr, Foote FW Jr. The relatively favorable prognosis of medullary carcinoma of the breast. Cancer. 1949;2(4):635–42.

416. Jacquemier JR-FJ, Lakhani SR, Rakha E. Carcinoma with medullary features. In: WHO Classification of Tumours. Editorial Board, editors. WHO Classification of Breast Tumours. 4th ed. Lyon: International Agency for Research on Cancer (IARC); 2012.

417. Jacquemier J, Padovani L, Rabayrol L, Lakhani SR, Penault-Llorca F, Denoux Y, et al. Typical medullary breast carcinomas have a basal/myoepithelial phenotype. J Pathol. 2005;207(3):260–8.

418. de Cremoux P, Salomon AV, Liva S, Dendale R, Bouchind'homme B, Martin E, et al. p53 mutation as a genetic trait of typical medullary breast carcinoma. J Natl Cancer Inst. 1999;91(7):641–3.

419. Denkert C, von Minckwitz G, Darb-Esfahani S, Lederer B, Heppner BI, Weber KE, et al. Tumour-infiltrating lymphocytes and prognosis in different subtypes of breast cancer: a pooled analysis of 3771 patients treated with neoadjuvant therapy. Lancet Oncol. 2018;19(1):40–50.

420. Loi S, Drubay D, Adams S, Pruneri G, Francis PA, Lacroix-Triki M, et al. Tumor-infiltrating lymphocytes and prognosis: a pooled individual patient analysis of early-stage triple-negative breast cancers. J Clin Oncol. 2019;37(7):559–69.

421. Loi S, Michiels S, Salgado R, Sirtaine N, Jose V, Fumagalli D, et al. Tumor infiltrating lymphocytes are prognostic in triple negative breast cancer and predictive for trastuzumab benefit in early breast cancer: results from the FinHER trial. Ann Oncol. 2014;25(8):1544–50.

422. Rakha EAAK, Bu H, Ellis IO, Foschini MP, Horii R, Masuda S, Penault-Llorca F, Schnitt SJ, Tsuda H, Vincent-Salomon A, Yang WT. Invasive breast carcinoma of no special type. In: WHO Classification of Tumours. Editorial Board, editors. WHO Classification of Breast Tumours. 5th ed. Lyon: International Agency for Research on Cancer (IARC); 2019. p. 104.

423. Fisher ER, Gregorio RM, Fisher B, Redmond C, Vellios F, Sommers SC. The pathology of invasive breast cancer. A syllabus derived from findings of the National Surgical Adjuvant Breast Project (protocol no. 4). Cancer. 1975;36(1):1–85.

424. Rapin V, Contesso G, Mouriesse H, Bertin F, Lacombe MJ, Piekarski JD, et al. Medullary breast carcinoma. A reevaluation of 95 cases of breast cancer with inflammatory stroma. Cancer. 1988;61(12):2503–10.

425. Huober J, Gelber S, Goldhirsch A, Coates AS, Viale G, Ohlschlegel C, et al. Prognosis of medullary breast cancer: analysis of 13 International Breast Cancer Study Group (IBCSG) trials. Ann Oncol. 2012;23(11):2843–51.

426. Richardson WW. Medullary carcinoma of the breast; a distinctive tumour type with a relatively good prognosis following radical mastectomy. Br J Cancer. 1956;10(3):415–23.

427. Bloom HJ, Richardson WW, Field JR. Host resistance and survival in carcinoma of breast: a study of 104 cases of medullary carcinoma in a series of 1,411 cases of breast cancer followed for 20 years. Br Med J. 1970;3(5716):181–8.

428. Pedersen L, Holck S, Schiodt T, Zedeler K, Mouridsen HT. Medullary carcinoma of the breast, prognostic importance of characteristic histopathological features evaluated in a multivariate Cox analysis. Eur J Cancer. 1994;30A(12):1792–7.

429. Maier WP, Rosemond GP, Goldman LI, Kaplan GF, Tyson RR. A ten year study of medullary carcinoma of the breast. Surg Gynecol Obstet. 1977;144(5):695–8.

430. Li CI, Uribe DJ, Daling JR. Clinical characteristics of different histologic types of breast cancer. Br J Cancer. 2005;93(9):1046–52.

431. Vu-Nishino H, Tavassoli FA, Ahrens WA, Haffty BG. Clinicopathologic features and long-term outcome of patients with medullary breast carcinoma managed with breast-conserving therapy (BCT). Int J Radiat Oncol Biol Phys. 2005;62(4):1040–7.

432. Rubens JR, Lewandrowski KB, Kopans DB, Koerner FC, Hall DA, McCarthy KA. Medullary carcinoma of the breast. Overdiagnosis of a prognostically favorable neoplasm. Arch Surg. 1990;125(5):601–4.

433. Neuman ML, Homer MJ. Association of medullary carcinoma with reactive axillary adenopathy. AJR Am J Roentgenol. 1996;167(1):185–6.

434. Kleer CG. Carcinoma of the breast with medullary-like features: diagnostic challenges and relationship with BRCA1 and EZH2 functions. Arch Pathol Lab Med. 2009;133(11):1822–5.

435. Meyer JE, Amin E, Lindfors KK, Lipman JC, Stomper PC, Genest D. Medullary carcinoma of the breast: mammographic and US appearance. Radiology. 1989;170(1 Pt 1):79–82.

436. Jeong SJ, Lim HS, Lee JS, Park MH, Yoon JH, Park JG, et al. Medullary carcinoma of the breast: MRI findings. AJR Am J Roentgenol. 2012;198(5):W482–7.

437. Yoo JL, Woo OH, Kim YK, Cho KR, Yong HS, Seo BK, et al. Can MR Imaging contribute in characterizing well-circumscribed breast carcinomas? Radiographics. 2010;30(6):1689–702.

438. Reinfuss M, Stelmach A, Mitus J, Rys J, Duda K. Typical medullary carcinoma of the breast: a clinical and pathological analysis of 52 cases. J Surg Oncol. 1995;60(2):89–94.

439. Marginean F, Rakha EA, Ho BC, Ellis IO, Lee AH. Histological features of medullary carcinoma and prognosis in triple-negative basal-like carcinomas of the breast. Mod Pathol. 2010;23(10):1357–63.

440. Salgado R, Denkert C, Demaria S, Sirtaine N, Klauschen F, Pruneri G, et al. The evaluation of tumor-infiltrating lymphocytes (TILs) in breast cancer: recommendations by an International TILs Working Group 2014. Ann Oncol. 2015;26(2):259–71.

441. Rosen PP, Lesser ML, Kinne DW. Breast carcinoma at the extremes of age: a comparison of patients younger than 35 years and older than 75 years. J Surg Oncol. 1985;28(2):90–6.

442. Rodriguez-Pinilla SM, Rodriguez-Gil Y, Moreno-Bueno G, Sarrio D, Martin-Guijarro Mdel C, Hernandez L, et al. Sporadic invasive breast carcinomas with medullary features display a basal-like phenotype: an immunohistochemical and gene amplification study. Am J Surg Pathol. 2007;31(4):501–8.

443. Vincent-Salomon A, Gruel N, Lucchesi C, MacGrogan G, Dendale R, Sigal-Zafrani B, et al. Identification of typical medullary breast carcinoma as a genomic sub-group of basal-like carcinomas, a heterogeneous new molecular entity. Breast Cancer Res. 2007;9(2):R24.

444. Chu Z, Lin H, Liang X, Huang R, Zhan Q, Jiang J, et al. Clinicopathologic characteristics of typical medullary breast carcinoma: a retrospective study of 117 cases. PLoS One. 2014;9(11):e111493.

445. Reiner A, Reiner G, Spona J, Schemper M, Holzner JH. Histopathologic characterization of human breast cancer in correlation with estrogen receptor status. A comparison of immunocytochemical and biochemical analysis. Cancer. 1988;61(6):1149–54.

446. Stierer M, Rosen H, Weber R, Hanak H, Spona J, Tuchler H. Immunohistochemical and biochemical measurement of estrogen and progesterone receptors in primary breast cancer. Correlation of histopathology and prognostic factors. Ann Surg. 1993;218(1):13–21.

447. Flucke U, Flucke MT, Hoy L, Breuer E, Goebbels R, Rhiem K, et al. Distinguishing medullary carcinoma of the breast from high-grade hormone receptor-negative invasive ductal carcinoma: an immunohistochemical approach. Histopathology. 2010;56(7):852–9.

448. Soomro S, Shousha S, Taylor P, Shepard HM, Feldmann M. c-erbB-2 expression in different histological types of invasive breast carcinoma. J Clin Pathol. 1991;44(3):211–4.

449. Somerville JE, Clarke LA, Biggart JD. c-erbB-2 overexpression and histological type of in situ and invasive breast carcinoma. J Clin Pathol. 1992;45(1):16–20.

450. Tot T. The cytokeratin profile of medullary carcinoma of the breast. Histopathology. 2000;37(2):175–81.

451. Larsimont D, Lespagnard L, Degeyter M, Heimann R. Medullary carcinoma of the breast: a tumour lacking keratin 19. Histopathology. 1994;24(6):549–52.

452. Kajiwara M, Toyoshima S, Yao T, Tanaka M, Tsuneyoshi M. Apoptosis and cell proliferation in medullary carcinoma of the breast: a comparative study between medullary and non-medullary carcinoma using the TUNEL method and immunohistochemistry. J Surg Oncol. 1999;70(4):209–16.

453. Domagala W, Harezga B, Szadowska A, Markiewski M, Weber K, Osborn M. Nuclear p53 protein accumulates preferentially in medullary and high-grade ductal but rarely in lobular breast carcinomas. Am J Pathol. 1993;142(3):669–74.

454. Guo X, Fan Y, Lang R, Gu F, Chen L, Cui L, et al. Tumor infiltrating lymphocytes differ in invasive micropapillary carcinoma and medullary carcinoma of breast. Mod Pathol. 2008;21(9):1101–7.

455. Kuroda H, Tamaru J, Sakamoto G, Ohnisi K, Itoyama S. Immunophenotype of lymphocytic infiltration in medullary carcinoma of the breast. Virchows Arch. 2005;446(1):10–4.

456. Yakirevich E, Izhak OB, Rennert G, Kovacs ZG, Resnick MB. Cytotoxic phenotype of tumor infiltrating lymphocytes in medullary carcinoma of the breast. Mod Pathol. 1999;12(11):1050–6.

457. Carter JM, Polley MC, Leon-Ferre RA, Sinnwell J, Thompson KJ, Wang X, et al. Characteristics and spatially-defined immune (micro)landscapes of early-stage PD-L1-positive triple-negative breast cancer. Clin Cancer Res. 2021;27(20):5628–37.

458. Dadmanesh F, Peterse JL, Sapino A, Fonelli A, Eusebi V. Lymphoepithelioma-like carcinoma of the breast: lack of evidence of Epstein-Barr virus infection. Histopathology. 2001;38(1):54–61.

459. Lespagnard L, Cochaux P, Larsimont D, Degeyter M, Velu T, Heimann R. Absence of Epstein-Barr virus in medullary carcinoma of the breast as demonstrated by immunophenotyping, in situ hybridization and polymerase chain reaction. Am J Clin Pathol. 1995;103(4):449–52.

460. Lakhani SR, Gusterson BA, Jacquemier J, Sloane JP, Anderson TJ, van de Vijver MJ, et al. The pathology of familial breast cancer: histological features of cancers in families not attributable to mutations in BRCA1 or BRCA2. Clin Cancer Res. 2000;6(3):782–9.

461. Shousha S. Medullary carcinoma of the breast and BRCA1 mutation. Histopathology. 2000;37(2):182–5.

462. Eisinger F, Jacquemier J, Charpin C, Stoppa-Lyonnet D, Bressac-de Paillerets B, Peyrat JP, et al. Mutations at BRCA1: the medullary breast carcinoma revisited. Cancer Res. 1998;58(8):1588–92.

463. Marcus JN, Watson P, Page DL, Narod SA, Lenoir GM, Tonin P, et al. Hereditary breast cancer: pathobiology, prognosis, and BRCA1 and BRCA2 gene linkage. Cancer. 1996;77(4):697–709.

464. Marcus JN, Watson P, Page DL, Narod SA, Tonin P, Lenoir GM, et al. BRCA2 hereditary breast cancer pathophenotype. Breast Cancer Res Treat. 1997;44(3):275–7.

465. Lakhani SR, Jacquemier J, Sloane JP, Gusterson BA, Anderson TJ, van de Vijver MJ, et al. Multifactorial analysis of differences between sporadic breast cancers and cancers involving BRCA1 and BRCA2 mutations. J Natl Cancer Inst. 1998;90(15):1138–45.

466. Breast Cancer Linkage Consortium. Pathology of familial breast cancer: differences between breast cancers in carriers of BRCA1 or BRCA2 mutations and sporadic cases. Lancet. 1997;349(9064):1505–10.

467. Esteller M, Silva JM, Dominguez G, Bonilla F, Matias-Guiu X, Lerma E, et al. Promoter hypermethylation and BRCA1 inactivation in sporadic breast and ovarian tumors. J Natl Cancer Inst. 2000;92(7):564–9.

468. Bertucci F, Finetti P, Cervera N, Charafe-Jauffret E, Mamessier E, Adelaide J, et al. Gene expression profiling shows medullary breast cancer is a subgroup of basal breast cancers. Cancer Res. 2006;66(9):4636–44.

469. Romero P, Benhamo V, Deniziaut G, Fuhrmann L, Berger F, Manie E, et al. Medullary breast carcinoma, a triple-negative breast cancer associated with BCLG overexpression. Am J Pathol. 2018;188(10):2378–91.

470. Teschendorff AE, Miremadi A, Pinder SE, Ellis IO, Caldas C. An immune response gene expression module identifies a good prognosis subtype in estrogen receptor negative breast cancer. Genome Biol. 2007;8(8):R157.

471. Fisher ER, Kenny JP, Sass R, Dimitrov NV, Siderits RH, Fisher B. Medullary cancer of the breast revisited. Breast Cancer Res Treat. 1990;16(3):215–29.

472. Rakha EA, Aleskandarany M, El-Sayed ME, Blamey RW, Elston CW, Ellis IO, et al. The prognostic significance of inflammation and medullary histological type in invasive carcinoma of the breast. Eur J Cancer. 2009;45(10):1780–7.

473. Leon-Ferre RA, Polley MY, Liu H, Gilbert JA, Cafourek V, Hillman DW, et al. Impact of histopathology, tumor-infiltrating lymphocytes, and adjuvant chemotherapy on prognosis of triple-negative breast cancer. Breast Cancer Res Treat. 2018;167(1):89–99.

474. Sabatier R, Finetti P, Cervera N, Lambaudie E, Esterni B, Mamessier E, et al. A gene expression signature identifies two prognostic subgroups of basal breast cancer. Breast Cancer Res Treat. 2011;126(2):407–20.

475. Weiss MC, Fowble BL, Solin LJ, Yeh IT, Schultz DJ. Outcome of conservative therapy for invasive breast cancer by histologic subtype. Int J Radiat Oncol Biol Phys. 1992;23(5):941–7.

476. Kurtz JM, Amalric R, Brandone H, Ayme Y, Jacquemier J, Pietra JC, et al. Local recurrence after breast-conserving surgery and radiotherapy. Frequency, time course, and prognosis. Cancer. 1989;63(10):1912–7.